UFC 3-220-01A
16 January 2004

UNIFIED FACILITIES CRITERIA (UFC)

DEEP FOUNDATIONS

APPROVED FOR PUBLIC RELEASE; DISTRIBUTION UNLIMITED

UNIFIED FACILITIES CRITERIA (UFC)

DEEP FOUNDATIONS

U.S. ARMY CORPS OF ENGINEERS (Preparing Activity)

NAVAL FACILITIES ENGINEERING COMMAND

AIR FORCE CIVIL ENGINEER SUPPORT AGENCY

Record of Changes (changes are indicated by **1**\ ... /**1**/)

Change No.	Date	Location

This UFC supersedes TI 818-02, dated 3 August 1998. The format of this UFC does not conform to UFC 1-300-01; however, the format will be adjusted to conform at the next revision. The body of this UFC is the previous TI 818-02, dated 3 August 1998.

TI 818-02
3 August 1998

US Army Corps
of Engineers®

Technical Instructions

Design of Deep Foundations

Headquarters
U.S. Army Corps of Engineers
Engineering Division
Directorate of Military Programs
Washington, DC 20314-1000

TECHNICAL INSTRUCTIONS

Design of Deep Foundations

Approved for public release; distribution is unlimited.

Record of Changes (changes indicated by \1\..../1/)
No. Date Location

This Technical Instruction supersedes EI 02C097, dated 1 July 1997.
(EI 02C097 text is included in this Technical Instruction and may carry EI 02C097 identification.)

FOREWORD

These technical instructions (TI) provide design and construction criteria and apply to all U.S. Army Corps of Engineers (USACE) commands having military construction responsibilities. TI will be used for all Army projects and for projects executed for other military services or work for other customers where appropriate.

TI are living documents and will be periodically reviewed, updated, and made available to users as part of the HQUSACE responsibility for technical criteria and policy for new military construction. CEMP-ET is responsible for administration of the TI system; technical content of TI is the responsibility of the HQUSACE element of the discipline involved. Recommended changes to TI, with rationale for the changes, should be sent to HQUSACE, ATTN: CEMP-ET, 20 Massachusetts Ave., NW, Washington, DC 20314-1000.

TI are effective upon issuance. TI are distributed only in electronic media through the TECHINFO Internet site *http://www.hnd.usace.army.mil/techinfo/index.htm* and the Construction Criteria Base (CCB) system maintained by the National Institute of Building Sciences at Internet site *http://www.nibs.org/ccb/.* Hard copies of these instructions produced by the user from the electronic media should be checked against the current electronic version prior to use to assure that the latest instructions are used.

FOR THE DIRECTOR OF MILITARY PROGRAMS:

KISUK CHEUNG, P.E.
Chief, Engineering and Construction Division
Directorate of Military Programs

DEPARTMENT OF THE ARMY
U.S. Army Corps of Engineers
Washington, DC 20314-1000

EI 02C097

CEMP-E

Engineering Instructions
No. 02C097

01 July 1997

DESIGN OF DEEP FOUNDATIONS

Table of Contents
(Click on chapter titles to view topics.)

List of Figures

List of Figures

List of Tables

Chapter 1
Introduction

1. Purpose

This publication presents data, principles, and methods for use in planning, design, and construction of deep foundations. Deep foundations are literally braced (supported) column elements transmitting structure loads down to the subgrade supporting medium.

2. Applicability

These instructions are applicable to all HQUSACE elements and USACE comands.

3. Scope

General information with respect to the selection and design of deep foundations is addressed herein. Single and groups of driven piles and drilled shafts under axial and lateral static loads are treated. Some example problems and the most widely accepted computer methods are introduced. This publication is not intended for hydraulic structures; however, it does provide the following:

a. Guidance is provided to assist the efficient planning, design, and quality verification of the deep foundation.

b. Guidance is not specifically provided for design of sheet piles used as retaining walls to resist lateral forces or for the design of stone columns. Other foundation structures may be designed as discussed below:

(1) Shallow foundations will be designed using TM 5-818-1, "Soils and Geology; Procedures for Foundation Design of Buildings and Other Structures (Except Hydraulic Structures)."

(2) Refer to *Foundations* (Pile Buck Inc. 1992) and *Pile Foundations in Engineering Practice* (Prakash and Sharma 1989) for guidance on design of deep foundations subject to dynamic load.

c. Guidance for construction of deep foundations is provided only in minor detail. For construction of deep foundations, the following references are offered:

(1) Some guidance for selection of pile driving equipment and construction of driven piles is provided in TM 5-849-1, "Pile Driving Equipment."

(2) Guidance for construction of drilled shafts is available in FHWA-HI-88-042, "Drilled Shafts: Construction Procedures and Design Methods" and Association of Drilled Shaft Contractors (ADSC) Publication, "Drilled Shaft Inspector's Manual."

4. References

Appendix A contains a list of references used in this publication.

5. General Design Methodology

A single drilled shaft or a group of driven piles is typically designed to support a column load. The number of driven piles in a group is determined by dividing the column load by the design load of a single pile. The piles should be arranged in the group to provide a spacing of about three to four times the pile diameter B up to $6B$. The diameter of the piles may be increased to reduce the size of the pile cap if appropriate. Table 1-1 describes a general design methodology. Other design methodology aspects are the following:

a. Load factor design. This publication applies load factors for design (LFD) of the structural capacity of deep foundations. The sum of the factored loads shall not exceed the structural resistance and the soil resistance. The LFD, the structural resistance, and the soil resistance are all related to the load factors as follows:

(1) Definition. The LFD may be defined as a concept which recognizes that the different types i of loads Q_i that are applied to a structure have varied probabilities of occurence. Examples of types of loads applied to a structure include the live load Q_{LL}, dead load Q_{DL}, wind load Q_{WL}, and earthquake load Q_{EL}. The probability of occurrence of each load is accounted for by multiplying each Q_i by a load factor F_i > 1.0. The value of F_i depends on the uncertainty of the load.

(2) Structural resistance. The sum of the factored loads shall be less than the design strength

Table 1-1
General Design Methodology for Deep Foundations

Step	Evaluate	Description
1	Soil profile of selected site	Develop depth profiles of water content, liquid and plastic limits, unit weight and overburden pressure, and unconsolidated-undrained shear strength to a depth of a least twice the width of a pile group or five times the tip diameter of drilled shafts. Estimate shear strength and elastic soil modulus from results of in situ and laboratory triaxial tests. Determine water table depth and extent of perched water. Perform consolidation/swell tests if soil is potentially expansive or collapsible and plot compression and swell indices and swell pressure with depth. Evaluate lateral modulus of subgrade reaction profile. Compare soil profile at different locations on the site. See Chapters 1-6 for further details.
2	Group similar soils	Group similar soils and assign average parameters to each group or strata.
3	Depth of base	Select a potentially suitable stratum that should support the structural loads such as a firm, nonswelling, and noncollapsing soil of low compressibility.
4	Select type of deep foundation	Select the type of deep foundation such as driven piles or drilled shafts depending on requirements that include vertical and lateral load resistance, economy, availability of pertinent construction equipment, and experience. Environmental considerations include allowable noise level, vibrations, overhead clearance, and accessibility of equipment to the construction site. Soil conditions such as potential ground rise (heave) or loss and expansion/collapse also influence type of foundation. See Chapter 1 for further information on type and selection of deep foundations.
5	Check Q_a with structural capacity	Allowable pile or shaft load Q_a shall be within the structural capacity of the deep foundation as described by methodology in Chapter 2.
6	Design	The design procedure will be similar for most types of deep foundations and requires evaluation of the ultimate pile capacity $Q_u = Q_{su} + Q_{bu}$ where Q_{su} = ultimate skin friction resistance and Q_{bu} = ultimate end bearing capacity. Reasonable estimates of vertical and lateral displacements under the probable design load Q_d are also required. Q_d should be within levels that can be tolerated by the structure over its projected life and should optimize operations. $Q_d \leq Q_a$ where Q_a = allowable pile capacity. $Q_a = Q_u/FS$ = factor of safety. A typical $FS = 3$ if load tests are not performed or if the deep foundation consists of a group of driven piles. $FS = 2$ if load tests are performed or 2.5 if wave equation analyses of the driven piles calibrated with results of pile driving analyzer tests. Design for vertical loads is given in Chapter 3, lateral loads in Chapter 4, and pile groups in Chapter 5.
7	Verify the design	The capability of the deep foundation to support the structure shall be verified by static load and dynamic tests. These tests are usually nondestructive and allow the tested piles or drilled shafts to be used as part of the foundation. See Chapter 6 for further details.
8	Addition to existing structure	Calculate displacements of existing deep or shallow foundations to determine the ability to carry existing and additional loads and to accommodate new construction.
9	Effect on adjacent structure	Evaluate changes in bearing capacity and groundwater elevation and effect of any action which can result in settlement or heave of adjacent structures.

$$\phi_{pf} Q_{cap} \geq \sum F_i Q_i \quad (1\text{-}1)$$

where

ϕ_{pf} = performance factor for structural capacity

Q_{cap} = nominal structural capacity, kips

F_i = Load factor of type *i*

Q_i = applied load of type *i*

Guidance for analysis of structural capacity is given in Chapter 2.

(3) Soil resistance. The sum of the factored loads shall be less than the ability of the soil to resist the loads. This evaluation may be determined by factors of safety (*FS*) or by load factors. Factors of safety are often empirical values based on past experience and may lead to a more conservative design than the LFD concept. The *FS* and the LFD are presented as:

(a) Global *FS*. The allowable load may be evaluated with global *FS*

$$Q_a = \frac{Q_u}{FS} \geq \Sigma F_i Q_i \quad (1\text{-}2a)$$

where

Q_a = allowable load that can be applied to the soil, kips

Q_u = ultimate pile capacity, kips

FS = global factor of safety

The approach taken throughout this publication is to select a global *FS* for analysis of soil resistance rather than partial *FS* or load factors. Chapters 3 through 5 provide guidance for design of deep foundations to maintain loads within the allowable soil bearing capacity and displacement. Chapter 6 provides guidance for design verification.

(b) Load factor design. Analysis of soil resistance may also be determined by the LFD concept using performance factors

$$\phi_{pfq} Q_u \geq \Sigma F_i Q_i \quad (1\text{-}2b)$$

where ϕ_{pfq} = performance factor appropriate to the ultimate pile capacity. Performance factors ϕ_{pfq} depend on the method of evaluating Q_u and the type of soil resistance, whether end bearing, skin friction, uplift, or a group capacity. Values for ϕ_{pfq} and examples of load factor analysis are available in National Cooperative Highway Research Program Report No. 343, "Manuals for the Design of Bridge Foundations" (Barker et al. 1991). Load factors and factors of safety taken in combination can lead to an uneconomical foundation design. The design should be verified by guidance in Chapter 6.

b. Unusual situations. Consideration should be given to obtaining the services and advice of specialists and consultants in foundation design where conditions are unusual or unfamiliar or structures are economically significant. Some unusual situations for deep foundations, discussed below, include expansive clay, underconsolidated soil, and coral sands.

(1) Expansive clay. The swell of expansive clay can cause an uplift force on the perimeter area of deep foundations that can force the foundation to move up and damage the structure connected to the deep foundation.

(2) Underconsolidated soil. The settlement of underconsolidated soil can cause negative skin friction on the perimeter area of the deep foundation that can increase the end-bearing load, which results in an increase in settlement of the foundation.

(3) Coral sands. Piles in coral sands may indicate low penetration resistance during driving and an apparent low bearing capacity, but the penetration resistance often increases over time as a result of the dissipation of excess pore pressure. Driving of piles into cemented, calcareous sands can crush the soil and lower the lateral stress, which results in a low value for skin friction and bearing capacity.

c. Computer program assistance. Design of a deep foundation is normally accomplished with the assistance of several computer programs. Brief descriptions of appropriate computer programs are provided in Chapters 3 through 6. Copies of user's manuals and programs are available through the Engineering Computer Programs Library, Information Technology Laboratory, U.S. Army Engineer Waterways Experiment Station, CEWES-IM-DS.

6. Types of Deep Foundations

Deep foundations are classified with respect to displacements as large displacement, small displacement, and nondisplacement, depending on the degree to which installation disturbs the soil supporting the foundation (Table 1-2). Large displacement and small displacement piles are fabricated prior to installation and driven into the ground, while nondisplacement piles are constructed in situ and often are called drilled shafts. Augered cast concrete shafts are also identified as drilled shafts in this publication.

Table 1-2
Types of Deep Foundations

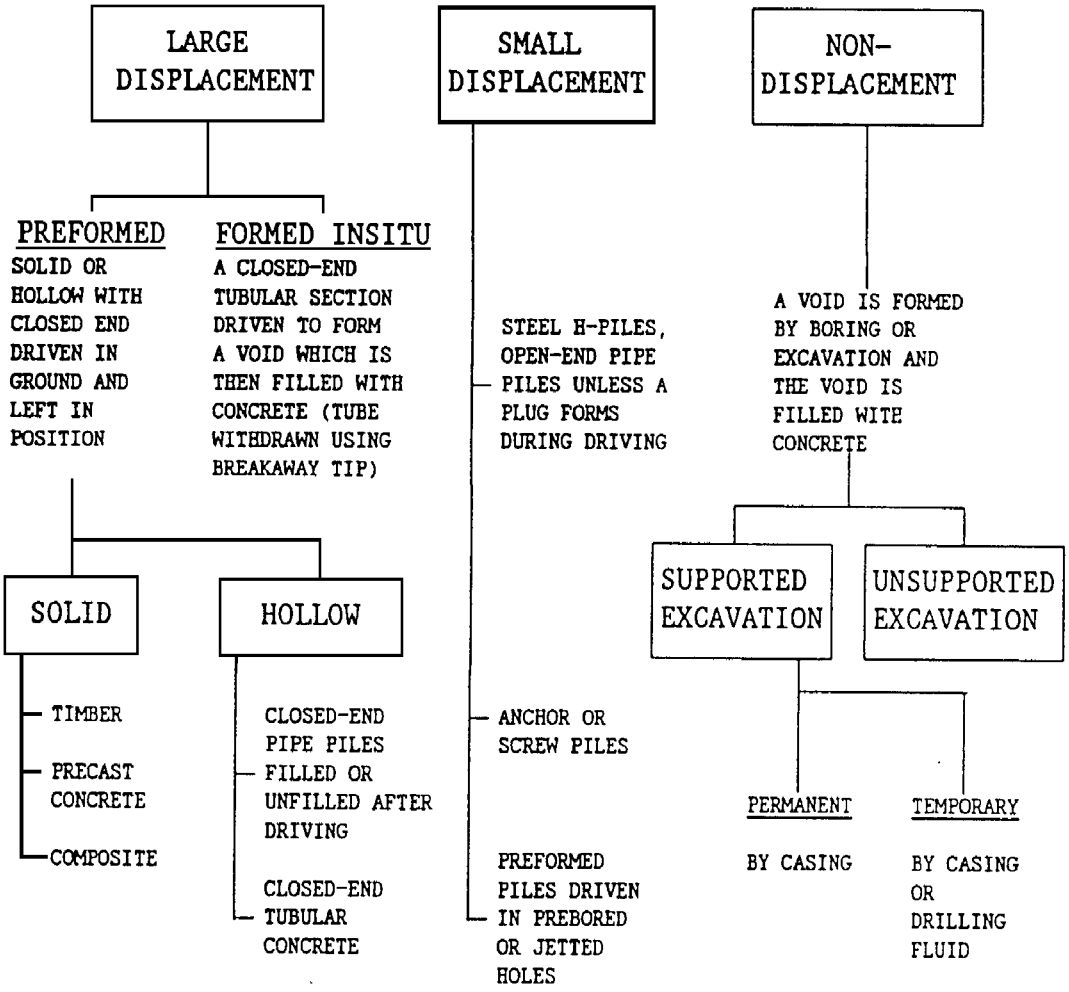

a. Large displacement piles. Driven piles are classified by the materials from which the pile is constructed, i.e., timber, concrete, or filled or unfilled steel pipe.

(1) Timber piles. These are generally used for comparatively light axial and lateral loads where foundation conditions indicate that piles will not be damaged by driving or exposed to marine borers. Overdriving is the greatest cause of damage to timber piles. Pile driving is often decided by a judgment that depends on the pile, soil condition, and driving equipment. Overdriving typically occurs when the dynamic stresses on the pile head exceed the ultimate strength of the pile. Timber piles can broom at the pile tip or head, split, or break when overdriven. Such piles have an indefinite life when constantly submerged or where cut off below the groundwater level. Some factors that might affect the performance of timber piles are the following:

(a) Splicing of timber piles is expensive and time-consuming and should be avoided. The full bending resistance of timber pile splices may be obtained by a concrete cover (Figure 1-1a) (Pile Buck Inc. 1992). Other transition splicers are available to connect timber with cast concrete or pipe piles.

(b) Tips of timber piles can be protected by a metal boot (Figure 1-1b).

(c) Timber piles are normally treated with creosote to prevent decay and environmental attack.

(d) American Society for Testing and Materials (ASTM) D 25 provides physical specifications of round timber piles. Refer to Federal Specifications TT-W-00571J, "Wood Preservation: Treating Practices," for other details.

(2) Precast concrete piles. These piles include conventionally reinforced concrete piles and prestressed concrete piles. Reinforced concrete piles are constructed with an internal reinforcement cage consisting of several longitudinal bars and lateral ties, individual hoops, or a spiral. Prestressed concrete piles are constructed using steel rods or wire strands under tension as reinforcement. Since the concrete is under continuous compression, transverse cracks tend to remain closed; thus, prestressed piles are usually more durable than conventionally reinforced piles. Influential factors for precast concrete piles include splices and steel points.

(a) Various splices are available to connect concrete piles. The splice will provide the tensile strength required during driving when the resistance to driving is low. Figure 1-2a illustrates the cement-dowel splice. Refer to "Foundations" (Pile Buck Inc. 1992) for additional splices.

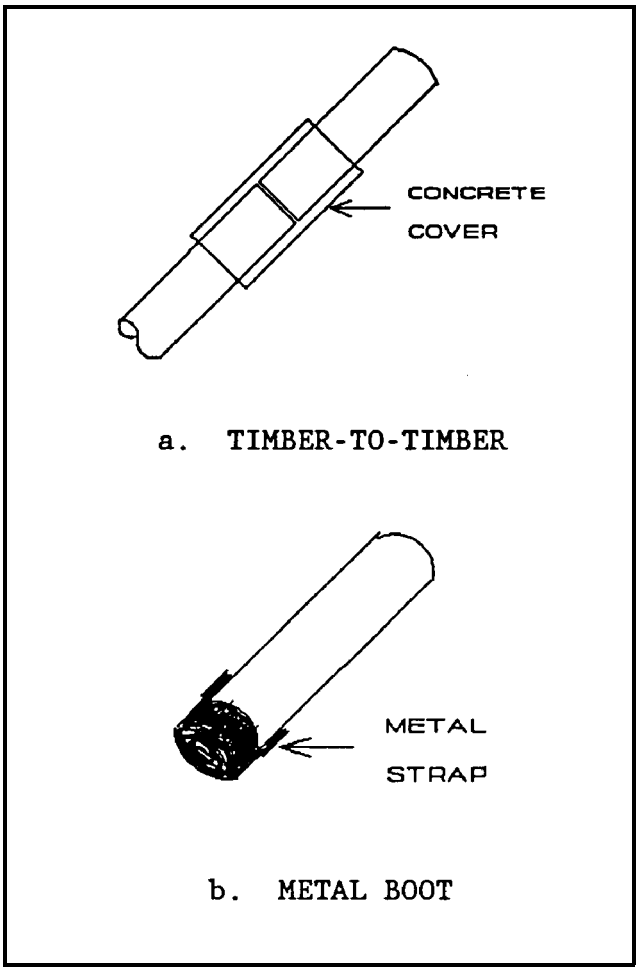

Figure 1-1. Timber pile splice and boot

(b) Special steel points can be attached to precast precast piles during casting of the piles and include steel H-pile tips or cast steel shoes (Figure 1-2).

(3) Raymond step-tapered piles. These consist of a corrugated steel shell driven into the ground using a mandrel. The shell consists of sections with variable diameters that increase from the tip to the pile head. A mandrel is a heavy, rigid steel tube shaped to fit inside the shell. The mandrel is withdrawn after the shell is driven and the shell filled with concrete. Raymond step-tapered piles are predecessors of drilled shafts and are still popular in the southern United States.

(4) Steel piles. These are generally H-piles and pipe piles. Pipe piles may be driven either "open-end" or "closed-end." Steel piles are vulnerable to corrosion, particularly in saltwater; however, experience indicates they are not

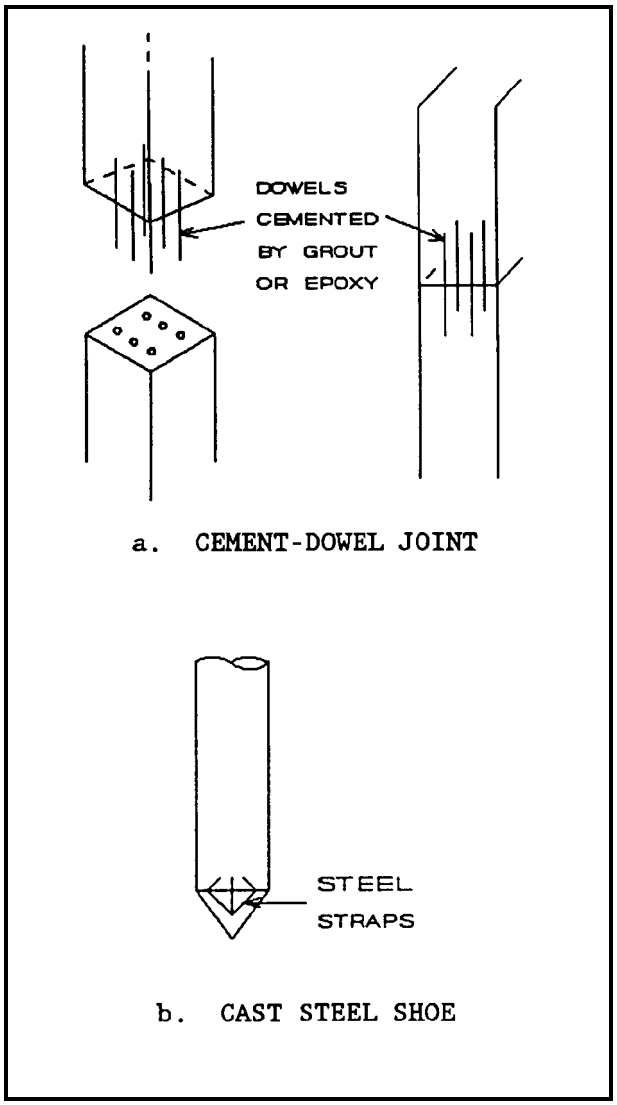

Figure 1-2. Concrete pile splice and boot

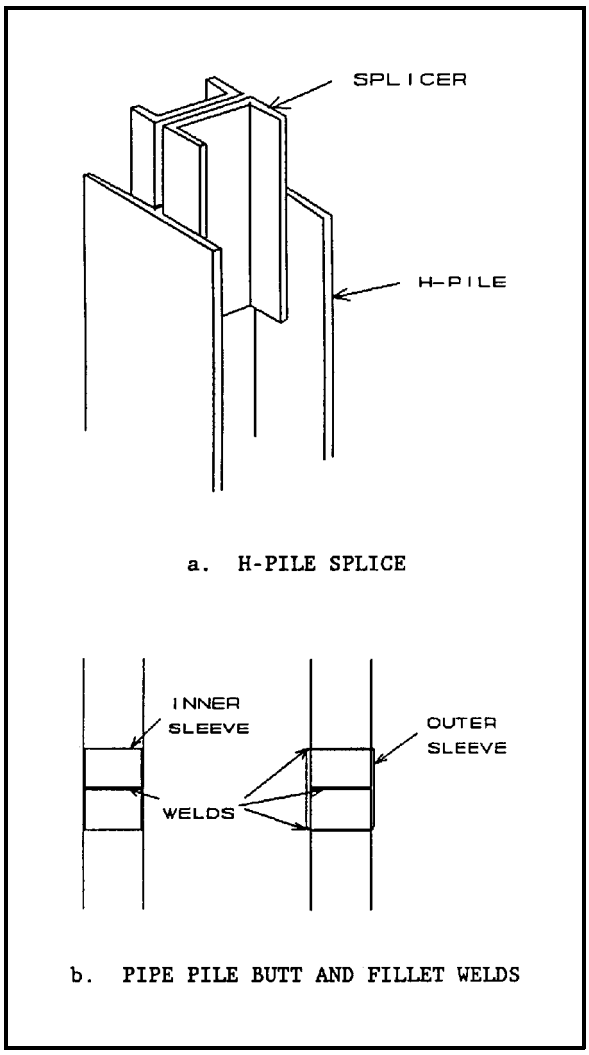

Figure 1-3. Steel pile splices

significantly affected by corrosion in undisturbed soil. Schematics of H-piles and pipe piles are presented in Figure 1-3.

(a) Steel H-piles. This type can carry larger loads, both axially and in bending, than timber piles and can withstand rough handling. H-piles can be driven into dense soil, coarse gravel, and soft rock with minimum damage, and cause minimal displacement of the surrounding soil while being driven. Hardened and reinforced pile tips should be used where large boulders, dense gravel, or hard debris may damage the pile. Splices are commonly made with full penetration butt welds or patented splicers (Figure 1-3a). H-piles can bend during driving and drift from planned location. Thus, H-piles may not be suitable when tolerance is small with respect to location and where absolute plumbness is required. Table 1-3 lists commonly available H-piles together with properties and dimensions.

(b) Steel pipe piles. Commonly used steel pipe piles are listed in Appendix B together with properties and dimensions. Steel pipe piles are generally filled with concrete after driving to increase the structural capacity. If the soil inside the pipe is removed during driving, open-end piles in cohesionless soil will cause less soil displacement and compaction, and in cohesive soils will cause less heaving of adjacent ground and nearby piles. If the soil inside the pipe is not removed during driving, the pipe becomes plugged and acts as a closed-end displacement pile. Criteria are presently unavailable for computing the depth at which a driven, open-end pile will plug. In cases where the foundation contains boulders, soft rock, or

other obstructions, the open-end pile permits inspection after removal of the plug material and ensures that the load will be transferred directly to the load-bearing stratum. Splices are commonly made by full penetration butt welds or fillet wells (Figure 1-3b) or patented splicers.

(5) Compaction piles. These are sometimes driven with the objective of increasing the density of loose, cohesionless soils and reducing settlement. Piles with a heavy taper are often most effective in deriving their support from friction.

b. Nondisplacement piles. This pile consists of a drilled shaft with a concrete cylinder cast into a borehole. Normally, the drilled shaft does not cause major displacement of the adjacent ground surface. The hole is usually bored with a short flight or bucket auger. Loss of ground could occur if the diameter of the hole is decreased because of inward displacement of soft soil or if there is caving of soil from the hole perimeter. Such unstable boreholes require stabilization by the use of slurry or slurry and casing. Drilled shafts are not subject to handling or driving stresses and therefore may be designed only for stresses under the applied service loads. Nondisplacement may be categorized as follows:

(1) Uncased shafts. Figure 1-4 illustrates a typical uncased drilled shaft with an enlarged base. The base is not perfectly flat because the shaft is drilled first, then the belling tool rotates in the shaft. Uncased shafts may be constructed in firm, stiff soils where loss of ground is not significant. Examples of uncased shaft are given in the American Concrete Institute (ACI) *Manual of Concrete Practice* (1986). Other terms used to describe the drilled shaft are "pier" or "caisson." Large shafts greater then 36 inches in diameter are often called caissons. The term "pile" is commonly associated with driven deep foundations of relatively small diameter or cross section.

(2) Cased shafts. A cased shaft is made by inserting a shell or casing into almost any type of bored hole that requires stabilization before placing concrete. Boreholes are caused where soil is weak and loose, and loss of ground into the excavation is significant. The bottom of the casing should be pushed several inches into an impervious stratum to seal the hole and allow removal of the drilling fluid prior to completion of the excavation and concrete placement. If an impervious stratum does not exist to push the casing into, the concrete can be placed by tremie to displace the drilling fluid.

(3) Drilling fluid shafts. Shafts can be installed in wet sands using drilling fluid, with or without casing. This procedure of installing drilled shafts can be used as an alternative to the uncased and cased shafts discussed previously.

(4) Pressure-grouted shafts. A special type of nondisplacement deep foundation is the uncased auger-placed grout shaft. This shaft is constructed by advancing a continuous-flight, hollow-stem auger to the required depth and filling the hole bored by the concrete grout under pressure as the auger is withdrawn. Careful inspection is required during installation, and shaft continuity should be verified by a combination of load tests and nondestructive testing as described in Chapter 6.

7. Selection of Deep Foundations

Deep foundations provide an efficient foundation system for soils that do not have a shallow, stable bearing stratum. Selection of a deep foundation requires knowledge of its characteristics and capacity.

a. Characteristics. Information adequate for reaching preliminary conclusions about types of driven piles or drilled shafts to be selected for a project is given in Table 1-4. This table lists major types of deep foundations with respect to capacity, application, relative dimensions, and advantages and disadvantages. Refer to *Foundations* (Pile Buck Inc. 1992) for additional information. Information in the table provides general guidelines in the selection of a type of deep foundation. Relevant codes and standards should be consulted with respect to allowable stresses. A cost analysis should also be performed that includes installation, locally available practices, time delays, cost of load testing program, cost of a pile cap, and other elements that depend on different types of deep foundations.

b. Capacity. Deep foundations transmit structural loads to deep strata that are capable of sustaining the applied loads. Accurate predictions of load capacity and settlement are not always possible. Adequate safety factors are therefore used to avoid excessive movement that would be detrimental to the structure that is supported and to avoid excessive stress in the foundation. Driven piles or drilled shafts are often used to resist vertical inclined, lateral, or uplift forces and overturning moments which cannot otherwise be resisted by shallow footings. These foundations derive their support from skin friction along the embedded length and by end bearing at the tip (base). Both factors contribute to the total ultimate pile capacity, but one or the other is usually dominant depending on the size, load, and soil characteristics. The capacity of deep foundation is influenced by several factors:

(1) Design limits. The limiting design criterion is normally influenced by settlement in soft and moderately stiff soil, and bearing capacity in hard soil or dense sand, and by pile or shaft structural capacity in rock.

Table 1-3
Standard H-piles; Dimensions and Properties (AISC 1969)

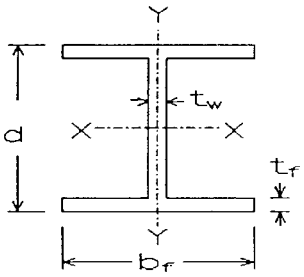

I = MOMENT OF INERTIA, $IN.^4$, mm^4
S = SECTION MODULUS, $IN.^3$, mm^3
r = RADIUS OF GYRATION, IN., mm

a. English Units

Designation	Area	Depth	Flange Width	Flange Thickness	Web Thickness	Section Properties Axis X-X			Axis Y-Y		
	A, in.²	d, in.	b_f, in.	t_f, in.	t_w, in.	I, in.⁴	S, in.³	r, in.	I, in.⁴	S, in.³	r, in.
HP14 x 117	34.4	14.21	14.885	0.805	0.805	1220	172.0	5.96	443.0	59.5	3.59
x 102	30.0	14.01	14.785	0.705	0.705	1050	150.0	5.92	380.0	51.4	3.56
x 89	26.1	13.83	14.695	0.615	0.615	904	131.0	5.88	326.0	44.3	3.53
x 73	21.4	13.61	14.585	0.505	0.505	729	107.0	5.84	261.0	35.8	3.49
HP13 x 100	29.4	13.15	13.205	0.765	0.765	886	135.0	5.49	294.0	44.5	3.16
x 87	25.5	12.95	13.105	0.665	0.665	775	117.0	5.45	250.0	38.1	3.13
x 73	21.6	12.75	13.005	0.565	0.565	630	98.8	5.40	207.0	31.9	3.10
x 60	17.5	12.54	12.900	0.460	0.460	503	80.3	5.36	165.0	25.5	3.07
HP12 x 84	24.6	12.28	12.295	0.685	0.685	650	106.0	5.14	213.0	34.6	2.94
x 74	21.8	12.13	12.215	0.610	0.610	569	93.8	5.11	186.0	30.4	2.92
x 63	18.4	11.94	12.125	0.515	0.515	472	79.1	5.06	153.0	25.3	2.88
x 53	15.5	11.78	12.045	0.435	0.435	393	66.8	5.03	127.0	21.1	2.86
HP10 x 57	16.8	9.99	10.225	0.565	0.565	294	58.8	4.18	101.0	19.7	2.45
x 42	12.4	9.70	10.075	0.420	0.420	210	43.4	4.13	71.7	14.2	2.41
HP8 x 36	10.6	8.02	8.155	0.445	0.445	119	29.8	3.36	40.3	9.88	1.95

b. Metric Units

Designation	Area	Depth	Flange Width	Flange Thickness	Web Thickness	Section Properties Axis X-X			Axis Y-Y		
	A, mm²	d, mm	b_f, mm	t_f, mm	t_w, mm	$I, 10^6 mm^4$	$S, 10^3 mm^3$	r, mm	$I, 10^6 mm^4$	$S, 10^3 mm^3$	r, mm
HP360 x 174	22200	361	378	20.4	20.4	504	2810	151	184	974	91.0
x 152	19400	356	376	17.9	17.9	439	2470	150	159	846	90.5
x 132	16900	351	373	15.6	15.6	375	2140	149	135	724	89.4
x 108	13800	346	370	12.8	12.8	303	1750	148	108	584	88.5
HP330 x 149	19000	334	335	19.4	19.4	368	2200	139	122	728	80.1
x 129	16400	329	333	16.9	16.9	315	1910	139	104	625	79.6
x 109	13900	324	330	14.4	14.4	263	1620	138	86.3	523	78.8
x 89	11300	319	328	11.7	11.7	211	1320	137	68.9	420	78.1
HP310 x 125	15900	312	312	17.4	17.4	270	1730	130	88.2	565	74.5
x 110	14100	308	310	15.5	15.4	237	1540	130	77.1	497	73.9
x 93	11900	303	308	13.1	13.1	196	1290	128	63.9	415	73.3
x 79	10000	299	306	11.0	11.0	163	1090	128	52.6	344	72.5
HP250 x 85	10800	254	260	14.4	14.4	123	969	107	42.3	325	62.6
x 62	7970	246	256	10.7	10.5	87.5	711	105	30.0	234	61.4
HP200 x 53	6820	204	207	11.3	11.3	49.8	488	85.5	16.7	161	49.5

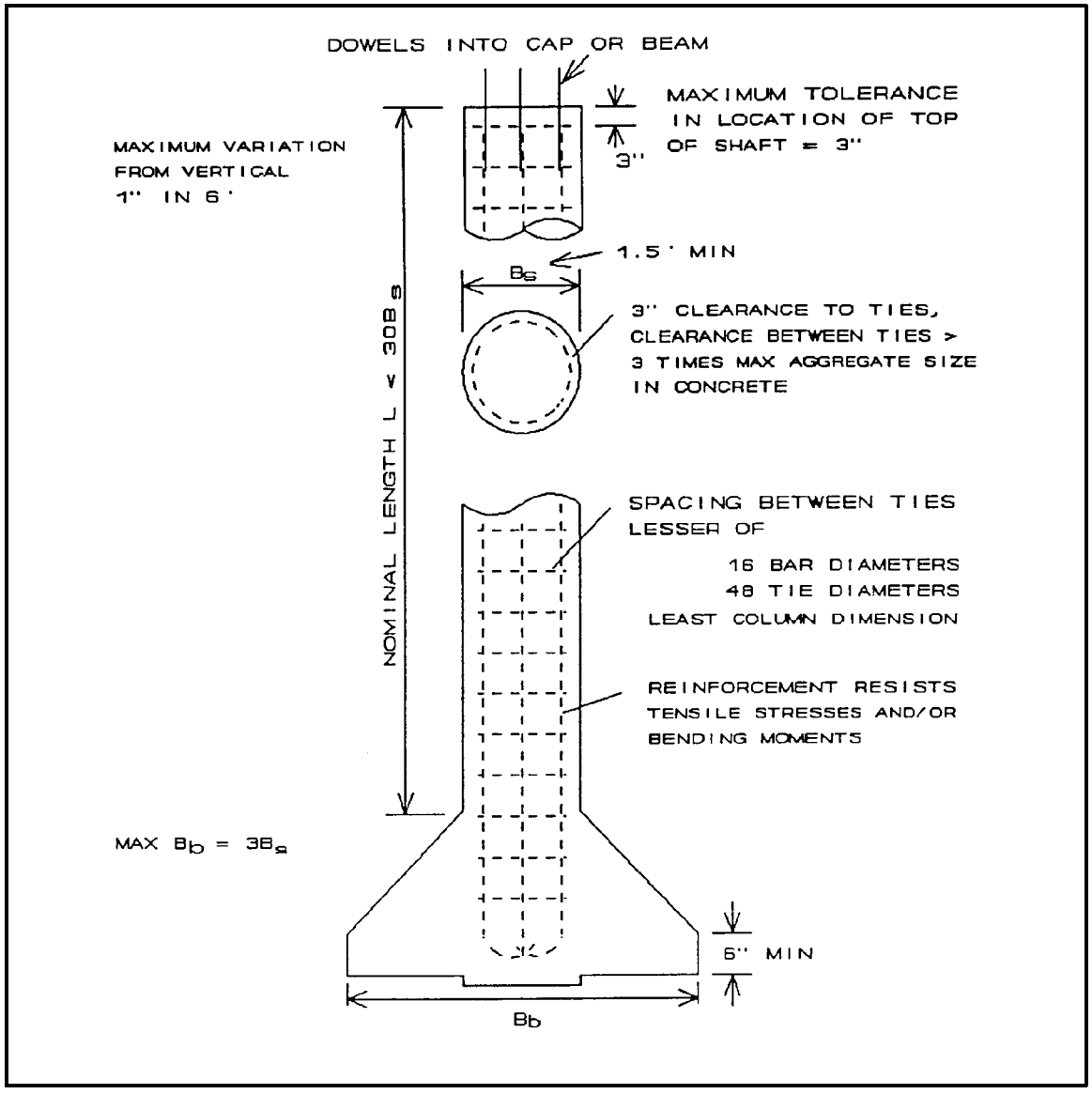

Figure 1-4. Drilled shaft details (1 in. = 25.4 mm)

(2) Skin resistance mobilization. Full skin resistance is typically mobilized within 0.5 inch of displacement, while end bearing may not be fully mobilized until displacements exceed 10 to 20 percent of the base diameter or underream for drilled shafts, unless the tip is supported by stiff clay, dense sand, or rock. Figure 1-5 illustrates an example of the vertical axial load displacement behavior of a single pile or drilled shaft. The load-displacement behavior and displacements that correspond to ultimate load are site specific and depend on the results of analyses. These analyses are given in Chapter 3.

(3) Lateral loads. Lateral load capacity of a pile or drilled shaft is directly related to the diameter, thus increasing the diameter increases the load-carrying capacity. For a drilled shaft that sustains no axial load, the cost of construction may be optimized by the selection of rigid shafts without underreams and with length/diameter ratios less than 10. The selected shaft dimensions should minimize the volume of concrete required and maximize constuction efficiency. The lateral load capacity of driven piles may be increased by increasing the number of piles

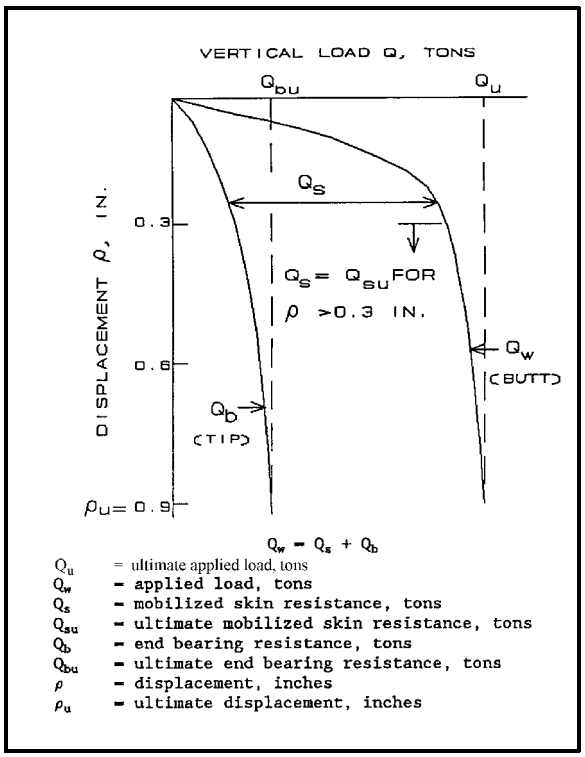

Figure 1-5. Axial-load deflection relationship

and battering piles in a pile group. Batter piles are efficient in resisting lateral loads but significantly reduce ductility of the pile group in the lateral direction, resulting in a brittle failure. Vertical piles, though less efficient in resisting lateral loads, are also less stiff and do not fail suddenly. These conflicting characteristics need to be balanced in design, and they are considered critical where seismic or dynamic lateral loads are involved.

c. Applications. Driven pile groups are typically used by the Corps of Engineers to support locks, dry docks, and other facilities constructed in river systems, lakes, lagoons, and other offshore applications. Drilled shafts typically support many permanent onshore structures such as administrative buildings, warehouses, dormitories, and clinics. Drilled shafts are divided into two groups: displacement and nondisplacement.

(1) Displacement. Driven pile foundations are usually preferable in loose, cohesionless, and soft soils, especially where excavations cannot support fluid concrete and where the depth of the bearing stratum is uncertain. Groundwater conditions can be a deciding factor in the selection of driven piles rather than drilled shafts. Uncased shafts are generally excluded from consideration where artesian pressures are present. Often more than one type of driven pile may meet all requirements for a particular structure. Driven piles according to their application are presented in Figure 1-6.

(a) Figures 1-6a and 1-6b illustrate piles classified according to their behavior as end-bearing or friction piles. A pile embedded a significant length into stiff clays, silts, and dense sands without significant end bearing resistance is usually a friction pile. A pile driven through relatively weak or compressible soil to an underlying stronger soil or rock is usually an end-bearing pile.

(b) Piles designed primarily to resist upward forces are uplift or tension piles (Figure 1-6c), and the resistance to the upward force is by a combination of side (skin) friction and self weight of the pile.

(c) Lateral forces are resisted either by vertical piles in bending (Figure 1-6d) or by batter piles or groups of vertical and batter piles (Figure 1-6e).

(d) Piles are used to transfer loads from above water structures to below the scour depth (Figure 1-6f). Piles are also used to support structures that may be endangered by future adjacent excavations (Figure 1-6g). In order to prevent undesirable movements of structures on shrink/swell soils, a pile anchored as shown in Figure 1-6h can be used.

(2) Nondisplacement. Drilled shafts are especially suitable for supporting large column loads of multistory structures and bridge abutments or piers. They are suitable for resisting large axial loads and lateral loads applied to the shaft butt (top or head) resulting from wind forces; these are also used for resisting uplift thrust applied to the shaft perimeter through soil-shaft interface friction and from heave of expansive soil. Figure 1-7 illustrates example load ranges for drilled shafts in different soils. The loads shown are for guidance only and can vary widely from site to site. Cylindrical shafts are usually preferred to underreamed ones because of ease

in construction and ease in inspection. Table 1-5 provides further details of the applications, advantages, and disadvantages of drilled shafts. Other aspects of drilled shafts include:

(a) Drilled shafts may secure much or all of their vertical load capacity from frictional side resistance (Figure 1-7a). An enlarged base using a bell or underream may also increase the vertical load capacity, provide uplift resistance to pullout loads, an resist uplift thrust from

EI 02C097
01 Jul 97

Table 1-4
Characteristics of Deep Foundations

Pile Type	Maximum Length, ft	Optimum Length, ft	Diameter Width, in.	Maximum Allowable Normal Stresses, psi	Maximum Allowable Bending Stresses, psi	Material Specifications Standards	Maximum Load tons	Optimum Load tons	Advantages	Disadvantages	Remarks
Driven Piles							150	40-100	Easy to inspect, easy to cut, resistant to deterioration, high lateral capacity, capable of being re-driven, cave-in prevented by shell	Difficult to splice, displacement pile, vulnerable to damage from hard driving	Best suited for medium-length friction pile
Cast-in-place concrete placed without mandrel	150	30-80	Butt: 12-18	Steel shell: 9,000 Concrete: 0.25 f'_c	Compression : 0.40 f'_c Tension: 0	ACI *Manual of Concrete Practice*					
Cast-in-place concrete driven with mandrel	Tapered: 40 Step tapered: 120	Tapered: 15-35 Step tapered: 40-60	Tip: 8, Butt: # 23 Step tapered: # 17	Steel: 9,000, $ 1 in. thick Concrete: 0.25 f'_c	Compression: 0.40 f'_c Tension: 0	ACI *Manual of Concrete Practice*	75	30-60	Easy to inspect, easy to cut, easy to handle, resistant to decay, high skin friction in sand, resistant to damage from hard driving	Not possible to re-drive, difficult to splice, displacement pile, vulnerable to collapse while adjacent piles are driven	Best suited for medium-length friction pile
Rammed concrete	60	---	17-26	0.25 f'_c	---	ACI *Manual of Concrete Practice*	300	60-100	Low initial cost, large bearing area, resistant to deterioration, resistant to damage from hard driving	Hard to inspect, displacement pile, not possible to form base in clay	Best suited where layer of dense sand is near ground surface
Composite	180	60-120	Depends on materials	Controlled by weakest materials	---	See Note	200	30-80	Resistant to deterioration, resistant to damage from driving, high axial capacity, long lengths at low initial cost	Hard to inspect, difficult in forming joint	Usual combinations are: cast-in-place concrete over timber or H-steel or pipe pile
Auger Cast Concrete Shafts	60	24	---	0.25 f'_c	---	ACI *Manual of Concrete Practice*	40	---	No displacement, low noise level, low vibration, low initial cost	Construction difficult when soils unfavorable, low capacities, difficult to inspect	Best suited where small loads are to be supported
Drilled Shafts	200	Shaft: # 120 Underreams: # 240	---	0.25 f'_c	---	ACI 318	Soil: 3,000 Rock: 7,000	200-400	Fast construction, high load capacity, no noise or vibration, no displacement, possible to drill through obstruction, can eliminate caps	Field inspection of construction critical, careful inspection necessary for casing method	Best suited for large axial lateral loads and small, isolated loads where soil conditions are favorable

Note: Creosote and creosote treatment: “Standards for Creosoted-Wood Foundation Piles,” C1-C12, American Wood-Preservers Institute (1977-1979)
Concrete: ACI Manual of Concrete Practice
Timber: ASTM Annual Book of Standards, Vol 04.09, D 2899, D 3200
Steel: ASTM Annual Book of Standards, Vol 01.01, Vol 01.04, A 252

heave of expansive soil. Shafts subject to pullout loads or uplift thrust must have sufficient reinforcement steel to absorb the tension load in the shaft and sufficient skin friction and underream resistance to prevent shaft uplift movements.

(b) The shaft may pass through relatively soft, compressible deposits and develop vertical load capacity from end bearing on hard or dense granular soil (Fig. 1-7b) or rock (Fig. 1-7c). End-bearing capacity should be sufficient to support vertical loads supplied by the structure as well as any downdrag forces on the shaft perimeter caused by negative skin friction from consolidating soil (Fig. 1-7b).

(c) Single drilled shafts may be constructed with large diameters, typically 10 feet or more, and can extend to depths of 200 feet or more. Drilled shafts can be made to support large loads and are seldom constructed in closely spaced groups.

(d) Drilled shafts tend to be preferred compared with driven piles as the soil becomes harder. Pile driving becomes difficult in these cases, and the driving vibration can adversely affect nearby structures. Also, many onshore areas have noise control ordinances which prohibit 24-hour pile driving (a cost impact).

(e) Good information on rock is required when drilled shafts are supported by rock. Drilled shafts placed in weathered rock or that show lesser capacity than expected may require shaft bases to be placed deeper than anticipated. This may cause significant cost overruns.

d. Location and topography. Location and topo-graphy strongly influence selection of the foundation. Local practice is usually an excellent guide. Driven piles are often undesirable in congested urban locations because of noise, inadequate clearance for pile driving, and the potential for damage caused by vibration, soil densification, and ground heave. Prefabricated piles may also be undesirable if storage space is not available. Other variables may restrict the utilization of deep foundation:

(1) Access roads with limited bridge capacity and head room may restrict certain piles and certain construction equipment.

(2) The cost of transporting construction equip-ment to the site may be significant for small, isolated structures and may justify piles that can be installed using light, locally available equipment.

e. Economy.

(1) Driven piles. Costs will depend on driving rig rental, local labor rates, fuel, tools, supplies, cost and freight of pile materials, driving resistance, handling, cutoffs, caps, splicing, and jetting. Jetting is the injection of water under pressure, usually from jets located on opposite sides of the pile, to preexcavate a hole and to assist pile penetration. Costs are also influenced by downtime for maintenance and repairs, insurance, overhead, and profit margin. An economic study should be made to determine the cost/capacity ratio of the various types of piles. Consideration should be given to including alternative designs in contract documents where practical.

(2) Drilled shafts. Drilled shafts are usually cost effective in soil above the water table and installation in cohesive soil, dense sand, rock, or other bearing soil overlaid by cohesive soil that will not cave when the hole is bored. Drilled shafts, particularly auger-placed, pressure-grouted shafts, are often most economical if the hole can be bored without slurry or casing.

*f. Length.*The length of the deep foundation is generally dependent on topography and soil conditions of the site.

(1) Driven piles. Pile length is controlled by soil conditions and location of a suitable bearing stratum, availability and suitability of driving equipment, total pile weight, and cost. Piles exceeding 300 feet have been installed offshore. Piles up to 150 feet are technically and economically acceptable for onshore installation.

(2) Drilled shafts. Shaft length depends on the depth to a suitable bearing stratum. This length is limited by the capability of the drilling equipment and the ability to keep the hole open for placement of the reinforcement steel cage and concrete.

8. Site and Soil Investigations

The foundation selected depends on functional requirements of the structure and results of the site investigation. Site investigation is required to complete foundation selection and design and to select the most efficient construction method. The first phase of the investigation is examination of site conditions that can influence foundation performance and construction methodology. The seond phase is to evaluate characteristics of the soil profile to determine the design and the construction method. These phases are accomplished bythe following:

a. Feasibility study. A reconnaissance study should be performed to determine the requiriements of a deep

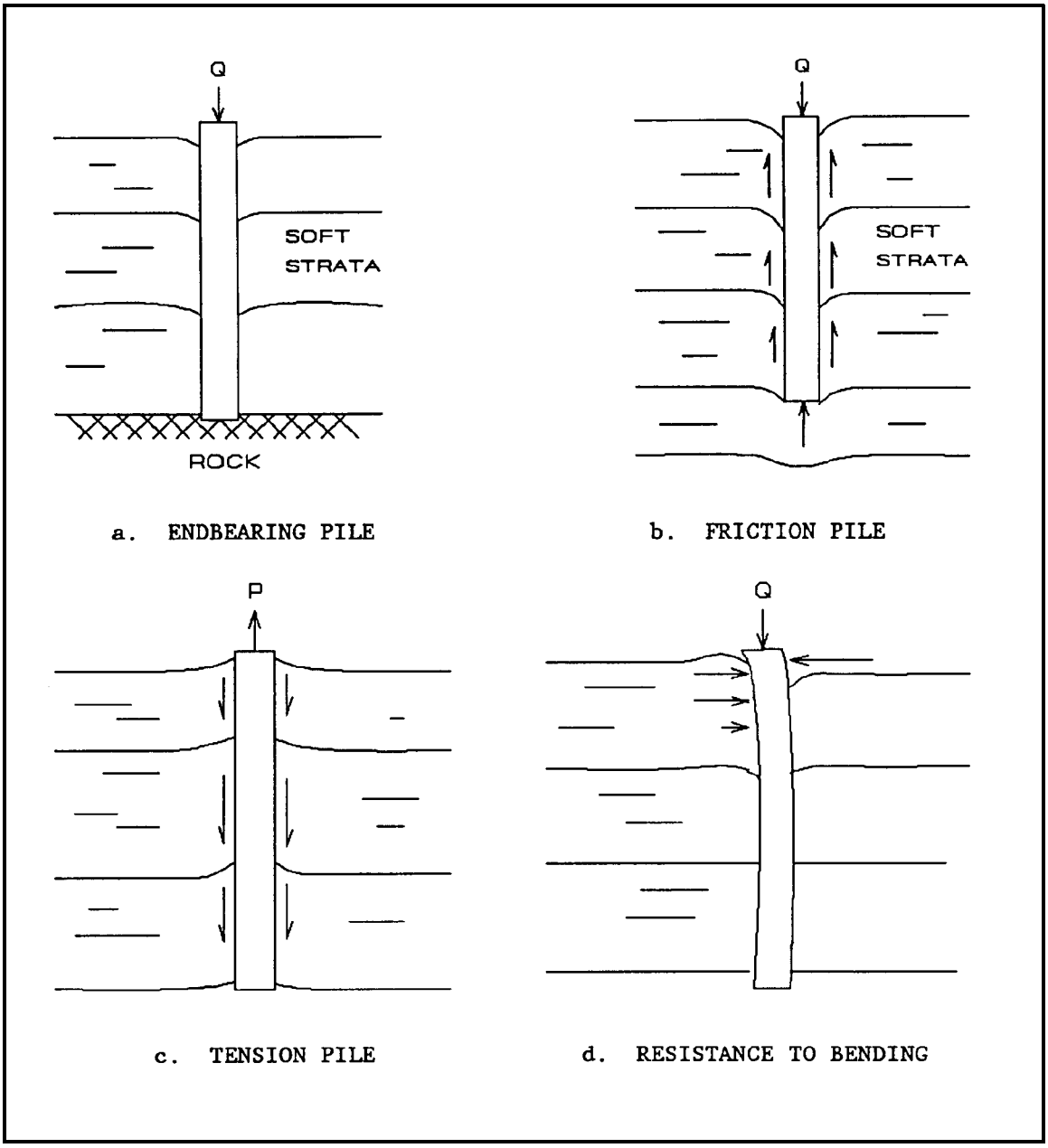

Figure 1-6. Driven pile applications (Continued)

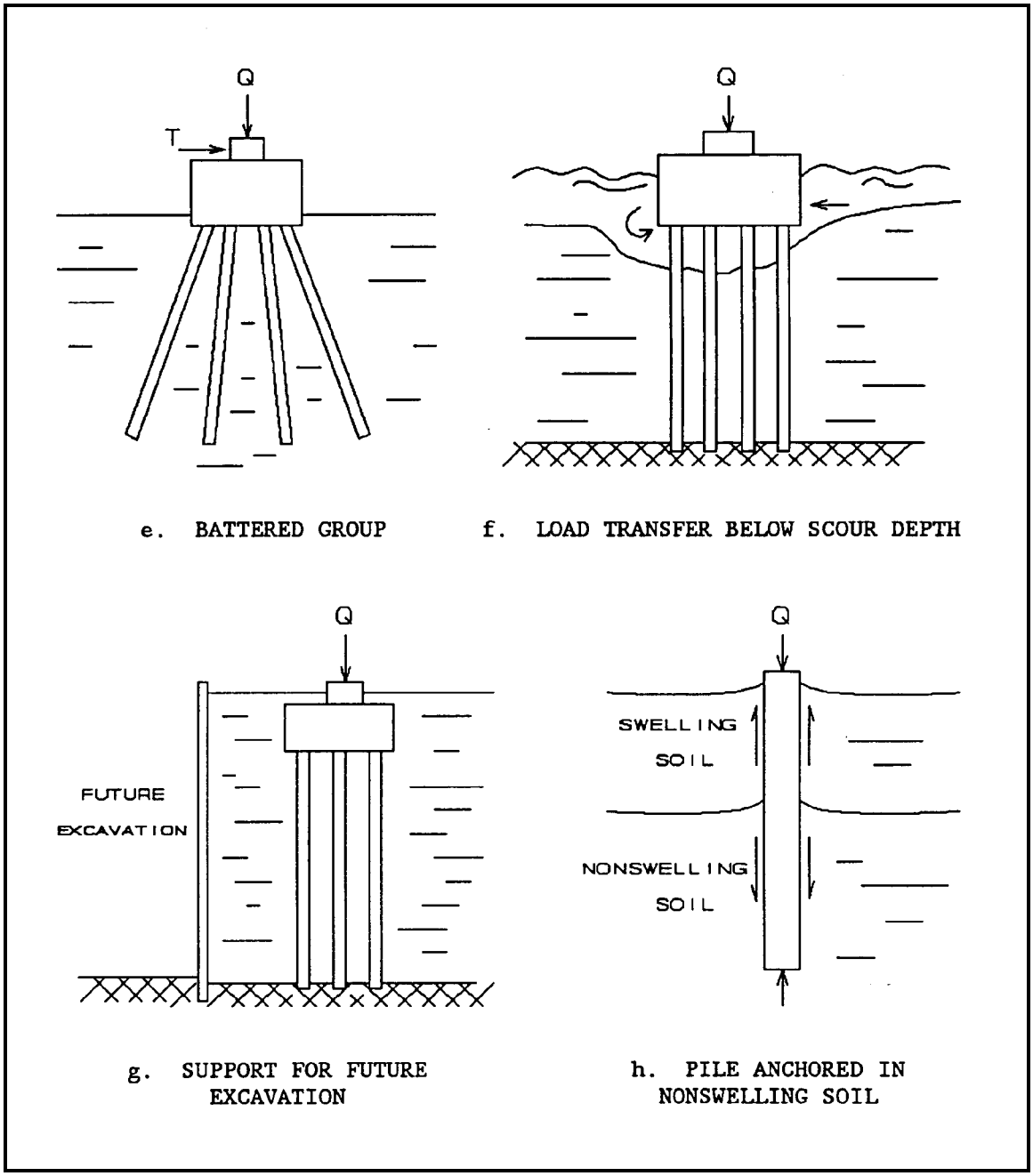

Figure 1-6. (Concluded)

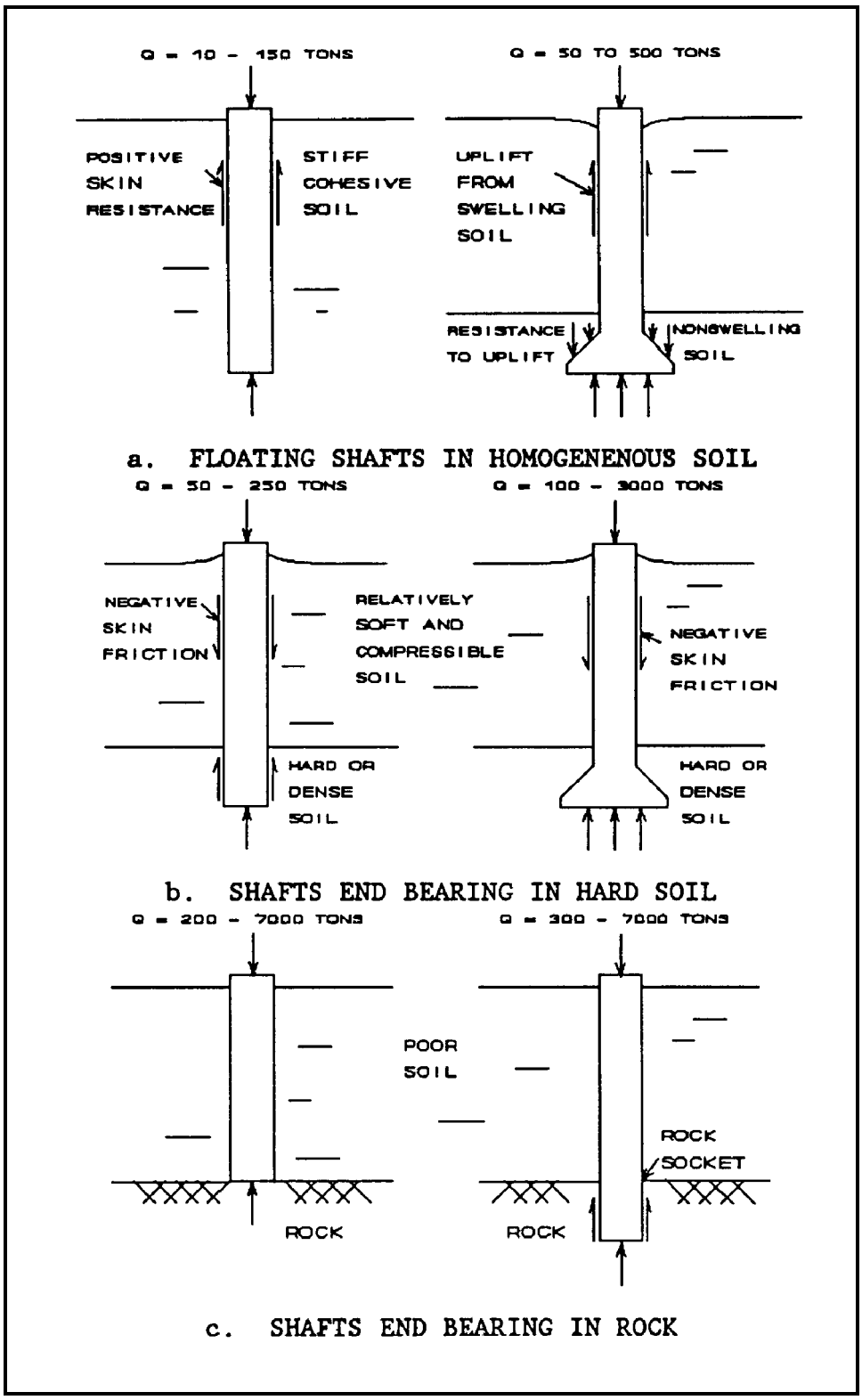

Figure 1-7. Load resistance of drilled shafts in various soils

Table 1-5
Drilled Shaft Applications, Advantages, and Disadvantages

Applications
Support of high column loads with shaft tips socketed in hard bedrock.
Support of moderate column loads with underreams seated on dense sand and gravel.
Support of light structures on friction shafts in firm, nonexpansive, cohesive soil.
Support of slopes with stability problems.
Resists uplift thrust from heave of expansive soil, downdrag forces from settling soil, and pullout forces.
Provides anchorage to lateral overturning forces.
Rigid limitations on allowable structural deformations.
Significant lateral variations in soils.
Advantages
Personnel, equipment, and materials for construction usually readily available; rapid construction due to mobile equipment; noise level of equipment less than some other construction methods; low headroom needed; shafts not affected by handling or driving stresses.
Excavation possible for a wide variety of soil conditions; boring tools can break obstructions that prevent penetration of driven piles; excavated soil examined to check against design assumption; careful inspection of excavated hole usually possible.
In situ bearing tests may be made in large-diameter boreholes; small-diameter penetration tests may be made in small boreholes.
Supports high overturning moment and lateral loads when socketed into rock.
Avoids high driving difficulties associated with pile driving.
Provides lateral support for slopes with stability problems.
Heave and settlement are negligible for properly designed drilled shafts.
Soil disturbance, consolidation, and heave due to remolding are minimal compared with pile driving.
Single shafts can carry large loads; underreams may be made in favorable soil to increase end-bearing capacity and resistance to uplift thrust or pullout forces.
Changes in geometry (diameter, penetration, underream) can be made during construction if required by soil conditions.
Pile caps unnecessary.
Disadvantages
Inadequate knowledge of design methods and construction problems may lead to improper design; reasonable estimates of performance require adequate construction control.
Careful design and construction required to avoid defective shafts; careful inspection necessary during inspection of concrete after placement difficult.

Table 1-5 (Concluded)

Disadvantages (Concluded)
Construction techniques sometimes sensitive to subsurface conditions; susceptible to "necking" in squeezing ground; caving or loss of ground in fissured or cohesionless soil.
Construction may be more difficult below groundwater level; concrete placement below slurry requires careful placement using tremie or pumping artesian water pressure can require weighting additives to drilling fluids to maintain stability; extraction of casing is sensitive to concrete workability, rebar cage placement must be done in a careful, controlled manner to avoid problems; underreams generally should be avoided below groundwater unless "watertight" formation is utilized for construction of underreams.
End-bearing capacity on cohesionless soil often low from disturbance using conventional drilling techniques.
Enlarged bases cannot be formed in cohesionless soil.
Heave beneath base of shaft may aggravate soil movement beneath slab-on-grade.
Failures difficult and expensive to correct.

foundation designs, and the scope of in situ soil and foundation load tests. Required cost estimates and schedules to conduct the soil investigation, load tests, and construction should be prepared and updated as the project progresses.

b. Site conditions. Examination of the site includes history, geology, visual inspection of the site and adjacent area, and local design and construction experience. Maps may provide data on wooded areas, ponds, streams, depressions, and evidence of earlier construction that can influence soil moisture and groundwater level. Existence of former solid waste disposal sites within the construction area should be checked. Some forms of solid waste, i.e., old car bodies and boulders, make installation of deep foundations difficult or result in unacceptable lateral deviation of driven piles. Guidance on determining potential problems of deep foundations in expansive clay is given in TM 5-818-7, "Foundations in Expansive Soils." Special attention should be payed to the following aspects of site investigation:

(1) Visual study. A visual reconnaissance should check for desiccation cracks and nature of the surface soil. Structural damage in nearby structures which may have resulted from excessive settlement of compressible soil or heave of expansive soil should be recorded. The visual study should also determine ways to provide proper drainage of the site and allow the performance of earthwork that may be required for construction.

(2) Accessibility. Accessibility to the site and equipment mobility also influence selection of construction methods. Some of these restrictions are on access, location of utility lines and paved roads, location of obstructing structures and trees, and topographic and trafficability features of the site.

(3) Local experience. The use of local design and construction experience can avoid potential problems with certain types of foundations and can provide data on successfully constructed foundations. Prior experience with and applications of deep foundations in the same general area should be determined. Local building codes should be consulted, and successful experience with recent innovations should be investigated.

(4) Potential problems with driven piles. The site investigation should consider sensitivity of existing structures and utilities to ground movement caused by ground vibration and surface heave of driven piles. The condition of existing structures prior to construction should be documented with sketches and photographs.

c. Soil investigation. A detailed study of the subsurface soil should be made as outlined in TM 5-818-1. The scope of this investigation depends on the nature and complexity of the soil, and size, functional intent, and cost of the structure. Results of the soil investigation are used to select the appropriate soil parameters for design as applied in Chapters 2 through 5. These parameters are frequently the consolidated-drained friction angle N for cohesionless soil, undrained shear strength C_u for cohesive soil, soil elastic modulus E_s for undrained loading, soil dry unit weight, and the groundwater table elevation. Refer to TM 5-818-1 for guidance on evaluating these parameters.Consolidation and potential heave characteristics may also be required for clay soils and the needed parameters may be evaluated following procedures presented in TM 5-818-7. Other tests associated with soil investigation are:

(1) In situ tests. The standard penetration test (SPT) according to ASTM D 1586 and the cone penetration test (CPT) according to ASTM D 3441 may be performed to estimate strength parameters from guidance in TM 5-818-1.

(2) Soil sampling. Most soil data are obtained from results of laboratory tests on specimens from disturbed and relatively undisturbed samples. Visual classification of soil is necessary to roughly locate the different soil strata as a function of depth and lateral variation.

(3) Location and sampling depth. Borings should be spaced to define the lateral geology and soil nonconformities. It may be sufficient to limit exploration to a depth that includes weathered and fissured material, to bedrock, or to depths influenced by construction. For individual drilled shafts, depths of at least five tip diameters beneath the tip of the deepest element of end-bearing foundations should be investigated. For driven pile groups, a much deeper investigation is appropriate and should extend a minimum of 20 feet or two pile group widths beneath the tip of the longest anticipated pile, or to bedrock, whichever is less. These depths are the minimum required to provide sufficient data for settlement analysis. The potential for settlement should be checked to ensure compliance with design specifications.

(4) Selection of soil parameters. Results of laboratory and in situ tests should be plotted as a function of depth to determine the characteristics of the subsurface soils. Typical plots include the friction angle ϕ for sands, undrained shear strength C_u for clays, and the elastic modulus E_s. These data should be grouped depending on the geological interpretation of the subsoil of similar types. Each soil type may be given representative values of strength, stiffness, and consolidation or swell indexes for estimating soil settlement or heave. Soil strength parameter could be estimated from established correlations from laboratory testing.

(a) Classification. Soil classification characteristics should be applied to estimate soil strength and other parameters from guidance in TM 5-818-1. Data such as gradation from sieve analysis, Atterberg limits, water content, and specific gravity should be determined from tests on disturbed specimens. Refer to ASTM D 2487 for soil classification procedures.

(b) Strength. Soil strength parameters are required to evaluate vertical and lateral load capacity. The strength of cohesive soil may be determined from triaxial test results performed on undisturbed soil specimens at confining pressures equal to the in situ total vertical overburden pressure σ_v. The unconsolidated undrained Q test will determine the undrained shear strength (cohesion) C_u of cohesive soils. The effective friction angle ϕ' and cohesion of overconsolidated soils may be determined from results of R tests with pore pressure measurements using a confining pressure similar to the effective overburden pressure ϕ'_v. However, analyses are usually performed assuming either cohesive or cohesionless soil. Mean strength values within the zone of potential failure may be selected for pile capacity analysis. Refer to TM 5-818-1 and NAVFAC DM-7.1, "Soil Mechanics," for further details.

(c) Elastic modulus. Young's Elastic modulus E_s is required for evaluation of vertical displacements of the deep foundation. The E_s may be estimated as the initial slope from the stress-strain curves of strength test results performed on undisturbed soil specimens. The E_s for clay may be estimated from the undrained shear strength C_u, the overconsolidation ratio, and the plasticity index (PI) shown in Figure 1-8. The E_s typically varies from 100 to 400 kips per square foot (ksf) for soft clay, 1,000 to 2,000 ksf for stiff clay, 200 to 500 ksf for loose sand, and 500 to 1,000 ksf for dense sand.

The E_s may also be estimated from results of

$$E_s = K_{cu} C_u \qquad (1\text{-}3a)$$

where

E_s = undrained elastic modulus

K_{cu} = factor relating E_s with C_u

C_u = undrained shear strength

The E_s may also be estimated from results of static cone penetration tests (Canadian Geotechnical Society 1985) as:

$$E_s = C_1 q_c \qquad (1\text{-}3b)$$

where

C_1 = constant depending on the relative compactness of cohesionless soil; i.e., C_1 = 1.5 for silts and sands, 2.0 for compact sand, 3.0 for dense sands, and 4.0 for sand and gravel

q_c = Static cone penetration resistance expressed in similar units of E_s

The E_s for cohesive soil may be estimated from the preconsolidation pressure (Canadian Geotechnical Society 1985) as:

$$E_s = C_2 P_c \qquad (1\text{-}3c)$$

where

C_2 = constant depending on the relative consistency of cohesive soils; i.e., 40 for soft, 60 for firm, and 80 for stiff clays

P_c = preconsolidation pressure, measured in similar units of E_s

(d) Lateral modulus of subgrade reaction. The modulus of horizontal subgrade reaction E_{ls} is required for evaluation of lateral displacements

$$E_{ls} = \frac{p}{y} \tag{1-4}$$

where

p = lateral soil reaction at a point on the pile per unit length, kips/ft

y = lateral displacement, ft

The E_{ls} is approximately $67C_u$ for cohesive soil (Davisson 1970), and for granular or normally consolidated clays is

$$E_{ls} = K_s Z \tag{1-5}$$

where

k_s = constant relating E_{ls} with depth z, ksf/ft

z = depth, ft

The value of k_s is recommended to be about 40, 150, and 390 ksf/ft for loose, medium, and dense dry or moist sands, respectively, and 35, 100, and 210 ksf/ft for submerged sands after FHWA-RD-85-106, "Behavior of Piles and Pile Groups Under Lateral Load." The value of k_s is also recommended to be about 500, 1,700, and 5,000 ksf/ft for stiff clays with average undrained shear strength of 1 to 2, 2 to 4, and 4 to 8 ksf, respectively. Refer to Chapter 4 for further information on E_{ls}.

(e) Consolidation. Consolidation tests using ASTM D 2435 or swell tests using ASTM D 4546 may be performed to determine preconsolidation pressure, compression and swell indexes, and swell pressures for estimating settlement and downdrag of consolidating soil and uplift forces and heave of expansive soil. Average parameters may be selected for analysis of deep foundations in consolidating or expansive soil by using the computer program Axial Load Transfer (AXILTR) (Appendix C). Refer to TM 5-818-7 for further details on the analysis of the potential heave of expansive soil.

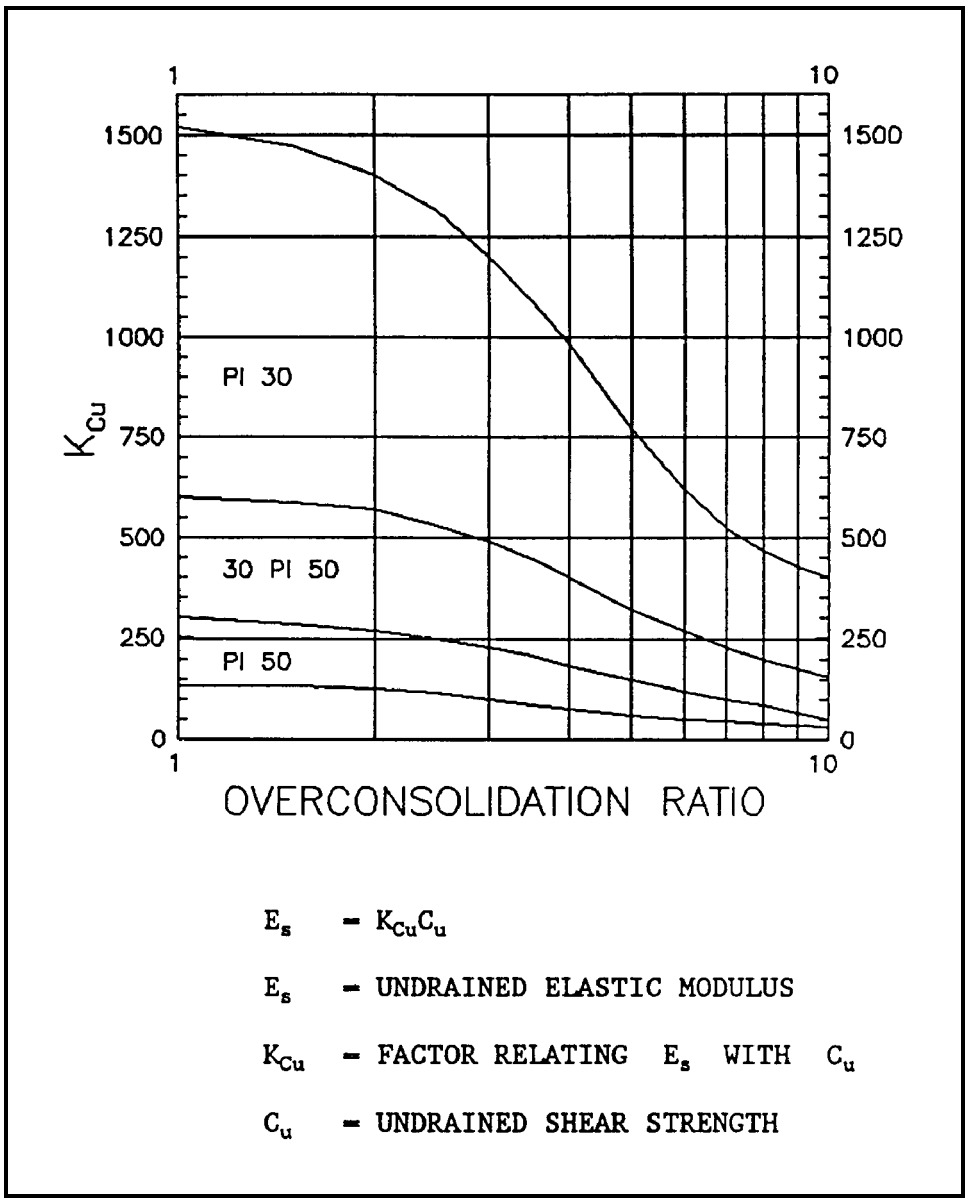

Figure 1-8. Variation K_{cu} for clay with respect to undrained shear strength and overconsolidation ratio

Chapter 2
Design Stresses

1. Constraints

The design of deep foundations is usually determined by limits specified for lateral or vertical displacement of the pile and placement tolerances. Limiting values of allowable stresses for different deep foundations are included in Table 1-4. Structural capacity rarely controls design, except when piles are founded on rock. Driven piles experience maximum stress during driving, while maximum vertical stresses in drilled shafts usually occur under static conditions.

a. Limiting deformations. Vertical and lateral live load displacements should be limited to 0.5 inch. However, operational requirements may necessitate additional restrictions. Long-term displacements may be larger than computed values due to creep. Cyclic loads and close spacings may increase displacements and should be considered in the design. Methods are presented later for the computation of displacements of deep foundations under vertical and lateral loadings.

b. Geometric constraints

(1) Driven piles. Piles are normally spaced three to four times the diameter from center to center. Typical tolerance of lateral deviation from the specified location at the butt is not more than 3 to 6 inches horizontally. The slope from vertical alignment is typically not more than 0.25 inch per foot of length for large pile groups. A deviation of ± 1 inch from the specified cutoff elevation is reasonable. Sloping land surfaces may require adjustment of the pile location if the surface varies from the reference plane used in the plans to depict pile locations. Other geometric constraints could be related to the following:

(a) Pile spacing. Bearing and lateral resistance of each pile will be reduced if piles are spaced too closely; close spacing might cause foundation heave or damage to other already driven piles. End bearing piles should usually be spaced not less than three pile diameters from center to center, while friction piles should be spaced a minimum of three to five pile diameters from center to center. Large groups of nine or more piles may be checked for pile interference using program CPGP (Wolff 1990). Methods presented later in Chapter 5 for computing the capacity of closely spaced piles may be used in a specific design to find the optimum spacing for piles of a given type.

(b) Pile batter. Batter piles are used to support structures subject to large lateral loads or for smaller lateral loads if the upper foundation stratum will not adequately resist lateral movement of vertical piles. Piles may be battered in opposite directions or used in combination with vertical piles. The axial load on a batter pile should not exceed the allowable design load for a vertical pile, and batter should not be greater than 1 horizontal to 2 vertical; the driving efficiency of the hammer decreases as the batter increases.

(c) Sweep. Specifications should include initial sweep (camber) limitations, because piles curved as a result of excessive sweep will be driven out of tolerance. Sweep for steel H-piles, for example, may be limited to 2 inches and for H-piles, up to 42 feet in length. Refer to the American Institute of Steel Construction "Manual of Steel Construction" (AISC 1989) for further information. The required number and locations of permissible pick-up points on the pile should also be clearly indicated in the specifications. Loading and unloading of long steel piles should be done by support at a minimum of two points about one-fourth of the pile length from each end of the pile. Precast concrete piles should be supported at several points.

(2) Drilled shafts. Drilled shafts are normally placed vertically and spaced at relatively large distances exceeding eight times the shaft diameter. Guidelines for placement tolerances are given in Table 2-1. Greater tolerances can be considered for drilled shafts in difficult subsoils. The additional axial and bending moments stresses caused by accidental eccentricity or batter can be calculated by methods in Chapter 4.

2. Factored Loads

The driven pile or drilled shaft in a group carrying the maximum factored load will be checked for structural failure.

a. Criterion. Calculation of the factored load from the dead and live loads on a pile or drilled shaft is given by equation 2-1:

$$F_e \, \phi_{pf} \, Q_{cap} \geq F_{DL} \, Q_{DL} + F_{LL} \, Q_{LL} \qquad (2\text{-}1)$$

where

F_e = eccentricity factor, Table 2-2

ϕ_{pf} = performance factor, Table 2-2

Q_{cap} = nominal structural capacity, kips

F_{DL} = dead load factor equals 1.35 for drilled shafts

F_{LL} = live load factors equals 2.25 for drilled shafts

Q_{DL} = dead load, kips

Q_{LL} = live load, kips

Table 2-1
Tolerances in Drilled Shaft Construction

Location of axis	Within 3 inches of the plan location
Vertical plumb or batter alignment	Within 1.5 inches for first 10 feet and 0.5 inch for each additional 10 feet of the total length; maximum 2 percent of shaft length for battered shafts
Top elevation	Not more than 1 inch above or 3 inches below the plan elevation
Cross sections of shafts and underreams	Not less than design dimensions; not more than 10 percent greater than design cross section in shrink/swell soil; underream diameter not to exceed three times the shaft diameter
Reinforcement cage	Not more than 6 inches above or 3 inches below the plan elevation; at least 3 inches of concrete cover around the cage perimeter

b. Calculation of maximum load. The maximum load on a single pile in a group or on a drilled shaft can be determined from computer or hand solutions.

(1) Computer solutions. The pile or drilled shaft carrying the maximum axial load in a group can be determined from computer program CPGA (U.S. Army Engineer Waterways Experiment Station Technical Report ITL-89-3), which computes the distribution of axial loads in a pile group for a rigid pile cap. The maximum inclined and eccentric load in a group can be determined from computer program BENT1 (U.S. Army Engineer Waterways Experiment Station Miscellaneous Paper K-75-2). The total vertical and lateral loads are input into program BENT1.

(2) Hand solutions. If all piles in a group have similar geometry, the axial load on any pile Q_{xy} of an eccentrically loaded pile group may be calculated by hand (Scott 1969)

$$Q_{xy} = Q_g \left[\frac{1}{n} + \frac{e_x X}{\Sigma x^2} + \frac{e_y Y}{\Sigma y^2} \right] \qquad (2\text{-}2)$$

where

Q_{xy} = load on a pile at a distance x and y from the centroid, kips

Q_g = total vertical load on a group of n piles at a distance e_x and e_y from the centroidal axes, Figure 2-1.

n = number of piles in the group

Σx^2 = sum of the square of the distance x of each pile from the centroid in the x direction, ft^2

Σy^2 = sum of the square of the distance y of each pile from the centroid in the y direction, ft^2

The x and y summations of the pile group in Figure 2-1 are: $\Sigma x^2 = 8 \times 1.5^2 = 18$ ft^2 and $\Sigma y^2 = 4 \times 1.5^2 + 4 \times 4.5^2 = 90$ ft^2. The pile with the maximum load is No. 4 in Figure 2-1, and it is calculated from equation 2-2

$$Q_4 = Q_g \left[\frac{1}{8} + \frac{0.8 \times 1.5}{18} + \frac{3.0 \times 4.5}{90} \right]$$
$$= Q_g \left[0.125 + 0.067 + 0.150 \right] = 0.342 Q_g$$

Pile No.5 carries the minimum load, which is a tension load

$$Q_5 = Q_g \left[\frac{1}{8} + \frac{0.8 \times (-1.5)}{18} + \frac{3.0 \times (-4.5)}{90} \right]$$
$$= Q_g \left[0.125 - 0.067 - 0.150 \right] = -0.092 Q_g$$

c. Buckling resistance. Driven piles or drilled shafts that extend above the ground surface through air or water, or when the soil is too weak to provide lateral support, may buckle under axial loads. Buckling failure may control axial load capacity of the pile.

(1) Buckling capacity. The critical buckling load Q_{cb} of partially embedded piles or drilled shafts may be estimated by (Davisson and Robinson 1965) as follows:

Table 2-2
Performance and Eccentricity Factors (Barker et al. 1991) (Copyright permission, National Cooperative Highway Research Program)

Type of Pile	Performance Factor, ϕ_{pf}	Eccentricity Factor, F_e
Prestressed concrete	Spiral columns: 0.75 Tied columns: 0.70	Spiral columns: 0.85 Tied columns: 0.80
Precast concrete	Spiral columns: 0.75 Tied columns: 0.70	Spiral columns: 0.85 Tied columns: 0.80
Steel H-piles	0.85	0.78
Steel pipe	0.85	0.87
Timber	1.20*	0.82
Drilled shafts	Spiral columns: 0.75 Tied columns: 0.70	Spiral columns: 0.85 Tied columns: 0.80

Note: ϕ_{pf} is greater than unity for timber piles because the average load factor for vertical loads is greater than the *FS*.

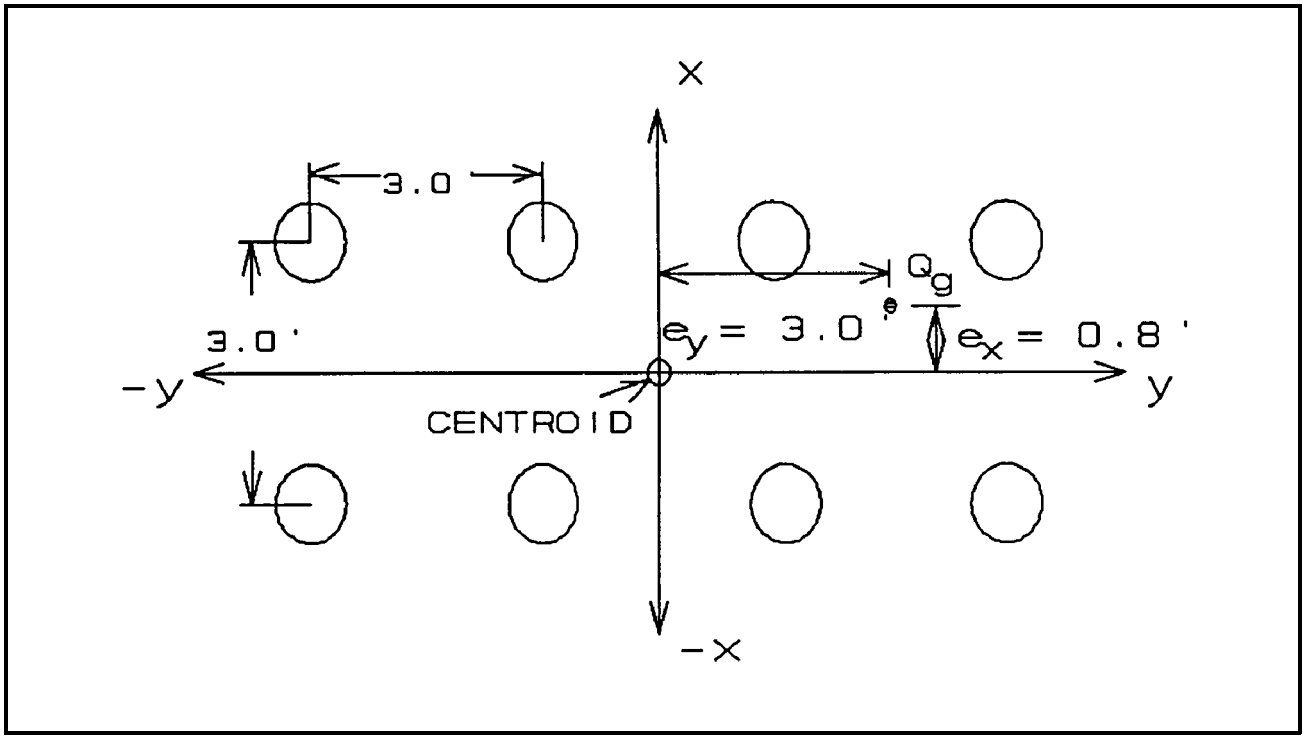

Figure 2-1. Eccentric load on a pile group

BRACED AT TOP

Rigid Cap: $Q_{cb} = \frac{4\pi^2 E_p I_p}{L_{eq}^2}$ (2-3a)

Flexible Cap: $Q_{cb} = \frac{2\pi E_p I_p}{L_{eq}^2}$ (2-3b)

UNBRACED AT TOP

Rigid Cap: $Q_{cb} = \frac{\pi^2 E_p I_p}{L_{eq}^2}$ (2-3c)

Flexible Cap: $Q_{cb} = \frac{\pi^2 E_p I_p}{4L_{eq}^2}$ (2-3d)

where

Q_{cb} = critical buckling load, kips

E_p = pile (shaft) elastic modulus, ksf

I_p = pile (shaft) moment of inertia, ft^4

L_{eq} = equivalent pile length, ft

The safe design load Q_d will be calculated using normal design procedures for columns and beam-columns when end moments and eccentricity are considered or by equation 2-1. This load will be less than Q_{cb}.

(2) Equivalent length. The equivalent length L_{eq} for long piles (where buckling may occur) can be calculated using the modulus of horizontal subgrade reaction, E_{1s}.

Constant E_{1s}: $L_{eq} = L_e + 1.4K_r$

where

$$K_r = \left(\frac{E_p I_p}{E_{1s}} \right)^{1/4} \quad (2\text{-}4a)$$

E_{1s} Increasing

Linearly with depth: $L_{eq} = L_e + 1.8K_r$

where

$$K_r = \left(\frac{E_p I_p}{K_s} \right)^{1/5} \quad (2\text{-}4b)$$

where

L_e = unsupported length extending above ground, ft

K_r = relative stiffness factor, ft

E_{1s} = modulus of horizontal subgrade reaction, ksf

k_s = constant relating E_{1s} with depth, ksf/ft

Refer to paragraph 1-7c (4)(d) for methods of estimating E_{1s}.

(3) Group effects. Adjacent piles at spacings greater than eight times the pile width or diameter have no influence on the soil modulus or buckling capacity. The E_{1s} decreases to one-fourth of that applicable for single piles when the spacing decreases to three times the pile diameter. The E_{1s} can be estimated by interpolation for intermediate spacings between piles in a group.

3. Structural Design of Driven Piles

Allowable stresses in piles should be limited to values described below for steel, concrete, and timber piles and will not exceed the factored structural capacity given by equation 2-1. Allowable stresses may be increased by 33 percent for unusual loads such as from maintenance and construction. Allowable stresses may be increased up to 75 percent for extreme loads such as accidental or natural disasters that have a very remote probability of occurrence and that require emergency maintenance following such disasters. Special provisions (such as field instrumentation, frequent or continuous field monitoring of performance, engineering studies and analyses, constraints on operational or rehabilitation activities) are required to ensure that the structure will not catastrophically fail during or after extreme loads. Figure 2-2 provides limiting axial driving stresses. Driving stresses may be calculated by wave equation analyses described in Chapter 6. Structural design in this publication is limited to steel, concrete, and timber piles.

a. Steel piles. Pile shoes should be used when driving in dense sand, gravel, cobble-boulder zones and when driving

Extended Driving and Seating Using Program GRLWEAP

Pile Material	Allowable Driving Stresses
Steel	$0.85f_y$
Reinforced Concrete	
Compression	$0.85f'_c$
Tension	500 psi
Timber	3000 psi

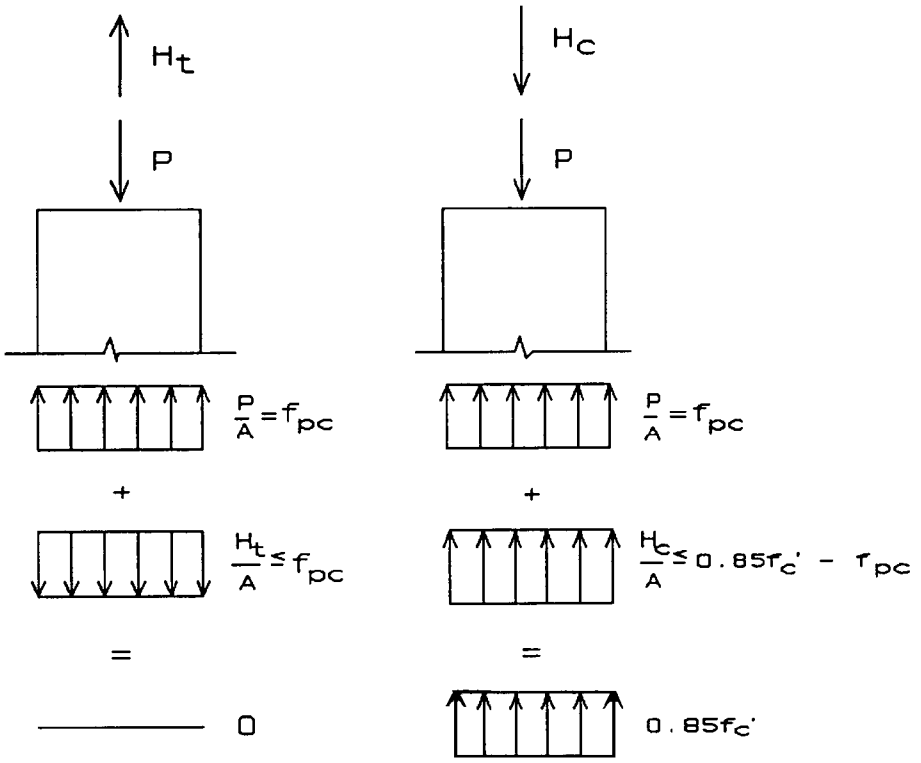

H_c = Compressive force induced by hammer, lb
H_t = Tensile force in pile during driving, lb
f_{pc} = Effective prestress after losses, psi
P = Prestressing force, lb
f'_c = 28 day concrete compressive strength, psi
f_y = Minimum steel yield strength, psi

Figure 2-2. Limits to pile driving stresses

piles to refusal on a hard layer such as bedrock. Bending is usually minimal in the lower part of the pile.

(1) The upper portion of a pile may be subject to bending and buckling as well as axial load. A higher allowable stress may be used when the pile experiences damage because the pile enters the inelastic range. This will cause some strain hardening of the steel and increase the pile load capacity. Since damage in the upper region is usually apparent during driving, a higher allowable stress is permitted.

(2) The upper portion of a pile is designed as a beam-column with consideration of lateral support. Allowable stresses for fully supported piles of A-36 steel of minimum yield strength f_y = 36 kips per square inch (ksi) are given in Table 2-3.

(a) Limits to combined bending and axial compression in the upper pile are given by

Table 2-3
Allowable Stresses for Fully Supported Piles. (English Units)

Concentric axial tension or compression in lower pile	Allowable stress, q_a, ksi (f_y = 36 ksi)
10 ksi, (1/3 × f_y × 5/6)	10
Driving shoes, (1/3) · f_y	12
Driving shoes, at least one axial load test and use of a pile driving analyzer to verify pile capacity and integrity, (1/2.5) · f_y	14.5

$$\left| \frac{f_a}{F_a} \pm \frac{f_{bx}}{F_b} \pm \frac{f_{by}}{F_b} \right| \le 1.0 \quad and \quad \frac{f_a}{F_a} \le 0.15 \qquad (2\text{-}5)$$

where

f_a = computed axial unit stress, ksi

F_a = allowable axial stress in absence of bending stress, $f_y/2$, ksi

f_y = minimum yield strength, ksi

f_{bx} = computed bending stress in x-direction, ksi

f_{by} = computed bending stress in y-direction, ksi

F_b = allowable bending stress in absence of axial stress, ksi

F_b = $0.6 \times f_y$ = 18 ksi for A-36 noncompact sections

F_b = $0.66 \times f_y$ = 20 ksi for A-36 compact sections

A noncompact section can develop yield stress in compression before local buckling occurs, but it will not resist inelastic local buckling at strain levels required for a fully plastic stress distribution. A compact section can develop a fully plastic stress distribution and possess rotation capacity of about 3 before local buckling occurs. Moment rotation capacity is $(\theta_u / \theta_p) - 1$ where θ_u is the rotation at the factored load state and θ_p is the idealized rotation corresponding to elastic theory when the moment equals the plastic moment. Refer to the ASIC Manual of Steel Construction (1989) for further information on noncompact and compact sections.

(b) Allowable stresses for laterally unsupported piles should be 5/6 of those for beam columns given by the AISC Manual of Steel Construction.

(c) A computer program for the analysis of beam columns under lateral loading, as provided in Chapter 4, may be used to compute combined stresses, taking into account all the relevant parameters.

(d) Cross sections of pipe piles may be determined from Appendix B.

(3) Allowable driving stresses are limited to $0.85f_y$, Figure 2-2.

b. Concrete piles.

(1) Prestressed concrete piles. Allowable concrete stresses should follow the basic criteria of ACI 318-89, except the strength performance factor ϕ_{pf} will be 0.7 for all failure modes and the load factors for both dead and live loads F_{DL} = F_{LL} will be 1.9. The specified load and performance factors provide an FS = 2.7 for all combinations of dead and live loads.

(a) The computed axial strength of the pile shall be limited to 80 percent of pure axial strength or the pile shall be designed for a minimum eccentricity of 10 percent of the pile width.

(b) Driving stresses should be limited as follows:

Compressive stresses: $0.85f'_c$ - effective prestress

Tensile stresses: effective prestress

(c) Cracking control in prestressed piles is achieved by limiting concrete compressive and tensile stresses under service conditions to values indicated in Table 2-4.

(d) Permissible stresses in the prestressing steel tendons should be in accordance with ACI 318-89.

Table 2-4
Allowable Concrete Stresses, Prestressed Concrete Piles

Uniform Axial Tension	0
Bending (extreme fiber)	
Compression	$0.45 \times f'_c$
Tension	0
Combined axial load and bending, the concrete stresses should be proportioned so that:	$f_a + f_b + f_{pc} \leq 0.4 \times f'_c$ $f_a - f_b + f_{pc} \geq 0$

where tension is negative for

f_a = computed axial stress, ksi
f_b = computed bending stress, ksi
f_{pc} = effective prestress, ksi
f'_c = concrete compressive strength, ksi

(e) Minimum effective prestress of 700 psi compression is required for piles greater than 50 feet in length. Excessively long or short piles may necessitate deviation from the minimum effective stress requirement.

(f) Strength interaction diagrams for prestressed concrete piles may be developed using computer program CPGC (WES Instruction Report ITL-90-2).

(2) Reinforced concrete piles. These piles will be designed for strength in accordance with ACI 318-89, except that the axial compression strength of the pile shall be limited to 80 percent of the ultimate axial strength or the pile shall be designed for a minimum eccentricity equal to 10 percent of the pile width. Strength interaction diagrams for reinforced concrete piles may be developed using the Corps computer program CASTR (U.S. Army Engineer Waterways Experiment Station Instruction Report ITL-87-2).

(3) Cast-in-place and Mandrel-driven piles. For a cast-in-place pile, the casing is top driven without the aid of a mandrel, typically using casing with wall thickness ranging from 9 gauge to 1/4 inch.

(a) Casing must be of sufficient thickness to withstand stresses due to the driving operation and to maintain the pile cross section. Casing thickness for mandrel-driven piles is normally 14 gauge.

(b) Cast-in-place and mandrel-driven piles should be designed for service conditions and stresses limited to those values listed in Table 2-5.

(c) Allowable compressive stresses are reduced from those recommended by ACI 543R-74 as explained for prestressed concrete piles.

(d) Cast-in-place and mandrel-driven piles will be used only when full embedment and full lateral support are assured and for loads that produce zero or small end moments so that compression always controls. Steel casing will be 14 gauge (U.S. Standard) or thicker, be seamless or have spirally welded seams, have a minimum yield strength of 30 ksi, be 16 inches or less in diameter, not be exposed to a detrimental corrosive environment, and not be designed to carry any working load. Items not specifically addressed will be in accordance with ACI 543R-74.

c. Timber piles. Representative allowable stresses for pressure-treated round timber piles for normal load duration in hydraulic structures are given in Table 2-6.

(1) Working stresses for compression parallel to the grain in Douglas Fir and Southern Pine may be increased by 0.2 percent for each foot of length from the tip of the pile to the critical section. An increase of 2.5 psi per foot of length is recommended for compression perpendicular to the grain.

(2) Values for Southern Pine are weighted for longleaf, ash, loblolly, and shortleaf.

(3) Working stresses in Table 2-6 have been adjusted to compensate for strength reductions due to conditioning and treatment. For piles, air-dried or kiln-dried before pressure treatment, working stresses should be increased by dividing the tabulated values as follows:

Pacific Coast Douglas Fir: 0.90

Southern Pine: 0.85

(4) The *FS* for allowable stresses for compression parallel to the grain and for bending are 1.25 and 1.3, respectively (International Conference of Building Officials 1991).

Table 2-5
Cast-in-Place and Mandrel-driven Piles, Allowable Concrete Stresses

Uniform axial compression	
Confined	0.33 × f'_c
Unconfined	0.27 × f'_c
Uniform axial tension	0
Bending (extreme fiber)	
Compression	0.40 × f'_c
Tension	0

Combined axial loading and bending

$$\left| \frac{f_a}{F_a} + \frac{f_b}{F_b} \right| \leq 1.0$$

where

f_a = computed axial stress, ksi
F_a = allowable axial stress, ksi
f_b = computed bending stress, ksi
F_b = allowable bending stress, ksi

Note: Participation of steel casing or shell is disallowed.

Table 2-6
Allowable Stresses for Pressure-treated Round Timber Piles for Normal Loads in Hydraulic Structures

	Allowable Stresses, psi	
	Pacific Coast Douglas Fir	**Southern Pine**
Compression parallel to grain, F_a	875	825
Bending, F_b	1,700	1,650
Horizontal shear	95	90
Compression perpendicular to grain	190	205
Modulus of elasticity	1,500,000	1,500,000

d. Design example. A 30-foot length L of A-36 unbraced H-pile, HP14 × 73, has a cross section area A_y = 21.4 in.^{2}, Table 1-3. This pile is made of A-36 steel with f_y = 36 ksi, E_p = 29,000 ksi, and $_pI$ = 729 in.^{4} for the X-X axis and 261 in.^{4} for the Y-Y axis. Dead load Q_{DL} = 40 kips and live load Q_{LL} = 60 kips. Load factors F_{DL} = 1.3 and F_{LL} = 2.17. Free-standing length above the ground surface is 10 feet. The soil is a clay with a constant modulus of horizontal subgrade reaction E_{1s} = 1 ksi. Spacing between piles is three times the pile width.

(1) Design load. The applied design load per pile Q_d from equation 2-1 is

$$Q_d = F_{DL} Q_{DL} + F_{LL} Q_{LL}$$

$$= 1.3 \times 40 + 2.17 \times 60 = 182.2 \text{ kips}$$

(2) Structural capacity. The unfactored structural capacity Q_{cap} is $f_y A_y$ = 36 × 21.4 = 770.4 kips. From Table 2-1, ϕ_{pf} = 0.85 and F_e = 0.78. The factored structural capacity is $F_e\phi_{pf}Q_{cap}$ = 0.78 × 0.85 × 770.4 = 508.4 kips > Q_d = 182.2 kips. Table 2-3 indicates that the allowable stress q_a = 10 ksi. $q_a A_y$ = 10 × 21.4 = 214 kips > $_dQ$ = 182.2 kips.

(3) Buckling capacity. A flexible cap unbraced at the top is to be constructed for the pile group. The E_{1s} = (1/4) × 1 ksi = 0.25 ksi because the spacing is three times the pile width. The equivalent length L_{eq} for the constant E_{1s} = 0.25 ksi from equation 2-4a for the minimum I_p of the X-X axis is

$$K_r = \left(\frac{E_p I_p}{E_{1s}} \right)^{1/4} = \left(\frac{29{,}000 \times 261}{0.25} \right)^{1/4} = 131.5 \text{ in.}$$

$$L_{eq} = L_e = 1.4 K_r = 10 \times 12 = 1.4 \times 131.5 = 304.1 \text{ in.}$$

The minimum critical buckling load Q_{cb} from equation 2-3d is

$$Q_{cb} = \frac{\pi^2 E_p I_p}{4 L_{eq}^2}$$

$$= \frac{9.87 \times 29{,}000 \times 261}{4 \times (304.1)^2} = 201 \text{ kips}$$

The Q_{cb} = 201 kips > Q_d = 182.2 kips. Buckling capacity is adequate.

Table 2-7
Minimum Requirements for Drilled Shaft Design

a. Nomenclature

Symbol	Description
A_c	Cross-sectional area of concrete within spiral or cage, inches^2
A_g	Gross area of the shaft section, inches^2
A_s	Area of reinforcement steel, inches^2
A_{sp}	Cross-sectional area of spirals or cage, inches^2
B_s	Shaft outside diameter, inches
Cover	Concrete cover over longitudinal steel, in.
d_b	Bar diameter, in.
d_t	Tie diameter, in.
d_{sp}	Spiral diameter, in.
D_m	Mean diameter of the equivalent steel ring, $B_s - 2(\text{Cover} + r_s)$, in.
e	Eccentricity, M_{max}/Q_w, in.
F_{DL}	Dead load factor to protect against material failure
F_{LL}	Live load factor to protect against material failure
FS	Factor of safety to limit vertical displacement in the foundation soil
f'_c	Ultimate concrete compressive strength, psi
f_y	Yield strength of reinforcement steel, psi
L_{sp}	Length of spiral in one path, in.
M_{max}	Maximum bending moment, lb-in.
N	Number of bars
pitch	Distance from any point of a spiral cage to the adjacent point on the cage measured parallel with the longitudinal axis of the cage
P_{max}	Maximum uplift thrust or pullout force, lb
Q_{ap}	Dependable axial load capacity of the shaft determined by $\phi_{pf}[0.85 \cdot f'_c(A_g - A_s) + A_s f_y]$, lb
Q_{DL}	Dead load, lb
Q_{LL}	Live load, lb
Q_{md}	Maximum downdrag force, lb
Q_w	Maximum factored axial load, lb
R_d	Diameter ratio of reinforcement steel, D_m/B_s
R_s	Ratio of reinforcement steel area to gross area, A_s/A_g
r_s	Radius of reinforcement steel, in.
S_t	Tie spacing, in.
T_{max}	Maximum applied lateral load, lb
v_{max}	Maximum applied shear stress, V_{max}/A_g
V_{max}	Maximum applied shear force, $T_{max}F_{LL}$
ρ_{sp}	Volumetric ratio of spiral reinforcement required
ϕ_{pf}	Capacity performance factor, 0.70 for a tied column of reinforcement steel 0.75 for a spiral column after ACI SP-17(1985)

(Sheet 1 of 3)

Table 2-7 (Continued)

b. Procedure

Step	Description
1	Determine that Q_w is well within Q_{cap}.

$$Q_{cap} > Q_w$$
$$Q_{cap} = \phi_{pf}[0.85 \cdot f'_c(A_g - A_s) + A_s f_y]$$
$$Q_w = F_{DL}Q_{DL} + F_{LL}Q_{LL}$$

For a shaft in compressible soil, evaluate downdrag force Q_{sd} (Chapter 3) and add to Q_w. For a shaft in expansive soil, evaluate uplift thrust P_{max} (negative, tensile force) and calculate the required reinforcement area from

$$A_s = -\frac{P_{max}}{\phi_{pf} f_y}$$

Percent steel for f_y = 60,000 psi is approximately $-0.003P_{max}/B_s^2$

2 Determine $v_{max} \leq 10 \cdot (f'_c)^{1/2}$.

3 Compute eccentricity e from given M_{max} and Q_w of the specifications, or 2 in. or $0.1B_s$, whichever is greater for tied columns or 1 in. or $0.05B_s$ for spiral columns of reinforcement steel. M_{max} may also be evaluated from lateral load analysis described in Chapter 4. Calculate eccentricity ratio e/B_s.

4 Calculate D_m. Estimate R_s from the trial ring of reinforcement steel.

5 Determine by interpolation steel ratio R_s from design charts in ACI SP-17, Vol I. If R_s < 1 percent, increase R_s to 1 percent. If R_s > 8 percent, increase the shaft diameter and repeat the above steps.

6 Select the actual steel reinforcement; i.e., size and number of bars. 6 bars minimum, 6 inches spacing maximum. Check for sufficient spacing for flow of concrete, spacing = $(\pi D_m - N d_b)/N$

7 Calculate R_s for the designed shaft cross section and check it against R_s assumed in step 4. Repeat steps 4 and 6 if the assumed R_s is significantly different from the calculated R_s.

8 Select appropriate ties or spirals to construct the reinforcement cage according to ACI 318-89 requirements or AASHTO specifications.

Ties (ACI): Vertical spacing shall not exceed the lesser of
(1) $S_t = 16d_b$
(2) $S_t = 48d_t$
(3) $S_t = B_s$

No. 3 ties may be used for longitudinal bars < No. 11; No. 4 or larger ties will be used for No. 11 bars or larger

Spirals (ACI):

$$\rho_{st} = 0.45\left(\frac{A_g}{A_c} - 1\right)\frac{f'_c}{f_y}$$
$$L_{st} = \sqrt{\pi (d_{st} + d_t)^2 + pitch^2}$$
$$A_{sp} = \frac{\rho_{st} \cdot pitch \cdot A_c}{L_{st}}$$

Table 2-7 (Concluded)

c. Example calculation of steel reinforcement for a tied reinforcement cage

Step	Calculation

1 Input parameters:

T_{max} = 10,000 lb	Cover = 3 in.	f'_c = 3,000 psi
Q_{DL} = 500,000 lb	B_s = 30 in.	f_y = 60,000 psi
Q_{LL} = 500,000 lb	F_{DL} = 1.35	M_{max} = $8 \cdot 10^6$ lb-in.
	F_{LL} = 2.25	ϕ_{pf} = 0.70

Assume initital R_t = 2 percent. Calculate $A_g = \pi B_s^2/4$ = 706.86 in.^{2}. Initial estimate of $A_s = 0.02 \cdot A_g$ = 14.14 inches. Fifteen No. 8 bars will be required for the initial estimate of steel reinforcement with r_s = 0.5 inch as shown in the sketch.

Q_w = $1.35 \cdot 500{,}000 + 2.25 \cdot 500{,}000$ = 1,800,000 lb

Q_{cap} = $0.7[0.85 \cdot 3{,}000(706.86 - 14.14) + 14.14 \cdot 60{,}000\}$ = 1,830,385 lb

1,830,385 > Q_w = 1,800,000 lb; Q_{cap} is adequate

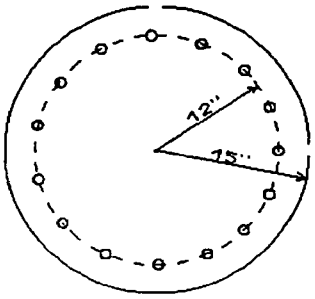

2 $v_{max} = T_{max}F_{LL}/A_g = 10{,}000 \cdot 2.25/706.86$ = 31.83 psi
$\leq 10 \cdot (f'_c)^{1/2}$

$10 \cdot (f'_c)^{1/2} = 10 \cdot (3{,}000)^{1/2}$ = 547.7 psi
Therefore, $v_{max} \leq 10 \cdot (f'_c)^{1/2}$

3 $e/B_s = M_{max}/(Q_w B_s) = 8 \cdot 10^6/(787{,}500 \cdot 30)$ = 0.339

4 $D_{sp} = B_s - 2(\text{Cover} + r_s)$ = 30 − 2(3 + 0.5) = 23 in.
R_d = 23/30 = 0.767

5 Determine R_t by interpolation from design charts, ACI SP-17 (85):
Therefore, R_t = 0.023 for R_d = 0.767

R_d	R_t
0.7	0.026
0.8	0.021

6,7 A_s = 0.023 · 706.86 = 16.26 in.^{2}

Spacing between bars:
- 21 No. 8 bars (A_s = 21 · 0.79 = 16.59 in^2, d_b = 1.000 inch):
  spacing = $(\pi \cdot 23 - 21 \cdot 1.000)/21$ = 2.44 in.
- 17 No. 9 bars (A_s = 17 · 1.00 = 17.00 in^2, d = 1.128 inch):
  spacing = $(\pi \cdot 23 - 17 \cdot 1.128)/17$ = 3.12 in.
- 13 No. 10 bars (A_s = 13 · 1.27 = 16.51 in.^{2}, d = 1.270 inch):
  spacing = $(\pi \cdot 23 - 13 \cdot 1.127)/13$ = 4.43 in.

17 No. 9 bars will be adequate assuming 1 inch maximum aggregate and spacing of at least 3 times the maximum aggregate size

8 Ties: (1) S_t = 16 · 1.000 = 16 in.
(2) S_t = 48 · 0.375 = 18 inches for No. 3 tie
(3) S_t = 30 in.
Select No. 3 bars at 16 inches center to center spacing

Spirals: (standard spiral sizes are 3/8, 1/2 and 5/8 inch; select 1/2 inch spiral size and 3-inch pitch)

A_g = 706.9 inches^2 $A_c = \pi \cdot 12^2$ = 452.4 inches^2
$\rho_s = 0.45 \cdot [(706.9/452.4) - 1] \cdot 3{,}000/60{,}000$ = 0.0152
$L_s = \{[\pi \cdot (24 + 0.5)]^2 + 3^2\}^{1/2}$ = 77 in.
$A_{sp} = \rho_s \cdot \text{pitch} \cdot A_c/L_s = 0.0152 \cdot 3 \cdot 452.4/77$ = 0.268 inches^2
Select No. 5 spiral at 3-inch pitch

(Sheet 3 of 3)

4. Structural Design of Drilled Shafts

Most drilled shaft foundations will be subject to lateral loads, bending moments, and shear stresses in addition to compressive stresses from vertical loads. Eccentrically vertical applied loads can generate additional bending moments.

a. Eccentricity. If bending moments and shears are not specified, the minimum eccentricity should be the larger of 2 inches or $0.1B_s$, where B_s is the shaft diameter, when tied cages of reinforcement steel are used and 1 inch or $0.05B_s$ when spiral cages are used. The minimum eccentricity should be the maximum permitted deviation of the shaft out of its plan alignment that does not require special computations to calculate the needed reinforcement if larger eccentricities are allowed.

b. Design example. Table 2-7 describes evaluation of the shaft cross section and percent reinforcement steel required for adequate shaft strength under design loads.

(1) The maximum bending moment, M_{max}, is required to determine the amount of reinforcement steel to resist bending. The maximum factored vertical working load, Q_w, and the estimate of the maximum applied lateral load, T_{max}, are used to calculate M_{max} . The full amount of reinforcing steel is not required near the bottom of the pile because bending moments are usually negligible near the pile bottom. Chapter 4 discusses procedures for calculating the distribution of bending moments to determine where steel will be placed in the pile.

(2) Load factors are applied to the design live and dead loads to ensure adequate safety against structural failure of the shaft. An example is worked out in Table 2-7c for F_{DL} = 1.35 and F_{LL} = 2.25 for a shaft supporting a bridge column.

(3) The minimum reinforcement steel, normally recommended, is 1 percent of the total cross-sectional area of drilled shaft expected to be exposed along their length by scour or excavation. Reinforcement steel should be full length for shafts constructed in expansive soil and for shafts requiring casing while the hole is excavated. Shaft diameter should be increased if the reinforcement steel required to resist bending such that adequate voids through the reinforcement cage will be provided to accommodate the maximum aggregate size of the concrete.

(4) The maximum applied axial load should also include maximum downdrag forces for a shaft in compressible soil and the maximum uplift thrust for a shaft in expansive soil. Uplift thrust may develop before the full structural load is applied to the shaft. Under such conditions, smaller amounts of reinforcement may be used if justified on the basis of relevant and appropriate computations.

Chapter 3
Vertical Loads

1. Design Philosophy

Analyses are performed to determine the diameter or cross section, length and number of driven piles or drilled shafts required to support the structure, and for procuring the correct materials and equipment to construct the foundation.

a. Type of loads. Loads applied to deep foundations consist of vertical forces and horizontal forces. These forces are resisted by the soil through bearing and friction. Therefore, the pile capacity analysis should be performed to determine that foundation failure by bearing or friction will be avoided, and load-displacement analysis performed to determine that foundation movements will be within acceptable limits.

(1) Load distribution. Loads on a deep foundation are simulated by a vertical force Q and a lateral force T, Figure 3-1. These vertical and horizontal forces are considered separately and their individual effects are superimposed. Unusual cross sections should be converted to a circular cross section for analysis when using computer programs such as CAXPILE (WES Instruction Report K-84-4) or AXILTR (Appendix C). Analysis for lateral loads is treated separately and given in Chapter 4.

(2) Construction influence. Construction methods, whether for driven piles or drilled shafts, influence pile capacity for vertical loads through soil disturbance and pore pressure changes.

(a) Driving resistance. A wave equation analysis shall be performed for driven piles to estimate the total driving resistance that will be encountered by the pile to assist in determining the required capability of the driving equipment. Refer to Chapter 6 for further details.

(b) Structural capacity. Total stresses that will be generated in the deep foundation during driving or by vertical and lateral loads will be compared with the structural capacity of the foundation. Structural capacity may be calculated by procedures in Chapter 2.

b. Analysis of vertical loads. The design philosophy for resisting vertical load is accomplished by calculating the ultimate pile capacity Q_u to determine the load to cause a bearing failure, then using FS to estimate the allowable pile capacity Q_a that can limit the settlement to permissible levels. Settlement of the individual piles or drilled shafts shall be calculated as presented later in this chapter, however settlement of a group of piles or drilled shafts shall be evaluated as given in Chapter 5. Table 3-1 illustrates this procedure.

(1) Ultimate pile capacity. Applied vertical loads Q (Figure 3-1) are supported by a base resisting force Q_b and soil-shaft skin resisting force Q_s. The approximate static load capacity Q_u resisting the applied vertical compressive forces on a single driven pile or drilled shaft is:

$$Q_u \approx Q_{bu} + Q_{su} \tag{3-1a}$$

$$Q_u \approx q_{bu} A_b + \sum_{i=1}^{n} Q_{sui}$$

where

Q_u = ultimate pile capacity, kips

Q_{bu} = ultimate end-bearing resisting force, kips

Q_{su} = ultimate skin resisting force, kips

q_{bu} = ultimate end-bearing resistance, ksf

A_b = area of tip or base, feet^2

Q_{sui} = ultimate skin resistance of pile element (or increment) i at depth z, kips

n = number of pile elements in pile length, L

Pile weight is negligible for deep foundations and neglected in practice. A drilled shaft or driven pile may be visualized to consist of a number of elements (as illustrated in Figure C-1, Appendix C), for calculation of ultimate pile capacity. The vertical pile resistance is a combination of the following:

(a) End-bearing resistance. Failure in end bearing is normally by punching shear with compression of the underlying supporting soil beneath the pile tip. Applied vertical compressive loads may lead to several inches of compression prior to plunging failure. Ultimate end-bearing resistance is

$$q_{bu} = cN_c\zeta_c + \sigma_L' N_q \zeta_q + \frac{B_b}{2} \gamma_b' N_\gamma \zeta_\gamma \tag{3-2}$$

where

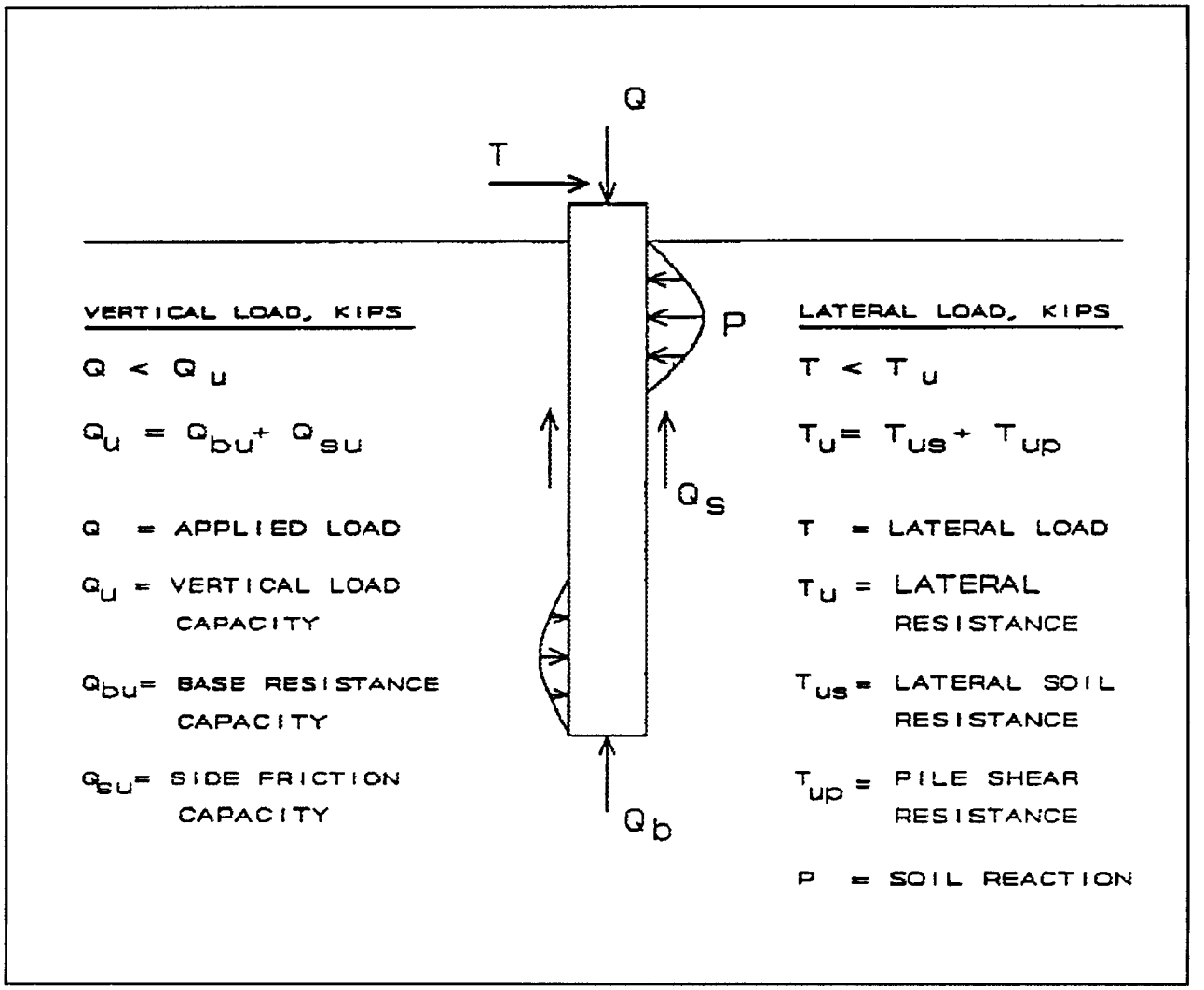

Figure 3-1. Loading support of deep foundation

c = cohesion of soil beneath the tip, ksf

σL = effective soil vertical overburden pressure at pile base, $\approx \gamma'_L L$, ksf

γ'_L = effective unit weight of soil along shaft length L, $\gamma_{sat} - \gamma_w$, kips/feet^3

γ_{sat} = saturated unit weight of soil, kips/feet^3

γ_w = unit weight of water, 0.064 kip/feet^3

γ_{sat} = saturated unit weight of soil, kips/feet^3

γ_w = unit weight of water, 0.064 kip/feet^3

B_b = base diameter, feet

γ'_b = effective unit weight of soil beneath base, kips/feet^3

N_c, N_q, N_γ = cohesion, surcharge, and wedge-bearing capacity factors

$\zeta_c, \zeta_q, \zeta_\gamma$ = cohesion, surcharge, and wedge geometry correction factors

The submerged unit weight of soil below the phreatic surface is $\gamma_{sat} - \gamma_w$. The wet unit weight γ is used instead of the effective unit weight if the soil is above the water table. The bearing capacity N_c, N_q, N_γ and geometry correction ζ_c, ζ_q, ζ_γ factors are given with the methods recommended below for calculating end bearing resistance q_{bu}.

Table 3-1
Vertical Load Analysis

Step	Procedure
1	Evaluate the ultimate bearing capacity Q_u using guidelines in this manual and equation 3-1.
2	Determine a reasonable *FS* based on sub-surface information, soil variability, soil strength, type and importance of the structure, and past experience. The *FS* recommended for normal design will typically be between 2 and 4, Table 3-2a. Variations in *FS* are permitted depending on how critical the foundation is to structural performance, Table 3-2b. Allowable loads may be increased when the soil performance investigation is thorough, settlements will remain tolerable, and performance will not be affected.
3	Evaluate allowable bearing capacity Q_a by dividing Q_u by *FS*, $Q_a = Q_u / FS$, equation 3-4.
4	Perform settlement analysis of driven pile groups and drilled shafts and adjust the bearing pressure on the top (head or butt) of the deep foundation until settlement is within permitted limits. The resulting design load Q_d should be $\leq Q_a$. Settlement analysis is particularly needed when compressible layers are present beneath the potential bearing stratum. Settlement analysis will be performed on important structures and those sensitive to settlement. Settlement analysis of individual piles or drilled shafts is presented in Chapter 3-3 and for pile groups is presented in Chapter 5.
5	Conduct a load test when economically feasible because bearing capacity and settlement calculations are, at most, approximate. However, load tests of normal duration will not reflect the true behavior of saturated compressible layers below the bearing stratum. Load tests permit a reduced *FS* = 2 in most situations, which can reduce the cost of the foundation. Refer to Chapter 6 for information on conducting load tests.

(b) Side friction resistance. Soil-shaft side friction develops from relatively small movements between the soil and shaft, and it is limited by the shear strength of the adjacent soil. Side friction often contributes the most bearing capacity in practical situations unless the base is located on stiff soil or rock. The maximum skin resistance that may be mobilized along an element *i* of pile at depth *z* may be estimated by

$$Q_{sui} = f_{sui} C_z \Delta L \qquad (3\text{-}3)$$

where

Q_{sui} = maximum load transferred to pile element *i* at depth *z*, kips

f_{sui} = maximum skin friction of pile element *i* at depth *z*, ksf

C_z = shaft circumference of pile element *i* at depth *z*, feet

ΔL = length of pile element *i*, feet

Ignoring effects due to the self-weight of the pile and residual stresses from pile driving, Figure 3-2 shows the distribution of skin friction and the associated load on a pile, where load is shown by the abscissa and depth is shown by the ordinate. The load carried in end bearing Q_b is shown in the sketch and the remainder Q is carried by skin friction. The slope of the curve in Figure 3-2c yields the rate that the skin friction f_s is transferred from the pile to the soil as shown in Figure 3-2b. Near the ground surface, f_s is usually small probably because vibrations from driving a pile form a gap near the ground surface and because of the low lateral effective stress near the top of the pile or drilled shaft. The relatively low values of f_s near the tip of a pile or drilled shaft in cohesive soils has been observed in experiments because of the decreasing soil movement against the pile as moving toward the tip. Therefore, the skin friction f_s, as a function of depth, frequently assumes a shape similar to a parabola (Figure 3-2b).

(2) Critical depth. The Meyerhof (1976) and Nordlund (1963) methods for driven piles assume that the effective vertical stress reaches a constant value after some critical depth D_c, perhaps from arching of soil adjacent to the shaft length. The critical depth ratio D_c/B, where B is the shaft diameter, is found in Figure 3-3a. For example, if the effective friction angle $\phi' = 35°$, then $D_c = 10B$, and end-bearing capacity will not increase below depth D_c, Figure 3-3b. End-bearing resistance q_{bu} will not exceed q given by Figure 3-4. Analysis of deep foundations using the pile driving analyzer has not supported this concept.

(3) Load Limits. Applied loads should be sufficiently less than the ultimate capacity to avoid excessive pile vertical and lateral displacements; e.g., $\leq$ 0.5 inch.

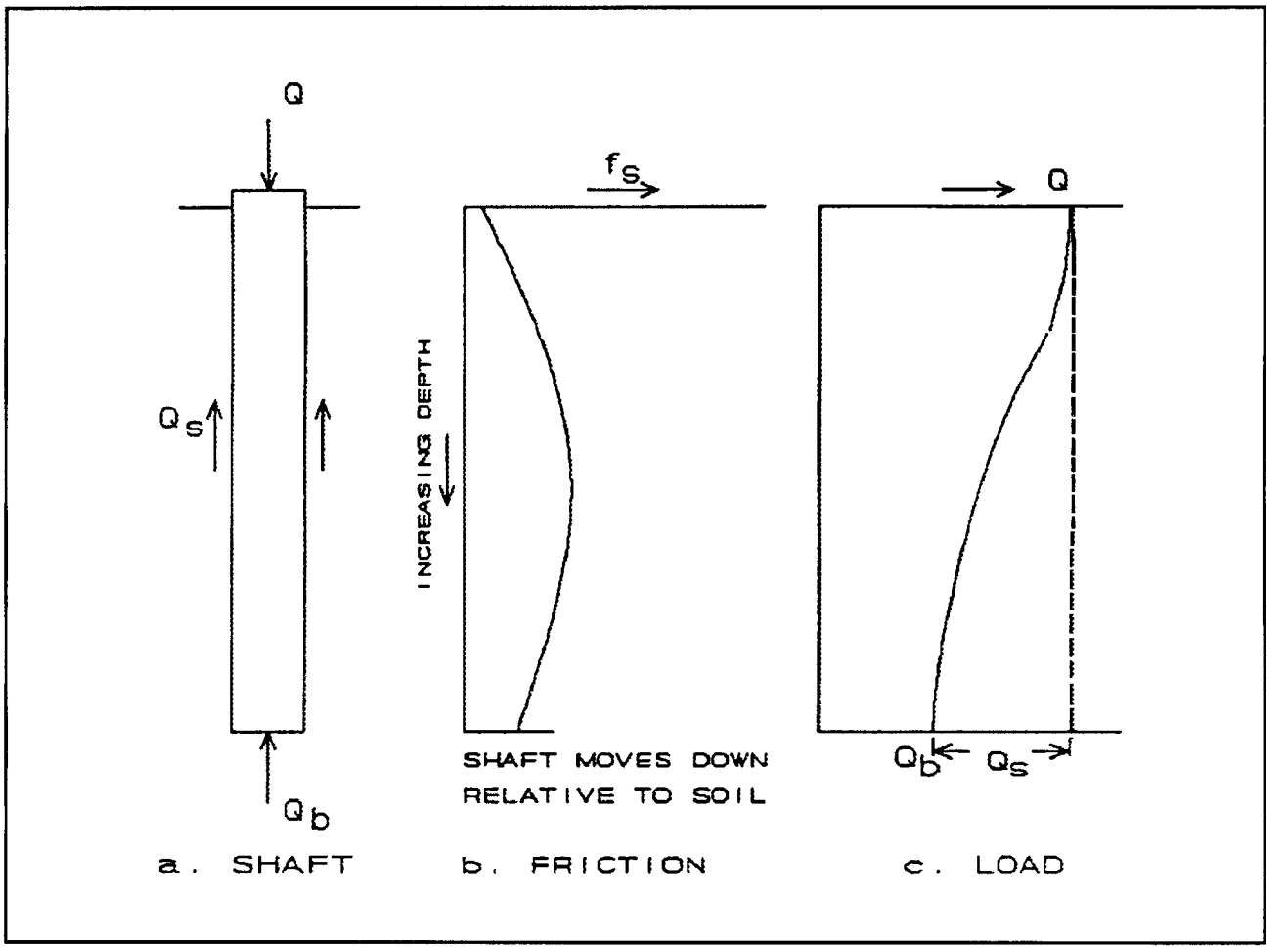

Figure 3-2. Distribution of skin friction and the associated load resistance

Applied loads one-half to one-fourth of the ultimate load capacity are often specified for design.

(a) Allowable pile capacity. The allowable pile capacity Q_a is estimated from the ultimate pile capacity using FS

$$Q_a = \frac{Q_u}{FS} \tag{3-4}$$

The design load $Q_d \leq Q_a$, depending on results of settlement analysis.

(b) Typical factors of safety. Table 3-2a provides typical FS for vertical load behavior. Typical or usual loads refer to conditions which are a primary function of a structure and can be reasonably expected to occur during the service life. Such loads may be long-term, constant, intermittent, or repetitive nature. Deviations from these minimum values may be justified by extensive foundation investigations and testing to reduce uncertainties related to the variability of the foundation soils and strength parameters. Load tests allow FS to be 2 for usual design and may lead to substantial savings in foundation costs for economically significant projects.

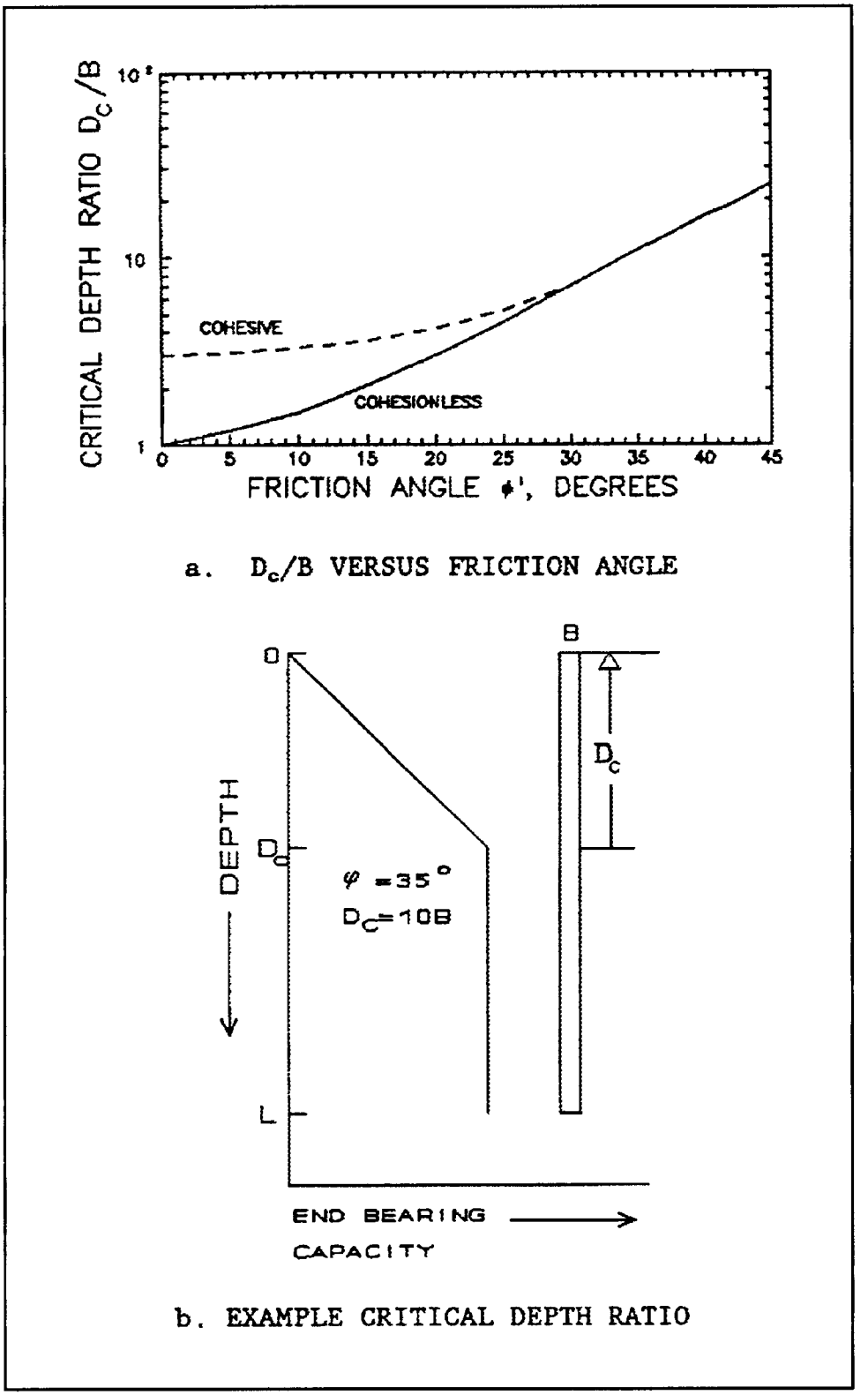

Figure 3-3. Critical depth ratio (Meyerhof 1976) (Copyright permission, American Society of Civil Engineers

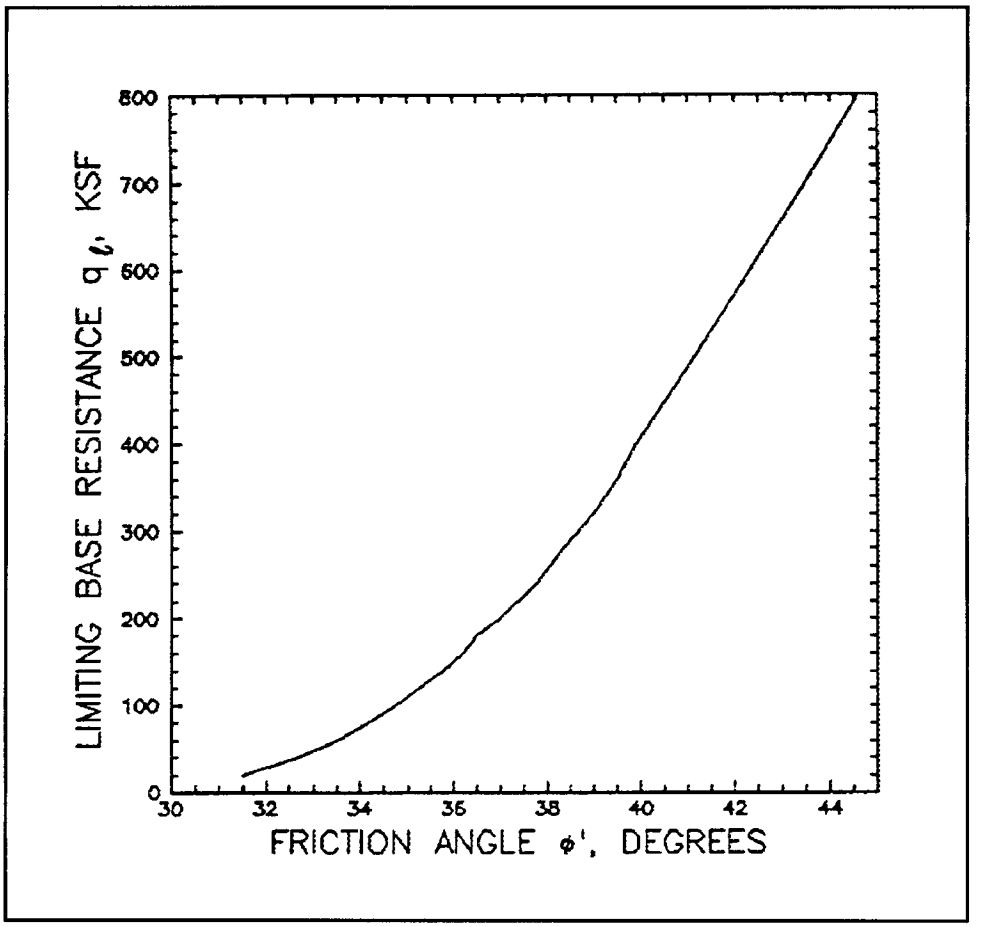

Figure 3-4. Limiting base resistance for Meyerhof and Nordlund methods

(c) Other factors of safety. Lower *FS* are possible for unusual or extreme loads, Table 3-2b, provided soil investigation is thorough and settlement will be within a tolerable range. Unusual loads refer to construction, operation, or maintenance conditions which are of relatively short duration or infrequent occurrence. Risks associated with injuries or property losses can be controlled by specifying the sequence or duration of activities and/or by monitoring performance. Extreme loads refer to events which are highly improbable and occur only during an emergency. Such events may be associated with major accidents involving impacts or explosions and natural disasters due to hurricanes. Extreme loads may also occur from a combination of unusual loads. The basic design for typical loads should be efficiently adapted to accommodate extreme loads without experiencing a catastrophic failure; however, structural damage which partially impairs the operational functions and requires major rehabilitation or replacement of the structure is possible. Caution is required to achieve an efficient design that will avoid unacceptable injuries or property losses.

(d) Group performance. Pile group analyses should be conducted as discussed in Chapter 5 to be sure that a state of ductile, stable equilibrium is attained even if individual piles will be loaded to or beyond their peak capacities.

(e) Field verification. Field instrumentation, frequent or continuous field monitoring of performance, engineering studies and analyses, and constraints on operational or rehabilitation activities may be required to ensure that the structure will not fail catastrophically during or after extreme loading. Deviations from these criteria for extreme loads should be formulated in consultation with and approved by CEMP-ET.

2. Driven Piles

The general procedure for calculating vertical loads of driven piles is given in Table 3-3. The total vertical capacity Q_u is calculated by equation 3-1 where methods for determining

end-bearing Q_{bu} and skin friction Q_{su} resistance

Table 3-2
Factors of Safety for Bearing Capacity (Pile Buck, Inc. 1992)

Usual Loads	
Condition	**Factor of Safety**
With load test	2.0
Base on bedrock	2.0
Driven piles with wave equation analysis calibrated to results of dynamic pile tests	
Compression	2.5
Tension	3.0
Resistance to uplift	2.5
Resistance to downdrag	3.0
Without load tests	3.0
Groups	3.0
Soil profile containing more than one type of soil or stratum	4.0

Influence of Loading Condition			
		Minimum Factor of Safety	
Method of Capacity Calculation	**Loading Condition[1]**	**Compression**	**Tension**
Verified by pile load test	Usual	2.0	2.0
	Unusual	1.5	1.5
	Extreme	1.15	1.15
Verified by pile driving analyzer, Chapter 6	Usual	2.5	3.0
	Unusual	1.9	2.25
	Extreme	1.4	1.7
Not verified by load test	Usual	3.0	3.0
	Unusual	2.25	2.25
	Extreme	1.7	1.7

[1] Defined in paragraph 3-1.b (3)(c)

are given below. In addition, a wave equation and pile driving analysis should be performed to estimate bearing capacity, maximum allowable driving forces to prevent pile damage during driving, and total driving resistance that will be encountered by the pile. These calculations assist in determining the required capability of the driving equipment

and to establish pile driving criteria.

a. End-bearing resistance. Ultimate end-bearing resistance is given by equation 3-2 neglecting the N_γ term

Table 3-3
General Design Procedure of a Driven Pile

Step	Procedure	Description
1	Select potentially suitable pile dimensions	Select several potentially suitable dimensions; final design selected to economize materials and while maintaining performance.
2	Evaluate end-bearing capacity Q_{bu}	Use equation 3-6 to compute end-bearing capacity q_{bu} for clay and equations 3-7 to 3-10 for sands. Use equations 3-11 to 3-13 to compute q_{bu} from in situ tests. $Q_{bu} = q_{bu} A_b$ from equation 3-1b.
3	Evaluate skin resisting force Q_{su}	Use equation 3-3 to compute skin resisting force Q_{su} for each element *i*. For clays, skin friction f_{su} is found from equation 3-16 using α from Table 3-5 or equation 3-17 with Figure 3-11. For sands, f_{su} is found from equation 3-20 using Figure 3-13 or Nordlund method in Table 3-4b. The Q_{su} for clays or sands is found from CPT data from equation 3-19 and Figures 3-12 and 3-14.
4	Compute ultimate pile capacity Q_u	Add Q_{bu} and Q_{su} to determine Q_u using equation 3-1.
5	Check that design load $Q_d \leq Q_a$	Calculate Q_a from equation 3-4 using factors of safety from Table 3-2 and compare with Q_d.

$$q_{bu} = cN_c\zeta_c + \sigma_L' (N_q - 1)\,\zeta_q \quad (3\text{-}5a)$$

or

$$q_{bu} = cN_c\zeta_c + \sigma_L' N_q \zeta_q \quad (3\text{-}5b)$$

Equation 3-5b is often used because omitting the "1" usually has negligible effect. The N_γ term is negligible for driven piles.

(1) Cohesive soil. The shear strength of cohesive soil is $c = C_u$, the undrained strength, the effective friction angle $\phi' = 0$ and $N_q = 1$. Thus, equation 3-5a may be reduced to

$$q_{bu} = N_c \times C_u = 9 \times C_u \quad (3\text{-}6)$$

where shape factor $\zeta_c = 1$ and $N_c = 9$. Undrained shear strength C_u may be taken as the mean value within $2B_b$ beneath the pile tip.

(2) Cohesionless soil. Several of the methods using equation 3-5 and in the following subparagraphs should be used for each design problem to provide a reasonable range of bearing capacity.

(a) Nordlund method. This semiempirical method (Nordlund 1963) taken from FHWA-DP-66-1 (Revision 1), "Manual on Design and Construction of Driven Pile Foundations," considers the shape of the pile taper and the influence of soil displacement on skin friction. Equations for calculating ultimate capacity are based on load test results that include timber, steel H, pipe, monotube, and Raymond step-taper piles. Ultimate capacity is

$$Q_u = \alpha_f N_q A_b \sigma_L' + \sum_{z=0}^{z=L} KC_f \sigma_z' \frac{\sin(\delta + \omega)}{\cos \omega} C_z \Delta L \quad (3\text{-}7a)$$

where

α_f = dimensionless pile depth-width relationship factor

A_b = pile point area, ft^2

σ_L' = effective overburden pressure at pile point, ksf

K = coefficient of lateral earth pressure at depth z

C_f = correction factor for K when $\delta \neq \phi'$

ϕ' = effective angle of internal friction for soil, degrees

δ = friction angle between pile and soil, degrees

ω = angle of pile taper from vertical, degrees

σ'_z = effective overburden pressure at the center of depth increment ΔL, $0 < z \leq L$, ksf

C_z = pile perimeter at depth z, feet

Δ = L
length of pile increment, feet

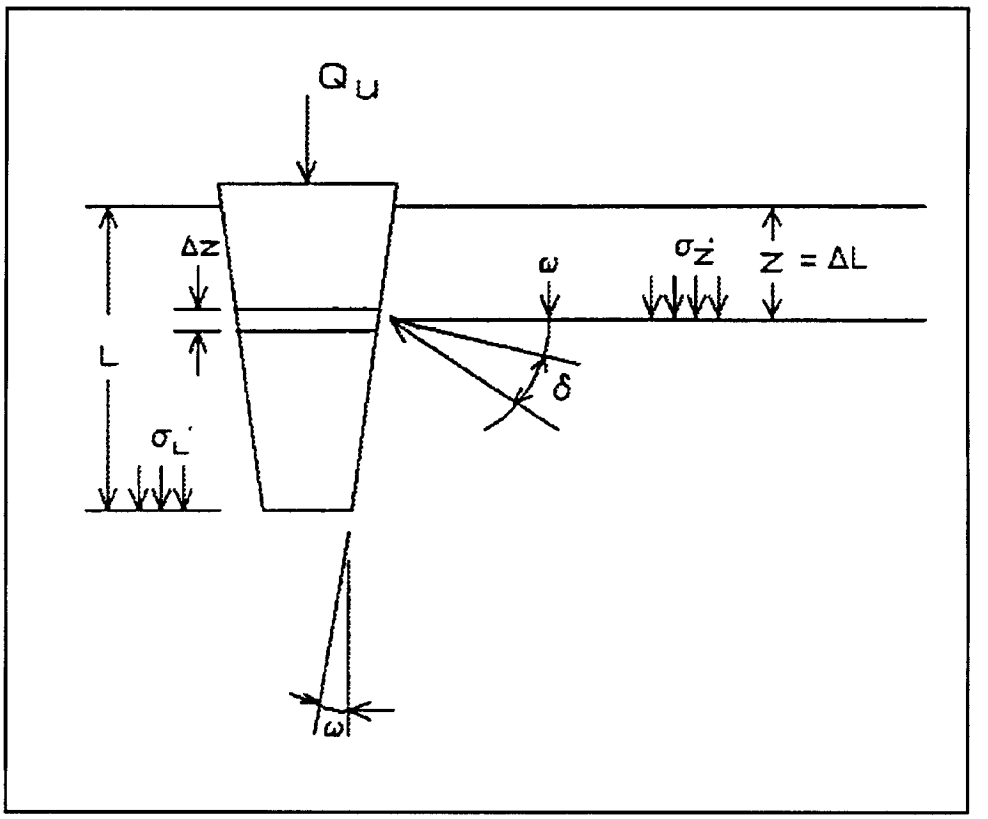

Figure 3-5. Illustration of input parameters for equation 3-7a

L = length of pile, feet

Some of these parameters are illustrated in Figure 3-5. End-bearing resistance $q_{bu} = \alpha_t N_q \sigma'_L A$ from equation 3-7a. As shown in Figure 3-4, q_{bu} should not exceed q_l where q is given. Other parameters can be determined as follows: α_f and N_q are found from Figure 3-6, K from Figure 3-7, δ from Figure 3-8 for a given ϕ' and V, and C_f from Figure 3-9. The volume V is displacement by the pile per given penetration length. The Q_u for a pile of uniform cross section ($\omega = 0$) and length L driven in a homogeneous soil with a single friction angle ϕ and single effective unit weight is

$$Q_u = \alpha_f N_q A \sigma'_L + K C_f \sigma'_m \sin\delta \, C_s L \qquad (3\text{-}7b)$$

where

A = pile cross section area

C_s = is the pile perimeter

σ'_m = mean effective vertical stress between the ground surface and pile tip, ksf.

The procedure for evaluating Q_{bu} by the Nordlund method is

given in Table 3-4.

(b) Vesic method. Bearing capacity factors of equation 3-5b are estimated by (Vesic 1977)

$$N_c = (N_q - 1) \cot \phi' \tag{3-8a}$$

$$N_q = \frac{3}{3 - \sin\phi'} e^{\frac{(90 - \phi')\pi}{180} \tan \phi'} \tan^2 \left[45 + \frac{\phi'}{2}\right] I_{rr}^{\frac{4\sin\phi'}{3(1 + \sin\phi')}} \tag{3-8b}$$

$$I_{rr} = \frac{I_r}{1 + \epsilon_v \times I_r} \tag{3-8c}$$

$$I_r = \frac{G}{C_u + \sigma_L' \tan\phi'} \tag{3-8d}$$

$$\epsilon_v = \frac{1 - 2\nu_s}{2(1 - \nu_s)} \times \frac{\sigma_L'}{G} \tag{3-8e}$$

where

ϵ_v = volumetric strain, fraction

υ_s = soil Poisson's ratio

G = soil shear modulus, ksf

C_u = undrained shear strength, ksf

ϕ' = effective friction angle, degrees

σ_L' = effective soil overburden pressure at pile base, ksf

The reduced rigidity index $I_{rr} \approx$ rigidity index I for undrained or dense soil where $\nu_s = 0.5$. $G = E / [2(1 + \upsilon)]$ where E is the soil elastic modulus. Shape factor $\zeta_c = 1.00$ and

$$\zeta_q = \frac{1 + 2K_o}{3} \tag{3-9a}$$

$$K_o = (1 - \sin\phi') \cdot OCR^{\sin\phi'} \tag{3-9b}$$

where

K_o = coefficient of earth pressure at rest

OCR = overconsolidation ratio

The OCR is the ratio of the preconsolidation pressure p_c to the vertical effective soil pressure. If the OCR is not known, then K_o can be estimated from the Jaky equation as follows

$$K_o = 1 - \sin\phi' \tag{3-9c}$$

(c) General shear method. The bearing capacity factors of equation 3-5b may be estimated, assuming the Terzaghi general shear failure (Bowles 1968), as

$$N_q = \frac{a^2}{2\cos^2(45 + \frac{\phi'}{2})}, \quad a = e^{(\frac{3\pi}{4} - \frac{\phi}{2}) \tan\phi} \tag{3-10}$$

Shape factor $\zeta_q = 1.00$. $N_c = (N_q - 1) \cot \phi'$.

(d) SPT Meyerhof Method. End-bearing capacity may be estimated from penetration resistance data of the SPT by (Meyerhof 1976)

$$q_{bu} = 0.8 \times N_{SPT} \times \frac{L_b}{B} < 8 \times N_{SPT}, \quad \frac{L}{B} \leq 10 \tag{3-11}$$

where

N_{SPT} = average uncorrected blow count within $8B$ above and $3B_b$ below the pile tip

L_b = depth of penetration of the pile tip into the bearing stratum

q_{bu} = is in units of ksf.

(e) CPT Meyerhof method. End-bearing capacity may be estimated from cone penetration resistance data by (Meyerhof 1976)

$$q_{bu} = \frac{q_c}{10} \times \frac{L_b}{B} < q_l \tag{3-12}$$

based on numerous load tests of piles driven to a firm cohesionless stratum not underlain by a weak deposit. The limiting static point resistance given by Figure 3-4 is q_l. q_{bu} and q_l are in units of ksf.

(f) CPT 1978 FHWA-Schmertmann method. End bearing capacity may be estimated by (FHWA-TS-78-209)

$$q_{bu} = \frac{q_{c1} + q_{c2}}{2} \tag{3-13}$$

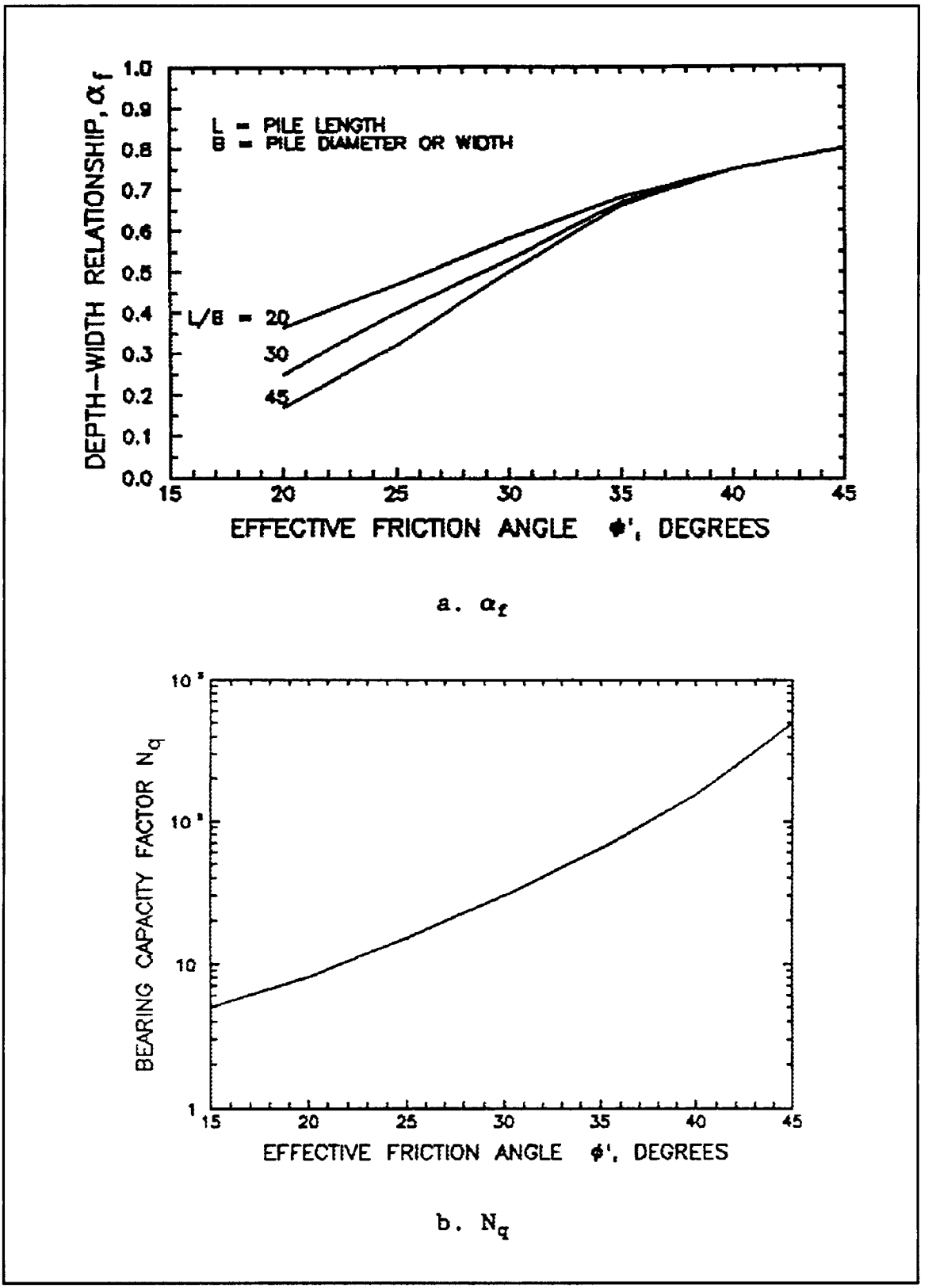

Figure 3-6. Variation of α_f and bearing capacity factor N_q with respect to ϕ' (FHWA-DP-66-1)

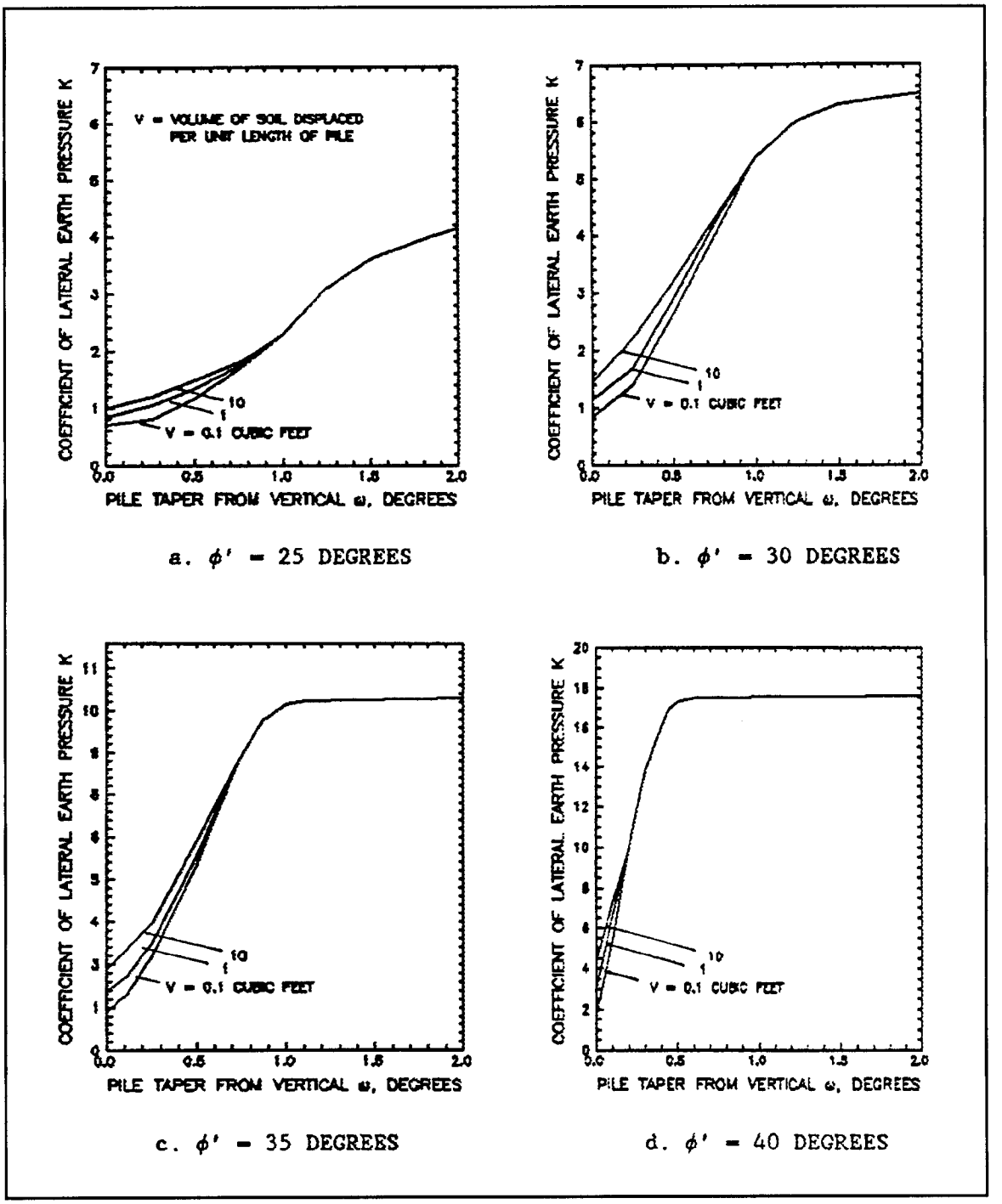

Figure 3-7. Variation of the coefficient *K* with respect to φ' (FHWA-DP-66-1)

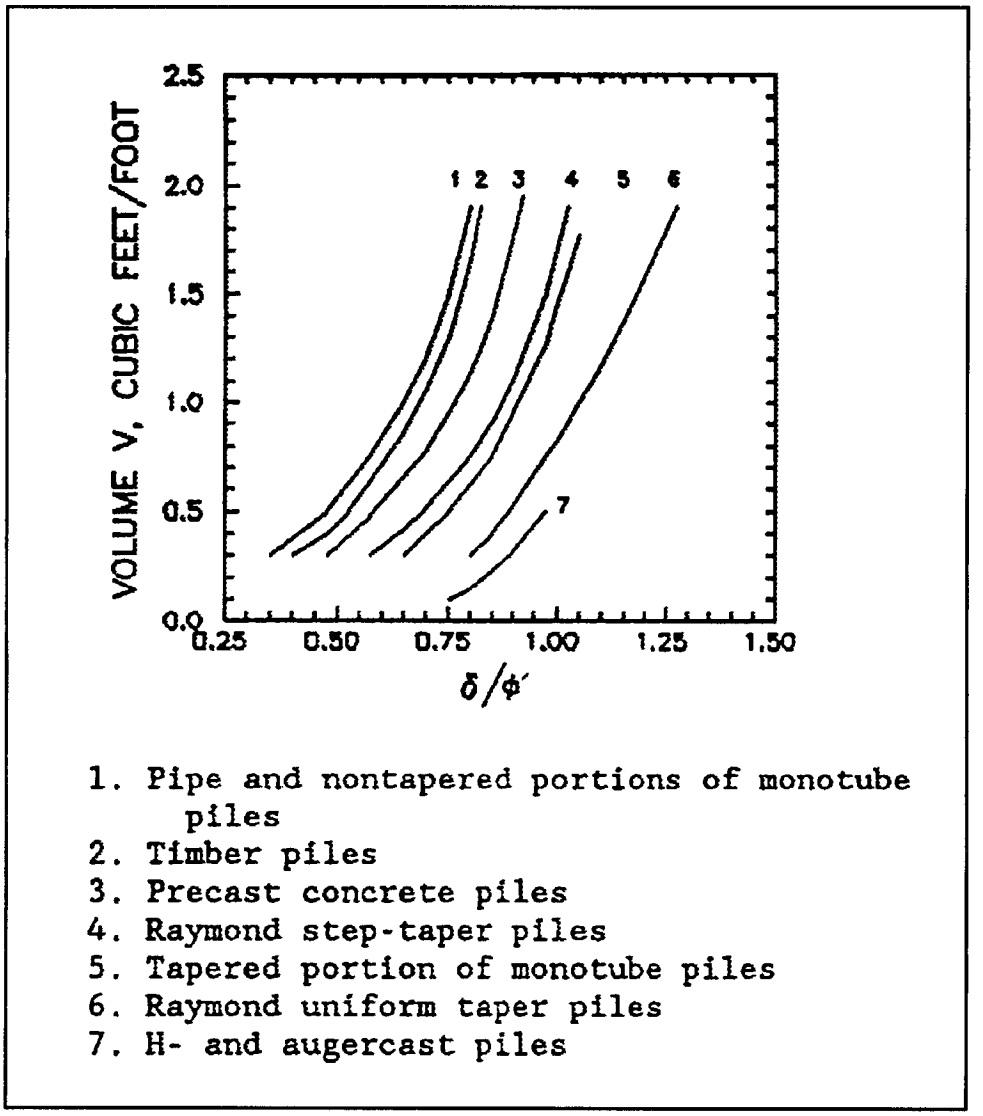

Figure 3-8. Ratio δ/ϕ′ for given displacement Volume *V*

where q_{c1} and q_{c2} are unit cone point resistances determined as given in Figure 3-10.

For example, q_{c1} calculated over the minimum path is as follows:

$$q_{c1} = \frac{180 + 170 + 170 + 170 + 170}{5}$$

$$= 172 \text{ ksf}$$

q_{c2} over the minimum path is:

$$q_{c2} = \frac{120 + 150 + 160 + 160 + 160 + 160 + 160 + 160}{8}$$

$$= 153.75 \text{ ksf}$$

From equation 3-13,

$$q_{bu} = (172 + 153.75)/2 = 162.9 \text{ ksf}$$

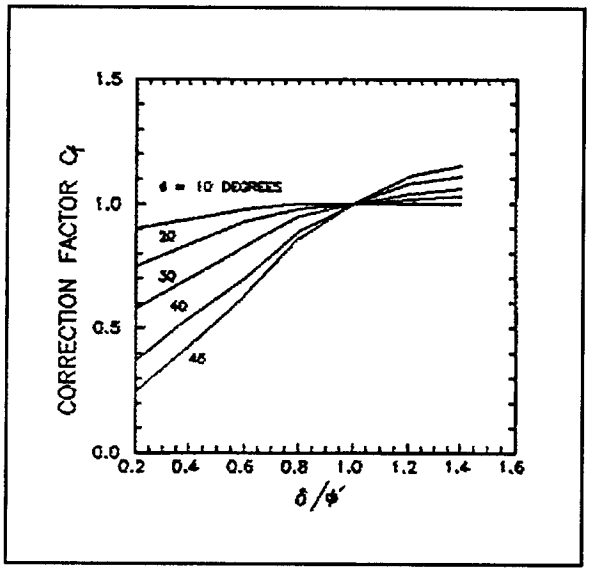

Figure 3-9. Correction factor C_f with respect to δ/φ' (FHWA-DP-66-1)

(3) Scale effects. Ultimate end-bearing capacity q_{bu} tends to be less for larger diameter driven piles and drilled shafts than that indicated by equation 3-11 or 3-12 or equation 3-5. Skin friction per unit circumferential area f_s is assumed to be independent of scale effects.

(a) Sands. The reduction in end-bearing capacity has been related with a reduction of the effective angle in internal friction ϕ' with larger diameter deep foundations. End-bearing capacity q_{bu} from equation 3-5 should be multiplied by a reduction factor (Meyerhof 1983) R_{bs}

$$R_{bs} = \left[\frac{B + 1.64}{2B}\right]^m \leq 1 \qquad (3\text{-}14a)$$

for $B > 1.64$ feet. The exponent $m = 1$ for loose sand, 2 for medium dense, and 3 for dense sand.

(b) Clays. A reduction in end-bearing capacity q_{bu} in clays appears to be related with soil structure and fissures. Equation 3-5 should be multiplied by the reduction factor R_{bc}. For driven piles in stiff fissured clay, $R_{bc} = R_{bs}$ from equation 3-14a where $m = 1$. For drilled shafts

$$R_{bc} = \left[\frac{B + 3.3}{2B + 3.3}\right] \leq 1 \qquad (3\text{-}14b)$$

for B from 0 to 5.75 ft.

(4) Base resistance of piles driven to rock. The ultimate end-bearing resistance may be estimated from the uniaxial compression strength of the rock by (Canadian Geotechnical Society 1985)

$$q_{bu} = 3\sigma_c K_{rock} f_d \qquad (3\text{-}15a)$$

$$K_{rock} = \frac{3 + \frac{s_d}{B_{sock}}}{10\left[1 + 300\,\frac{w_d}{s_d}\right]^{0.5}} \qquad (3\text{-}15b)$$

where

σ_c = uniaxial compressive strength of rock, ksi

f_d = $1 + 0.4 D_{sock}/B_{sock}$

w_d = width of discontinuities in rock, inches

s_d = spacing of discontinuities in rock, inches

B_{sock} = socket diameter, inches

D_{sock} = depth of embedment of pile socketed into rock, inches

The rock quality designation (RQD) should be greater than 50 percent, s_d should be greater than 12 inches, w_d should be less than 0.25 inch for unfilled discontinuities or w_d should be less than 1.0 inch for discontinuities filled with soil or rock debris, and B should be greater than 12 inches. Rocks are sufficiently strong that the structural capacity of the piles will govern the design. This method is not applicable to soft, stratified rocks such as shale or limestone. Piles supported on these rocks should be designed from the results of pile load tests.

b. Skin friction resistance. The maximum skin resistance between the soil and the shaft is $Q_{sui} = A_i f_{ui}$, equation 3-3.

(1) Cohesive soil. Skin friction resisting applied loads are influenced by the soil shear strength, soil disturbance, and changes in pore pressure and lateral earth pressure. The mean undrained shear strength should be used to estimate skin friction by the alpha and Lambda methods (Barker et al. 1991).

Table 3-4
Q_u by the Nordlund Method

Step	Procedure
	a. End-Bearing Capacity
1	Determine friction angle ϕ' for each soil layer. Assume $\phi = \phi'$.
2	Determine α_t using ϕ for the soil layer in which the tip is embedded and the pile L/B ratio from Figure 3-6a.
3	Determine N_q using ϕ for the soil layer in which the tip is embedded from Figure 3-6b.
4	Determine effective overburden pressure at the pile tip σ'_L and limiting stress q_l according to Figure 3-4.
5	Determine the pile point area, A_b.
6	Determine end-bearing resistance pressure $q_{bu} = \alpha_t N_q \sigma'_L$. Check $q_{bu} \leq q_l$. Calculate end-bearing capacity $Q_{bu} = q_{bu} A_b$.
	b. Skin Friction Capacity
7	Compute volume of soil displaced per unit length of pile.
8	Compute coefficient of lateral earth pressure K for ϕ' and ω using Figure 3-7; use linear interpolation.
9	Determine δ/ϕ' for the given pile and volume of displaced soil V from Figure 3-8. Calculate δ for friction angle ϕ'.
10	Determine correction factor C_f from Figure 3-9 for ϕ and the δ/ϕ' ratio.
11	Calculate the average effective overburden pressure σ'_z of each soil layer.
12	Calculate pile perimeter at center of each soil layer C_z.
13	Calculate the skin friction capacity of the pile in each soil layer i from $Q_{sui} = KC_f\sigma_z' \frac{\sin(\delta + \omega)}{\cos \omega} C_z \Delta L$. Add Q_{sui} of each soil layer to obtain Q_{su}, $Q_{su} = \sum Q_{sui}$ of each layer.
14	Compute ultimate total capacity, $Q_u = Q_{bu} + Q_{su}$.

(a) Alpha method. The soil-shaft skin friction of a length of a pile element at depth z may be estimated by

$$f_{sui} = \alpha_a \times C_u \tag{3-16}$$

where

α_a = adhesion factor

C_u = undrained shear strength, ksf

Local experience with existing soils and load test results should be used to estimate appropriate α_a. Estimates of α_a may be made from Table 3-5 in the absence of load test data and for preliminary design.

(b) Lambda method. This semiempirical method is based on numerous load test data of driven pipe piles embedded in clay assuming that end-bearing resistance was evaluated from equation 3-6. Skin friction is (Vijayvergiya and Focht 1972)

$$f_{sui} = \lambda \times (\sigma'_m + 2C_{um}) \tag{3-17}$$

where

λ = correlation factor, Figure 3-11

σ'_m = mean effective vertical stress between the ground surface and pile tip, ksf

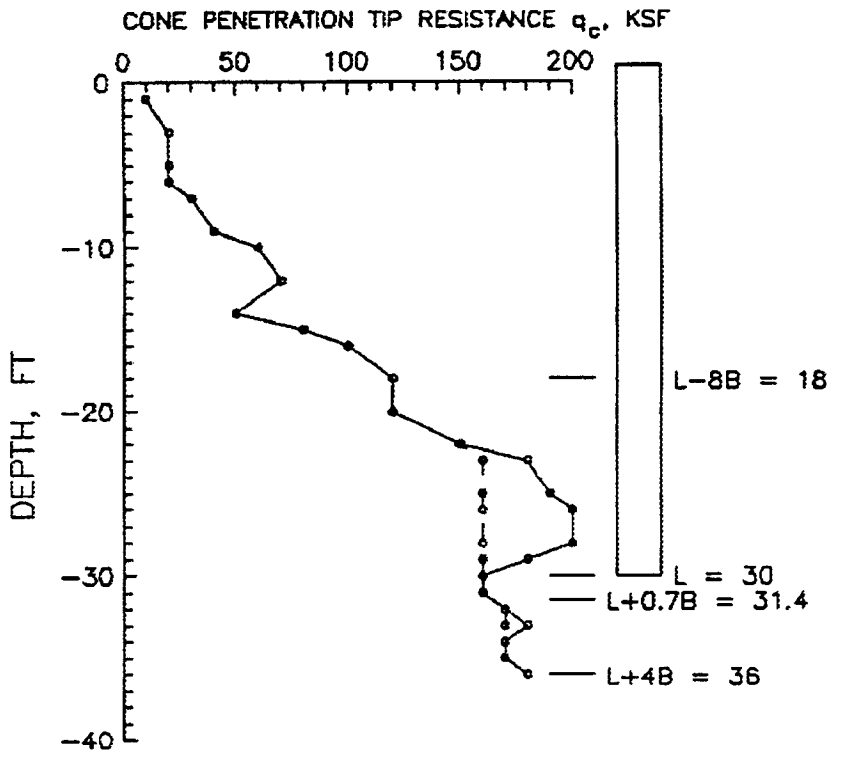

$$q_{bu} = \frac{q_{c1} + q_{c2}}{2}$$

q_{c1} = Average q_c over a distance L + 0.7B to L + 4B below the pile tip; use the minimum path, which is a vertical line spanning the minimum measured q_c between L + 0.7B and L + 4B, ksf

q_{c2} = Average q_c over a distance of L to L - 8B above the pile tip; use the minimum path as above

B = Pile diameter, ft

Figure 3-10. Estimating pile tip capacity from CPT data (FHWA-TS-78-209)

C_{um} = mean undrained shear strength along pile length, ksf

λ may also be given approximately by

$$\lambda = L^{-0.42} \qquad L \geq 10 \text{ ft} \tag{3-18a}$$

$$\lambda = 0.5 - 0.01L \qquad L < 10 \text{ ft} \tag{3-18b}$$

where L is the pile length, feet, λ may also be estimated as follows (Kraft, Focht, and Amarasinghe 1981)

Normally consolidated:

$$\lambda = 0.296 - 0.032 \ln L \quad (3\text{-}18c)$$

Overconsolidated:

$$\lambda = 0.488 - 0.078 \ln L \quad (3\text{-}18d)$$

The ratio of the mean undrained shear strength to the effective overburden pressure should be greater than 0.4 for overconsolidated soil.

(c) CPT field estimate. The cone penetration test provides a sleeve friction f_{sl} which can be used to estimate the ultimate skin resistance Q_{su} (Nottingham and Schmertmann 1975)

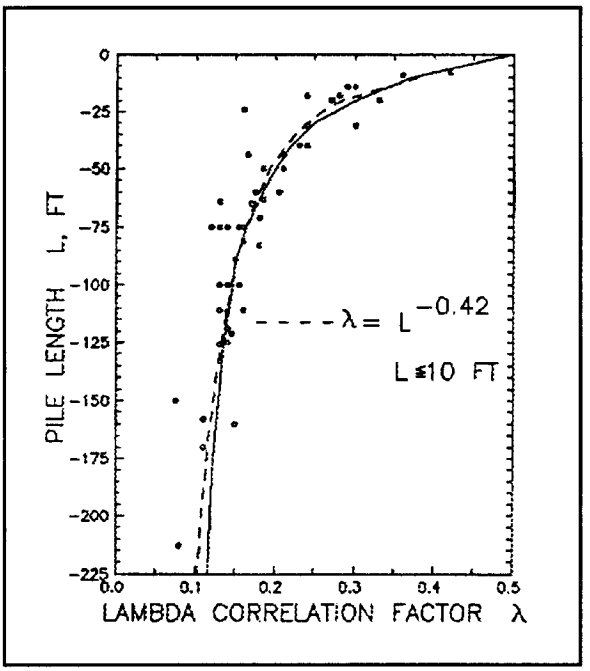

Figure 3-11. Lambda correlation factor for clay (Copyright permission, Offshore Technology Conference, Society of Petroleum Engineers)

$$Q_{su} = k_{sl}\left[\sum_{z_L=0}^{8B} \frac{z_L}{8B} f_{slz} C_z + \sum_{z_L=8B}^{L} f_{slz} C_z\right] \quad (3\text{-}19)$$

where

k_{sl} = sleeve friction factor, Figure 3-12

f_{slz} = cone sleeve friction at depth z, ksf

C_z = pile circumference at depth z, feet

B = pile diameter or width, feet

z_L = depth to point considered, feet

L = length of embedded pile, feet

Equation 3-19 corrects for the cone (mechanical or electrical), pile material (steel, concrete, or wood), type of soil through sleeve friction f_{sl}, and corrects for the depth of the pile embedment. f_{sl} for high OCR clays is 0.8 times f_{sl} measured by the mechanical cone. The cone penetration test procedure is given in ASTM D 3441.

(2) Cohesionless soil. The soil-shaft friction may be estimated using effective stresses

$$f_{sui} = \beta_f \times \sigma_i' \quad (3\text{-}20a)$$

$$\beta_f = K \times \tan \delta_a \quad (3\text{-}20b)$$

where

f_{sui} = soil shaft skin friction

β_f = lateral earth pressure and friction angle factor

K = lateral earth pressure coefficient

δ_a = soil-shaft effective friction angle, $\leq \phi'$, degrees

σ_i' = effective vertical stress in soil adjacent to pile element i, ksf

Cohesion c is zero. The σ_i' is limited to the effective overburden pressure calculated at the critical depth D_c of Figure 3-3.

(a) Values of β_f as a function of the effective friction angle ϕ' of the soil prior to installation of the deep foundation are shown in Figure 3-13. Values in Figure 3-13 are lower bound estimates.

(b) The Nordlund method in Table 3-4b provides an alternative method of estimating skin resistance.

Table 3-5
Adhesion Factors for Cohesive Soil

Length/Width Ratio $\frac{L}{B}$	Undrained Shear Strength C_u, ksf	Adhesion Factor α_s
< 20	< 3	$1.2 - 0.3C_u$
	> 3	0.25
> 20	0.0 - 1.5	1.0
	72 - 4.0	$1.25 - 0.24C_u$
	> 4	0.3

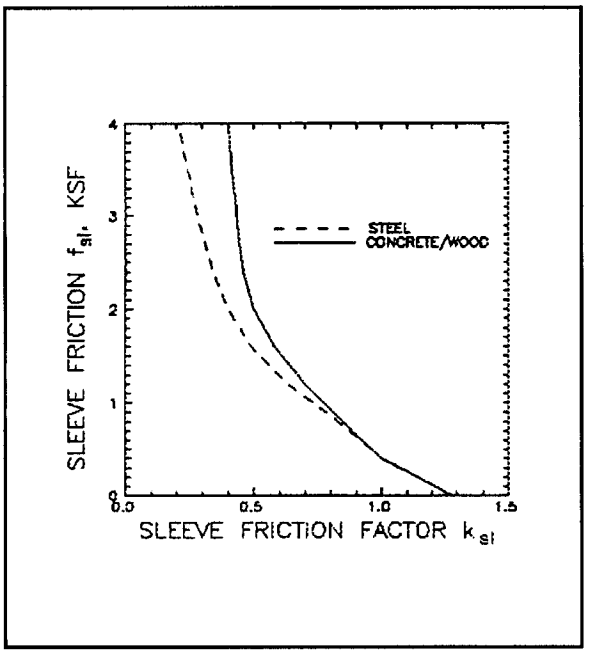

Figure 3-12. Sleeve friction factor for clays (Copyright permission, Florida Department of Transportation)

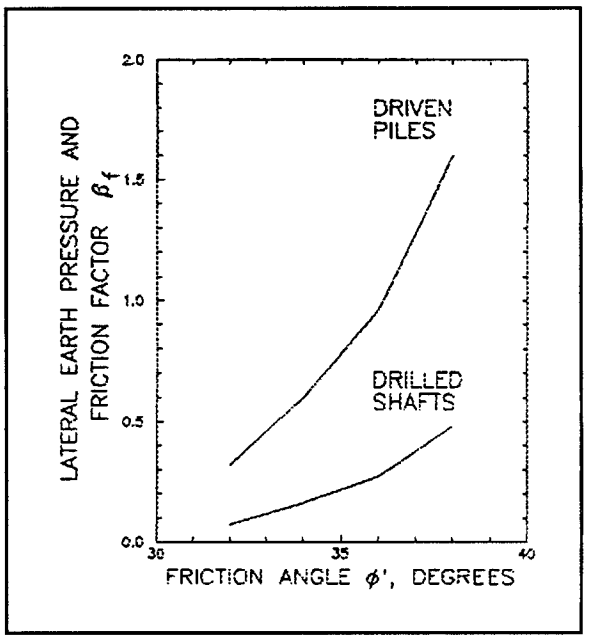

Figure 3-13. Lateral earth pressure and friction angle factor β_f (Copyright permission, American Society of (Civil Engineers)

(3) CPT field estimate. The ultimate skin resistance may be estimated from the cone sleeve friction similar to that for clays from equation 3-19 where the sleeve friction factor k_{sl} is estimated for sands from Figure 3-14 (Nottingham and Schmertmann 1975). The factor k_{sl} for wood piles is 1.25 times the k_s for steel piles.

c. Computer programs. Pile capacity can be calculated using computer programs CAXPILE (WES IR-K-84-4), AXILTR (Appendix C), and GRLWEAP (Goble et al. 1988). CAXPILE AND AXILTR solve for axial load-displacement behavior of single piles by load transfer curves. Several base and shaft load transfer curves applicable to different types of soils are available in these programs. Other curves may be input if data are available. Refer to Chapter 6 for further details on wave equation program GRLWEAP.

d. Load-displacement relationships. The settlement of a pile group is of more interest than that of a single pile because most piles are placed as groups, Chapter 5. If required, the settlement of single piles can be estimated using methods in paragraph 3-3 for drilled shafts.

e. Application. Each pile for a certain project is required to support Q_d = 100 kips. Steel circular, 1.5-foot-diameter, closed-end pipe piles are tentatively selected, and they are to be driven 30 feet through a two-layer soil of clay over fine uniform sand, Figure 3-15. The water level (phreatic surface) is 15 feet below ground surface at

the clay-sand interface. The pile will be filled with concrete with density γ_{conc} = 150 pounds per cubic foot. The strength and density of the soils are given in Figure 3-15. The friction angle ϕ of 36 degrees for the lower sand layer given in Figure 3-15 is an average value. ϕ increases from 34 degrees at the top to 38 degrees at the base of the pile to be consistent with the cone penetration data given in Fig. 3-10.

(1) Soil parameters

(a) Mean effective vertical stress. The mean effective vertical stress σ_s' in the sand layer below the surface clay layer may be estimated by

$$\sigma_s' = L_{clay} \times \gamma_c + \frac{L_{sand}}{2} \times \gamma_s' \qquad (3\text{-}21a)$$

where

L_{clay} = thickness of a surface clay layer, feet

γ_c = wet unit weight of surface clay layer above the phreatic surface, kips/cubic foot

L_{sand} = thickness of an underlying sand clay layer, feet

γ_s' = submerged unit weight of underlying sand layer below the phreatic surface, kips/cubic feet

The mean effective vertical stress in the sand layer adjacent to the embedded pile from equation 3-21a is

$$\sigma_s' = L_{clay} \times \gamma_c + \frac{L_{sand}}{2} \times \gamma_s' = 15 \times 0.12 + \frac{15}{2} \times 0.04 = 1.8 + 0.3$$

$$\sigma_s' = 2.1 \text{ ksf}$$

The effective vertical soil stress at the pile tip is

$$\sigma_L' = L_{clay} \times \lambda_c + L_{sand} \times \lambda_s' = 1.5 \times 0.12 + 15 \times 0.04 = 1.8 + 0.6 = 2.4 \text{ ksf} \qquad (3\text{-}21b)$$

Figure 3-3 indicates that the D_c/B ratio is 10 for an average ϕ' = 36 degrees. Therefore, D_c = 10 · 1.5 = 15 feet. The effective stress is limited to σ_s' = 1.8 ksf below 15 feet and the effective stress at the pile tip is σ_L' = 1.8 ksf for the Meyerhof and Nordlund methods. The remaining methods use σ_L' = 2.4 ksf.

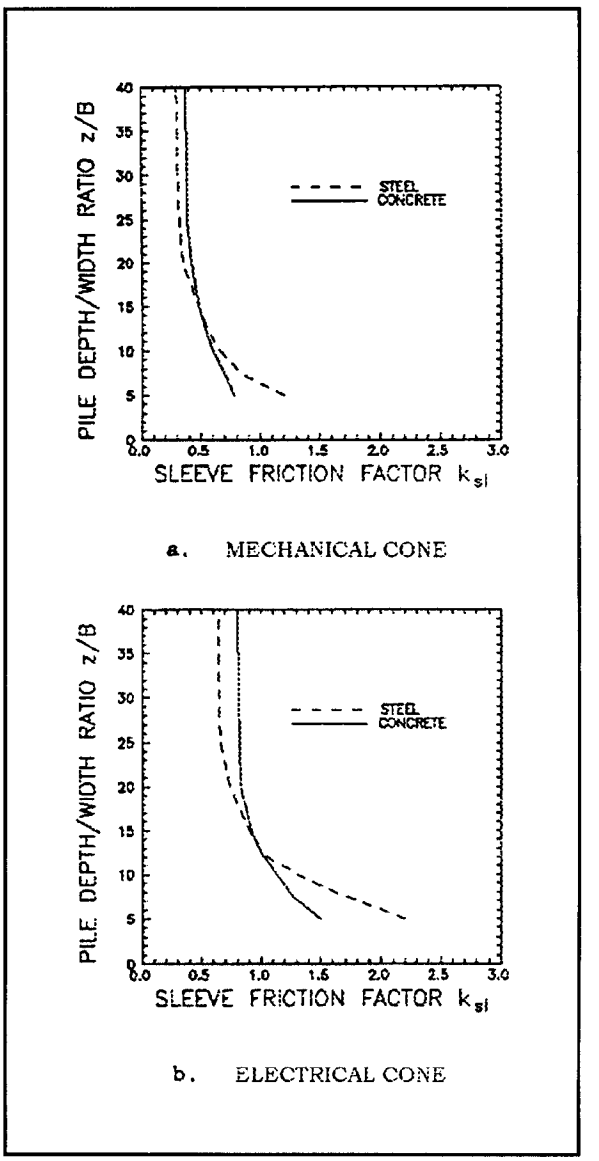

Figure 3-14. Sleeve friction factors for sands (Copyright permission, Florida Department of Transportation)

(b) Cone penetration resistance. Penetration tests using an electrical cone indicate that an average cone tip resistance q_c in the clay is 40 ksf and in the sand it is 160 ksf. The shear modulus $G = E_s / [\,2\,(1 + \upsilon_s)\,] = 250 / [\,2\,(1 + 0.3)\,] = 96$ ksf or about 100 ksf using an assumed elastic soil modulus E_s = 250 ksf and Poisson's ratio υ_s = 0.3. These E_s and υ_s values are typical of soft to medium stiff clay or loose to medium dense sands. E_s is consistent with that calculated for sands from equation 1-3a. Sleeve friction f_{sl} in the clay is 1.0 ksf and in the sand it is 1.5 ksf.

(c) Coefficient of earth pressure. Coefficient of earth pressure at rest from the Jaky equation is $K_o = 1 - \sin \phi = 1 - \sin 36 \text{ degrees} = 0.42$.

(2) Vertical load capacity. Solution of the vertical load capacity of a single pile using Table 3-3 is given in Table 3-6.

3. Drilled Shafts

The general procedure for design of a single drilled shaft is given in Table 3-7. The vertical capacity Q_u is given by equation 3-1 where the end bearing Q_{bu} and skin friction Q_{su} capacities are calculated by methods given below. Load tests to confirm the design should be performed where economically feasible. Refer to Chapter 6 for further information on load tests.

a. End-bearing resistance. Ultimate end bearing resistance for single drilled shafts with enlarged bases should be evaluated using equation 3-2. Equation 3-2 may be simplified for shafts without enlarged tips by eliminating N_γ

$$q_{bu} = cN_c\zeta_c + \sigma_L' (N_q - 1)\, \zeta_q \qquad \text{(3-5a, bis)}$$

or

$$q_{bu} = cN_c\zeta_c + \sigma_L' N_q \zeta_q \qquad \text{(3-5b, bis)}$$

Equations 3-5 also adjust for pile weight W_p assuming $\gamma_p \approx \gamma_L'$.

(1) Cohesive soil. The undrained shear strength of saturated cohesive soil for deep foundations in saturated clay subjected to a rapidly applied load is $c = C_u$ and the friction angle $\phi = 0$. Equations 3-5 simplifies to (FHWA-HI-88-042)

$$q_{bu} = F_r N_c C_u, \quad q_{bu} \le 80 \text{ ksf} \qquad \text{(3-22)}$$

where the shape factor $\zeta_c = 1$ and $N_c = 6\,[\,1 + 0.2\,(L/B_b)\,] \le 9$. The limiting q_{bu} of 80 ksf is the largest value that has so far been measured for clays. The undrained shear strength C_u may be reduced by about one-third in cases where the clay at the base has been softened and could cause local bearing failure due to high strain. F_r should be 1.0, except when B_b exceeds about 6 feet. For $B_b > 6$ feet

$$F_r = \frac{2.5}{aB_b + 2.5b}, \quad F_r \le 1.0 \qquad \text{(3-23)}$$

where

$a = 0.0852 + 0.0252\,(L/B_b)$, $a \le 0.18$

$b = 0.45C_u^{0.5}$, $0.5 \le b \le 1.5$, where C_u is in units of ksf

Equation 3-22 limits q_{bu} to bearing pressures for a base settlement of 2.5 inches. C_u should be the average shear strength within $2B_b$ beneath the tip of the shaft.

(2) Cohesionless soil. Vesic method and the general shear methods discussed for driven piles in paragraph 2a, Chapter 3, and the Vesic Alternate Method are recommended for solution of ultimate end bearing capacity using equation 3-5 (Vesic 1977).

(a) Vesic Alternate Method. This method assumes a local shear failure and provides a lower bound estimate of bearing capacity

$$N_q = e^{\pi \tan \phi'} \left[\tan^2\left(45 + \frac{\phi'}{2}\right)\right] \qquad \text{(3-24)}$$

The shape factor may be estimated by equation 3-9. A local shear failure occurs at the base of deep foundations only in poor soils such as loose silty sands or weak clays or in soils subject to disturbance due to the construction of drilled shafts. The Vesic Alternate Method may be more appropriate for deep foundations constructed under difficult conditions, for drilled shafts placed in soil subject to disturbance, and when a bentonite-water slurry is used to keep the hole open during drilled shaft construction.

(b) SPT field estimate. The end bearing resistance q_{bu} in units of ksf may be estimated from standard penetration data (Reese and Wright 1977) by

$$q_{bu} = \frac{4}{3} N_{SPT} \qquad N_{SPT} \le 60 \qquad \text{(3-25a)}$$

$$q_{bu} = 80 \text{ ksf} \qquad N_{SPT} > 60 \qquad \text{(3-25b)}$$

where N_{SPT} is the uncorrected standard penetration resistance in blows per foot.

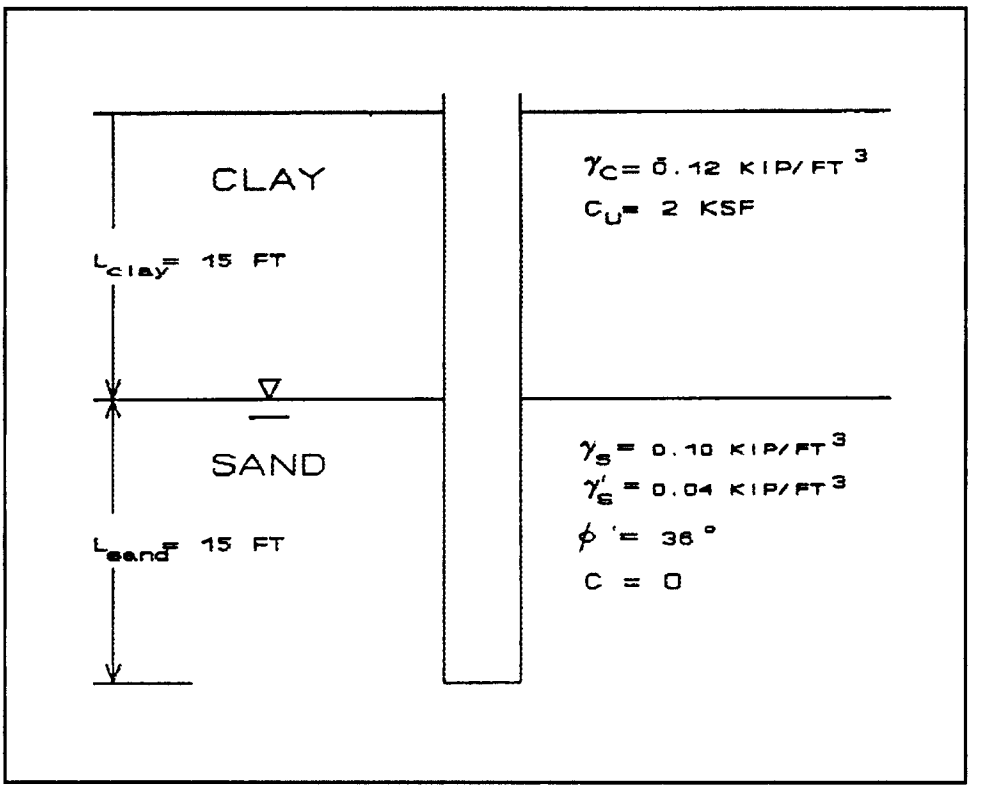

Figure 3-15. Driven steel pipe pile

b. Skin friction resistance. The maximum skin resistance that may be mobilized between the soil and shaft perimeter is $Q_{sui} = A_{si} f_{sui}$, equation 3-3, where A_{si} is the perimeter area of element *i*. Several methods of estimating skin friction f_{sui}, based on past experience and the results of load tests, are described below.

(1) Cohesive soil. Skin friction between the soil and shaft is estimated by using the average undrained shear strength and an empirical adhesion factor α_a.

(a) Alpha method. The soil-shaft skin friction f_{sui} of a length of shaft (or pile) element may be estimated by

$$f_{sui} = \alpha_a C_u \qquad \text{(3-16 bis)}$$

where

α_a = adhesion factor

C_u = undrained shear strength, ksf

Local experience with existing soils and load test results should be used to estimate appropriate α_a. Estimates of α_a may be made from Table 3-8 in the absence of load test data and for preliminary design.

(b) Adhesion factor. The adhesion factor may also be related to the plasticity index PI for drilled shafts constructed dry. For cohesive soil, the following expression (Stewart and Kulhawy 1981) may be used

Overconsolidated:

$$\alpha_a = 0.7 - 0.01 \times \text{PI} \qquad \text{(3-26a)}$$

Slightly over-consolidated ($OCR \leq 2$):

$$\alpha_a = 0.9 - 0.01 \times \text{PI} \qquad \text{(3-26b)}$$

Normally consolidated:

$$\alpha_a = 0.9 - 0.004 \times \text{PI} \qquad \text{(3-26c)}$$

where $15 < \text{PI} < 80$. Drilled shafts constructed using the bentonite-water slurry should use α_a of about 1/ 2 to 2/3 of those given by equation 3-26.

Table 3-6
Calculations of Vertical Loads in a Single Pile

Step	Procedure	Description
1	Select suitable dimensions	Select a trial 1.5-ft-diameter by 30-ft-long steel closed-end pipe pile. Pile circumference C_z = 4.71 ft and area of base A_b = 1.77 ft^2
2	Evaluate end bearing capacity Q_{bu}	$Q_{bu} = q_{bu} A_b$ from equation 3-1b; q_{bu} is found using several methods in the sand: (a) Nordlund method: Use Table 3-4a α_t = 0.72 for ϕ' = 38 deg, Figure 3-6a N_q = 105 ϕ' = 38 deg, Figure 3-6b σ'_L = 1.8 ksf $q_{bu} = \alpha_t N_q \sigma'_L$ = 0.72 × 105 × 1.8 = 136.1 ksf q_l = 150 ksf from Figure 3-4 Therefore, q_{bu} = 136.1 ksf ≤ q_l (b) Vesic method: Reduced rigidity index from equation 3-8c $$I_{rr} = \frac{I_r}{1 + \epsilon_v \times I_r} = \frac{53.3}{1 + 0.006 \times 53.3} = 40.4$$ $$\epsilon_v = \frac{1 - 2\nu_s}{2(1 - \nu_s)} \times \frac{\sigma'_L}{G_s} = \frac{1 - 2 \times 0.3}{2(1 - 0.3)} \times \frac{2.4}{100}$$ $$= 0.006$$ $$I_r = \frac{G_s}{\sigma'_L \times \tan\phi'} = \frac{100}{2.4 \times \tan 38} = 53.3$$ From equation 3-8b $$= \frac{3}{3 - \sin\phi} e^{\frac{(90 - \phi)}{180}\pi \tan\phi} \tan^2\left[45 + \frac{\phi}{2}\right] I_{rr}^{\frac{4\sin\phi}{3(1 + \sin\phi)}}$$ $$= \frac{3}{3 - \sin 38} e^{\frac{(90 - 38)}{180}\pi \tan 38} \tan^2\left[45 + \frac{38}{2}\right] I_{rr}^{\frac{4\sin 3}{3(1 + si}}$$ $$= 1.258 \times 2.032 \times 4.023 \times 6.549$$ $$= 70.4$$ Shape factor equation 3-9a $$\zeta_q = \frac{1 + 2K_o}{3} = \frac{1 + 2 \times 0.42}{3} = 0.61$$ where K_o was found from equation 3-9c

Table 3-6 (Continued)

Step	Procedure	Description

From equation 3-5b,

$$q_{bu} = \sigma_L' \times N_q \times \zeta_q = 2.4 \times 70.4 \times 0.61 = 103 \text{ ksf}$$

(c) General Shear (Bowles method (Bowles 1968)): From equation 3-10

$$N_q = \frac{e^{\frac{270 - \phi}{180} \pi \tan \phi}}{2\cos^2\left[45 + \frac{\phi}{2}\right]}$$

$$= \frac{e^{\frac{270 - 38}{180} \pi \tan 38}}{2\cos^2\left[45 + \frac{38}{2}\right]}$$

$$= \frac{e^{3.164}}{2 \times 0.192} = \frac{23.65}{0.384} = 61.5$$

The shape factor $\zeta_q = 1.00$ when using equation 3-10; from equation 3-5b,

$$q_{bu} = \sigma_L' \times N_q \times \zeta_q = 2.4 \times 61.5 \times 1.00$$

$$= 147.7 \text{ ksf}$$

(d) CPT Meyerhof method: From equation 3-12,

$$q_{bu} = \frac{q_c}{10} \times \frac{L_{sand}}{B} < q_\ell$$

$$= \frac{160}{10} \times \frac{15}{1.5} = 160 \text{ ksf}$$

q_ℓ = 150 ksf from Figure 3-4; therefore, q_{bu} = 150 ksf

(e) CPT FHWA & Schmertmann: Data in Figure 3-10 are used to give q_{bu} = 163 ksf as illustrated in paragraph 2a, Chapter 3

(f) Comparison:

Table 3-6 (Continued)

Step	Procedure	Description

Method	q_{bu}, ksf
Friction Angle ϕ = 38 deg	
Nordlund	136
Vesic	103
General Shear	148
Cone Penetration Test	
CPT Meyerhof	150
CPT FHWA & Schmertmann	163

q_{bu} varies from 103 to 148 ksf for ϕ' = 38 deg and 150 to 163 ksf for the cone data. Select lower bound $q_{bu,l}$ = 103 ksf and upper bound q_{bu} = 163 ksf. Scale effects of equation 3-14 are not significant because B < 1.64 ft

$Q_{bu,l} = q_{bu,l} \times A_b$ = (103) (1.77) = 182 kips
$Q_{bu,u} = q_{bu,u} \times A_b$ = (163) (1.77) = 289 kips

3 Evaluate skin resistance Q_{su}

ToTop Layer: Cohesive soil; average skin friction using the alpha method, equation 3-16 is

$$f_{su} = \alpha_a \times C_u = 0.6 \times 2.0 = 1.2 \text{ ksf}$$

where α_a = 1.2 - 0.3C_u = 0.6 for L/B = 20 from Table 3-5

Q_{su} from equation 3-3 is

$$Q_{su} = f_{su} \times C_z \times L_{\text{clay}} = (1.2) \times (4.71) \times (15)$$
$$= 84.8 \text{ kips}$$

Average skin friction using the lambda method and equation 3-17 is

$$f_{su} = \lambda\ (\sigma_m + 2C_{um}) = 0.32\,(0.9 + 2.2)$$
$$= 1.57 \text{ ksf}$$

where $\lambda = L_{\text{clay}}^{-0.42} = 15^{-0.42} = 0.32$ from equation 3-18a; σ'_m is found from

$$\sigma'_m = \frac{L_{\text{clay}}}{2} \times \gamma'_{\text{clay}} = \frac{15}{2} \times 0.12 = 0.9 \text{ ksf}$$

Q_{su} from equation 3-3 is

$$Q_{su} = f_{su} \times C_z \times L_{\text{clay}} = 1.57 \times 4.71 \times 15$$
$$= 110.9 \text{ kips}$$

Table 3-6 (Continued)

Step	Procedure	Description

Q_{su} using the CPT field estimate method is found from equation 3-19 where k_{sl} = 0.75 for f_{sl} = 1.0 ksf, Figure 3-12

$$Q_{su} = 0.75\ [12 \times 1.0 \times 1.0 \times 4.71 + 3 \times 1.0 \times 4.71]$$
$$= 0.75\ [56.5 + 14.1] = 53.0 \text{ kips}$$

$$Q_{su} = k_{sl}\left[8B \times \frac{8B}{8B} \times f_{sl} C_z + \sum_{8B}^{L_{clay}} f_{sl} C_z\right]$$

Lower bound $Q_{su,l}$ = 53 kips and upper bound $Q_{su,u}$ = 111 kips

Bottom Layer: Cohesionless soil; average skin friction from equation 3-20a using $\sigma'_s \leq$ limiting stress 1.8 ksf is

$$f_{su} = \beta_f \times \sigma'_s = 0.96 \times 1.8 = 1.7 \text{ ksf}$$

where β_f is from Figure 3-13 for average ϕ' = 36 deg

Q_{su} from equation 3-3 is

$$Q_{su} = f_{su} \times C_z \times L_{clay} = 1.7 \times 4.71 \times 15$$
$$= 120 \text{ kips}$$

An alternative estimate from the Nordlund method, Table 3-4b, is

$V = \pi \times (1.5^2/2) \times 1 = 1.77$ ft^3/ft
K = 2.1 from Figure 3-7 for ω = 0 deg
δ/ϕ = 0.78 for V = 1.77 and pile type 1 from Figure 3-8
$\delta = 0.78 \cdot 36 = 28$ deg
C_f = 0.91 for δ/ϕ = 0.78, ϕ = 36 deg from Figure 3-9
$C_z = \pi \times B_e = \pi \times 1.5 = 4.71$ ft

$$Q_{su} = KC_f \sigma'_s \sin\delta \times C_z L_{sand}$$
$$= 2.1 \times 0.91 \times 1.8 \times \sin 28 \times 4.71 \times 15$$
$$= 114 \text{ kips}$$

Q_{su} using the CPT field estimate method is found from equation 3-19 where k_{sl} varies from 1.3 to 0.7, Figure 3-14b, for $z/B = L_{clay}/B$ = 15/1.5 = 10 to $z/B = (L_{clay} + L_{sand})/B$ = 30/1.5 = 20

$$Q_{su} = k_{sl}\left[\sum_{L_{clay}}^{L_{clay}+L_{sand}} f_{sl} C_z\right]$$

Table 3-6 (Concluded)

Step	Procedure	Description
		$Q_{su} = (1.3 + 0.7)/2[15 \times 1.5 \times 4.71]$ $= 106$ kips Lower bound $Q_{su,l}$ in sand is 106 kips and upper bound $Q_{su,u}$ = 120 kips Total Q_{su} in both clay and sand is: Lower bound: $Q_{su,l}$ = 53 + 106 = 159 kips Upper bound: $Q_{su,u}$ = 111 + 120 = 231 kips
4	Compute ultimate capacity Q_u	The total bearing capacity from equation 3-1a is $Q_u = Q_{bu} + Q_{su}$ Lower bound: $Q_{u,l} = Q_{bu,l} + Q_{su,l}$ $= 182 + 159 = 341$ kips Upper bound: $Q_{u,u} = Q_{bu,u} + Q_{su,u}$ $= 289 + 231 = 520$ kips Q_u ranges from a low of 341 to a high of 520 kips for a difference of 179 kips or 42 percent of the mean (341 + 520) /2 = 430 kips. This difference is reasonable because of assumptions used by various methods
5	Check $Q_d \leq Q_a$	Q_d = 100 kips; for FS = 3 and using $Q_{u,l}$ lower bound $Q_a = \frac{Q_u}{FS} = \frac{341}{3} = 114$ kips Therefore, Q_d is less than the lower bound estimate. A load test should be performed to failure to assure that the pile has adequate capacity. The FS may also be reduced to 2.0 and permit the design load Q_d to be increased leading to fewer piles and a more economical foundation when load tests are performed as a part of the design

(2) Cohesionless soil. Skin friction is estimated using effective stresses, the soil friction angle, and empirical correlations.

(a) The soil-shaft skin friction of a length of pile element is estimated by

$$f_{sui} = \beta_f \sigma_i' \qquad \text{(3-20a, bis)}$$

$$\beta_f = K \tan \delta_a \qquad \text{(3-20b, bis)}$$

where

β_f = lateral earth pressure and friction angle factor

K = lateral earth pressure coefficient

Table 3-7
Design of a Drilled Shaft

Step	Procedure	Description
1	Select shaft length	Length depends on location of a bearing stratum of sufficient strength and load bearing requirements for the foundation.
2	Evaluate ultimate base resistance q_{bu}	Use equation 3-22 to compute end bearing in clay (total stress analysis $\phi = 0$); $N_c = 9$ or 7 with hammer grab or bucket auger. Use equations 3-8, 3-9, and 3-10 with equations 3-5 for sands setting cohesion c to zero.
3	Evaluate maximum mobilized skin friction f_{sui}	f_{sui} is estimated from equation 3-16 and adhesion factors from equations 3-26 and Table 3-8 for clays. Q_{su} is estimated from equation 3-19 and Figures 3-12 or 3-14, then dividing by $C_z \Delta L$ where C_z is pile circumference and ΔL is length in sand or clay.
4	Evaluate Q_{bu} and Q_{su} for several shaft and base diameters	Select several shaft and base diameters; $Q_{bu} = q_{bu} A_b$, equation 3-1b; Q_{sui} is found from equation 3-3 and adding increments of Q_{sui} over shaft length L less top and bottom 5 ft or from Table 3-8.
5	Check that design load $Q_d \leq Q_a$	Q_a is evaluated from equation 3-4 using FS in Table 3-2.
6	Evaluate shaft resistance to other loads	If pullout, uplift thrust, or downdrag is significant, use program AXILTR, Appendix C.
7	Evaluate maximum settlement from design load Q_d	Estimate settlement for design load Q_d using equations 3-36 to 3-38, load transfer functions, or program CAXPILE or AXILTR.
8	Check computed $\leq$ specified settlement or heave	Adjust design load or shaft dimensions.

δ_a = soil-shaft effective friction angle, $\leq \phi'$, degree

σ'_i = effective vertical stress in soil at shaft element i, ksf

The cohesion c is taken as zero.

(b) Figure 3-13 indicates values of β_f as a function of the effective friction angle ϕ' of the soil prior to installation of the deep foundation. σ'_i is limited to the effective overburden pressure calculated at the critical depth D_c in Figure 3-3.

(c) SPT field estimate. The skin friction f_s in units of ksf may be estimated for drilled shafts in sand (Reese and Wright 1977) by

$$f_s = \frac{N_{SPT}}{17} \quad \text{for } N_{SPT} \leq 53 \tag{3-27a}$$

$$f_s = \frac{N_{SPT} - 53}{225} \quad \text{for } 53 < N_{SPT} \leq 100 \tag{3-27b}$$

c. Drilled shafts socketed in rock. This calculation of pile capacity of drilled shafts socketed in rock assumes that the load is carried either entirely by skin resistance or by end-bearing resistance depending on the value of the estimated settlement of the shaft in the socket (FHWA-HI-88-042). If the settlement is greater than 0.4 inch, loads are assumed to be carried by base resistance. Loads are carried by skin friction if settlement is less than 0.4 inch. This assumption is conservative because no allowance is provided for loads carried by a combination of both skin and end-bearing resistances.

(1) Calculation of socket settlement. Settlement of the portion of the drilled shaft socketed in the rock is

$$\rho_{sock} = \rho_{e,\,sock} + \rho_{b,\,sock} \tag{3-28a}$$

Table 3-8
Adhesion Factors for Drilled Shafts in Cohesive Soil

Shaft Depth, ft	Adhesion Factor α_a
0 – 5	0.0
diameter of shaft from bottom of straight or from top of underream	0.0
All Other Points	0.55

Note: skin friction f_{si} should be limited to 5.5 ksf

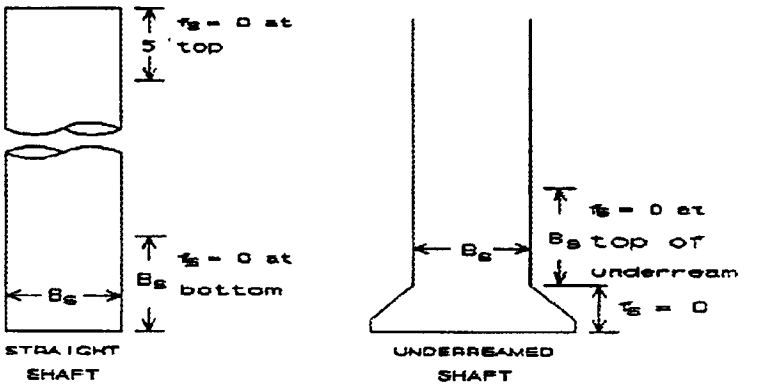

$$\rho_{e,\,sock} = \frac{Q_{sock} D_{Sock}}{A_{sock} E_p} \qquad (3\text{-}28b)$$

$$\rho_{b,\,sock} = \frac{Q_{sock} I_{sock}}{B_{sock}} E_{mass} \qquad (3\text{-}28c)$$

where

ρ_{sock} = settlement in socket, inches

$\rho_{e,\,sock}$ = elastic shortening of drilled shaft in socket, mm (inches)

$\rho_{b,\,sock}$ = settlement of base of drilled shaft in socket, mm (inches)

Q_{sock} = load at top of socket, kips

D_{sock} = depth of embedment in socket, inches

A_{sock} = cross section area of socket, inches^2

E_p = Young's modulus of concrete in socket, ksi

B_{sock} = socket diameter, inches

I_{sock} = settlement influence factor, Figure 3-16

E_{mass} = Young's modulus of the mass rock, ksi

Elastic shortening of the shaft not in the socket should also be calculated to determine the total elastic settlement

$$\rho_e = \rho_{sock} + \frac{Q + Q_{sock}}{2} \frac{(L - D_{sock})}{AE_p} \qquad (3\text{-}28d)$$

where

Q = load at shaft top, kips

L = embedded shaft length, inches

A = cross section area of shaft, inches^2

Further information for the derivation of Figures 3-16, 3-17, and 3-18 is available from FHWA-HI-88-042, "Drilled Shafts: Construction Procedures and Design Methods." Young's modulus of the mass rock is estimated from the Young's modulus of the intact (core) rock by

$$E_{mass} = K_e E_{core} \qquad (3\text{-}29)$$

where

K_e = modulus reduction ratio, E_{mass}/E_{core}, Figure 3-17

E_{core} = Young's modulus of the intact rock, ksi

E_{core} is given as a function of the uniaxial compressive strength σ_c in Figure 3-18.

(2) Skin resistance. The capacity of the drilled shaft in the rock socket is determined by skin resistance if $\rho_{sock} < 0.4$ inch. Ultimate skin resistance Q_{su} is (Barker et al. 1991)

$$Q_{su} = 0.15\sigma_c C_z D_{sock} \qquad \sigma_c \le 0.28 \text{ ksi} \qquad (3\text{-}30a)$$

$$Q_{su} = 2.5\sqrt{\sigma_c} C_z D_{sock} \qquad \sigma_c > 0.28 \text{ ksi} \qquad (3\text{-}30b)$$

where

Q_{su} = ultimate skin resistance of drilled shaft in socket, kips

σ_c = uniaxial compressive strength of the rock (or concrete, whichever is less), ksi

C_z = circumference of socket, inches

D_{sock}= depth of embedment of socket, inches

(3) Base resistance. The capacity of the drilled shaft in the rock socket is determined by base resistance if $\rho_{sock} >$ 0.4 inch.

(a) Base resistance is computed the same as that for driven piles on rock by equation 3-15 in paragraph 2a, Chapter 3.

(b) The base resistance q_{bu} in units of KN/M2 (ksf) of drilled shafts socketed in rock may also be estimated from pressuremeter data (Canadian Geotechnical Society 1985) by

$$q_{bu} = K_b (P_l - P_o) + \sigma_v \qquad (3\text{-}31)$$

where

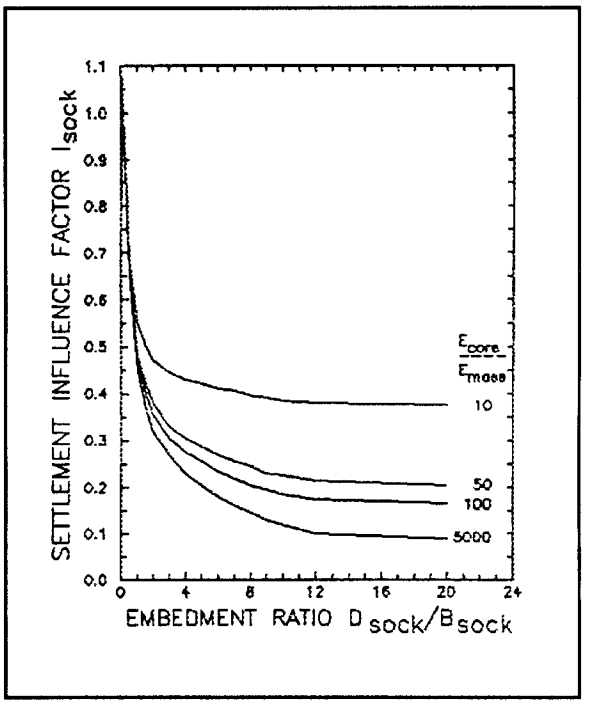

Figure 3-16. Settlement influence factor, I_{sock}

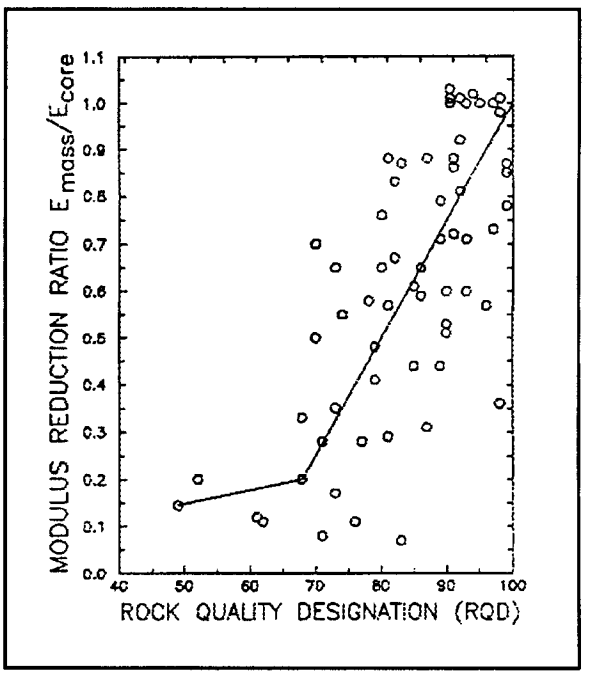

Figure 3-17. Modulus reduction ratio E_{mass} / E_{core}

K_b = pressuremeter coefficient, dimensionless, Table 3-9

P_l = pressuremeter limit pressure, ksf

P_o = pressuremeter at rest, horizontal pressure measured at the base elevation, ksf

σ_v = vertical pressure, kfs

Table 3-9
Dimensionless Pressuremeter Coefficient (from Canadian Geotechnical Society 1985, BiTech Publishers Ltd.)

D_{sock}/B_{sock}	k_b
0	0.8
1	2.8
2	3.6
3	4.2
5	4.9
7	5.2

(4) Limitations for analysis of the socket capacity.

(a) The strength of the rock will not deteriorate during construction from values measured during the site investigation.

(b) The drilling fluid will not form a lubricated film on the sides of the excavation.

(c) The bottom of the rock socket is properly cleaned out. This limitation is important if pile capacity is based on the end-bearing resistance. Depth of the rock socket is typically one to three times the diameter of the socket.

(d) Shaft load tests are required if the RQD is less than 50 percent.

d. Vertical capacity to resist other loads. Deep foundations may be subject to other vertical loads such as uplift and downdrag forces. Uplift forces are caused by pullout loads from structures or heave of expansive soils surrounding the shaft tending to drag the shaft up. Downdrag forces are caused by settlement of soil surrounding the shaft that exceeds the downward displacement of the shaft and increases the downward load on the shaft. A common cause of settlement is a lowering of the water table. These forces influence the skin friction that is developed between the soil and the shaft perimeter and influence bearing capacity.

(1) Method. Analysis of bearing capacity with respect to these vertical forces requires an estimate of the relative movement between the soil and the shaft perimeter and the location of neutral point *n*, the position along the shaft length where there is no relative movement between the soil and the shaft. In addition, tension or compression stresses in the shaft or pile caused by uplift or downdrag shall be considered to properly design the shaft. These shaft movements are time-dependent and complicated by soil movement. Background theory for analysis of pullout, uplift, and downdrag forces of single circular drilled shafts and a method for computer analysis of these forces are provided.

(2) Pullout. Deep foundations are frequently used as anchors to resist pullout forces. Pullout forces are caused by overturning moments such as from wind loads on tall structures, utility poles, or communication towers.

(a) Force distribution. Deep foundations may resist pullout forces by shaft skin resistance and resistance mobilized at the tip contributed by enlarged bases illustrated in Figure 3-19. The shaft resistance is defined in terms of negative skin friction f_n to indicate that the shaft is moving up relative to the soil. This is in contrast to compressive loads that are resisted by positive skin friction where the shaft moves down relative to the soil, Figure 3-2. The shaft develops a tensile stress from pullout forces. Bearing capacity resisting pullout may be estimated by

$$P_u = Q_{bu} + P_{nu} \tag{3-32a}$$

$$P_u = q_{bu}A_{bp} + \sum_{i=1}^{n} P_{nui} \tag{3-32b}$$

$$P_{ni} = \sum_{i=1}^{n} P_{nui}C_z\Delta L \tag{3-32c}$$

where

P_u = ultimate pullout resistance , kips

Q_{bu} = ultimate end-bearing force available to resist pullout force P, kips

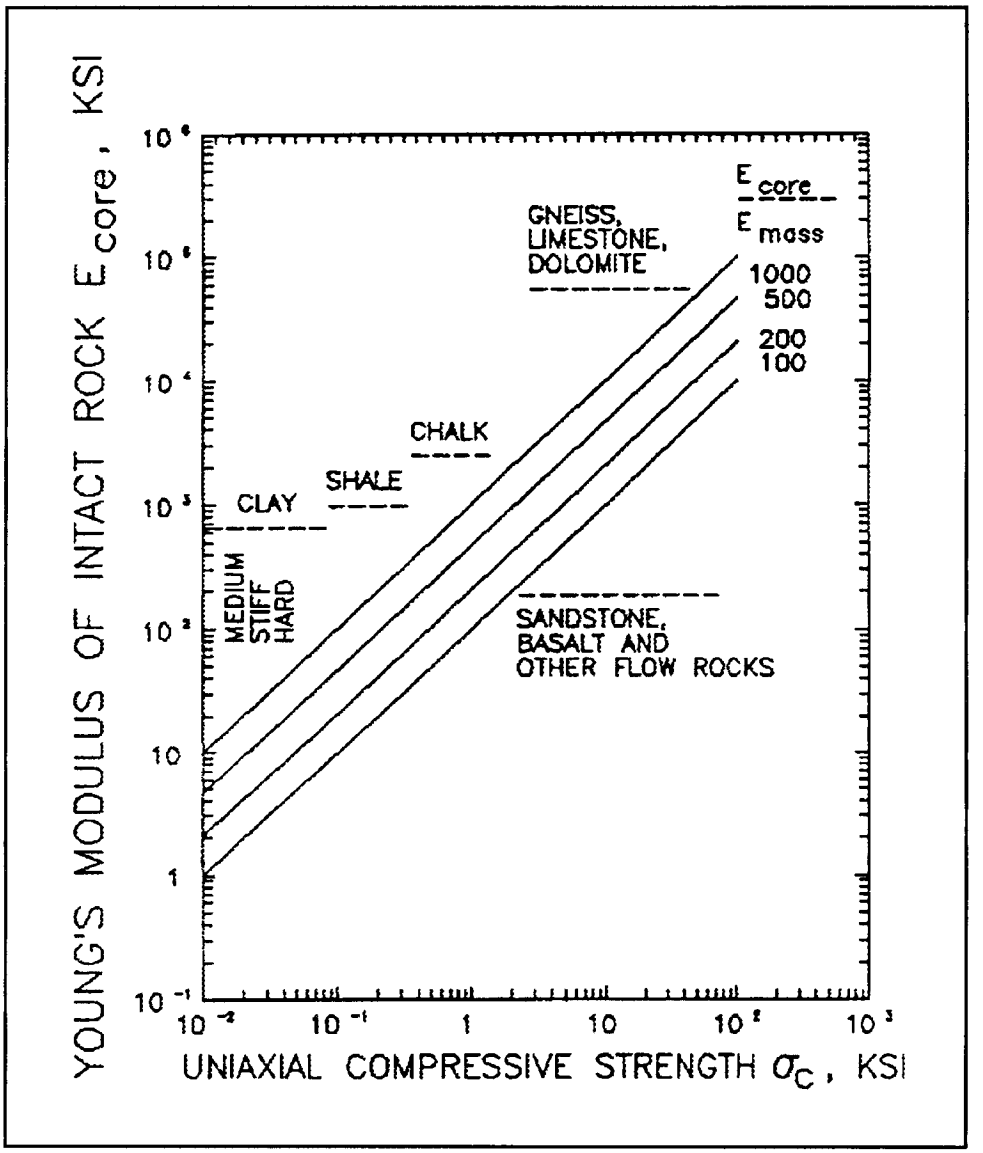

Figure 3-18. Elastic modulus of intact rock

P_{mu} = ultimate skin resistance available to resist pullout force P, kips

q_{bu} = ultimate end-bearing resistance available to resist pullout force P, kips

A_{bp} = area of base resisting pullout force P, ft^2

P_{nui} = pullout skin resistance for pile element i, kips

f_{ni} = negative skin friction resisting pullout force P at element i, ksf

C_z = circumference of shaft, feet

ΔL = length of pile element i, feet

(b) P_n in Figure 3-19 is the skin resistance force that is resisting pullout force P.

(3) Uplift. Deep foundations constructed in expansive soil are subject to uplift forces caused by swelling of expansive soil adjacent to the shaft. These uplift forces cause a friction on the upper length of the shaft perimeter tending to move the shaft up. The portion of the shaft perimeter subject to uplift thrust is in the soil subject to heave. This soil is often within the top 7 to 20 feet of the soil profile

referred to as the depth of the active zone for heave Z_a. The shaft located within Z_a is sometimes constructed in such a manner that isolates the shaft perimeter from the expansive soil to reduce uplift thrust.

(a) Stiffened and ribbed mats as well as drilled shafts are frequently used to support structures in expansive soil areas. Uplift forces may be controlled by minimizing the shaft diameter consistent with that required for downloads and to counter the uplift thrust, by extending the shaft length into nonswelling soil to depths of twice the depth of the active zone for heave. Such force can be reduced by the construction of widely spaced shafts to reduce differential movement, and by making shafts vertically plumb (maximum variation of 1 inch in 6 feet) and smooth to reduce adhesion between the swelling soil and the shaft.

(b) End-bearing resistance. The q_{bu} of enlarged bases may be estimated by equation 3-5b. For sands, cohesion c is set to zero and N_q is calculated by the Nordlund (1963), Vesic (1977), general shear , and Vesic Alternate Methods (1977). For clays, the friction angle is set to zero and N_c varies from zero at the ground surface to a maximum of 9 at a depth of $2.5B_b$ below the ground surface where B_b is the diameter of the base of the shaft (Vesic 1971). The undrained shear strength C_u is the average strength from the base to a distance $2B_b$ above the base. Base area A_b, resisting pullout to be used in equation 3-1b for underreamed drilled shafts, is

$$A_{bp} = \frac{\pi}{4} \times (B_b^2 - B_s^2) \qquad (3\text{-}33)$$

where

B_b = diameter of base, feet

B_s = diameter of shaft, feet

The soil above the underream is assumed to shear as a cylinder of diameter B_b.

(c) Skin resistance. The shaft diameter may be slightly reduced from pullout forces by a Poisson effect that reduces lateral earth pressure on the shaft perimeter. Thus, skin resistance may be less than that developed for shafts subject to compression loads because horizontal stress is slightly reduced (Stewart and Kulhawy 1980).

(d) Force distribution. During uplift, the shaft moves down relative to the soil above neutral point n, figure 3-20, and moves up relative to the soil below point n. The negative skin friction f_n below point n and enlarged bases of drilled shafts resist the uplift thrust of expansive soil. The positive skin friction f_s above point n contributes to uplift thrust from heaving soil and puts the shaft in tension. End-bearing and skin friction capacity resisting uplift thrust may be estimated by equations 3-32.

(e) End bearing. End-bearing resistance may be estimated similar to that for pullout forces. Bearing capacity factor for pullout in clays N_{cp} should be assumed to vary from 0 at the depth of the active zone of heaving soil to 9 at a depth $2.5B_b$ below the depth of the active zone of heave. The depth of heaving soil may be at the bottom of the expansive soil layer or it may be estimated by guidelines provided in TM 5-818-7.

(f) Skin friction. Skin friction from the top of the shaft to the neutral point n contributes to uplift thrust, while skin friction from point n to the base contributes to skin friction that resists the uplift thrust. The magnitude of skin friction f_s above point n that contributes to uplift thrust will be as much or greater than that estimated for compression loads. Skin friction f_n that resists uplift thrust should be estimated similar to that for pullout loads because uplift thrust places the shaft in tension tending to pull the shaft out of the ground and slightly reduces lateral pressures below point n.

(4) Downdrag. Deep foundations constructed through compressible soils and fills can be subject to an additional downdrag force. This downdrag force is caused by the soil surrounding the drilled shaft or pile settling downward more than the deep foundation. The deep foundation is dragged downward as the soil compresses. The downward load applied to the shaft is significantly increased and can even cause a structural failure of the shaft as well as excessive settlement of the foundation. Settlement of the loose soil after installation of the deep foundation can be caused by the weight of overlying fill, compaction of the fill, and lowering of the groundwater level. The effects of downdrag can be reduced by isolating the shaft from the soil using a bituminous coating or by allowing the consolidating soil to settle before construction. Downdrag loads can be considered in the design by adding them to column loads.

(a) Force distribution. The shaft moves up relative to the soil above point n, Figure 3-21, and moves down relative to the soil below point n. The positive skin friction f_s below point n and end bearing capacity resists the downward loads applied to the shaft by the settling soil and the structural loads. Negative skin friction f_n above the neutral point contributes to the downdrag load and increases the compressive stress in the shaft.

(b) End bearing. End-bearing capacity may be estimated similar to methods for compressive loads given by equation 3-5.

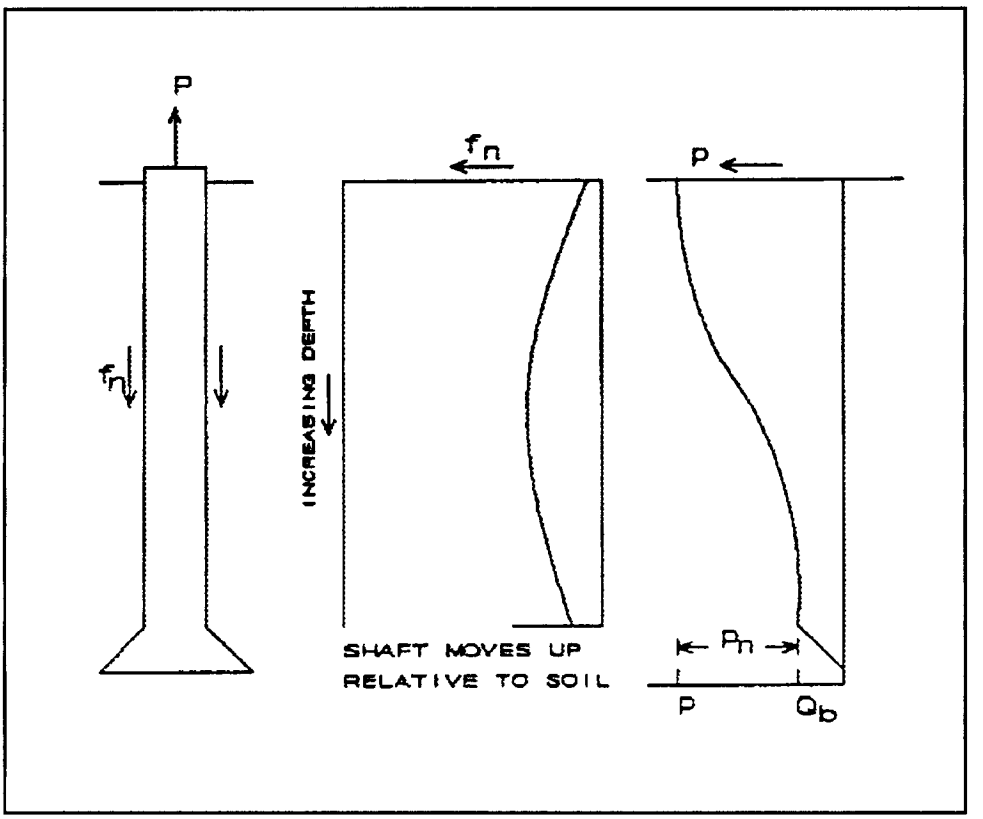

Figure 3-19. Pullout force in underreamed shaft

(c) Skin friction. Skin friction may be estimated by equation 3-3 where the positive skin friction is given by equations 3-16 and 3-20.

(5) Computer analysis. Program AXLITR (Axial Load-Transfer), Appendix C, computes the vertical shaft and soil displacements for axial down-directed structural, axial pullout, uplift and downdrag forces as described above using load-transfer functions to relate base pressures and skin friction with displacements. Some load-transfer functions available in program AXILTR are presented in Figure 3-22. AXILTR also calculates the load and displacement distribution with depth permitting evaluation of the load distribution illustrated in Figures 3-19 to 3-21. Refer to Appendix C for example applications of AXILTR for pullout, uplift, and downdrag loads.

(a) Load-transfer principle. Vertical loads are transferred from the top of the shaft to the supporting soil adjacent to the shaft using skin friction-load transfer functions and to soil beneath the base using base load-transfer functions or consolidation theory. The total bearing capacity of the shaft $Q_u = Q_{su} + Q_{bu}$ is given by equation 3-1. The program should be used to provide a minimum and maximum range for the load-displacement behavior for given soil conditions.

(b) Base resistance. The maximum base resistance q_{bu} in equation 3-1b is computed by AXILTR from equation 3-5b. Correction factors ζ are considered equal to unity. Program AXILTR does not set a limit for σ'_L. For effective stress analysis, N_q is evaluated by equation 3-24 for local shear and by equation 3-10 for general shear. For effective stress analysis, N_c is given by equation 3-8a. For total stress analysis, N_c is equal to 9 when general shear is specified and 7 when local shear is specified. In total stress analysis, the angle of internal friction ϕ is zero. Additional resistance provided by an underream to pullout loads or uplift thrust is seven-ninths (7/9) of the end-bearing resistance.

(c) Base displacement. Base displacement is computed using the Reese and Wright (1977) or Vijayvergiya (1977) base load-transfer functions (Figure 3-22a) or consolidation theory. Ultimate base displacement for the Reese and Wright model is

$$\rho_{bu} = 2B_b \cdot \epsilon_{50} \tag{3-34}$$

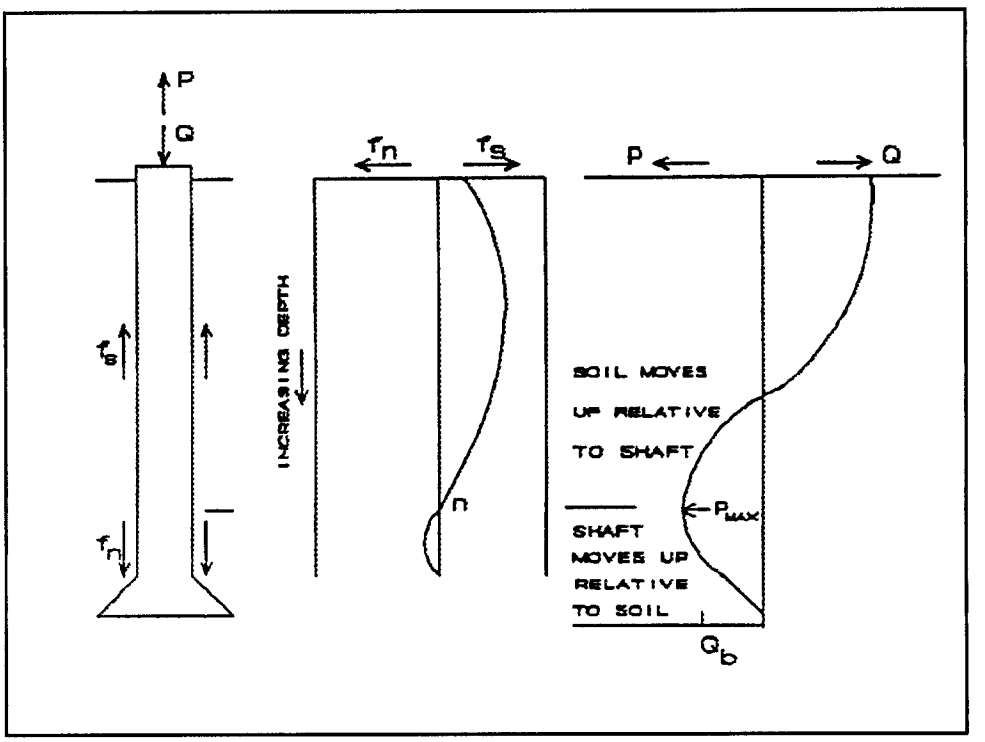

Figure 3-20. Deep foundation resisting uplift thrust

where

ρ_{bu} = ultimate base displacement, inches

B_b = base diameter, inches

ϵ_{50} = strain at 1/2 of maximum deviator stress from consolidated undrained or unconsolidated undrained triaxial test conducted at a confining pressure equal to the soil overburden pressure, fraction

Typical values for ϵ_{50} are 0.007, 0.005, and 0.004 for stiff clays with cohesion C_u of 1 to 2, 2 to 4, and 4 to 8 ksf, respectively (FHWA-RD-85-106). The ultimate base displacement ρ_{bu} for the Vijayvergiya model is 4 percent of the base diameter, where ρ_{bu} occurs at loads equal to the bearing resisting force of the soil Q_{bu}. Plunging failure occurs if an attempt is made to apply greater loads. Base displacement from consolidation theory is calculated relative to the initial effective stress on the soil beneath the base of the shaft prior to placing the structural loads. AXILTR may calculate large settlements for small applied loads on the shaft if the preconsolidation stress (maximum past pressure) is less than the initial effective stress (i.e., an underconsolidated soil). Effective stresses in the soil below the shaft base caused by shaft loads are calculated using the Boussinesq stress theory.

(d) Skin resistance. The shaft skin friction load-transfer functions applied by AXILTR as shown in Figure 3-22b are the Seed and Reese (1957) model, and of Kraft, Ray, and Kagawa (1981) models. The Kraft, Ray, and Kagawa model requires an estimate of a curve fitting constant R that can be obtained from

$$G = G_i\left[1 - \frac{\tau R}{\tau_{max}}\right] \tag{3-35}$$

where

G = soil shear modulus at an applied shear stress τ, ksf

G_i = initial shear modulus, ksf

τ = shear stress, ksf

τ_{max} = shear stress at failure, ksf

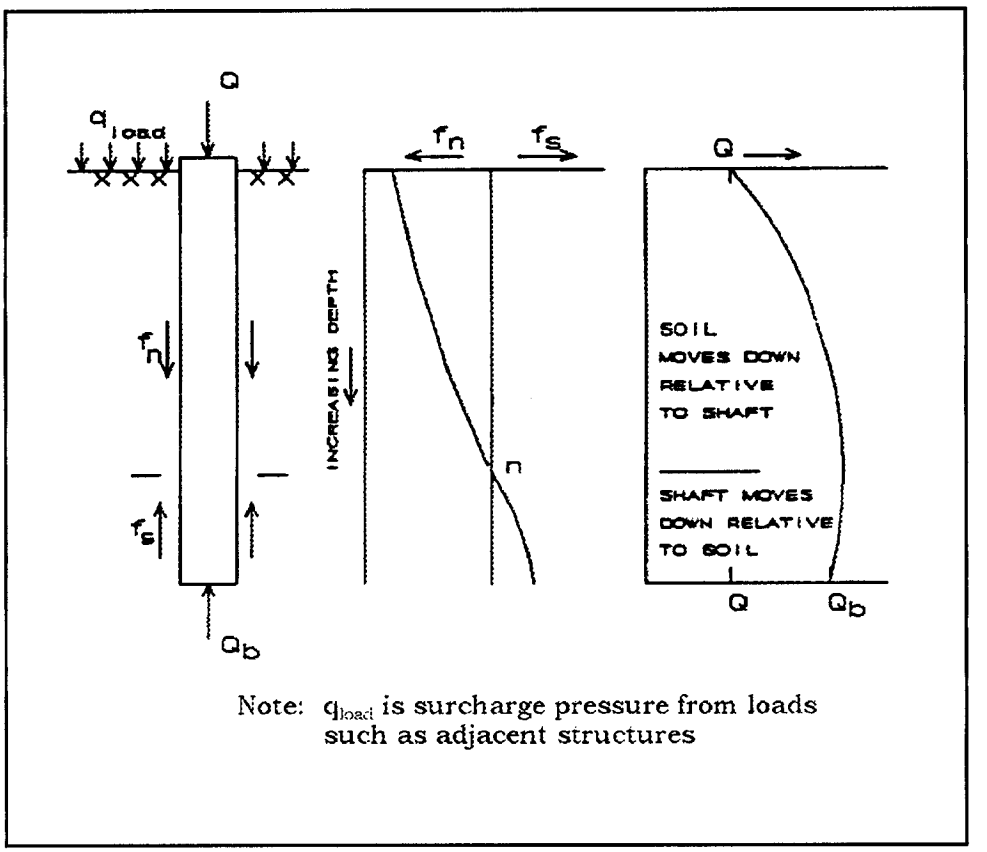

Figure 3-21. Deep foundation resisting downdrag

R = curve fitting constant, usually near 1.0

Curve fitting constant R is the slope of $1 - G/G_i$ versus τ/τ_{max} and should be assumed unity it not known.

(e) Other load-transfer functions. Other functions may be input into AXILTR for each soil layer up to 11. Each function consists of 11 data points that are the ratio of the mobilized skin friction/maximum mobilized skin friction f_s/f_{su} correlated with displacement such as in Figure 3-22b. The value f_{su} is taken as the soil shear strength if not known. The 11 displacement points in meters (inches) are input only once and become applicable to all of the load-transfer functions; therefore, f_s/f_{su} of each load-transfer function must be correlated with displacement.

(f) Influence of soil movement. Soil movement, whether heave or settlement, alters shaft performance. The magnitude of soil heave or settlement is calculated in AXILTR using swell or recompression indexes, compression indexes, swell pressure of each soil layer, maximum past pressure, water table depth, and depth of the soil that is subject to soil movement. The swell index is the slope of the rebound log pressure/void ratio curve of consolidation test results as described in ASTM D 4546. The recompression index is the slope of the log pressure/void ratio curve for pressures less than the maximum past pressure. AXILTR assumes that the swell and recompression indexes are the same. The compression index is the slope of the linear portion of the log pressure-void ratio for pressures exceeding the maximum past pressure. The maximum past pressure is the greatest effective pressure applied to a soil. Swell pressure is defined as the pressure when it prevents soil swell described in Method C of ASTM D 4546.

e. Load-dispalcement relationship. Settlement for given loads should be estimated to check that the expected settlement will be within acceptable limits. Load-displacement relationships are estimated by theory of elasticity and empirical load-transfer relationships. Settlement analysis using computer programs based on nonlinear load-transfer functions applicable to actual soil conditions are also reasonably reliable and cost effective. The skin friction and base load transfer curves should be used together to estimate

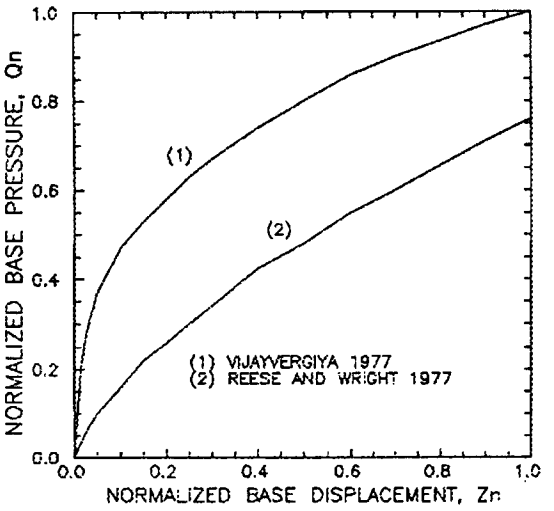

$$Q_n = \frac{\text{BASE PRESSURE, } q_b}{\text{ULTIMATE BASE PRESSURE, } q_{bu}}$$

$$Z_n = \frac{\text{BASE DISPLACEMENT, } \rho_b}{\text{ULTIMATE BASE DISPLACEMENT, } \rho_{bu}}$$

a. BASE TRANSFER (q-z) FUNCTIONS

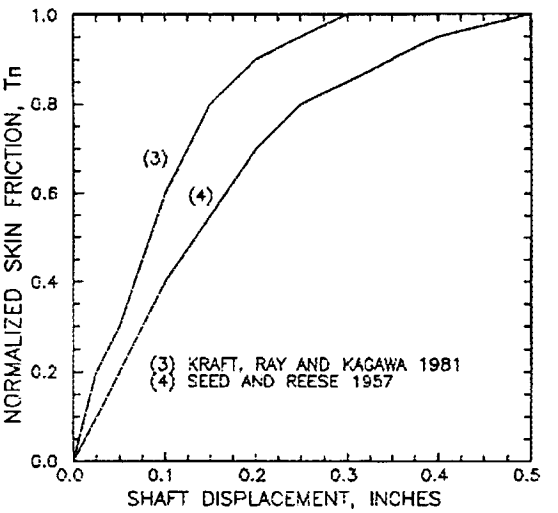

$$T_n = \frac{\text{MOBILIZED SKIN FRICTION, } f_s}{\text{MAXIMUM MOBILIZED SKIN FRICTION, } f_{su}}$$

$$\rho_s = \text{SHAFT DISPLACEMENT, INCHES}$$

b. SHAFT TRANSFER (t-z) FUNCTIONS

Figure 3-22. Load-transfer curves used in AXILTR

settlement for a wide variety of load conditions and to provide a complete analysis of load-displacement behavior. Settlement due to consolidation and creep are site specific and will be considered depending on the types of soils in which the foundation is to be constructed.

(1) Elastic method. Linear elastic analysis is used to determine short-term settlement, but may underestimate long-term settlement. Loads at the pile or shaft base applied to underlying soil should be checked for consolidation settlement using methods in TM 5-818-1 of AXILTR if a highly compressible soil layer exists beneath the tip. The Randolph and Wroth method (1978) is recommended to quickly estimate settlement for piles or straight shafts:

$$\rho = \frac{Q\xi\mu}{2\pi G_L' \tanh(\mu L)} \qquad (3\text{-}36a)$$

A similar equation for underreamed shafts can be deduced as follows:

$$\rho = \frac{Q\xi\mu\eta(1 - \nu_s)}{2[\pi\eta(1 - \nu_s)\tanh(\mu L) + \xi B_b \mu]G_L'} \qquad (3\text{-}36b)$$

where

$$\xi = \ln\left[\frac{5LG_L'\eta(1 - \nu_s)}{B_s G_L}\right]$$

$$\mu = \left[\frac{8G_L}{\xi E_p B_s^2}\right]^{1/2}$$

L = embedded length of pile of shaft, feet

Q = applied load, kips

ρ = settlement for load Q, feet

ν_s = Poisson's ratio

η = interaction factor of upper with lower soil layer, $0.85B_s/B_b$

E_p = shaft elastic modulus, ksf

G_L = soil shear modulus at depth L, ksf

G_L' = average soil shear modulus, ksf

B_b = base diameter, feet

B_s = shaft diameter, feet

This method accounts for local softening or a weak stratum near the shaft.

(2) Semiempirical method. Total settlement for piles or drilled shafts ρ (Vesic 1977) is

$$\rho = \rho_p + \rho_b + \rho_s \qquad (3\text{-}37)$$

where

ρ = total settlement at the pile or shaft top, feet

ρ_p = settlement from axial pile or shaft deformation, feet

ρ_b = tip (base) settlement from load transferred through the shaft to the tip, feet

ρ_s = tip settlement from load transmitted to the soil from skin friction along the shaft length, feet

(a) Axial compression (Vesic 1977) is

$$\rho_p = (Q_b + \alpha_s Q_s)\frac{L}{AE_p} \qquad (3\text{-}38a)$$

where

Q_b = load at the pile tip, kips

α_s = load distribution factor along pile length, 0.5 to 0.7; usually assume 0.5

Q_s = load taken by skin friction, kips

L = pile or shaft length, feet

A = cross section area of pile, feet^2

E_p = pile or shaft modulus of elasticity, ksf

Axial compression should usually be calculated by assuming that $Q_s = Q_{su}$, the ultimate skin resistance in equation 3-1 or 3-3, because most skin friction will be mobilized before end bearing is significant, unless the pile is bearing on a hard stratum. The value of Q_b is then calculated by subtracting Q_s from the design load Q_d. Otherwise, loads Q_b and Q_s supporting the pile load Q_d should be estimated using load-transfer curves as follows:

(b) Settlement at the pile or shaft tip (Vesic 1977) is

$$\rho_b = \frac{C_b Q_b}{B_s q_{bu}} \qquad (3\text{-}38b)$$

$$\rho_s = \frac{C_s Q_s}{L q_{bu}} \qquad (3\text{-}38c)$$

where

C_b = empirical tip coefficient, Table 3-10

C_s = empirical shaft coefficient, $[\, 0.93 + 0.16\,(L/B_s)^{0.5}\,]\, C_b$

Table 3-10
Empirical Tip Coefficient C_b

Soil	Driven Piles	Drilled Shafts
Sand (dense to loose)	0.02 to 0.04	0.09 to 0.18
Clay (stiff to soft)	0.02 to 0.03	0.03 to 0.06
Silt (dense to loose)	0.03 to 0.05	0.09 to 0.12

The bearing stratum extends a minimum $10B_b$ beneath the pile or shaft tip, and stiffness in this stratum is equal to or greater than stiffness at the tip elevation. C_b will be less if rock is closer to the pile tip than $10B_b$. Settlement is $0.88\rho_b$ if rock exists at $5B_b$ and 0.5ρ if rock is B below the pile or shaft tip. Consolidation settlement should not be significant and should not exceed 15 percent of the total settlement.

(3) Load-transfer functions. Skin friction *t-z* curves and base resistance *q-z* curves may be used to transfer vertical loads to the soil. Curves in Figure 3-23 for clays and Figure 3-24 for sands were determined from drilled shafts with internal instruments for separating skin friction and base resistance. These curves include elastic compression and may be used to estimate settlements ρ_s and ρ_b which include ρ_p for shafts < 20 feet long. The value ρ_p from equation 3-38a should be added for long shafts.

(4) Computer programs. Programs available at WES for estimating settlement from axial loads using base and shaft load-transfer functions are CAXPILE and AXILTR. These programs may be applied to either piles or shafts and consider multilayer soils. Some load-transfer functions are included and others may be input. Noncircular piles or shafts should be converted to circular cross sections by assuming equivalent area for square or rectangular cross sections. The cross-sectional area of H-piles calculated as the flange width b_f times section depth d, shown in Table 1-3, should be converted to an equivalent circular cross section.

(a) CAXPILE. This program considers downward vertical loads on shaft with variable diameter (WES Instruction Report-K-84-4).

(b) AXILTR. This program, Appendix C (available from the Soil and Rock Mechanics Division, Geotechnical Laboratory, U.S. Army Engineer Waterways Experiment Station), considers straight shafts with uniform cross sections are/or underreamed drilled shafts. AXILTR calculates settlement or uplift of piles caused by pullout loads and by soil heave or settlement.

f. Application. A drilled shaft is to be constructed in expansive soil characterized as two layers as shown in the tabulation on the following page. Soil Poisson's ratio $\nu_s = 0.4$. The shaft elastic modulus E_p = 432,000 ksf. A cone penetration test indicated q_c > 24 ksf. The shaft must support a design load Q_d = 300 kips with displacement less than 1 inch. The FS = 3. A schematic diagram of this shaft divided into 50 increments NEL = 50 and placed 10 feet into layer 2 is given in Figure C-1. Solution for the design according to Table 3-8 is given in Table 3-11. The shaft should also be checked for structural integrity as described in Chapter 2.

Parameter	Layer 1 0 - 40 ft	Layer 2 40 - 50 ft
Specific gravity, G_s	2.68	2.65
Initial void ratio, e_o	0.80	0.37
Water content, percent	30.00	13.10
Swell pressure, σ_s, ksf	4.80	6.00
Swell index, C_s	0.10	0.10
Compression index, C_c	0.20	0.20
Cohesion, C_u, ksf	2.00	4.00
Friction angle, ϕ, deg	0.00	0.00
Coefficient of earth pressure at rest, K_o	0.70	2.00
Maximum past pressure, σ_p, ksf	7.00	10.00
Plasticity index, PI, percent	38.00	32.00
Liquid limit, *LL*, percent	70.00	60.00
Elastic soil modulus, E_s, ksf	400.00	1,000.00
Shear soil modulus, *G*, ksf	143.00	357.00

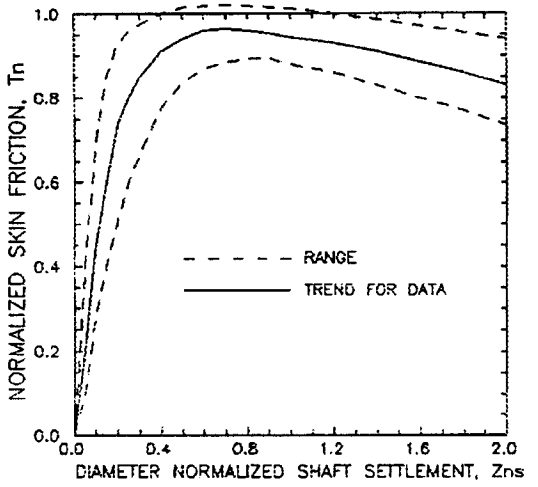

$$T_n = \frac{\text{MOBILIZED SKIN FRICTION, } f_s}{\text{MAXIMUM MOBILIZED SKIN FRICTION, } f_{su}}$$

$$Z_{ns} = \frac{\text{SETTLEMENT, } \rho_s}{\text{SHAFT DIAMETER, } B_s}, \text{ PERCENT}$$

b. SHAFT TRANSFER (t-z) FUNCTION

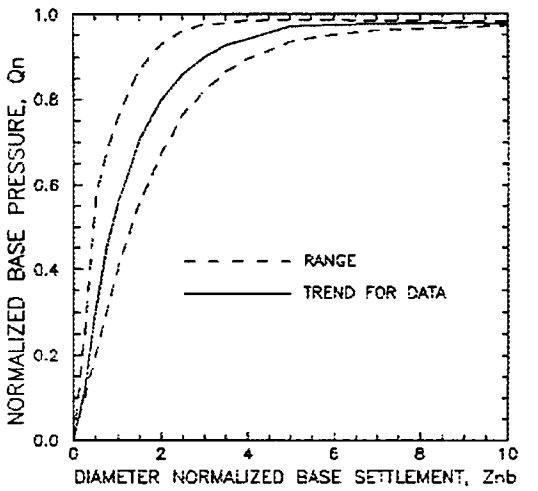

$$Q_n = \frac{\text{END BEARING PRESSURE, } q_b}{\text{ULTIMATE END BEARING, } q_{bu}}$$

$$Z_{nb} = \frac{\text{BASE SETTLEMENT, } \rho_b}{\text{BASE DIAMETER, } B_b}, \text{ PERCENT}$$

a. BASE TRANSFER (q-z) FUNCTION

Figure 3-23. General load-transfer curves for clay

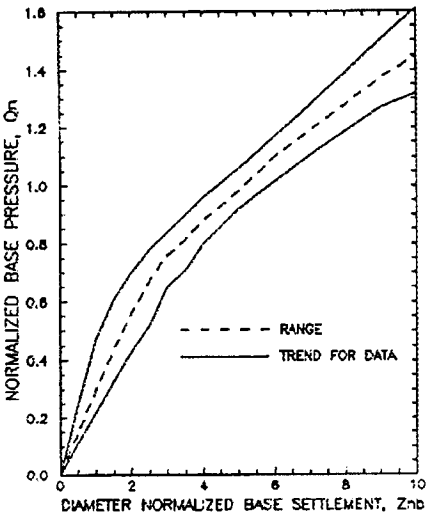

$$Q_n = \frac{\text{END BEARING PRESSURE, } q_b}{\text{ULTIMATE END BEARING, } q_{bu}}$$

$$Z_{nb} = \frac{\text{BASE SETTLEMENT, } \rho_b}{\text{BASE DIAMETER, } B_b}, \text{ PERCENT}$$

a. BASE TRANSFER (q-z) FUNCTION

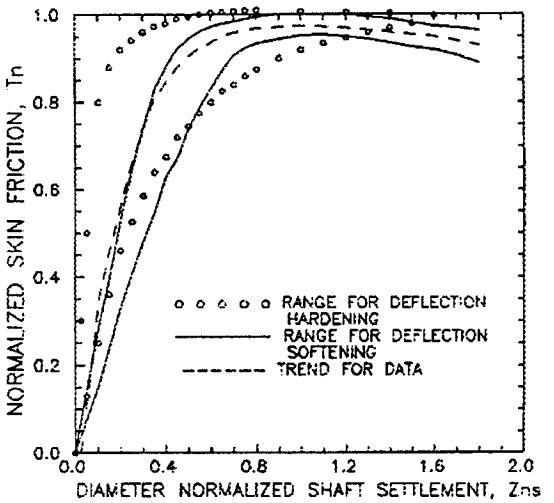

$$T_n = \frac{\text{MOBILIZED SKIN FRICTION, } f_s}{\text{MAXIMUM MOBILIZED SKIN FRICTION, } f_{su}}$$

$$Z_{ns} = \frac{\text{SETTLEMENT, } \rho_s}{\text{SHAFT DIAMETER, } B_s}, \text{ PERCENT}$$

b. SHAFT TRANSFER (t-z) FUNCTION

Figure 3-24. General load-transfer curves for sand

Table 3-11
Application of Drilled Shaft Design

Step	Procedure	Description
1	Select shaft length	The shaft is selected to penetrate 10 ft into layer 2, a firm stratum, with L = 50 ft; additional analyses can be performed with L < 50 ft to determine an optimum length
2	Evaluate q_{bu}	From equation 3-22, $q_{bu} = F_r N_c C_c \leq 80$ ksf $F_r = 1, \quad C_u = 4$ ksf, $N_c = 6[(1 + 0.2(L/B_b)] \leq 9$ $= 6[1 + 0.2(50/5)] = 18$; so $N_c = 9$ $q_{bu} = 1 \times 9 \times 4 = 36$ ksf
3	Evaluate f_{sui}	From equation 3-16, $f_{sui} = \alpha_a \times C_u$ Layer 1, equation 3-26b: 0-40 ft $\alpha_a = 0.9 - 0.01PI$ $= 0.9 - 0.01 \times 38$ $= 0.52$ $f_{su1} = 0.52 \times 2 = 1.04$ ksf Layer 2, equation 3-26a: 50 - 60 ft $\alpha_a = 0.7 - 0.01PI$ $= 0.7 - 0.1 \times 32$ $= 0.38$ $f_{su2} = 0.38 \times 4 = 1.52$ ksf From Table 3-8, $\alpha_a = 0.55$ Layer 1: $f_{su1} = 0.55 \times 2$ $= 1.1$ ksf ≤ 5.5 ksf Layer 2: $f_{su2} = 0.55 \times 4$ $= 2.2$ ksf ≤ 5.5 ksf

Table 3-11 (Continued)

Step	Procedure	Description
4	Evaluate Q_{bu} and Q_{su} for the shaft and base diameters	From equation 3-1b, $Q_{bu} = q_{bu} \times A_b = 36 \times \pi \times 2.5^2 = 706.9$ kips From equation 3-3, $Q_{sui} = A_{si} f_{sui} = \pi B_s \Delta L f_{sui}$ $Q_{su1} = \pi \times 2 \times 35 \times f_{su1} = 219.9 f_{su1}$ $Q_{su2} = \pi \times 2 \times 5 \times f_{su2} = 31.4 f_{su2}$ From equations 3-26, $Q_{su1} = 219.9 \times 1.04 = 228.7$ kips $Q_{su2} = 31.4 \times 1.52 = 47.7$ kips $Q_{su} = 228.7 + 47.7 = 276.4$ kips From Table 3-8, $\alpha_s = 0.55$ $Q_{su1} = 219.9 \times 1.1 = 241.9$ kips $Q_{su2} = 31.4 \times 2.2 = 69.1$ kips $Q_d = 300 < 327.8 = Q_a$; okay $Q_{su} = 241.9 + 69.1 = 311.0$ kips Select the least Q_{su} = 276.4 kips
5	Check $Q_d \leq Q_a$	$Q_u = Q_{bu} + Q_{su}$ $= 706.9 + 276.4 = 983.3$ kips; $Q_a = 983.3/3 = 327.8$ kips
6	Evaluate shaft for other loads	Figure C-2c, Appendix C, for this shaft in expansive soil indicates heave < 1 inch even when subject to 300-kip pullout force
7	Evaluate maximum settlement ρ for given Q_d	From equation 3-36b, $\rho = \frac{12 Q \xi \mu \eta (1 - \nu_s)}{2 [\pi \eta (1 - \nu_s) \tanh(\mu L) + \xi B_b \mu] G_L'}$ $= \frac{12 \times 300 \times 2.323 \times 0.34 \times 0.6 \times 0.267}{2 [\pi \times 0.34 \times 0.6 \times 0.87 + 2.323 \times 5 \times 0.0267] \times 143}$ $= 0.18$ inch

Table 3-11 (Continued)

Step	Procedure	Description

where

$$\xi = \ln\left[\frac{5LG_L'\eta(1 - \nu_s)}{B_sG_L}\right]$$

$$= \ln\left[\frac{5 \times 50 \times 143 \times 0.34(1 - 0.4)}{2 \times 357}\right]$$

$$= 2.323$$

$$\mu = \left[\frac{8G_L}{\xi EB_s^2}\right]^{1/2}$$

$$= \left[\frac{8 \times 357}{2.323 \times 432{,}000 \times 2^2}\right]^{1/2}$$

$$= 0.0267$$

$$\tanh \mu L = \tanh 1.335 = 0.87$$

$$\eta = 0.85 \times (B_s/B_b) = 0.85 \times (2/5) = 0.34$$

$$G_L = 357 \text{ ksf}$$

$$G_L' = 143 \text{ ksf}$$

From equation 3-37,

$$\rho = \rho_p + \rho_b + \rho_s$$

From equation 3-38a,

$$\rho_p = (Q_b + \alpha_s Q_s)\frac{L}{AE}$$

$$= (23.6 + 0.5 \times 276.4)\frac{50}{\pi 1^2 \times 432{,}000}$$

$$= 0.07 \text{ inch}$$

where

$$Q_s = Q_{su} = 276.4 \text{ kips}$$

$$Q_b = Q_d - Q_s = 300 - 276.4 = 23.6 \text{ kips}$$

Table 3-11 (Continued)

Step	Procedure	Description

From equation 3-38b,

$$\rho_b = \frac{12 C_b Q_b}{B_s q_{bu}}$$

$$= \frac{12 \times 0.06 \times 23.6}{2 \times 36}$$

$$= 0.24 \text{ inch}$$

From equation 3-38c,

$$\rho_s = \frac{12 C_s Q_s}{L q_{bu}}$$

$$= \frac{12 \times 0.1 \times 276.4}{50 \times 36}$$

$$= 0.18 \text{ inch}$$

where

$$C_s = [0.93 + 0.16(L/B_s)^{0.5}] C_b$$

$$= [0.93 + 0.16(50/2)^{0.5}] \times 0.06$$

$$= 0.1$$

Therefore,

$$\rho = 0.07 + 0.24 + 0.18 = 0.49 \text{ inch}$$

Settlement should be < 0.49 inch because resistance from the 5-ft underream is disregarded

From Figure 3-23, base load-transfer functions (assume 90-percent skin friction is mobilized:

$$Q_b = Q_d - 0.9 Q_{su}$$

$$= 300 - 248.8 = 51.2 \text{ kips}$$

$Q_b/Q_{bu} = 51.2/706.9 = 0.07$; therefore,

$Z_{nb} = 0.2$ percent Figure 3-23a

$$\rho = 12 \times B_b Z_{nb}/100$$

$$= 12 \times 5 \times 0.2/100 = 0.12 \text{ inch}$$

Shaft: assume $f_s/f_{su} = 0.9$; therefore,

$Z_{ns} = 0.4$ percent from Figure 3-23b

Table 3-11 (Concluded)

Step	Procedure	Description
		$\rho = 12 \times B_s Z_{ns}/100$ $= 12 \times 2 \times 0.4/100 = 0.10$ inch
		The shaft is longer than 20 ft, $\rho_p = 0.07$ inch must be added to determine total settlement ρ
		$\rho = 0.07 + 0.12 + 0.10 = 0.29$ inch
		Program AXILTR , Figure C-2a, Appendix C, indicates 0.2 inch for a 300-kip load using $\alpha_e = 0.9$
		All of the above analyses indicate total settlement < 0.5 inch
8	Check computed ≤ specified settlement	Specified settlement is 1.0 inch; this exceeds the calculated settlement; okay

Chapter 4[1]
Lateral Loads

1. Description of the Problem

a. Design philosophy. Deep foundations must often support substantial lateral loads as well as axial loads. While axially loaded, deep foundation elements may be adequately designed by simple statis methods, design methodology for lateral loads is more complex. The solution must ensure that equilibrium and soil-structure-interation compatability are satisfied. Nonlinear soil response complicates the solution. Batter piles are included in pile groups to improve the lateral capacity when vertical piles alone are not sufficient to support the loads.

b. Cause of lateral loads. Some causes of lateral loads are wind forces on towers, buildings, bridges and large signs, the centripetal force from vehicular traffic on curved highway bridges, force of water flowing against the substructure of bridges, lateral seismic forces from earthquakes, and backfill loads behind walls.

c. Factors influencing behavior. The behavior of laterally loaded deep foundations depends on stiffness of the pile and soil, mobilization of resistance in the surrounding soil, boundary conditions (fixity at ends of deep foundation elements), and duration and frequency of loading.

2. Nonlinear Pile and *p-y* Model for Soil.

a. General concept. The model shown in Figure 4-1 is emphasized in this document. The loading on the pile is general for the two-dimensional case (no torsion or out-of-plane bending). The horizontal lines across the pile are intended to show that it is made up of different sections; for example, steel pipe could be used with the wall thickness varied along the length. The difference-equation method is employed for the solution of the beam-column equation to allow the different values of bending stiffness to be addressed. Also, it is possible, but not frequently necessary, to vary the bending stiffness with bending moment that is computed during interation

b. Axial load. An axial load is indicated and is considered in the solution with respect to its effect on bending and not in regard to computing the required length to support a given axial load. As shown later, the computational procedure allows the detrmination of the axial load at which the pile will buckle.

c. Soil representation. The soil around the pile is replaced by a set of mechanisms indicating that the soil resistance p is a nonlinear function of pile deflection y. The mechanisms, and the corresponding curves that represent their behavior, are widely spaced but are considered to be very close in the analysis. As may be seen in Figure 4-1, the *p-y* curves are fully nonlinear with respect to distance x along the pile and pile deflection y. The curve for $x = x_1$ is drawn to indicate that the pile may deflect a finite distance with no soil resistance. The curve at $x = x_2$ is drawn to show that the soil is deflection-softening. There is no reasonable limit to the variations that can be employed in representing the response of the soil to the lateral deflection of a pile.

d. The p-y curve method. The *p-y* method is extremely versatile and provides a practical means for design. The method was suggested over 30 years ago (McCelland and Focht 1958). Two developments during the 1950's made the method possible: the digital computer for solving the problem of the nonlinear, fourth-order differential equation for the beam-column; and the remote-reading strain gauge for use in obtaining soil-response (*p-y*) curves from field experiments. The method has been used by the petroleum industry in the design of pile-supported platforms and extended to the design of onshore foundations as, for example by publications of the Federal Highway Administration (USA) (Reese 1984).

(1) Definition of p and y. The definition of the quantities p and y as used here is necessary because other approaches have been used. The sketch in Figure 4-2a shows a uniform distribution of unit stresses normal to the wall of a cylindrical pile. This distribution is correct for the case of a pile that has been installed without bending. If the pile is caused to deflect a distance y (exaggerated in the sketch for clarity), the distribution of unit stresses would be similar to that shown in Figure 4-2b. The stresses would have decreased on the back side of the pile and increased on the front side. Both normal and a shearing stress component may developed along the perimeter of the cross section. Integration of the unit stresses will result in the quanity p which acts opposite in direction to y. The dimensions of p are load per unit length along the pile. The definitions of p and y that are presented are convenient in the solution of the differential equation and are consistent with the quantities used in the solution of the ordinary beam equation.

(2) Nature of soil response. The manner in which the soil responds to the lateral deflection of a pile can be examined by examined by considering the pipe pile shown

[1]Portions of this chapter were abstracted from the writings of Dr. L. C. Reese and his colleagues, with the permission of Dr. Reese.

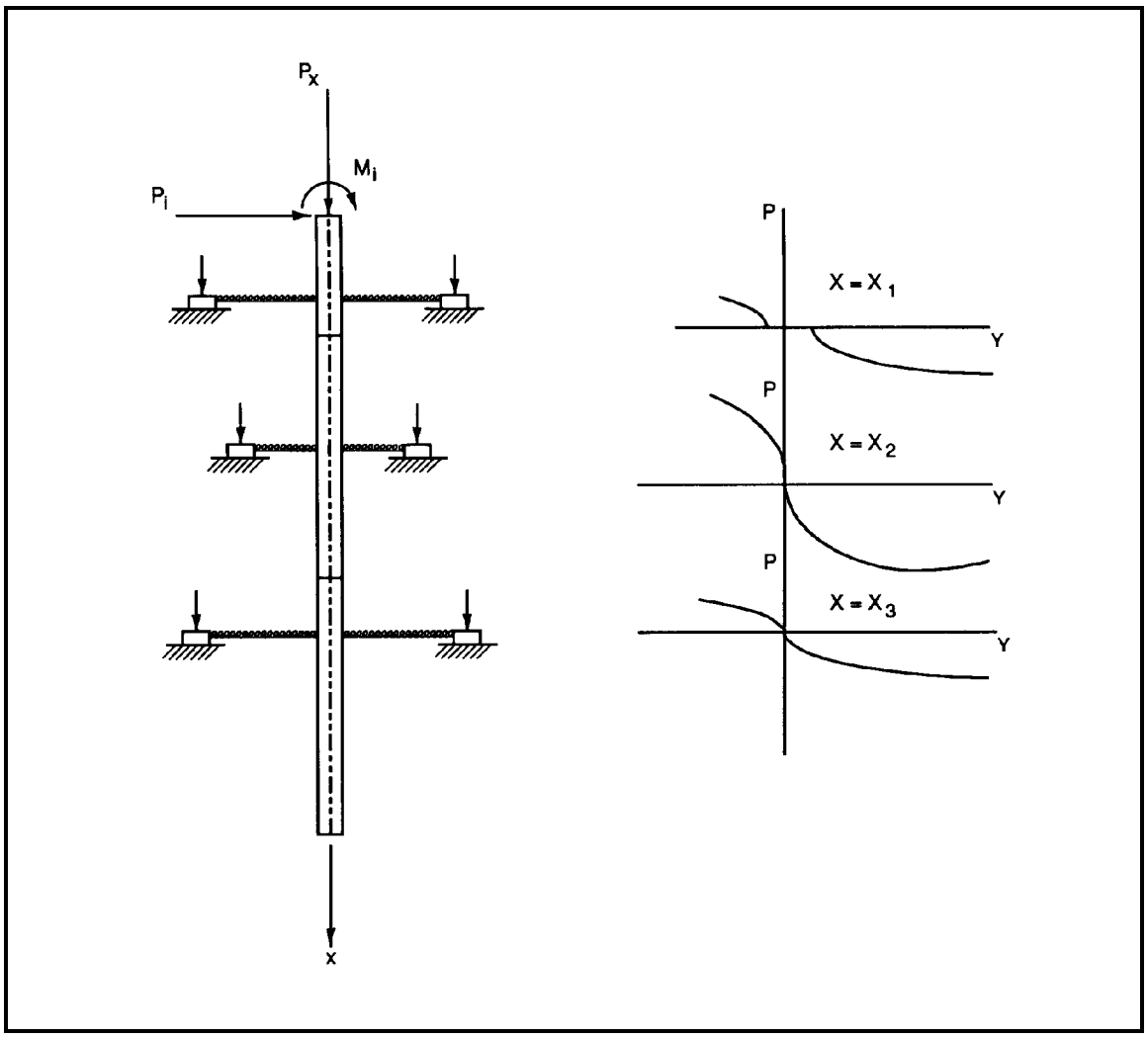

Figure 4-1. Model of pile under lateral loading with *p-y* curves

in Figure 4-3. Two slices of soil are indicated; the element *A* is near the ground surface and the element *B* is several diameters below the ground surface. Consideration will be given here to the manner in which those two elements of soil react as the pile deflects under an applied lateral load. Figure 4-4 shows a *p-y* curve that is conceptual in nature. The curve is plotted in the first quadrant for convenience and only one branch is shown. The curve properly belongs in the second and fourth quadrants because the soil response acts in opposition to the deflection. The branch of the *p-y* curves 0-a is representative of the elastic action of the soil; the deflection at point *a* may be small. The branch *a-b* is the transition portion of the curve. At point *b* the ultimate soil resistance is reached. The following paragraphs will deal with the ultimate soil resistance.

(a) Ultimate resistance to lateral movement. With regard to the ultimate resistance at element *A* in Figure 4-3, Figure 4-5 shows a wedge of soil that is moved up and away from a pile. The ground surface is represented by the plane ABCD, and soil in contact with the pile is represented by the surface CDEF. If the pile is moved in the direction indicated, failure of the soil in shear will occur on the planes ADE, BCF, and AEFB. The horizontal force F_p against the pile can be computed by summing the horizontal components of the forces on the sliding surfaces, taking into account ote gravity force on the wedge of soil. For a given value of *H*, it is assumed that the value of the horizontal force on the pile is

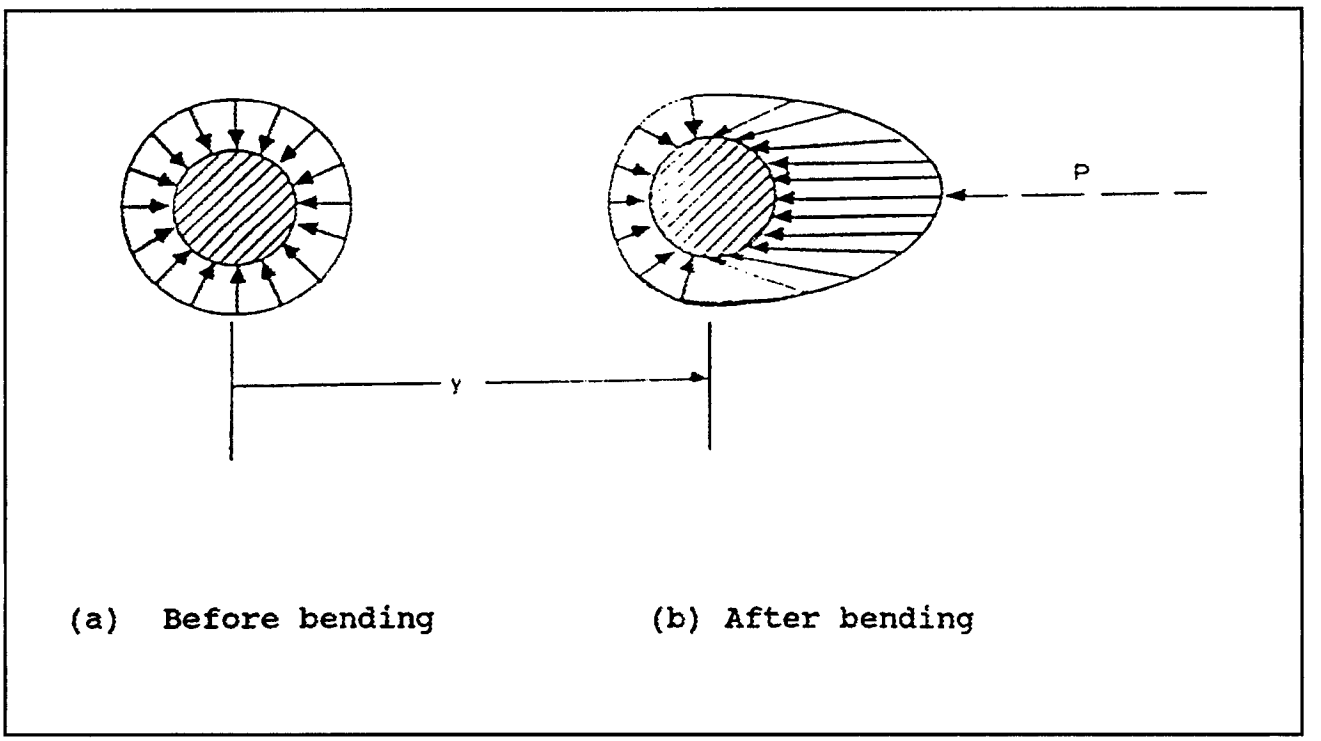

Figure 4-2. Distribution of unit stresses against a pile before and after lateral deflection

F_{p1}. If a second computation is made with the depth of the wedge increased by ΔH, the horizontal force will be F_{p2}. The value of p_u for the depth z where z is equal approximately to $(2H + \Delta H)/2$ can be computed: $(p_u)_z = (F_{p2} - F_{p1})/\Delta H$.

(b) Resistance at ground level. At the ground surface, the value of p_u for sand must be zero because the weight of the wedge is zero and the forces on the sliding surfaces will be zero. At the ground surface for clay, on the other hand, the values of p_u will be larger than zero because the cohesion of the clay, which is independent of the overburden stress, will generate a horizontal force.

(c) Resistance below ground level. A plan view of a pile at several diameters below the ground surface,corresponding to the element at B in Figure 4-3, is shown in Figure 4-6. The potential failure surfaces that are shown are indicative of plane-strain failure; while the ultimate resistance p_u cannot be determined precisely, elementary concepts can be used to develop approximate expressions.

(3) Effects of loading . As will be shown in detail in the next sections, the soil response can be affected by the way the load is applied to a pile. Recommendations are given herein for the cases where the load is short-term (static) or is repeated (cyclic). The latter case is frequently encountered in design. Loadings that are sustained or dynamic (due to machinery or a seismic event) are special cases; the methods of dealing with these types of loading are not well developed and are not addressed herein. The cyclic loading of sands also causes a reduced resistance in sands, but the reduction is much less severe than experienced by clays.

(4) Presence of water. The presence of water will affect the unit weight of the soil and will perhaps affect other properties to some extent; however, water above the ground surface has a pronounced effect on the response of clay soils, particularly stiff clay. Cyclic loading has two types of deleterious effects on clays; there is likely to be (1) strain softening due to repeated deformations and (2) scour at the pile-soil interface. This latter effect can be the most serious. If the deflection of the pile is greater that at point a in Figure 4-4 or certainly if the deflection is greater than that at point b, a space will open as the load is released. The space will fill with water and the water will be pushed upward, or through cracks in the clay, with the next cycle of loading. The velocity of the water cxan be such that considerable quantities of soil are washed ot the ground surface, causing a significant loss in soil resistance.

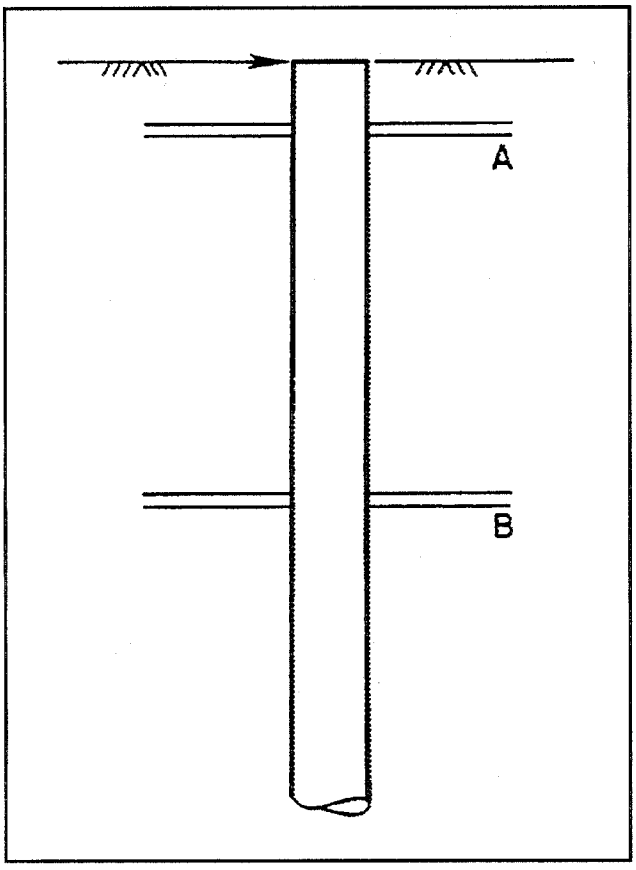

Figure 4-3. Pipe pile and soil elements

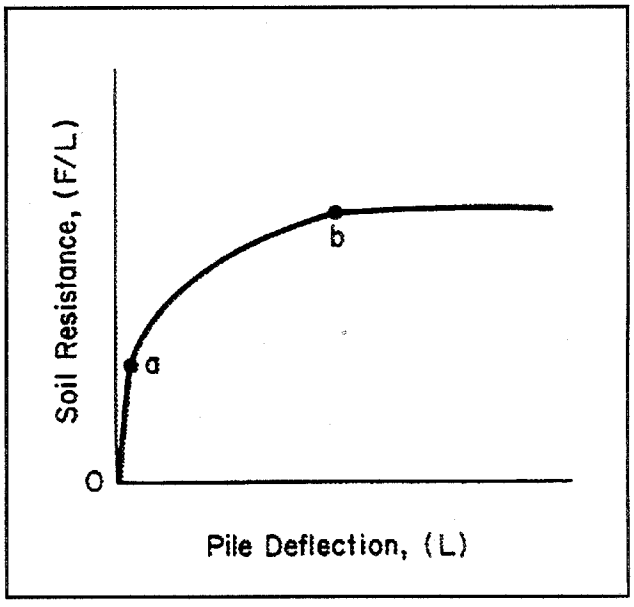

Figure 4-4. Conceptual *p-y* curve

3. Development of *p-y* Curve for Soils

Detailed methods for obtaining *p-y* curves are presented in the following paragraphs. Recommendations are given for clay and sand, for static and cyclic loading, and for cases where the water table is above or below the ground surface. As will be seen, the soil properties that are needed for clay refer to undrained shear strength; there are no provisions for dealing with soils having both c and ϕ parameters.

a. p-y curves for soft clay. As noted earlier, there is a significant influence of the presence of water above the ground surface. If soft clay exists at the ground surface, it is obvious that water must be present at or above the ground surface or the clay would have become desiccated and stronger. If soft clay does not exist at the ground surface but exists at some distance below the ground surface, the deleterious effect of water moving in and out of a gap at the interface of the pile and soil will not occur; therefore, the *p-y* curves for clay above the ground surface should be used (Welch and Reese 1972). The *p-y* curves presented here are for soft clay, with water above the group surface, and the clay experienced the deteriorating effects noted earlier.

(1) Field experiments. Field experiments using full-sized, instrumented piles provide data from which *p-y* curves from static and cyclic loading can be generated. Such experimental curves are correlated with available theory to provide the basis to recommend procedures for developing *p-y* curves. Therefore, field experiments with instrumented piles are essential to the recommendations for *p-y* curves. Matlock (1970) performed lateral load tests employing a steel-pipe pile that was 12.75 inches in diameter and 42 feet long. It was driven into clays near Lake Austin that had a shear strength of about 800 pounds per square foot. The pile was recovered, taken to Sabine Pass, Texas, and driven into clay with a shear strength that averaged about 300 pounds per square foot in the significant upper zone. The studies carried out by Matlock led to the recommendations shown in the following paragraphs.

(2) Recommendations for computing *p-y* curves. The following procedure is for short-term static loading and is illustrated in Figure 4-7a.

(a) Obtain the best possible estimate of the variation with depth of undrained shear strength c and submerged unit weight γ'. Also obtain the values of ε_{50}, the strain corresponding to one-half the maximum principal-stress difference. If no stress-strain curves are available, typical values of ε_{50} are given in Table 4-1.

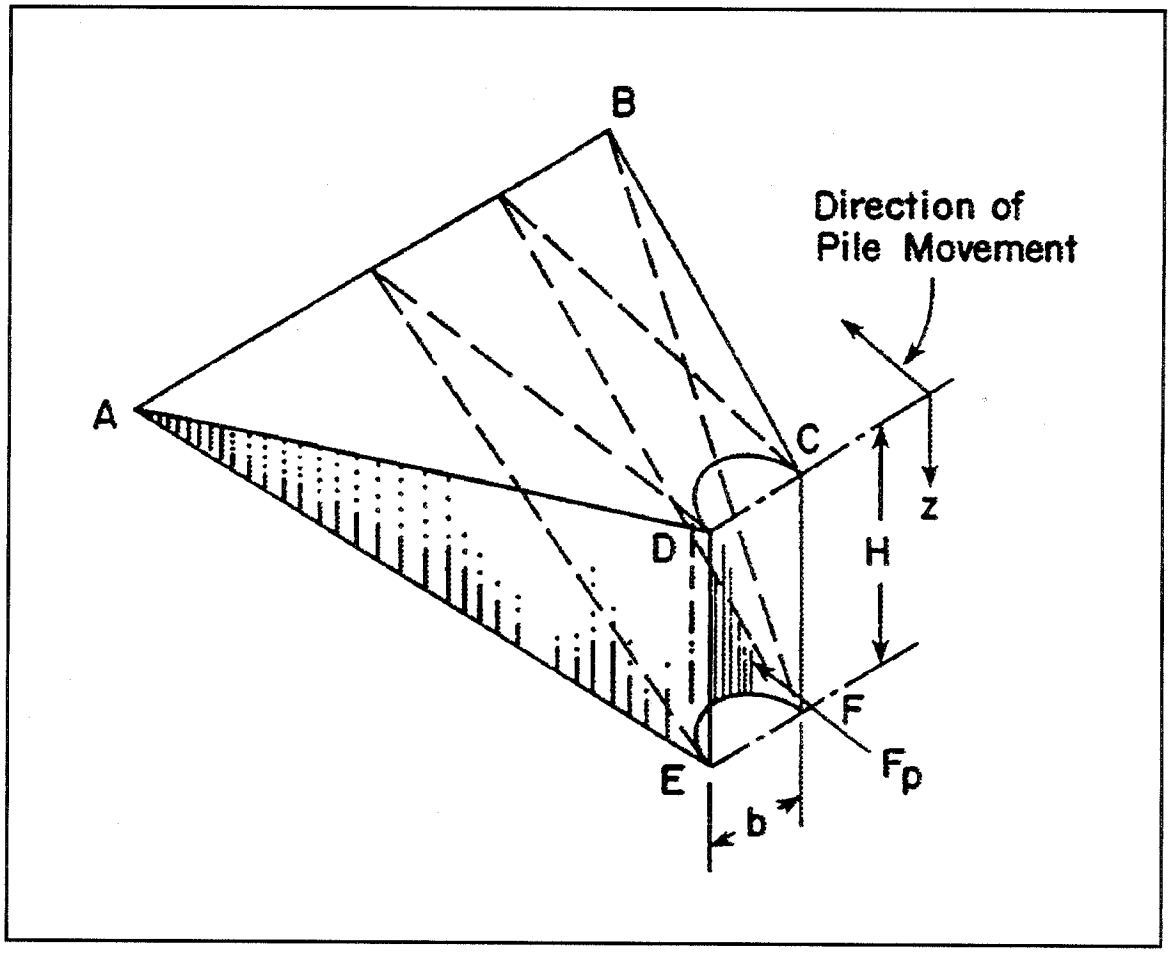

Figure 4-5. Wedge-type failure of surface soil

Table 4-1
Representative Values of ε_{50}

Consistency of Clay	ε_{50}
Soft	0.020
Medium	0.010
Stiff	0.005

(b) Compute the ultimate soil resistance per unit length of pile, using the smaller of the values given by equations below

$$p_u = [3 + \frac{\gamma'}{c} \times + \frac{J}{b} \times]\ cb \qquad (4\text{-}1)$$

$$p_u = 9\ cb \qquad (4\text{-}2)$$

where

p_u = ultimate soil resistance

x = depth from ground surface to p-y curve

γ' = average effective unit weight from ground surface to depth x

c = shear strength at depth x

b = width of pile

J = empirical dimensionless parameter

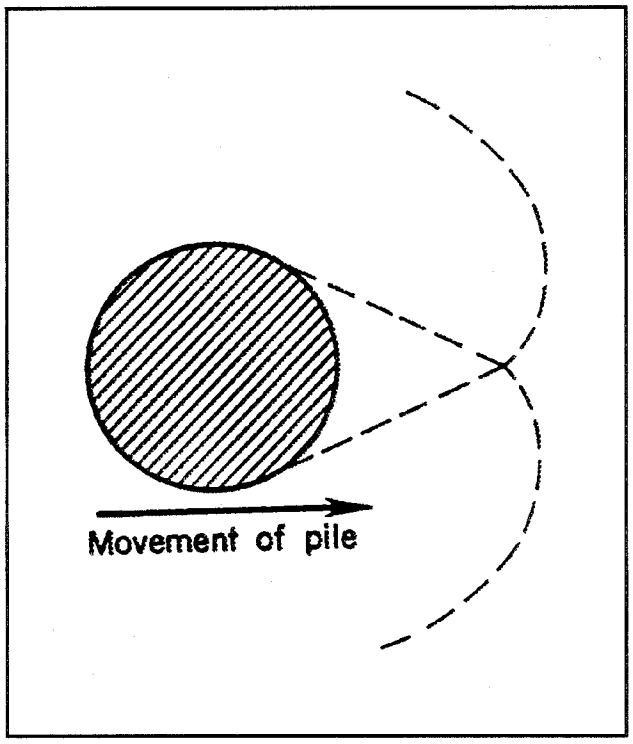

Figure 4-6. Potential failure surfaces generated by pile at several diameters below ground surface

Matlock (1970) stated that the value of J was determined experimentally to be 0.5 for a soft clay and about 0.25 for a medium clay. A value of 0.5 is frequently used for J. The value of p_u is computed at each depth where a p-y curve is desired, based on shear strength at that depth. A computer obtains values of y and the corresponding p-values at close spacings; if hand computations are being done, p-y curves should be computed at depths to reflect the soil profile. If the soil is homogeneous, the p-y curves should be obtained at close spacings near the ground surface where the pile deflection is greater.

(c) Compute the deflection, y_{50}, at one-half the ultimate soil resistance for the following equation:

$$y_{50} = 2.5\ \varepsilon_{50} b \qquad (4\text{-}3)$$

(d) Points describing the p-y curve are now computed from the following relationship.

$$\frac{p}{p_u} = 0.5\left(\frac{y}{y_{50}}\right)^{0.333} \qquad (4\text{-}4)$$

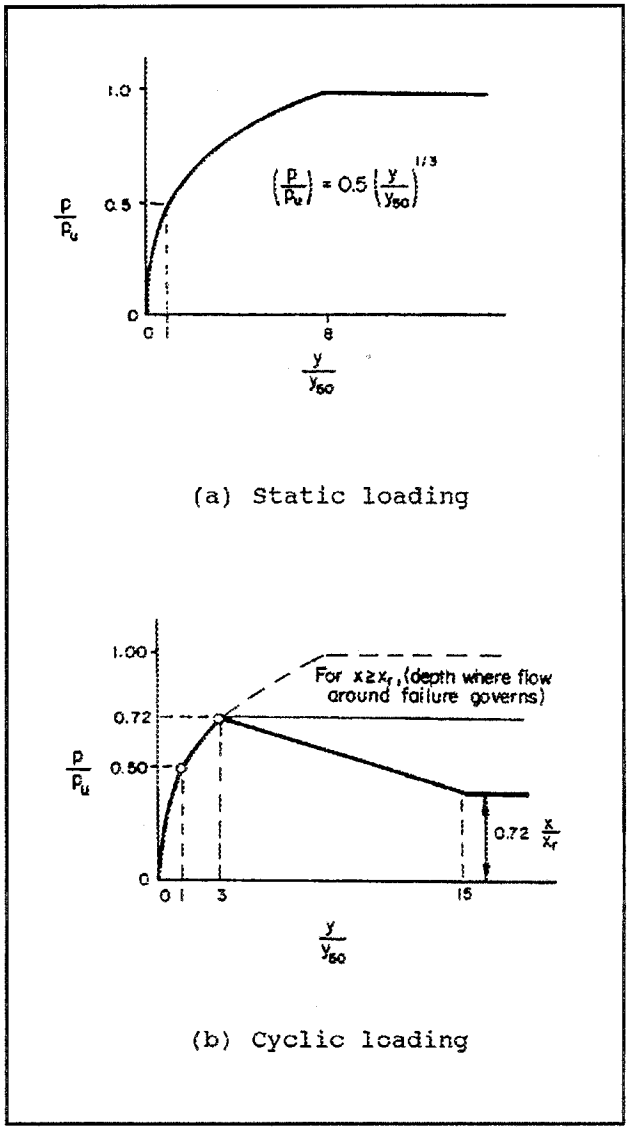

Figure 4-7. Characteristic shapes of the *p-y* curves for soft clay below the water table

The value of p remains constant beyond $y = 8y_{50}$.

(3) Procedure for cyclic loading. The following procedure is for cyclic loading and is illustrated in Figure 4-7b.

(a) Construct the p-y curve in the same manner as for short-term static loading for values of p less than $0.72p_u$.

(b) Solve equations 4-1 and 4-2 simultaneously to find the depth, x_r, where the transition occurs from the wedge-type failure to a flow-around failure. If the unit weight and shear strength are constant in the upper zone, then

$$x_r = \frac{6\ cb}{(\gamma' b + Jc)} \quad (4\text{-}5)$$

If the unit weight and shear strength vary with depth, the value of x_r should be computed with the soil properties at the depth where the *p-y* curve is desired.

(c) If the depth to the *p-y* curve is greater than or equal to x_r, then p is equal to $0.72p_u$ from $y = 3y_{50}$ to $y = 15y_{50}$.

(d) If the depth to the *p-y* curve is less than x_r, then the value of p decreases from $0.72p_u$ at $y = 3y_{50}$ to the value given by the following expression at $y = 15y_{50}$.

$$p = 0.72\ p_u\left(\frac{x}{x_r}\right) \quad (4\text{-}6)$$

The value of p remains constant beyond $y = 15y_{50}$.

(4) Recommended soil tests. For determining the values of shear strength of the various layers of soil for which *p-y* curves are to be constructed, Matlock (1970) recommended the following tests in order of preference:

(a) In situ vane-shear tests with parallel sampling for soil identification.

(b) Unconsolidated-undrained triaxial compression tests having a confining stress equal to the overburden pressure with c being defined as half the total maximum principal stress difference.

(c) Miniature vane tests of samples in tubes.

(d) Unconfined compression tests.

b. p-y curves for stiff clay below the water table.

(1) Field experiments. Reese, Cox, and Koop (1975) performed lateral load tests employing steel-pipe piles that were 24 inches in diameter and 50 feet long. The piles were driven into stiff clay as a site near Manor, TX. The clay had an undrained shear strength ranging from about 1 ton per square foot at the ground surface to about 3 tons per square foot at a depth of 12 feet. The studies that were carried out led to the recommendations shown in the following paragraphs.

(2) Recommendations for computing *p-y* curves. The following procedure is for short-term static loading and is illustrated by Figure 4-8. The empirical parameters, A_s and A_c shown in Figure 4-9 and k_s and k_c shown in Table 4-2 were determined from the results of the experiments.

(a) Obtain values for undrained soil shear strength c, soil submerged unit weight γ' and pile diameter b.

(b) Compute the average undrained soil shear strength c_a over the depth x.

(c) Compute the ultimate soil resistance per unit length of pile using the smaller of the values given by the equation below

$$p_{ct} = 2c_a b + \gamma' bx + 2.83\ c_a x \quad (4\text{-}7)$$

$$p_{cd} = 11\ cb \quad (4\text{-}8)$$

(d) Choose the appropriate values of the empirical parameter A_s from Figure 4-9 for the particular nondimensional depth.

(e) Establish the initial straight-line portion of the *p-y* curve:

$$p = (kx)y \quad (4\text{-}9)$$

Use the appropriate value of k_s or k_c from Table 4-2 for k.

(f) Compute the following:

$$y_{50} = \varepsilon_{50} b \quad (4\text{-}10)$$

Use an appropriate value of ε_{50} from results of laboratory tests or, in the absence of laboratory tests, from Table 4-3.

Table 4-2
Representative Values of *k* for Stiff Clays

	Average Undrained Shear Strength[1] ksf T/sq ft		
	1-2	2-4	4-8
k_s (Static) lb/cu in.	500	1,000	2,000
k_c (Static) lb/cu in.	200	400	800

[1] The average shear strength should be computed to a depth of five pile diameters. It should be defined as half the total maximum principal stress difference in an unconsolidated undrained triaxial test.

Table 4-3
Representative Values of ε_{50} for Stiff Clays

	Average Undrained Shear Strength ksf		
	1-2	2-4	4-8
ε_{50} (in./in.)	0.007	0.005	0.004

(g) Establish the first parabolic portion of the *p-y* curve, using the following equation and obtaining p_c from equations 4-7 or 4-8.

$$p = 0.5p_c\left(\frac{y}{y_{50}}\right)^{0.5} \tag{4-11}$$

Equation 4-11 should define the portion of the *p-y* curve from the point of the intersection with equation 4-9 to a point where y is equal to $A_s y_{50}$ (see note in step j).

(h) Establish the second parabolic portion of the *p-y* curve,

$$p = 0.5p_c\left(\frac{y}{y_{50}}\right)^{0.5} - 0.555p_c\left(\frac{y - A_s y_{50}}{A_s y_{50}}\right)^{1.25} \tag{4-12}$$

Equation 4-12 should define the portion of the *p-y* curve from the point where y is equal to $A y_{50}$ to a point where y is equal to $6A_s y_{50}$ (see note in step j).

(i) Establish the next straight-line portion of the *p-y* curve,

$$p = 0.5p_c(6A_s)^{0.5} - 0.411p_c - \left(\frac{0.0625}{y_{50}}\right)p_c\,(y - 6A_s y_{50}) \tag{4-13}$$

Equation 4-13 should define the portion of the *p-y* curve from the point where y is equal to $6A_s y_{50}$ to a point where y is equal to $18A_s y_{50}$ (see note in step j).

(j) Establish the final straight-line portion of the curve,

$$p = 0.5p_c(6A_s)^{0.5} - 0.411p_c - 0.75p_cA_s \tag{4-14}$$

or

$$p_c = p_c(1.225\sqrt{A_s} - 0.75A_s - 0.411) \tag{4-15}$$

Equation 4-15 should define the portion of the *p-y* curve from the point where y is equal to $18A_s y_{50}$ and for all larger values of y (see following note).

Note: The step-by-step procedure is outlined, and Figure 4-8 is drawn, as if there is an intersection between equations 4-9 and 4-11. However, there may be no intersection of equation 4-9 with any of the other equations defining the *p-y* curve. If there is no intersection, the equation should be employed that gives the smallest value of p for any value of y.

(3) Procedure of cyclic loading. The following procedure is for cyclic loading and is illustrated in Figure 4-10.

(a) Step a is same as for static case.

(b) Step b is same as for static case.

(c) Step c is same as for static case.

(d) Choose the appropriate value of A_c from Figure 4-9 for the particular nondimensional depth.

Compute the following:

$$y_p = 4.1A_s y_{50} \tag{4-16}$$

(e) Step e is same as for static case.

(f) Step f is same as for static case.

(g) Establish the parabolic portion of the *p-y* curve,

$$p = A_c p_c\left[1 - \left|\frac{y - 045y_p}{0.45y_p}\right|^{2.5}\right] \tag{4-17}$$

Equation 4-17 should define the portion of the *p-y* curve from the point of the intersection with equation 4-9 to where y is equal to $0.6y_p$ (see note in step i).

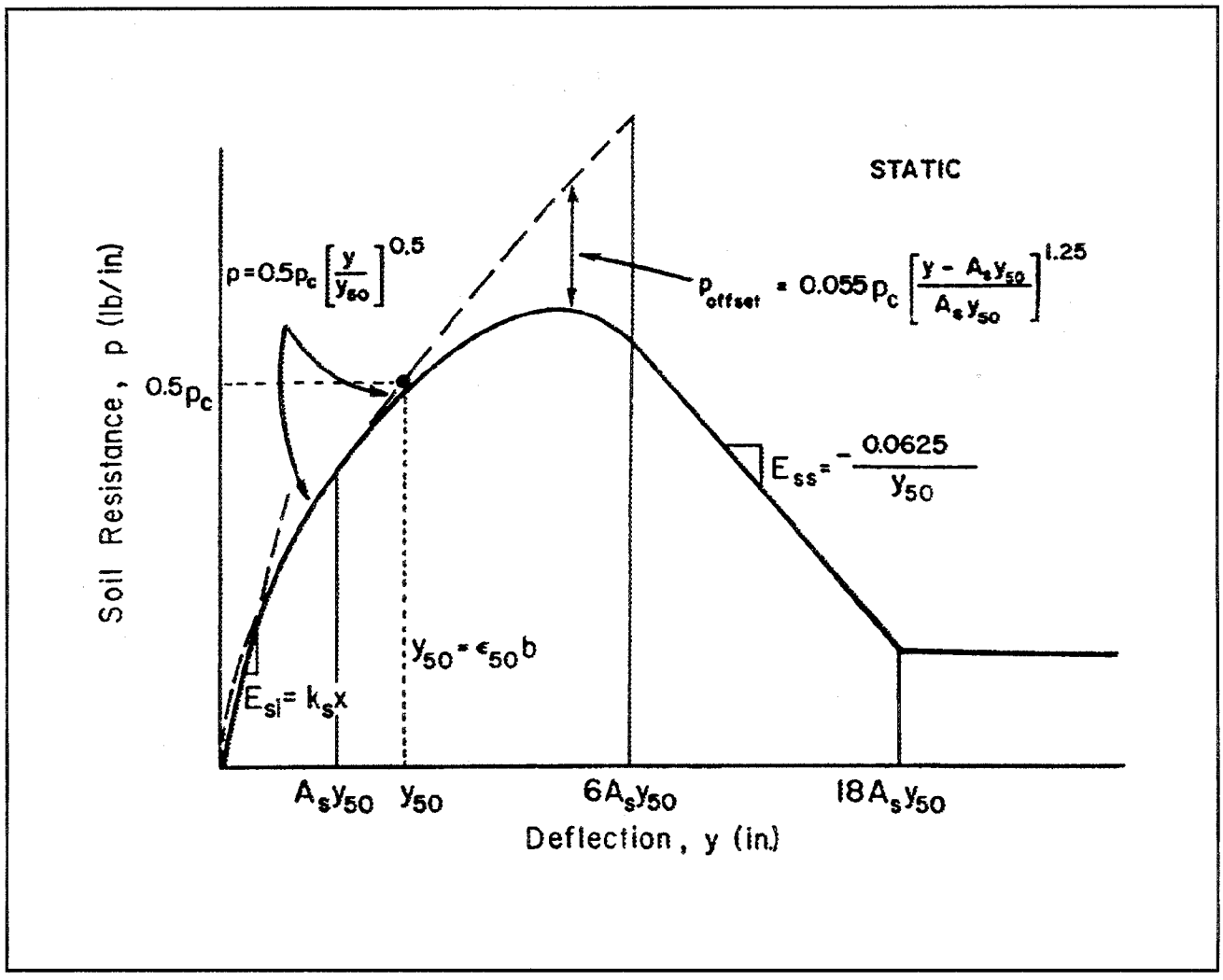

Figure 4-8. Charactertistic shape of *p-y* curve for static loading in stiff clay below the water table

(h) Establish the next straight-line portion of the *p-y* curve,

$$p = 0.936\, A_c p_c - \frac{0.085}{y_{50}}\, p_c (y - 0.6y_p) \qquad (4\text{-}18)$$

Equation 4-18 should define the portion of the *p-y* curve from the point where y is equal to $0.6y_p$ to the point where y is equal to $1.8y_p$ (see note in step h).

(i) Establish the final straight-line portion of the *p-y* curve,

$$p = 0.936\, A_c p_c - \frac{0.102}{y_{50}}\, p_c y_p \qquad (4\text{-}19)$$

Equation 4-19 should define the portion of the *p-y* curve from the point where y is equal to $1.8y_p$ and for all larger values of y (see following note).

Note: The step-by-step procedure is outlined, and Figure 4-10 is drawn, as if there is an intersection between equations 4-9 and 4-17. However, there may be no intersection of those two equations and there may be no intersection of equation 4-9 with any of the other equations defining the *p-y* curve. If there is no intersection, the equation should be employed that gives the smallest value of p for any value of y.

(4) Recommended soil tests. Triaxial compression tests of the unconsolidated-undrained type with confining pressures conforming to the in situ total overburden pressures are

illustrated in Figure 4-11.

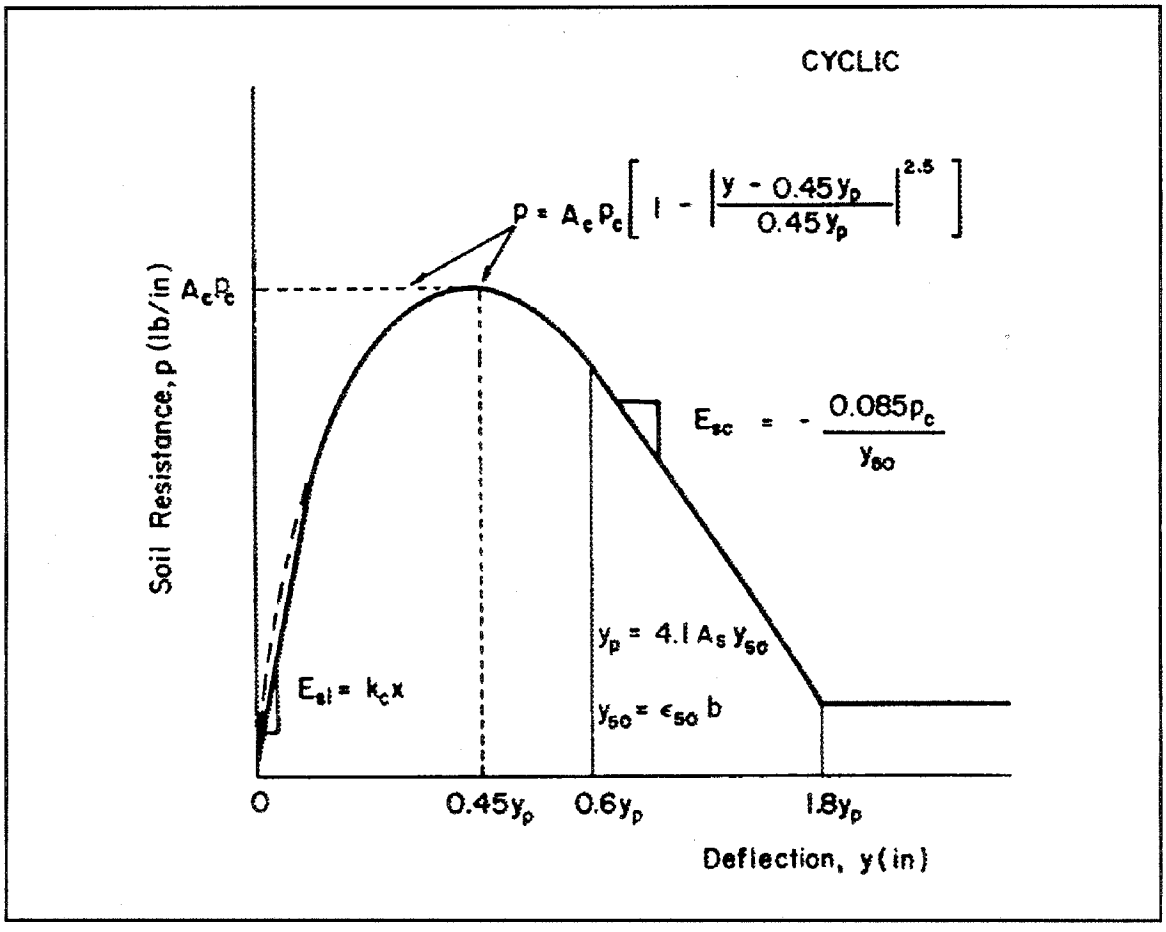

Figure 4-10. Characteristic shape of *p-y* curve for cyclic loading in stiff clay below the water table

ε_{50} from stress-strain curves. If no stress-strain curves are available, use a value from ε_{50} of 0.010 or 0.005 as given in Table 4-1, the larger value being more conservative.

(b) Compute the ultimate soil resistance per unit length of shaft, p_u, using the smaller of the values given by equations 4-1 and 4-2. (In the use of equation 4-1, the shear strength is taken as the average from the ground surface to the depth being considered and J is taken as 0.5. The unit weight of the soil should reflect the position of the water table.)

(c) Compute the deflection, y_{50} at one-half the ultimate soil resistance from equation 4-3.

(d) Points describing the *p-y* curve may be computed from the relationship below.

$$\frac{p}{p_u} = 0.5\left(\frac{y}{y_{50}}\right)^{0.25} \qquad (4\text{-}20)$$

(e) Beyond $y = 16y_{50}$, p is equal to p_u for all values of y.

(3) Procedure for cyclic loading. The following procedure is for cyclic loading and is illustrated in Figure 4-12.

(a) Determine the *p-y* curve for short-term static loading by the procedure previously given.

(b) Determine the number of times the design lateral load will be applied to the pile.

(c) For several values of p/p_u, obtain the value of C, the parameter describing the effect of repeated loading on deformation, from a relationship developed by laboratory tests

(Welch and Reese 1972), or in the absence of tests, from the following equation.

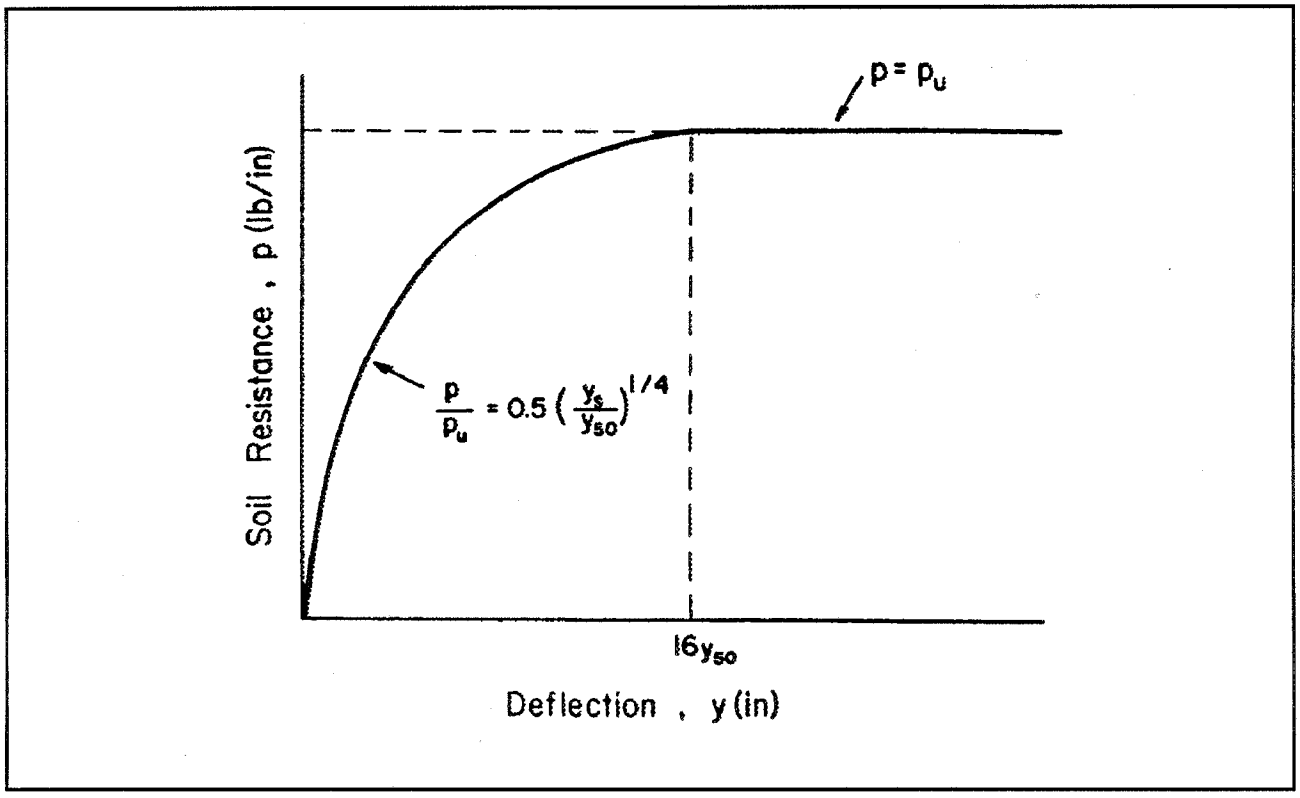

Figure 4-11. Characteristic shape of *p-y* curve for static loading in stiff clay above the water table

$$C = 9.6\left(\frac{p}{p_u}\right)^4 \qquad (4\text{-}21)$$

(d) At the value of p corresponding to the values of p/p_u selected in step c, compute new values of y for cyclic loading from the following equation.

$$y_c = y_s + y_{50} \times C \times \log N \qquad (4\text{-}22)$$

where

y_c = deflection under N-cycles of load

y_s = deflection under short-term static load

y_{50} = deflection under short-term static load at one-half the ultimate resistance

N = number of cycles of load application

(e) Define the soil response after N-cycles of load, using the *p-y* curve.

(4) Recommended soil tests. Triaxial compression tests of the unconsolidated-undrained type with confining stresses equal to the overburden pressures at the elevations from which the samples were taken are recommended to determine the shear strength. The value of ε_{50} should be taken as the strain during the test corresponding to the stress equal to half the maximum total principal stress difference. The undrained shear strength, c, should be defined as one-half the maximum total-principal-stress difference. The unit weight of the soil must also be determined.

d. p-y curves for sand. A major experimental program was conducted on the behavior of laterally loaded piles in sand below the water table. The results can be extended to sand above the water table by making appropriate adjustments in the values of the unit weight, depending on the position of the water table.

(1) Field experiments. An extensive series of tests were performed as a site on Mustang Island, near Corpus Christi

(Cox, Reese, and Grubbs 1974). Two steel-pipe piles, 24 inches in diameter, were driven into sand in a manner to simulate the driving of an open-ended pipe and were subjected to lateral oading. The embedded length of the piles was 69 feet. One of the piles was subjected to short-

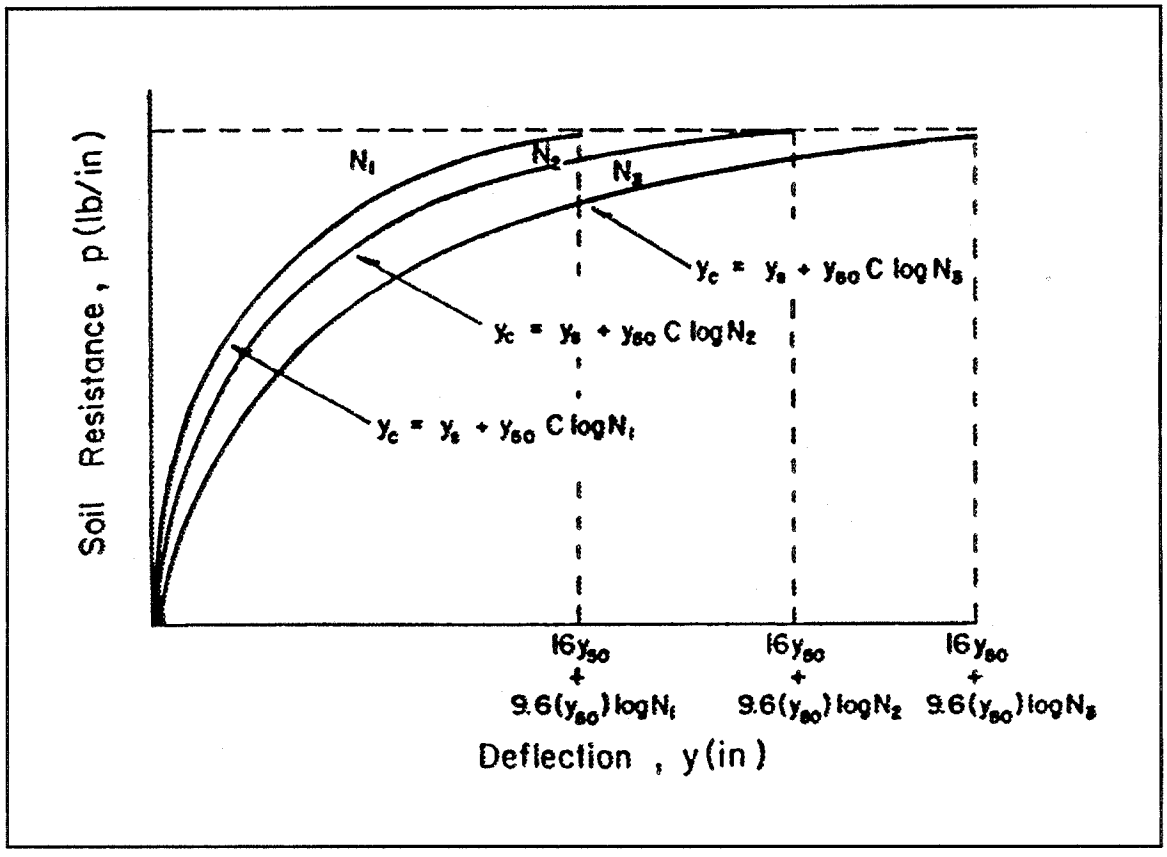

Figure 4-12. Characteristic shape of *p-y* curve for cyclic loading in stiff clay above the water table

term loading and the other to repeated loading. The soil at the site was a uniformly graded, fine sand with an angle of internal friction of 39 degrees. The submerged unit weight was 66 pounds per cubic foot. The water surface was maintained a few inches above the mudline throughout the test program.

(2) Recommendations for computing *p-y* curves. The following procedure is for short-term static loading and for cyclic loading and is illustrated in Figure 4-13 (Reese, Cox, and Koop 1974).

(a) Obtain values for the angle of internal friction ϕ, the soil unit weight γ, and pile diameter b.

(b) Make the following preliminary computations.

$$\alpha = \frac{\phi}{2};\ \beta = 45 + \frac{\phi}{2};\ K_o = 0.4;\ \text{and}$$
$$K_a = \tan^2(45 - \frac{\phi}{2});\ K_p = \tan^2(45 - \frac{\phi}{2}) \quad (4\text{-}23)$$

(c) Compute the ultimate soil resistance per unit length of pile using the smaller of the values given by the equations below, where x is equal to the depth below the ground surface.

$$p_{st} = \gamma b^2 \left[S_1 (\frac{x}{b}) + S_2 (\frac{x}{b})^2 \right] \quad (4\text{-}24)$$

$$p_{sd} = \gamma b^2 [S_3 (\frac{x}{b})] \quad (4\text{-}25)$$

where

$$S_1 = (K_p - K_a) \quad (4\text{-}26)$$

$$S_2 = (\tan\beta)(K_{\tan\alpha} + K_o[\tan\phi \sin\beta (\sec\alpha + 1) - \tan\alpha]) \quad (4\text{-}27)$$

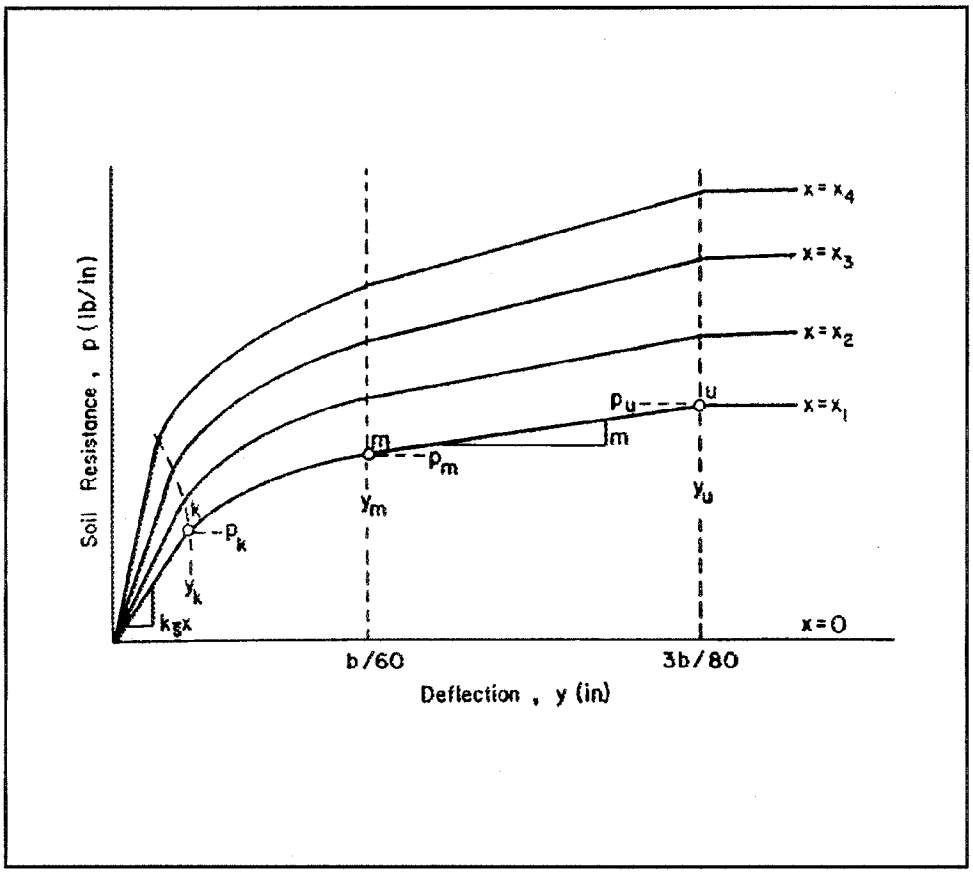

Figure 4-13. Characteristic shape of a family of *p-y* curves for static and cyclic loading in sand

$$S_3 = K^2 p (K_p + K_o \tan \phi) - K_a \qquad (4\text{-}28)$$

(d) The depth of transition x_t can be found by equating the expressions in equations 4-24 and 4-25, as follows:

$$\frac{x_t}{b} = \frac{(S_3 - S_1)}{S_2} \qquad (4\text{-}29)$$

The appropriate γ for the position of the water table should be employed. Use equation 39 above, x_t, and equation 40 below. It can be seen that S_1, S_2, S_3, x_t / b are functions only of ϕ; therefore, the values shown in Table 4-4 can be computed.

(e) Select a depth at which a *p-y* curve is desired.

(f) Establish y_u as 3b/80. Compute p by the following equation:

$$p_u = \overline{A_s} p_s \quad \text{or} \quad p_u = \overline{A_c} p_s \qquad (4\text{-}30)$$

Use the appropriate value of $\overline{A_s}$ or $\overline{A_c}$ from Figure 4-14 for the particular nondimensional depth and for either the static or cyclic case. Use the appropriate equation for p_s, equation 4-24 or 4-25 by referring to the computation in step d.

(g) Establish y_m as b/60. Compute p by the following equation:

$$p_m = B_s p_s \quad \text{or} \quad p_m = B_c p_s \qquad (4\text{-}31)$$

Use the appropriate value of B_s or B_c from Figure 4-15 for the particular nondimensional depth, and for either the static or cyclic case. Use the appropriate equation for p_s. The two

Table 4-4
Nondimensional Coefficients for *p-y* Curves for Sand

ϕ, deg	S_1	S_2	S_3	x_t / b
25.0	2.05805	1.21808	15.68459	11.18690
26.0	2.17061	1.33495	17.68745	11.62351
27.0	2.28742	1.46177	19.95332	12.08526
28.0	2.40879	1.59947	22.52060	12.57407
29.0	2.53509	1.74906	25.43390	13.09204
30.0	2.66667	1.91170	28.74513	13.64147
31.0	2.80394	2.08866	32.51489	14.22489
32.0	2.94733	2.28134	36.81400	14.84507
33.0	3.09733	2.49133	41.72552	15.50508
34.0	3.25442	2.72037	47.34702	16.20830
35.0	3.41918	2.97045	53.79347	16.95848
36.0	3.59222	3.24376	61.20067	17.75976
37.0	3.77421	3.54280	69.72952	18.61673
38.0	3.96586	3.87034	79.57113	19.53452
39.0	4.16799	4.22954	90.95327	20.51883
40.0	4.38147	4.62396	104.14818	21.56704

straight-line portions of the *p-y* curve, beyond the point where y is equal to b/60, can now be established.

(h) Establish the initial straight-line portion of the *p-y* curves,

$$p = (kx)y \tag{4-32}$$

Use Tables 4-4 and 4-5 to select an appropriate value of k.

(i) Establish the parabolic section of the *p-y* curve,

$$p = \overline{C}\, y^{1/n} \tag{4-33}$$

(3) Parabolic section. Fit the parabola between points k and m as follows:

(a) Get the slope of line between points m and u by,

$$m = \frac{p_u - p_m}{y_u - y_m} \tag{4-34}$$

(b) Obtain the power of the parabolic section by,

$$n = \frac{p_m}{m_{ym}} \tag{4-35}$$

(c) Obtain the coefficient $\overline{C}$ as follows:

$$\overline{C} = \frac{p_m}{y^{m^{1/n}}} \tag{4-36}$$

(d) Determine point k as

$$yk = \left(\frac{\overline{C}}{kx}\right) \quad n/n-1 \tag{4-37}$$

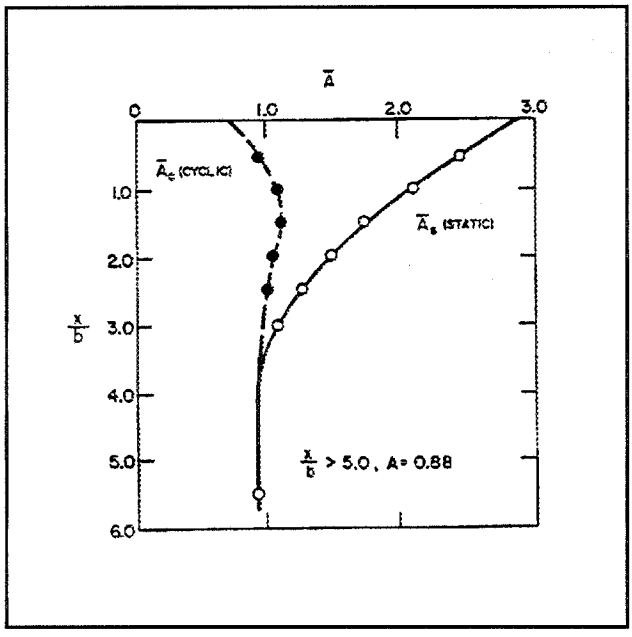

Figure 4-14. Values of coefficients $\bar{A}_c$ and $\bar{A}_s$

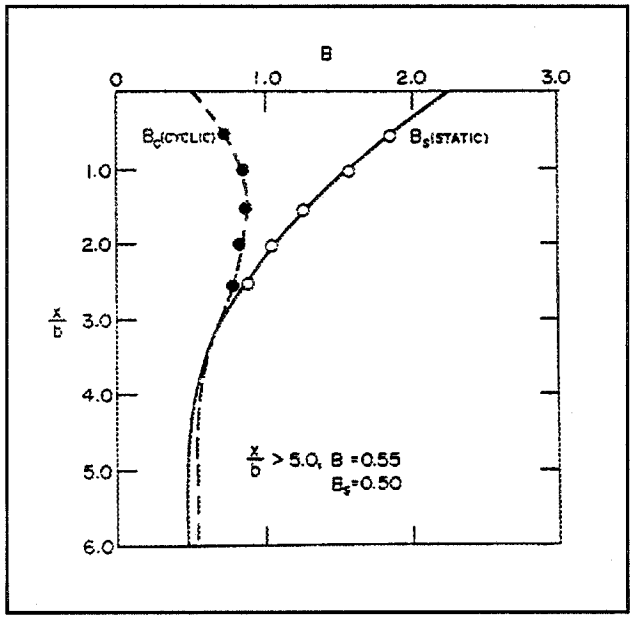

Figure 4-15. Nondimensional coefficient *B* for soil resistance versus depth

(e) Compute appropriate number of points on the parabola by using equation 4-33.

Note: The step-by-step procedure is outlined, and Figure 4-13 is drawn, as if there is an intersection between the initial straight-line portion of the *p-y* curve and the parabolic portion of the curve at point *k*. However, in some instances there may be no intersection with the parabola. Equation 4-32 defines the *p-y* curve until there is an intersection with another branch of the *p-y* curve or if no intersection occurs, equation 4-32 defines the complete *p-y* curve. The soil-response curves for other depths can be found repeating the above steps for each desired depth.

(4) Recommended soil tests. Triaxial compression tests are recommended for obtaining the angle of internal friction of the sand. Confining pressures should be used which are close or equal to those at the depths being considered in the analysis. Tests must be performed to determine the unit weight of the sand. In many instances, however, undisturbed samples of sand cannot be obtained and the value of ϕ must be obtained from correlations with static cone penetration tests or from dynamic penetration tests (Table 4-4).

4. Analytical Method

The solution of the problem of the pile under lateral load must satisfy two general conditions. The equations of equilibrium must be solved and deflections and deformations must be consistent and compatible. These two requirements are fulfilled by finding a solution to the following differential equation (Hetenyi 1946).

$$EI\frac{d^4y}{dx^4} + P_x\frac{d^2y}{dx^2} - p - W = 0 \qquad (4\text{-}38)$$

where

P_x = axial load on the pile

y = lateral deflection of the pile at a point x along the length of the pile

p = soil reaction per unit length

EI = flexural rigidity

W = distributed load along the length of the pile

Other beam formulae which are useful in the analysis are:

$$EI\frac{d^3y}{dx^3} = V \qquad (4\text{-}39)$$

Table 4-5
Representative Values of *k* (lb/cu in.) for Sand

	Relative Density		
	below 35%	**35% to 65%**	**above 65%**
Recommended *k* for sand below water table	20	60	125
Recommended *k* for sand above water table	25	90	225

$$EI \frac{d^2y}{dx^2} = M \qquad (4\text{-}40)$$

and

$$\frac{dy}{dx} = S \qquad (4\text{-}41)$$

where

V = shear at point x along the length of the pile

M = bending moment of the pile

S = slope of the elastic curve

Solutions of the above equations can be made by use of the computer program described in this chapter. Nondimensional methods, described later, can frequently be used to obtain acceptable solutions but those methods are much less versatile than the computer method. An acceptable technique for getting solutions to the equations governing the behavior of a laterally loaded pile is to formulate the differential equation in difference terms. The pile is divided into n increments of constant length h. Equation 4-38 can be represented at point m along the pile as follows:

$$\begin{aligned} y_m - 2^R m - 1 &+ y_{m-1}(-2R_{m-1} - 2Rm \\ &+ P_x h^2) + y_m(R_{m-1} + 4R_m \\ &+ R_{m+1} - 2P_x h^2 + k_m h^4) \\ &+ y_{m+1}(-2R_m - 2R_m + 1 \\ &+ P_x h^2) + y_{m+2} R_m + 1 - W_m = 0 \end{aligned} \qquad (4\text{-}42)$$

where

y_m = deflection at point m

R_m $E_m I_m$ = flexural rigidity at point m

P_x = axial load (causes no moment at $x = 0$)

k_m = $\frac{p_m}{y_m}$ = soil modulus at point m

W_m = distributed load at point m

Because the pile is divided into n increments, there are $n + 1$ points on the pile and $n + 1$ of the above equations can be written. The differential equation in difference form uses deflections at two points above and at two points below the point being considered. Therefore, four imaginary deflections are introduced, two at the top of the pile and two at the bottom. The introduction of four boundary conditions, two at the bottom of the pile and two at the top, yields $n + 5$ simultaneous equations of a sort to be easily and quickly solved by the digital computer. After solving the simultaneous equations, shear moment and slope can be found at all points along the pile by solving equations 4-39, 4-40, and 4-41. The soil resistance p can be found to be the product $k_m y_m$. It is obvious that an iterative solution must be made with the computer because the values of the soil moduli k_m are not known at the outset. Convergence to the correct solution is judged to have been achieved when the difference between the final two sets of computed deflections are less than the value of the tolerance selected by the engineer.

a. Boundary conditions. At the bottom of the pile the two boundary conditions employed are the shear and the moment, and both are equal to zero. Thus, a solution can be obtained for a short pile such that there is a significant amount of deflection and slope at the bottom of the pile.

Sometimes the question arises about the possibility of forces at the base of the pile due to development of shearing stresses from the soil when the bottom of the file is deflected. That possibility can readily be accommodated by placing a *p-y* curve with appropriate numerical values at the bottom increment of the pile. There are three boundary conditions to be selected at the top of the pile, but one of those, the axial load, provides no specific information on pile-head deflection. Thus, two other boundary conditions must be selected. The computer is programmed to accept one of the following three sets. (The axial load is assumed to be used with each of these sets).

(1) The lateral load (P_t) and the moment (M_t) at the top of the pile are known.

(2) The lateral load (P_t) and the slope of the elastic curve (S_t) at the top of the pile are known.

(3) The lateral load (P_t) and the rotational-restraint constant (M_t/S_t) at the top of the pile are known.

The first set of boundary conditions applies to a case such as a highway sign where wind pressure applies a force some distance above the groundline. The axial load will usually be small and a free body of the pile can be taken at the groundline where the shear and the moment will be known. The second set of boundary conditions can be employed if a pile supports a retaining wall or bridge abutment and where the top of the pile penetrates some distance into a reinforced concrete mat. The shear will be known, and the pile-head rotation in most cases can be assumed to be zero. The third set of boundary conditions is encountered when a pile frames into a superstructure that is flexible. In some bridge structures, the piles could continue and form the lower portion of a column. A free body of the pile can be taken at a convenient point, and the rotational restraint (M_t/S_t) of the portion of the structure above the pile head can be estimated. The magnitude of the shear will be known. Iteration between pile and superstructure will lead to improved values of rotational restraint and convergence to an appropriate solution can be achieved.

b. U.S. Army Engineer Waterways Experiment Station (WES) computer program COM624G (IOO12). The method for solving the governing equations for the single pile under lateral loading and the recommendations for *p-y* curves have been incorporated into a computer program that is available from WES. The user is urged to read the documentation that accompanies the computer diskettes and to solve the examples that are included. Users are assumed to be engineers who can understand the importance of verifying the accuracy of any given solution. Solutions are obtained rapidly to allow the user to investigate the importance and influence of various parameters. For example, upper-bound and lower-bound values of the soil properties can be input and the outputs compared. This exercise will give the user an excellent idea of the possible variation of behavior across a site and may indicate the desirability of performing a full-scale field test.

c. Nondimensional method of analysis.

(1) Variation of soil modulus with depth. Prior to presenting the details of nondimensional analysis, it is desirable to discuss the nature of the soil modulus. A pile under lateral loading is shown in Figure 4-16a and a set of *p-y* curves is shown in Figure 4-16b. As shown in the figure, the ultimate value of *p* and the initial slope of the curves increase with depth, as is to be expected in many practical cases. Also shown in Figure 4-16b is the possible deflected shape of the pile under load and the secants to the point on the curves defined to be the respective deflection. The values of soil modulus E_s so obtained are plotted as a function of depth in Figure 4-16c. The line passing through the plotted points defines the variation of E_s with depth. In the case depicted in Figure 4-16, the following equation defines the variation in the soil modulus.

$$E_s = kx \tag{4-43}$$

It is of interest to note that neither E_s nor k are constants, but each of them decrease as the load and deflection increase. In many cases encountered in practice, the value E_s would not be zero at the groundline and would not increase linearly with depth, as shown in Figure 4-16. However, these are two things that suggest that equation 4-43 will frequently define, at least approximately, the variation of the soil modulus with depth. First, the soil strength and stiffness will usually increase with depth. Second, the pile deflection will always be larger at and near the groundline. Furthermore, experience with nondimensional solutions has shown that it is not necessary to pass a curve precisely through the soil-modulus values, as is done by the computer, to obtain an acceptable solution.

(2) Nondimensional equations and curves. The derivation of the equations for the nondimensional solutions are not shown here but may be seen in detail elsewhere (Reese and Matlock 1956; Matlock and Reese 1961). The following sections present the equations and nondimensional curves for three cases: pile head free to rotate, pile head fixed against rotation, and pile head restrained against rotation. The nondimensional solutions are valid only for piles that have constant stiffness *EI* and no with axial load. These restrictions are not very important in many cases because computer solutions usually show that deflections and bending moments are only moderately influenced by changes in *EI* and by the presence of an axial load. Also, the principal benefits from the nondimensional method are in

checking computer solutions and in allowing an engineer to gain insight into the nature of the problem; thus, precision is not required. As may be seen by examining published derivations (Matlock and Reese 1961), nondimensional curves can be developed for virtually any conceivable variation in soil modulus with depth. However, studies show (Reese 1984) that the utility of some more complex forms of variation ($E_s = k_1 + k_2 x, E_s = kx^n$) is limited when compared to the simpler form ($E_s = kx$).

d. Pile head free to rotate (Case I). The procedure shown in this section may be used when the shear and moment are known at the groundline. A single pile that serves as the foundation for an overhead sign, such as those that cross a highway, is an example of the Case I category. The shear and moment at the groundline may also be known, or computed, for some structural configurations for bridges.

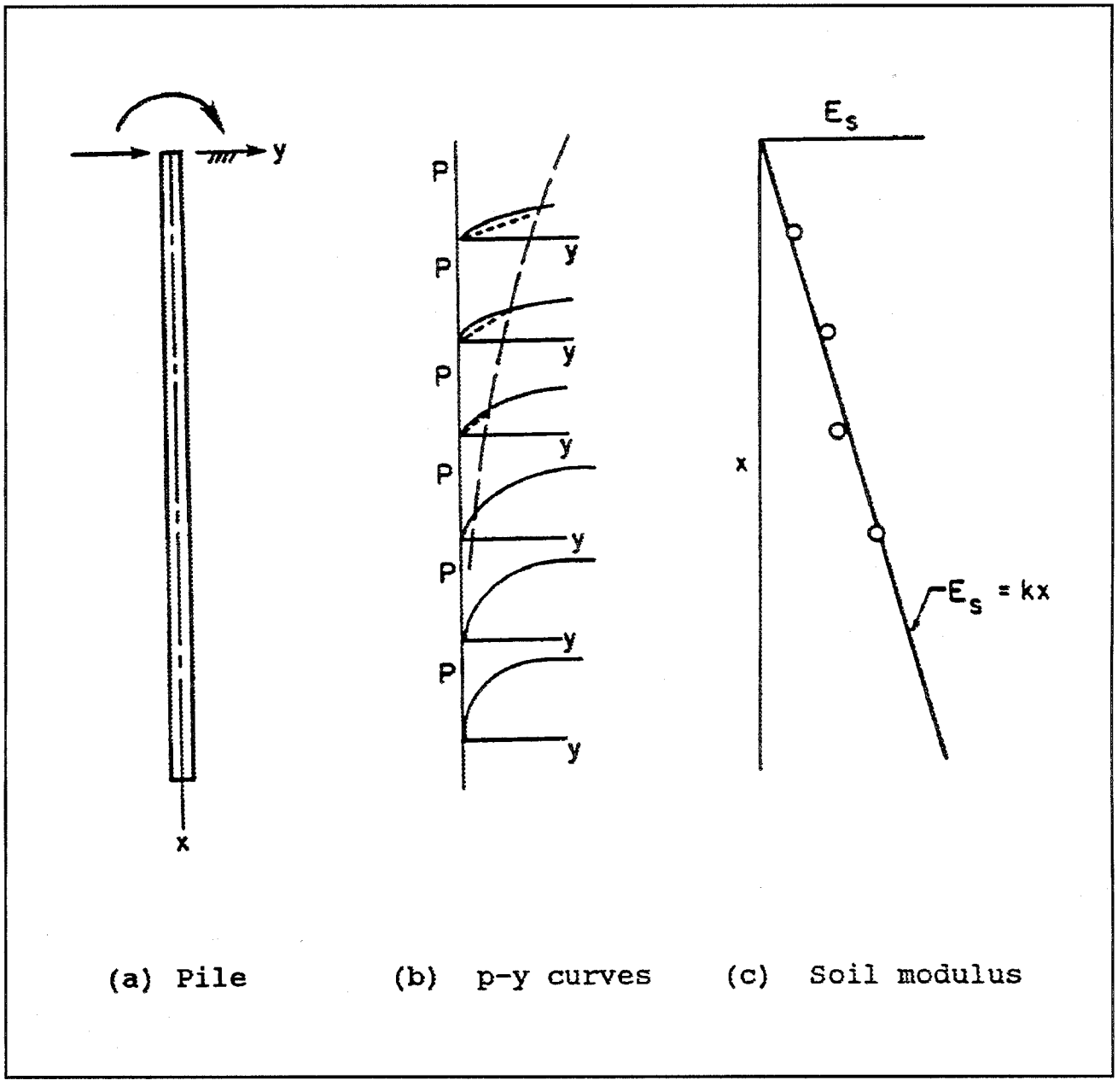

Figure 4-16. Form of variation of soil modulus with depth

(1) Construct *p-y* curves at various depths by procedures recommended herein, with the spacing between *p-y* curves being closer near the ground surface than near the bottom of the pile.

(2) Assume a convenient value of a relative stiffness factor *T*, perhaps 100 inches. The relationship is given as:

$$T = \left(\frac{EI}{k} \right)^{1/5} \tag{4-44}$$

where

EI = flexural rigidity of pile

k = constant relating the secant modulus of soil and reaction of depth ($E_s = kx$)

(3) Compute the depth coefficient z_{max}, as follows:

$$z_{\max} = \frac{x_{\max}}{T} \tag{4-45}$$

where x_{max} equals the embedded length of the pile.

(4) Compute the deflection y at each depth along the pile where a *p-y* curve is available by using the following equation:

$$y = A_y \frac{P_t T^3}{EI} + B_y \frac{M_t T^2}{EI} \tag{4-46}$$

where

A_y = deflection coefficient, found in Figure 4-17

P_t = shear at top of pile

T = relative stiffness factor

B_y = deflection coefficient, found in Figure 4-18

M_t = moment at top of pile

EI = flexural rigidity of pile

The particular curves to be employed in getting the A_y and B_y coefficients depend on the value of z_{max} computed in step 3. The argument for entering Figures 4-17 and 4-18 is the nondimensional depth z, where z is equal to x/T.

(5) From a *p-y* curve, select the value of soil resistance p that corresponds to the pile deflection value y at the depth of the *p-y* curve. Repeat this procedure for every *p-y* curves that is available.

(6) Compute a secant modulus of soil reaction E_s ($E_s = -p/y$). Plot the E_s values versus depth (see Figure 4-16c).

(7) From the E_s versus depth plotted in step 6, compute the constant k which relates E_s to depth ($k = E_s/x$). Give more weight to E_s values near the ground surface.

(8) Compute a value of the relative stiffness factor T from the value of k found in step 7. Compare this value of T to the value of T assumed in step 2. Repeat steps 2 through 8 using the new value of T each time until the assumed value of T equals the calculated value of T.

(9) When the iterative procedure has been completed, the values of deflection along the pile are known from step 4 of the final iteration. Values of soil reaction may be computed from the basic expression: $p = E_s y$. Values of slope, moment, and shear along the pile can be found by using the following equations:

$$S = A_s \frac{P_t T^2}{EI} + B_s \frac{M_t T}{EI} \tag{4-47}$$

$$M = A_m P_t T + B_m M_t \tag{4-48}$$

$$V = A_v P_t + B_v \frac{M_t}{T} \tag{4-49}$$

The appropriate coefficients to be used in the above equations may be obtained from Figures 4-19 through 4-24.

e. Pile head fixed against rotation (Case II). The method shown here may be used to obtain solution for the case where the superstructure translates under load but does not rotate and where the superstructure is very, very stiff in relation to the pile. An example of such a case is where the top of a pile is embedded in a reinforced concrete mat as for a retaining wall or bridge abutment.

(1) Perform steps 1, 2, and 3 of the solution procedure for free-head piles, Case I.

(2) Compute the deflection y_F at each along the pile where a *p-y* curve is available by using the following equation:

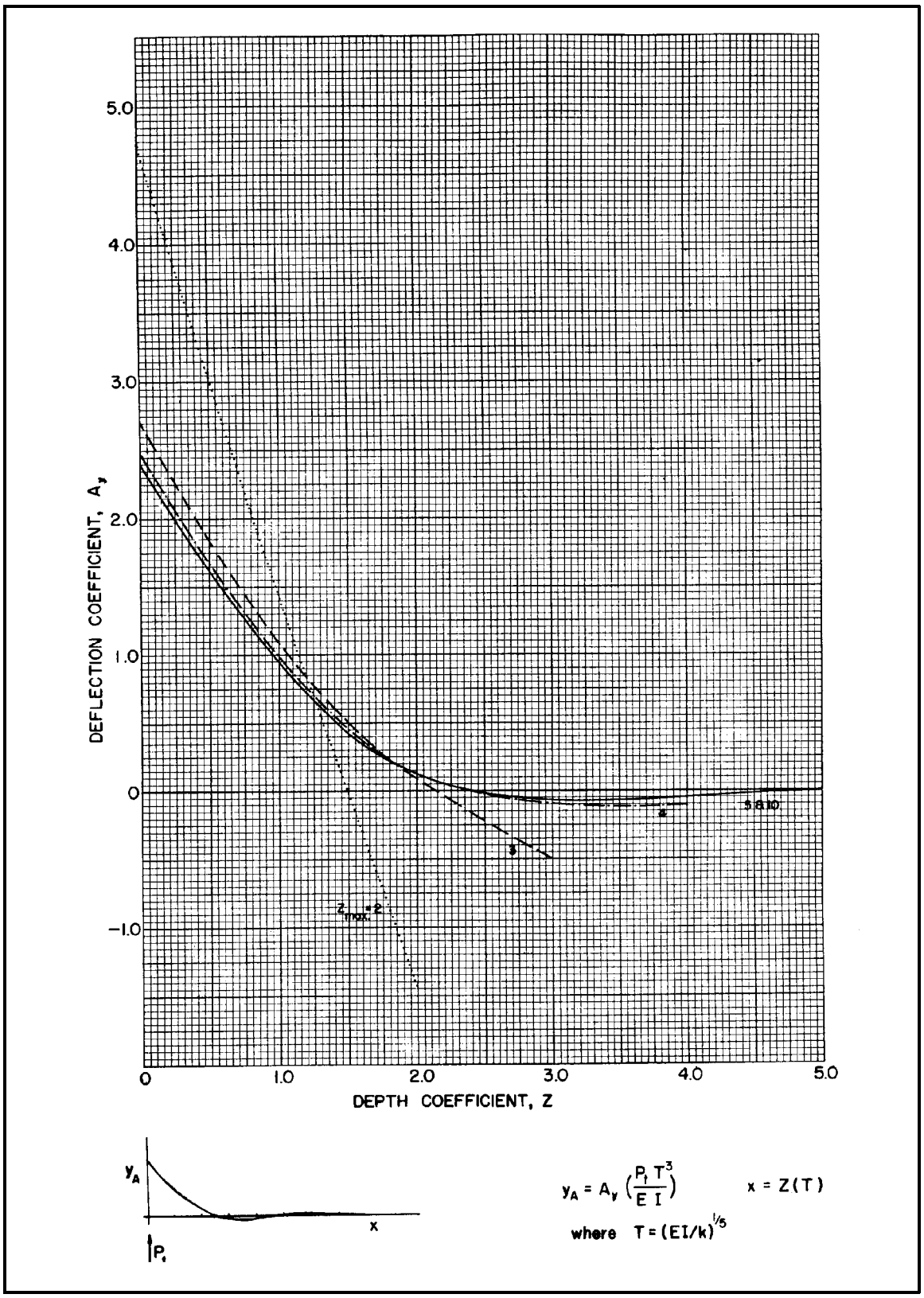

Figure 4-17. Pile deflection produced by lateral load at mudline

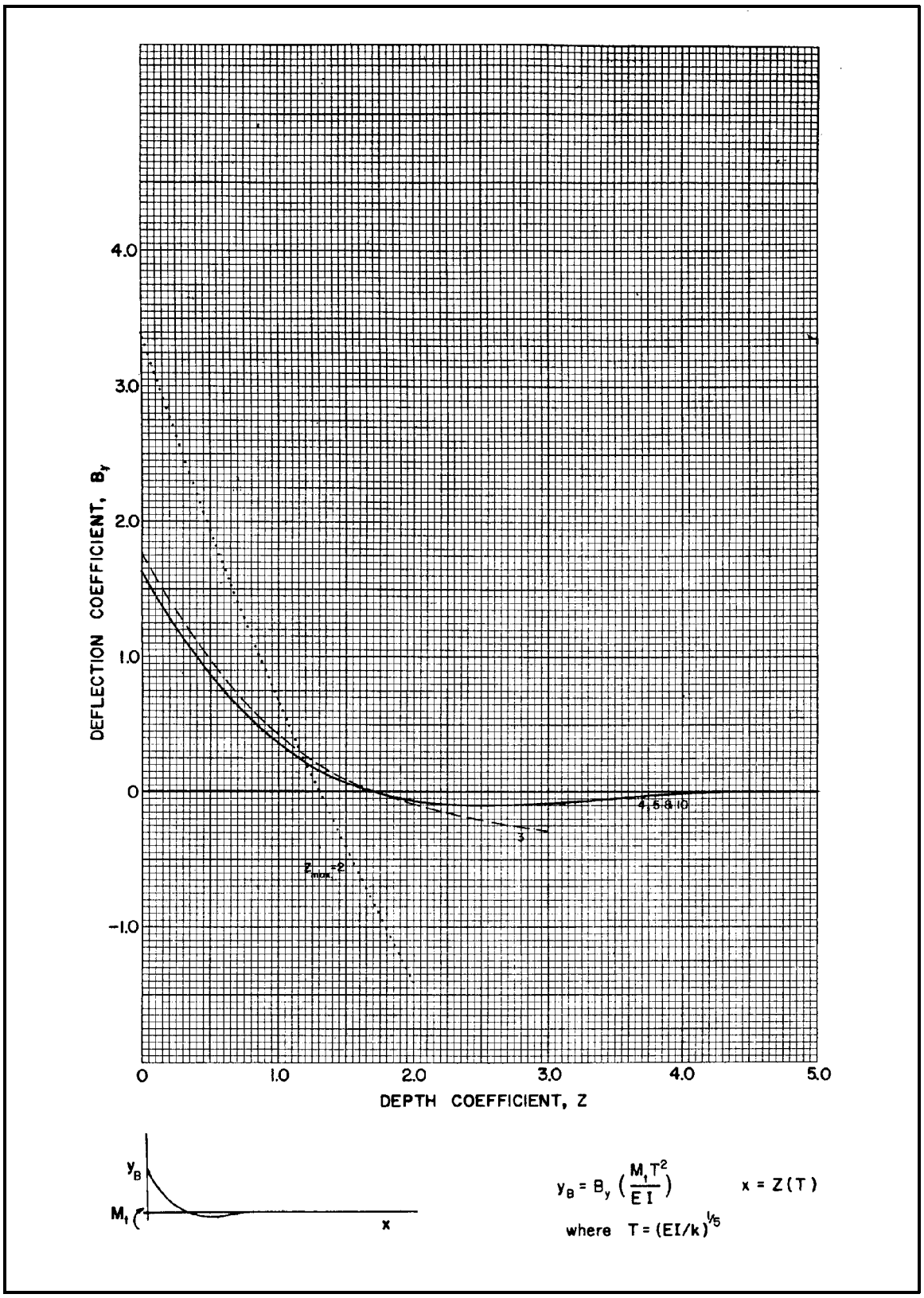

Figure 4-18. Pile deflection produced by moment applied at mudline

$$y_F = F_y \frac{P_t T^3}{EI} \quad (4\text{-}50)$$

The deflection coefficients F_y may be found by entering Figure 4-25 with the appropriate value of z_{max}.

(3) The solution proceeds in steps similar to those of steps 5 through 8 for the free-head case.

(4) Compute the moment at the top of the pile M_t from the following equation:

$$M_t = F_{Mt} P_t T \quad (4\text{-}51)$$

The value of F_{Mt} may be found by entering Table 4-6 with the appropriate value of z_{max}, where z_{max} is the maximum depth coefficient.

Table 4-6
Moment Coefficients at Top of Pile for Fixed-Head Case

z_{max}	F_{Mt}
2	-1.06
3	-0.97
4	-0.93
5 and above	-0.93

(5) Compute the values of slope, moment, shear, and soil reaction along the pile by following the procedure in step 9 for the free-head pile.

f. Pile head restrained against rotation (Case III). Case III may be used to obtain a solution for the case where the superstructure translates under load, but rotation at the top of the pile is partially restrained. An example of Case III is when the pile is extended and becomes a beam-column of the superstructure. A moment applied to the bottom of the beam-column will result in a rotation, with the moment-rotation relationship being constant. That relationship, then, becomes one of the boundary conditions at the top of the pile.

(1) Perform steps 1, 2, 3 of the solution procedures for free-head piles, Case I.

(2) Obtain the value of the spring stiffness k_θ of the pile superstructure system. The spring stiffness is defined as follows:

$$k_\theta = \frac{M_t}{S_t} \quad (4\text{-}52)$$

where

M_t = moment at top of pile

S_t = slope at top of pile

(3) Compute the slope at the top of pile S_t as follows:

$$S_t = A_{st} \frac{P_t T^2}{EI} + B_{st} \frac{M_t T}{EI} \quad (4\text{-}53)$$

where

A_{st} = slope coefficient at $z = 0$, found in Figure 4-19

B_{st} = slope coefficient at $z = 0$, found in Figure 4-20

(4) Solve equations 4-52 and 4-53 for the moment at the top of the pile M_t.

(5) Perform steps 4 through 9 of the solution procedure for free-head piles, Case I.

g. Solution of example problem. To illustrate the solution procedures, an example problem is presented. The example will be solved principally by the nondimensional method. The solution, while somewhat cumbersome, yields an excellent result in the case selected. The nondimensional method has several advantages: (1) the elements of a solution are clearly indicated; (2) the method is useful for practical cases if a computer and the necessary software are unavailable; and (3) the method is capable of providing a check to the output of the computer.

(1) Select pile dimensions and calculate ultimate bending moment (step 1). The pile is an HP 12 by 84 with the load applied perpendicular to the major axis. The width is 12.295 inches and the depth is 12.28 inches. The moment of inertia about the major axis is 650 in.^{4}, the cross-sectional area is 24.6 square inches, and the ultimate bending moment is 4,320 inch-kips, assuming a yield strength of the steel of 36 kips per square inch ignoring the effect of axial load. The length, penetration below the ground surface, is assumed to be 80 feet.

(2) Study soil profile and idealize soil as clay with $\phi = 0$ or as sand with $c = 0$ (step 2). This step would normally require the evaluation of the results of field exploration and

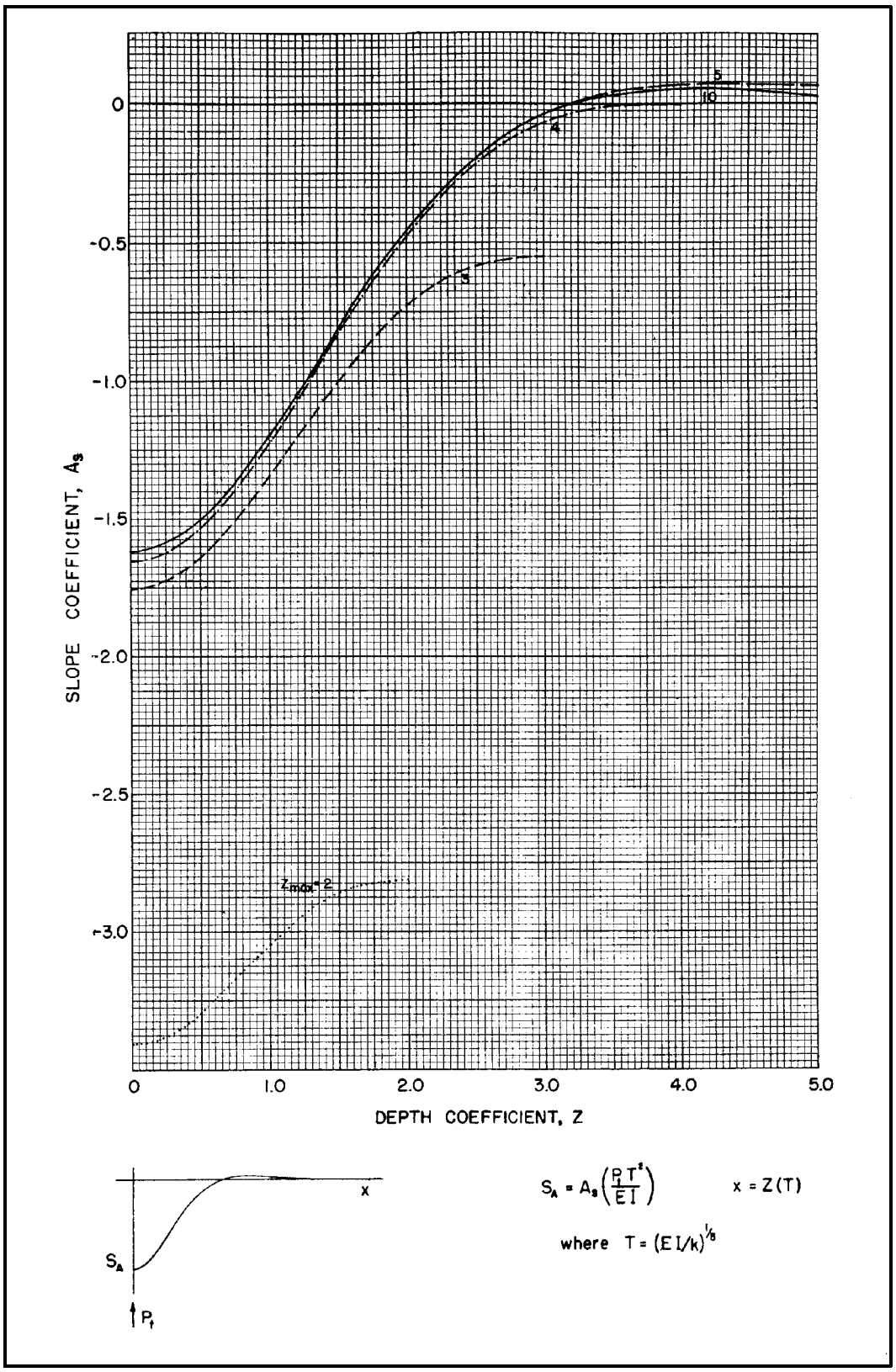

Figure 4-19. Slope of pile caused by lateral load at mudline

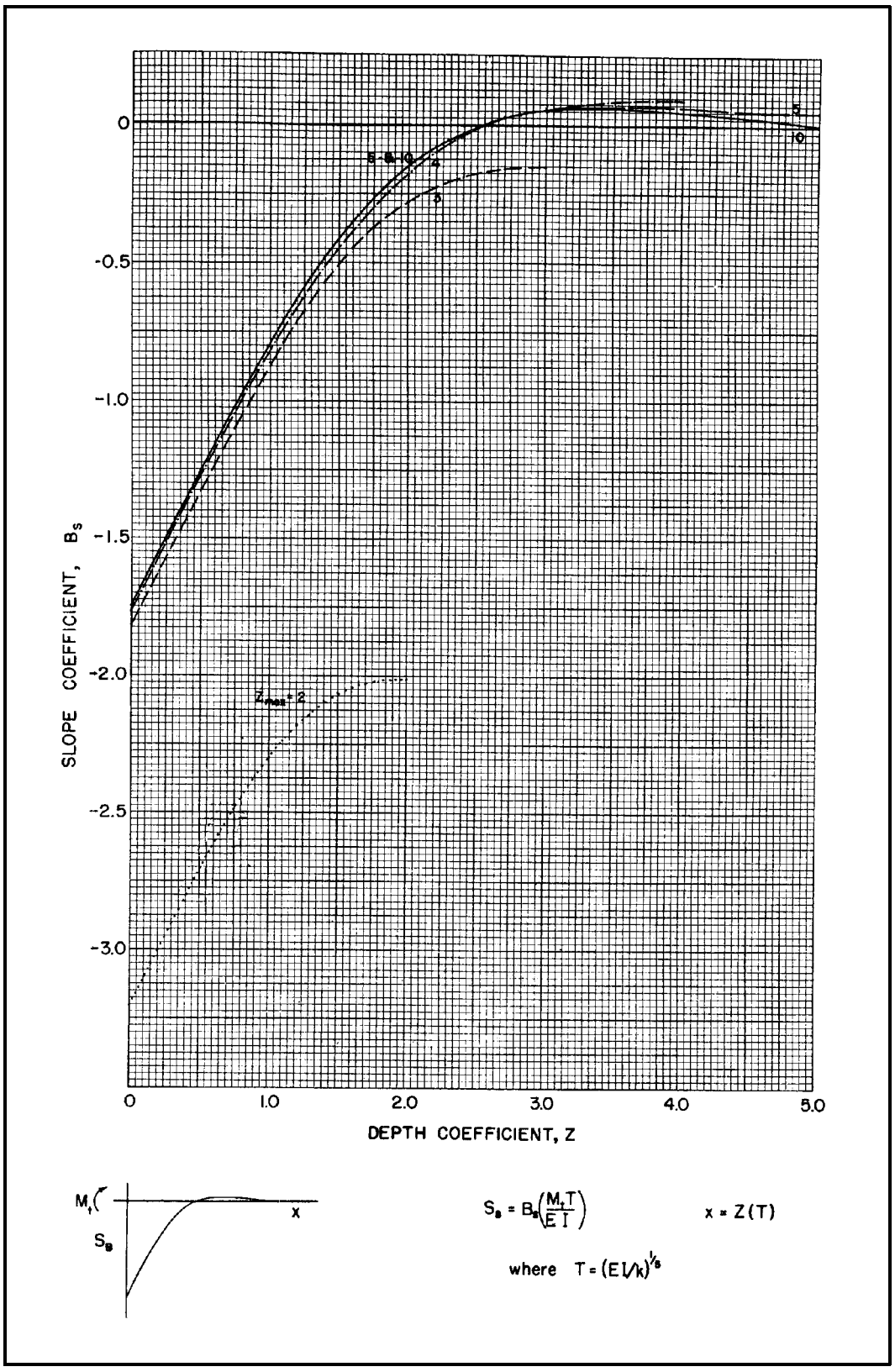

Figure 4-20. Slope of pile caused by moment applied at mudline

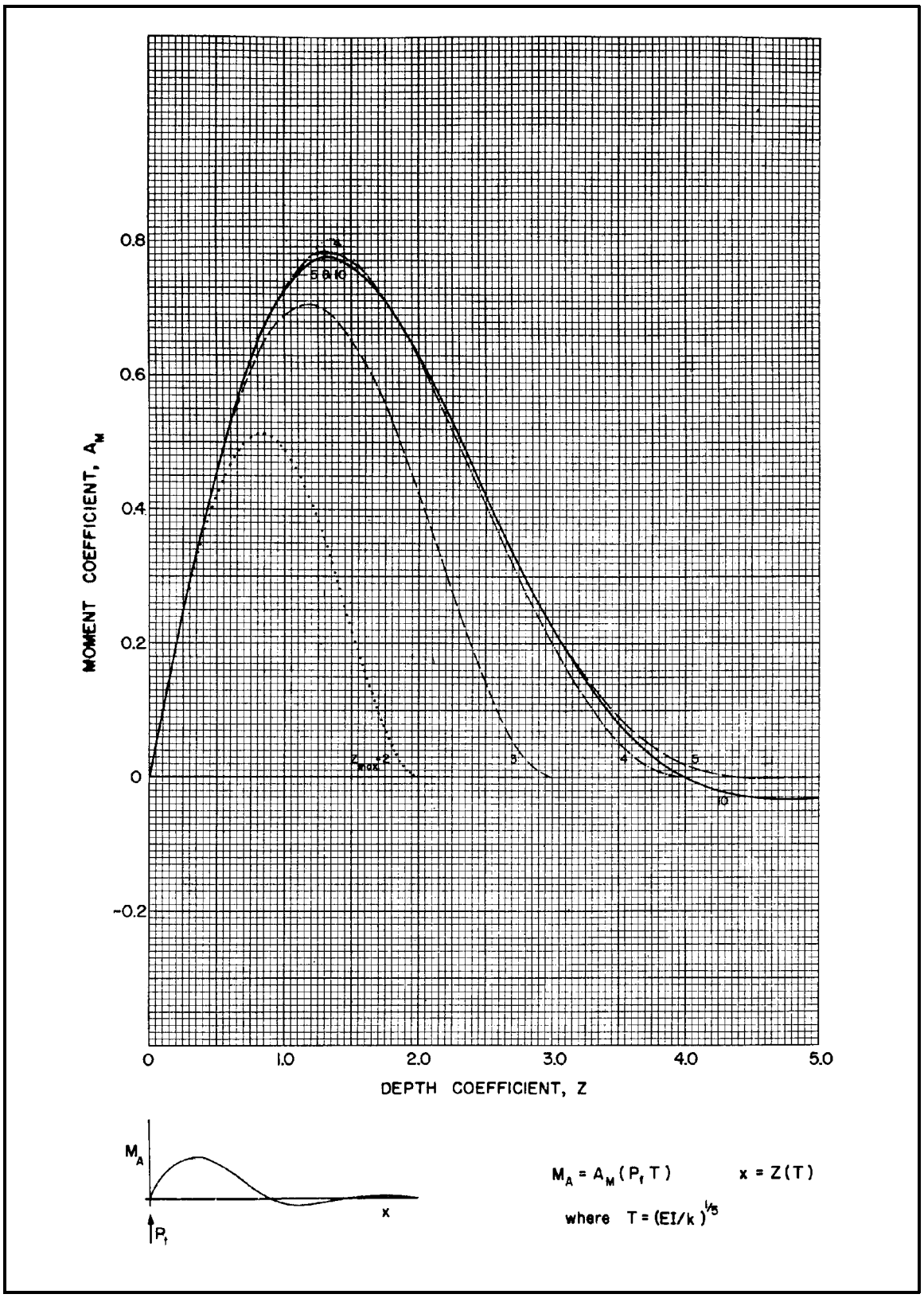

Figure 4-21. Bending moment produced by lateral load at mudline

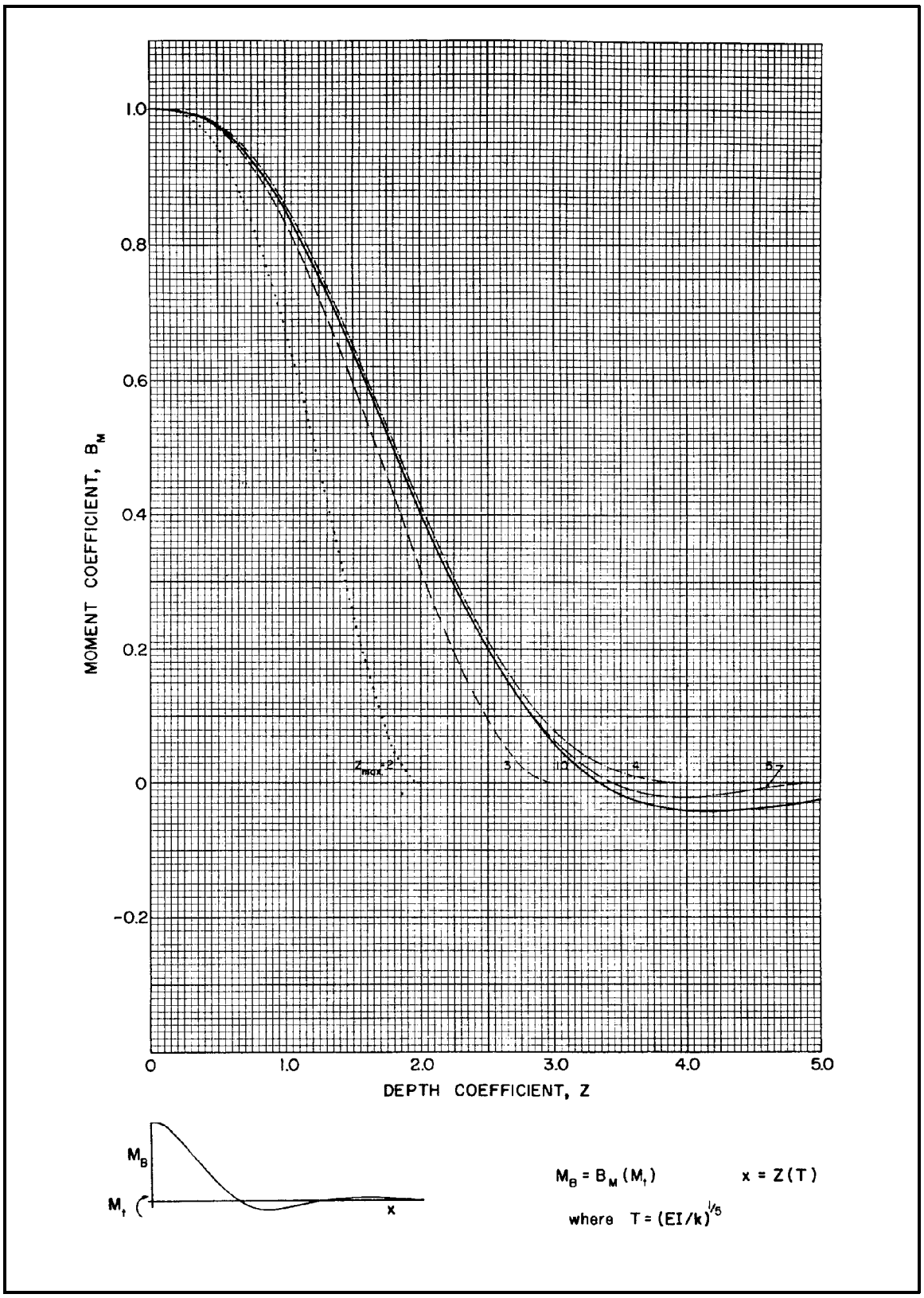

Figure 4-22. Bending moment produced by moment applied at mudline

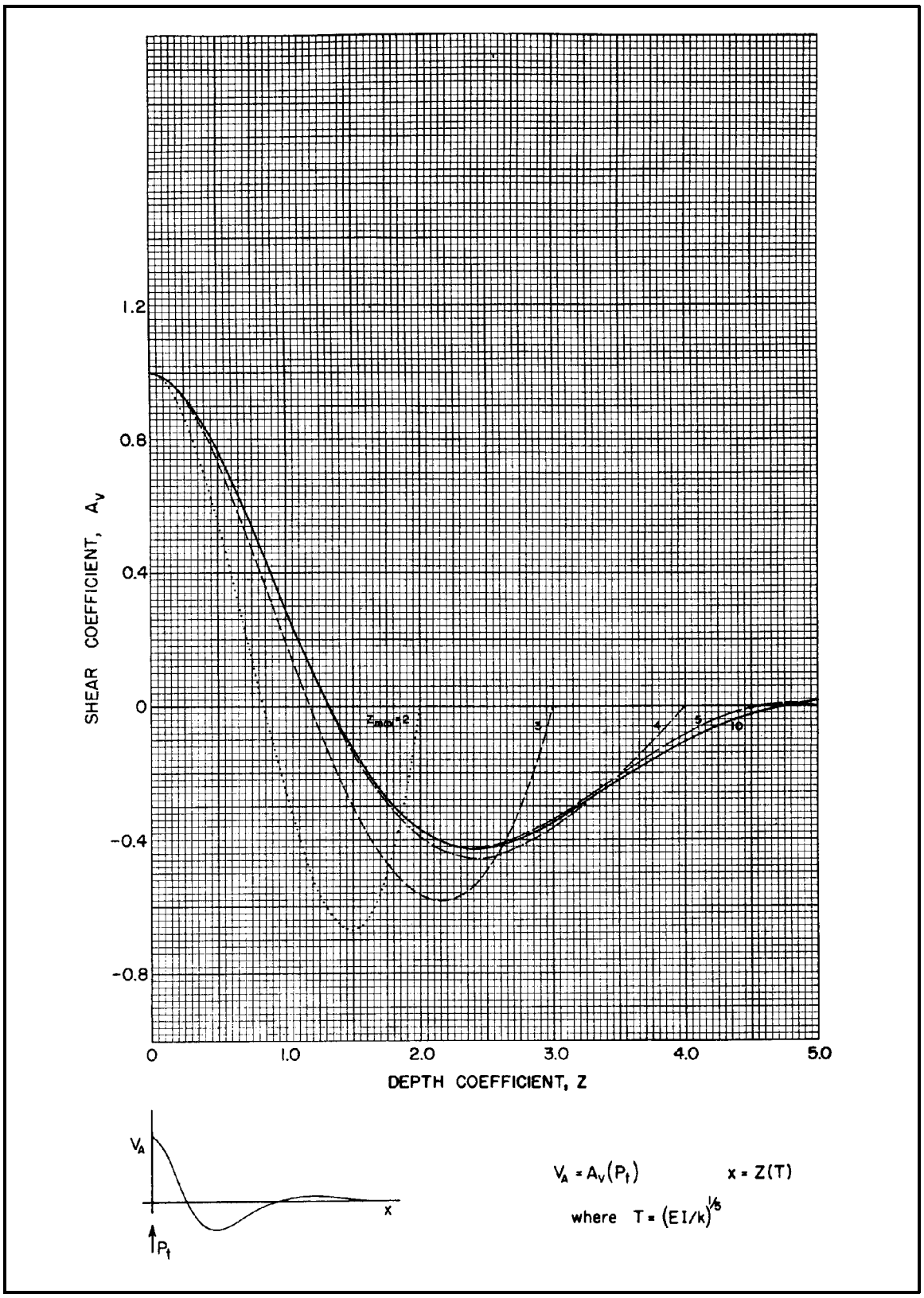

Figure 4-23. Shear produced by lateral load at mudline

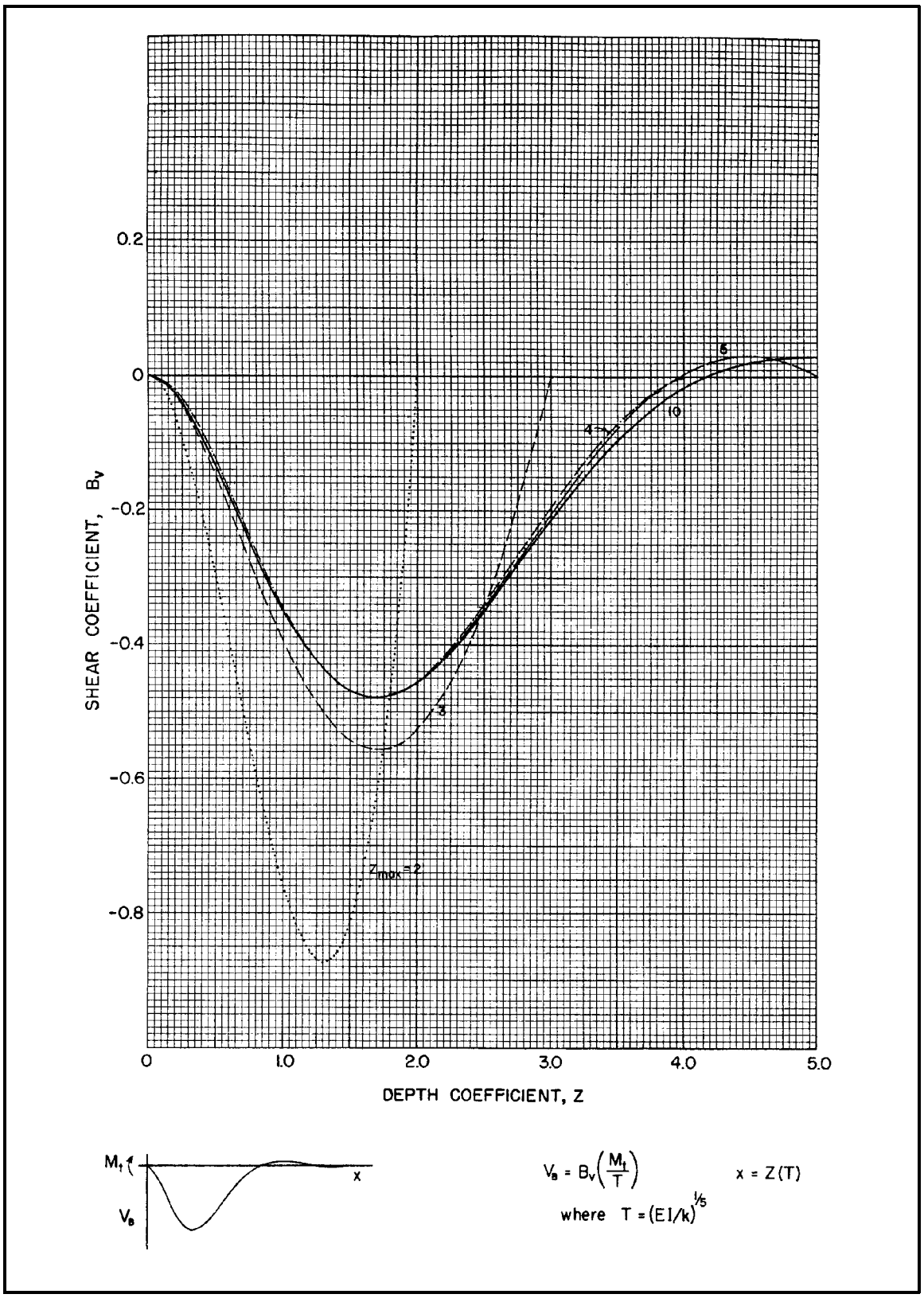

Figure 4-24. Shear produced by moment applied at mudline

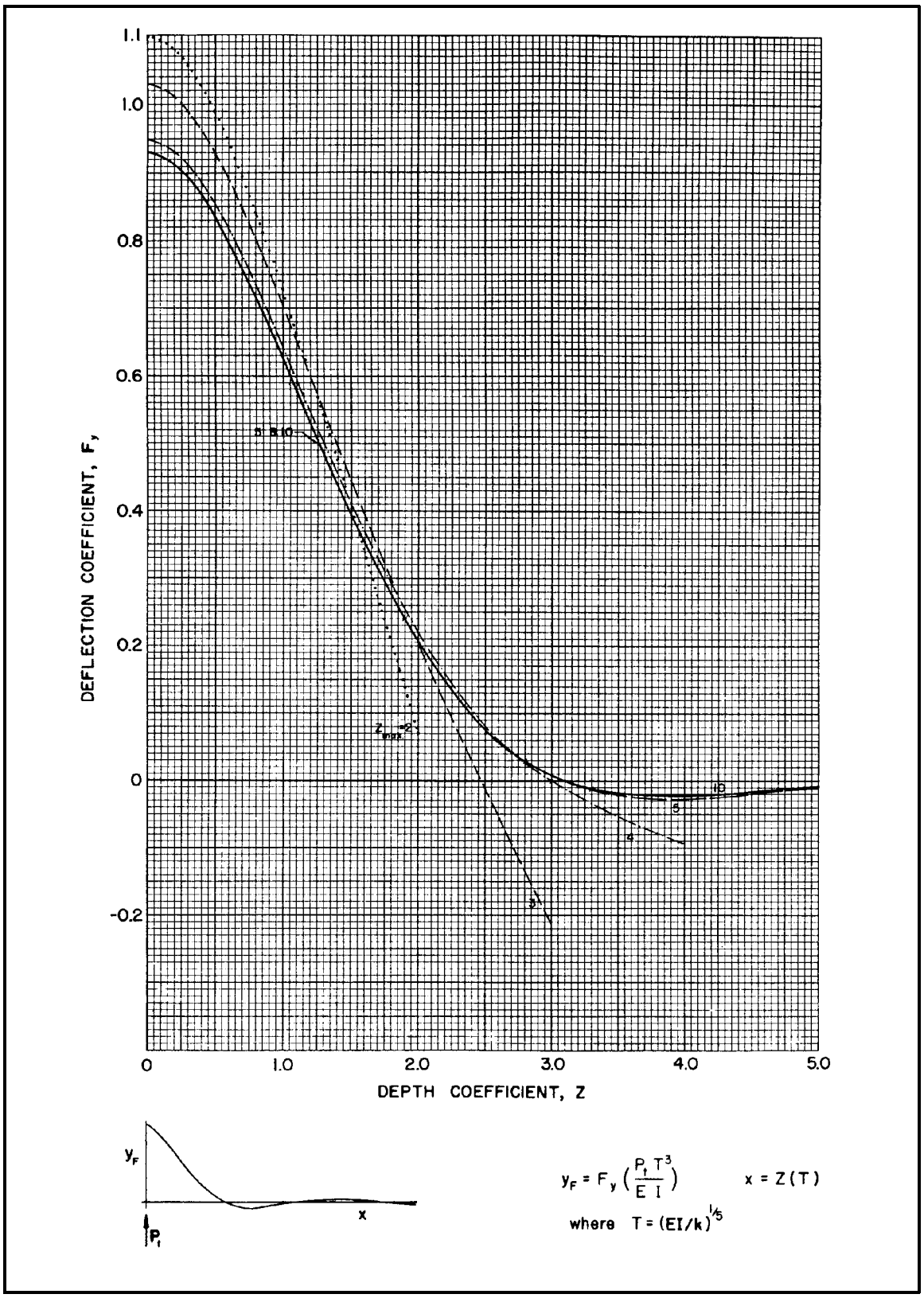

Figure 4-25. Deflection of pile fixed against rotation at mudline

laboratory testing, but for the example problem the soil is assumed to be a sand with an angle of internal friction of 35 degrees and with the water table at the ground surface. The submerged unit weight of the soil is assumed to be 0.04 pounds per cubic inch.

(3) Study soil-response (p-y) curves (step 3). The procedures described earlier for sand were used and the p-y curves were developed. For the structural shape, the diameter of the pile was selected as equal to the width. The curves are presented in Figure 4-26. The curves are spaced closer near the top of the pile where deflection is the largest. If the computer is employed, this step is unnecessary because the subroutines for the responses of the soil are implemented in the program. However, the user may have p-y curves produced for examination, if desired. For the hand solution, demonstrated herein, the p-y curves are shown in Figure 4-26. For the curve of the ground surface, zero depth, the p-values are zero for all values of y. The nonlinearity in the curves is evident, but it is of interest to note that there is no deflection-softening for the sand.

(4) Select set of loads and boundary conditions (step 4). If the computer program, COM624G, is being used, the engineer may select a set of loads and input the set into the program. Only a minimum set of output could be specified for each load; for example, pile-head deflection and maximum bending moment. The boundary conditions at the pile head can also be varied during these computations. The computer will rapidly produce the results, and the engineer may monitor the results on the screen and select another set for more complete output by hard copy and/or graphics. The deflection and bending moment, and other values, will be produced for points along the pile. In any case, the plan should be to find the loading that will generate the maximum bending moment or the maximum allowable deflection. A global factor of safety can be used and the results obtained for the case of the working load. All of the computations could be by the hand solution except that the axial loading cannot be included as affecting the lateral deflection and except that the pile cannot be shown as having different stiffnesses with depth. In any case, the hand solutions will be very time-consuming. However, to indicate the analytical process, a lateral load P_t of 30 kips was selected and the pile head was assumed to be free to rotate. This case might be similar to one of the piles that support a lock and dam, where the pile head extends only a short distance into the concrete base.

(5) Solve for deflection and bending moment (step 5). The first part of this step is to use the method for a hand solution and to solve for the response of the pile to the loading and boundary condition shown above. There is little information to be used in the selection of the initial value of the relative stiffness factor T, so a convenient value is selected. It is noted that the computations are with units of pounds and inches, for convenience.

(a) Trial 1

L = 80 ft (960 in.)

T = 100 in.

= L/T

z_{max} = 960/100 = 9.6; use curves for a "long" pile

$$y = A_y \frac{P_t T^3}{EI} = A_y \frac{(30{,}000)\ (100)^3}{(29{,}000{,}000)\ (650)}$$

$$= 1.592\ A_y$$

The computational table should be set up to correspond to the depths of the p-y curves.

The values of E_s are plotted in Figure 4-27a as a function of x with the result for k as shown below.

$$k = 270/100 = 2.70\ \text{lb/in.}^3$$

The value of the relative stiffness factor T that was obtained can now be found.

$$T = \sqrt[5]{\frac{EI}{K}} \sqrt[5]{\frac{(29 \times 10^6)\ (650\ \text{in.}^4)}{2.70}}$$

$$= 93.1\ \text{inches}$$

The value of T that was obtained is lower than the one that was tried. The second trial needs to use a still lower value to help to achieve a convergence.

(b) Trial 2

T = 50 inches

z_{max} = 960/50 = 19.2; use curves for a "long" pile

$$y = A_y \frac{P_t T^3}{EI} = A_y \frac{(30{,}000)\ (50)^3}{(29{,}000{,}000)\ (650)}$$

$$= 0.1989\ A_y$$

The values of E_s are plotted in Figure 4-27a as a function of x with the result for k as shown below.

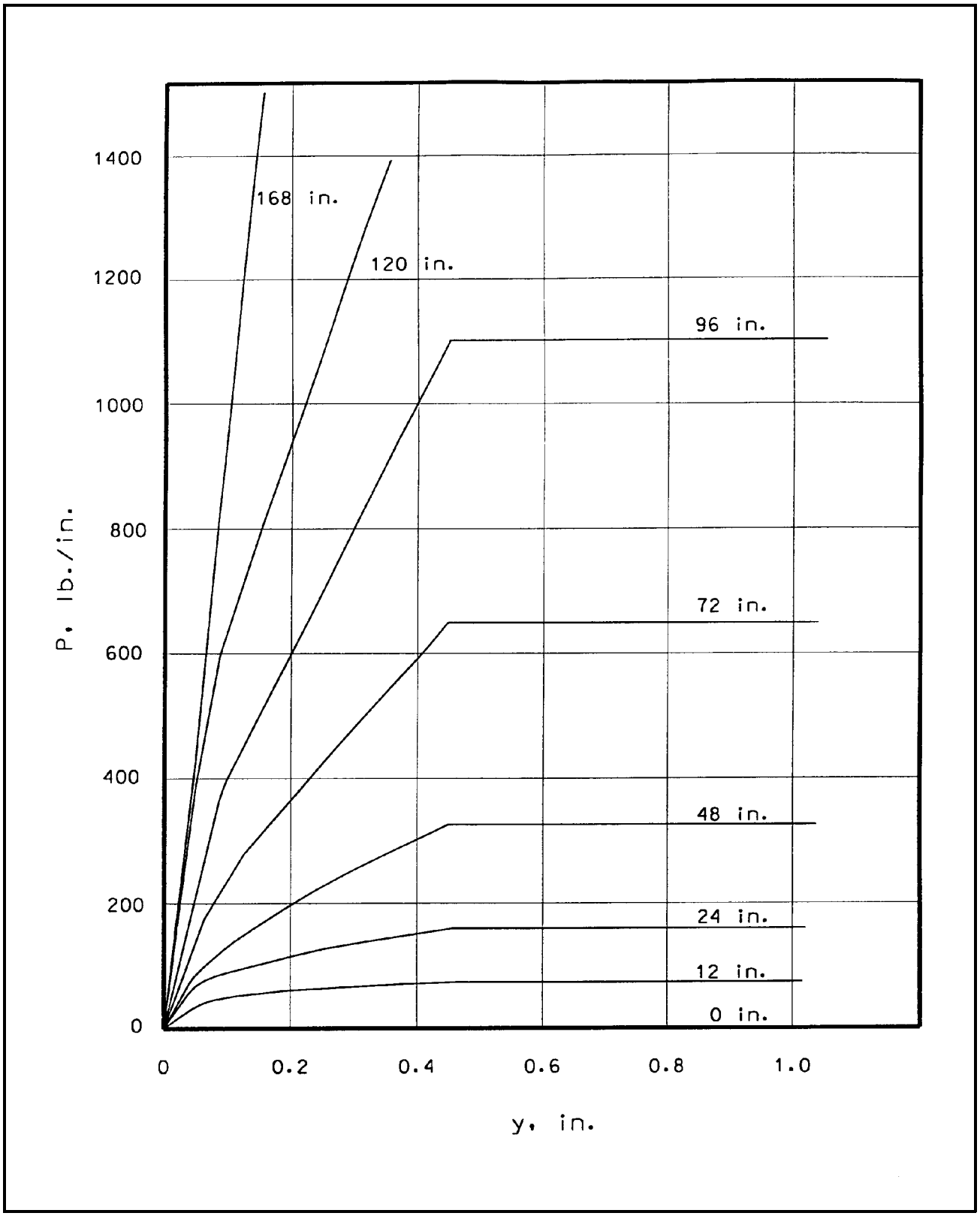

Figure 4-26. Soil-response curves

Depth (in.)	$z = x/t$	A_y	Deflection (in.)	Soil Resistance (lb/in.)	E_s (lb/sq in.)
0	0.00	2.4	3.82	0	0
12	0.12	2.25	3.58	77	22
24	0.24	2.0	3.18	165	52
48	0.48	1.7	2.71	320	118
72	0.72	1.3	2.07	625	302
96	0.96	1.0	1.59	1,125	708
120	1.2	0.75	1.19	---	---
168	1.68	0.2	0.32	---	---

Depth (in.)	$z = x/t$	A_y	Deflection (in.)	Soil Resistance (lb/in.)	E_s (lb/sq in.)
0	0.00	2.4	0.477	0	0
12	0.24	2.0	0.398	75	188
24	0.48	1.7	0.338	135	399
48	0.96	1.0	0.199	185	930
72	1.44	0.5	0.100	225	2,250
96	1.92	0.15	0.030	---	---
120	2.40	0.00	0.000	---	---
168	3.32	---	---	---	---

$$k = 1{,}000/47 = 21.28 \text{ lb/in.}^3$$

The value of the relative stiffness factor T that was obtained can now be found.

$$T = \sqrt[5]{\frac{EI}{K}} \sqrt[5]{\frac{(29 \times 10^6)\ (650 \text{ in.}^4)}{21.28}}$$

$$= 61.6 \text{ inches}$$

The values of T obtained are plotted versus T tried in Figure 4-27b. The converged value for T is approximately 84 inches. The reader may see that values for the A_y coefficients were obtained only approximately from the curve and that the values for the soil resistance corresponding to a computed deflection were obtained only approximately from the Figure giving the p-y curves. Also, there is no assurance that a straight line is correct between the plotted points for the two trials shown in Figure 4-27b. However, for the purposes of this demonstration no additional trials are made and the result is accepted as shown. The value of T of 84, a value of P_t of 30,000 pounds, and a value of EI of 18.85×10^9 lb-in.^{2} are employed in obtaining the curves of deflection and bending moment as a function of depth. The equations are shown below and the computations merely involve the selection of values from the nondimensional curves for the depths desired.

$$y = A_y \frac{P_t T^3}{EI} = A_y \frac{(30{,}000)\ (84)^3}{(29{,}000{,}000)\ (650)}$$

$$= 0.943\ A_y$$

$$M = A_m\ P_t\ T = 2.52 \times 10^6 \text{ in.-lb}$$

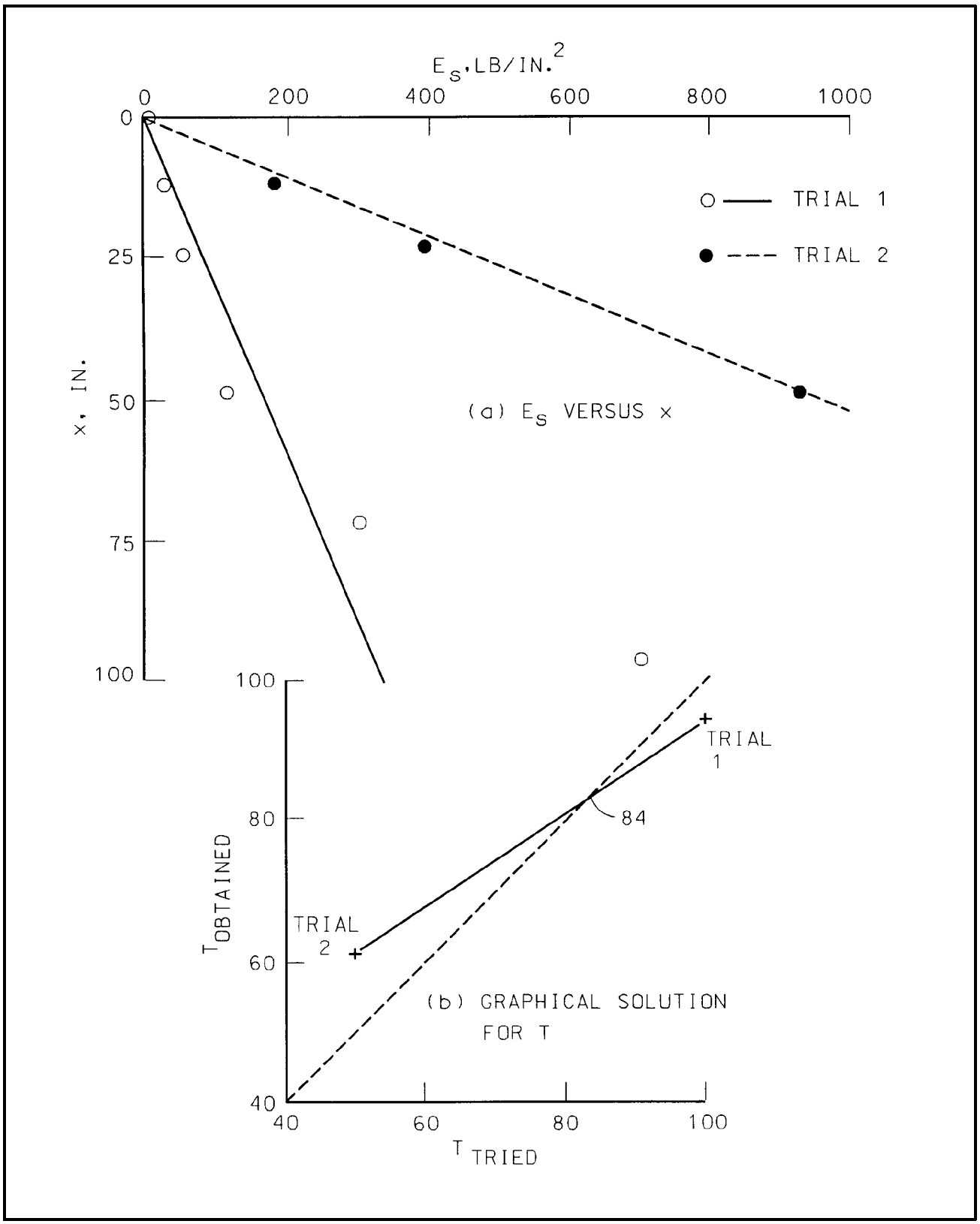

Figure 4-27. Graphical solution for relative stiffness factor

The following table shows the computation of the values of deflection and bending moment as a function of depth, using the above equations. The same problem was solved by computer and results from both methods are plotted in Figure 4-28. As may be seen, the shapes of both sets of curves are similar, the maximum moment from the hand method and from computer agree fairly well, but the computed deflection at the top of the pile is about one-half the value from the nondimensional method. One can conclude that a closed convergence may have yielded a smaller value of the relative stiffness factor to obtain a slightly better agreement between the two methods, but it is certain that the two methods could not have been brought into perfect agreement. An examination of Figure 4-27a shows that is impossible to fit a straight line through the plotted values of E_s versus depth; therefore, $E_s = kx$ will not yield a perfect solution to the problem, as demonstrated in Figure 4-28. However, even with imperfect fitting in Figure 4-27a and with the crude convergence shown in Figure 4-27b, the computed values of maximum bending moment from the hand solution and from computer agreed remarkably well. The effect of the axial loading on the deflection and bending moment was investigated with the computer by assuming that the pile had an axial load of

Depth (in.)	z	A_y	y (in.)	A_M	M (in. lb/10^6)
0	0.0	2.43	2.29	0.0	0
17	0.2	2.11	1.99	0.198	0.499
34	0.4	1.80	1.70	0.379	0.955
50	0.6	1.50	1.41	0.532	1.341
67	0.8	1.22	1.15	0.649	1.636
84	1.0	0.962	0.91	0.727	1.832
101	1.2	0.738	0.70	0.767	1.933
118	1.4	0.544	0.51	0.772	1.945
151	1.8	0.247	0.23	0.696	1.754
210	2.5	-0.020	-0.02	0.422	1.063
252	3.0	-0.075	-0.07	0.225	0.567
294	3.5	-0.074	-0.07	0.081	0.204
336	4.0	-0.050	-0.05	0.0	0

100 kips. The results showed that the groundline deflection increased about 0.036 inches, and the maximum bending moment increased about 0.058×10^6 in-lb; thus, the axial load caused an increase of only about 3 percent in the values computed with no axial load. However, the ability to use an axial load in the computations becomes important when a portion of a pile extends above the groundline. The computation of the buckling load can only be done properly with a computer code.

(6) Repeat solutions for loads to obtain failure moment (step 6). As shown in the statement about the dimensions of the pile, the ultimate bending moment was incremented to find the lateral load P_t that would develop that moment. The results, not shown here, yielded an ultimate load of 52 kips. The deflection corresponding to that load was about 3.2 inches.

(7) Apply global factor of safety (step 7). The selection of the factor of safety to be used in a particular design is a function of many parameters. In connection with a particular design, an excellent procedure is to perform computations with upper-bound and lower- bound values of the principal factors that affect a solution. A comparison of the results may suggest in a particular design that can be employed with safety. Alternatively, the difference in the results of such computations may suggest the performance of further tests of the soil or the performance of full-scale field tests at the

construction site.

5. Status of the Technology

The methods of analysis presented herein will be improved in time by the development of better methods of characterizing soil and by upgrading the computer code. In this latter case, the codes are being constantly refined to make them more versatile, applicable to a wider range of problems, and easier to use. From time to time tests are being performed in the field with instrumented piles. These tests, when properly interpreted, can lead to better ideas about the response of the soil. However, it is unlikely that there will be much changein the basic method of analysis. The solution of the difference equations by numerical techniques, employing curves at discrete locations along a pile to represent the response of the soil or distributed loading, is an effective method. The finite element method may come into more use in time but, at present, information on the characterization of the soil by that method is inadequate.

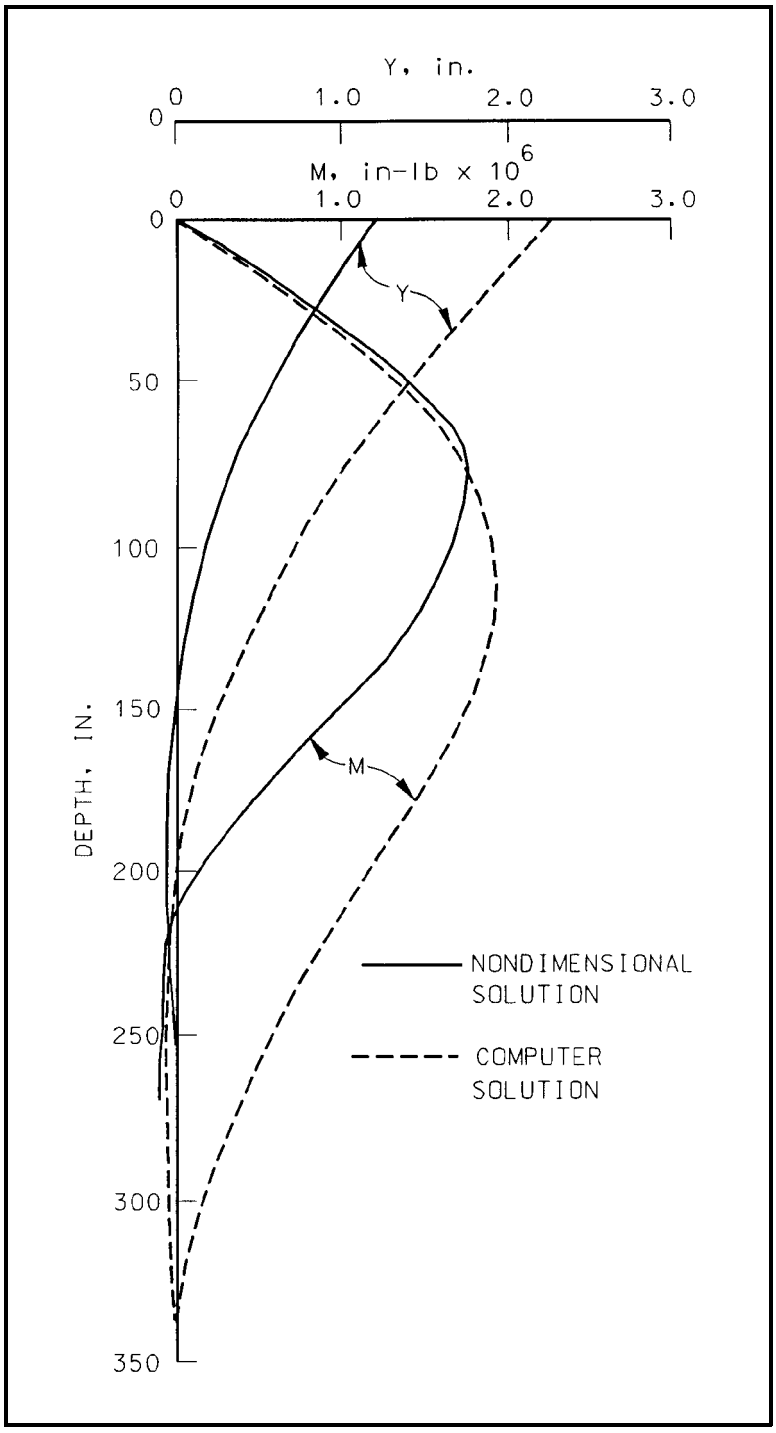

Figure 4-28. Comparison of deflection and bending moment from nondimensional and computer solutions

Chapter 5
Pile Groups

1. Design Considerations

This chapter provides several hand calculation methods for a quick estimate of the capacity and movement characteristics of a selected group of driven piles or drilled shafts for given soil conditions. A computer assisted method such as described in Chapter 5, paragraph 4, is recommended for a detailed solution of the performance of driven pile groups. Recommended factors of safety for pile groups are also given in Table 3-2. Calculation of the distribution of loads in a pile group is considered in paragraph 2b, Chapter 2.

a. Driven piles. Driven piles are normally placed in groups with spacings less than 6*B* where *B* is the width or diameter of an individual pile. The pile group is often joined at the ground surface by a concrete slab such as a pile cap, Figure 5-1a. If pile spacing within the optimum range, the load capacity of groups of driven piles in cohesionless soils can often be greater than the sum of the capacitites of isolated piles, because driving can compact sands and can increase skin friction and end-bearing resistance.

b. Drilled shafts. Drilled shafts are often not placed in closely spaced groups, Figure 5-1b, because these foundations can be constructed with large diameters and can extend to great depths. Exceptions include using drilled shafts as retaining walls or to improve the soil by replacing existing soil with multiple drilled shafts. Boreholes prepared for construction of drilled shafts reduce effective stresses in soil adjacent to the sides and bases of shafts already in place. The load capacity of drilled shafts in cohesionless soils spaced less than 6*B* may therefore be less than the sum of the capacities of the individual shafts. For end-bearing drilled shafts, spacing of less than 6*B* can be used without significant reduction in load capacity.

2. Factors Influencing Pile Group Behavior

Piles are normally constructed in groups of vertical, batter, or a combination of vertical and batter piles. The distribution of loads applied to a pile group are transferred nonlinearly and indeterminately to the soil. Interaction effects between adjacent piles in a group lead to complex solutions. Factors considered below affect the resistance of the pile group to movement and load transfer through the pile group to the soil.

a. Soil modulus. The elastic soil modulus E_s and the lateral modulus of subgrade reaction E_{1s} relate lateral, axial, and rotational resistance of the pile-soil medium to displacements. Water table depth and seepage pressures affect the modulus of cohesionless soil. The modulus of submerged sands should be reduced by the ratio of the submerged unit weight divided by the soil unit weight.

b. Batter. Battered piles are used in groups of at least two or more piles to increase capacity and loading resistance. The angle of inclination should rarely exceed 20 degrees from the vertical for normal construction and should never exceed 26½ degrees. Battered piles should be avoided where significant negative skin friction and downdrag forces may occur. Batter piles should be avoided where the structure's foundation must respond with ductility to unusually large loads or where large seismic loads can be transferred to the structure through the foundation.

c. Fixity. The fixity of the pile head into the pile cap influences the loading capacity of the pile group. Fixing the pile rather than pinning into the pile cap usually increases the lateral stiffness of the group, and the moment. A group of fixed piles can therefore support about twice the lateral load at identical deflections as the pinned group. A fixed connection between the pile and cap is also able to transfer significant bending moment through the connection. The minimum vertical embedment distance of the top of the pile into the cap required for achieving a fixed connection is 2*B* where *B* is the pile diameter or width.

d. Stiffness of pile cap. The stiffness of the pile cap will influence the distribution of structural loads to the individual piles. The thickness of the pile cap must be at least four times the width of an individual pile to cause a significant influence on the stiffness of the foundation (Fleming et al. 1985). A ridgid cap can be assumed if the stiffness of the cap is 10 or more times greater than the stiffness of the individual piles, as generally true for massive concrete caps. A rigid cap can usually be assumed for gravity type hydraulic structures.

e. Nature of loading. Static, cyclic, dynamic, and transient loads affect the ability of the pile group to resist the applied forces. Cyclic, vibratory, or repeated static loads cause greater displacements than a sustained static load of the same magitude. Displacements can double in some cases.

f. Driving. The apparent stiffness of a pile in a group may be greater than that of an isolated pile driven in cohesionless soil because the density of the soil within and around a pile group can be increased by driving. The pile group as a whole may not reflect this increased stiffness because the soil around and outside the group may not be favorably affected by driving and displacements larger than anticipated may occur.

g. Sheet pile cutoffs. Sheet pile cutoffs enclosing a pile group may change the stress distribution in the soil and influence the group load capacity. The length of the cutoff should be determined from a flow net or other seepage analysis. The net pressure acting on the cutoff is the sum of the unbalanced earth and water pressures caused by the

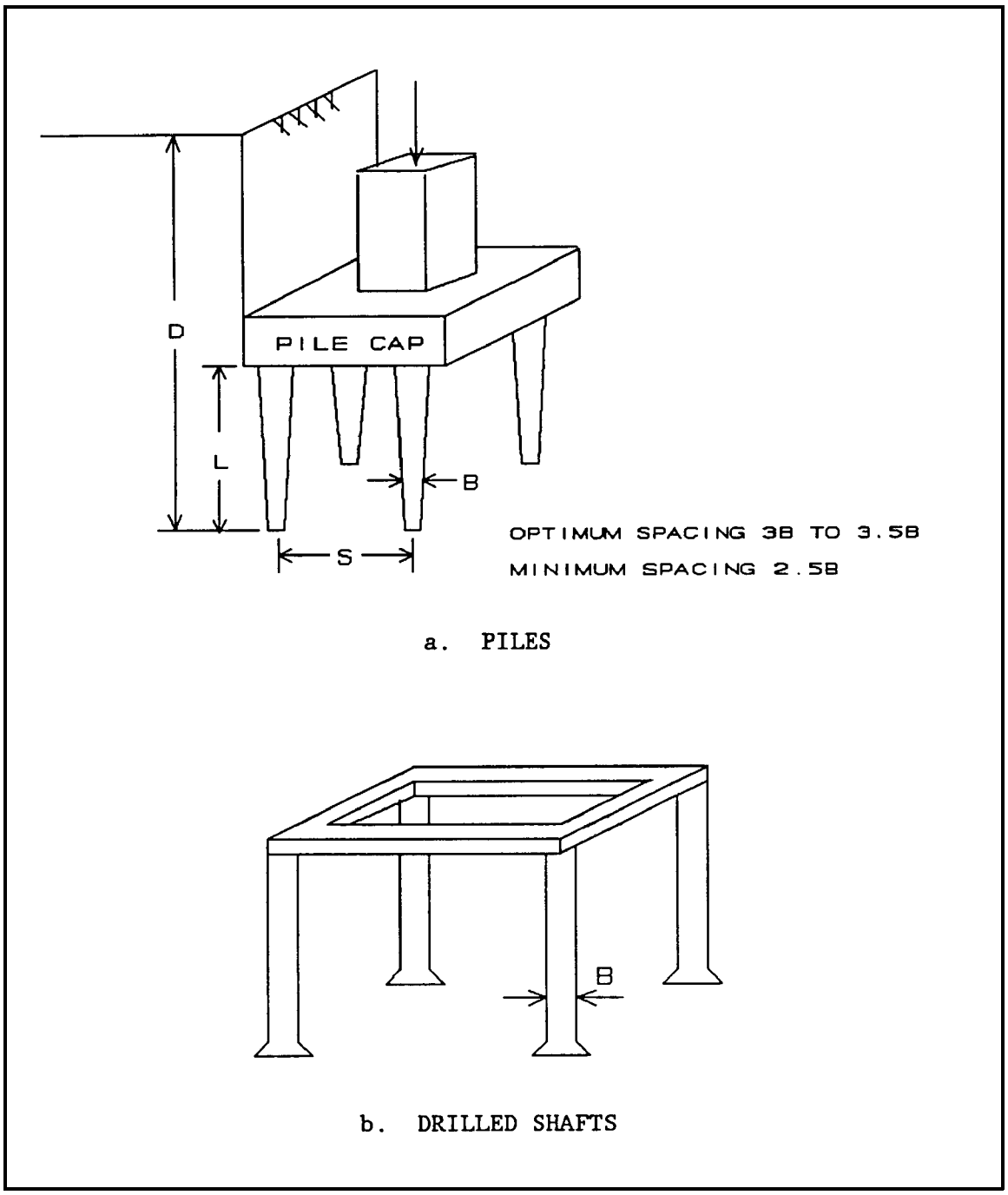

Figure 5-1. Groups of deep foundations

cutoff. Steel pile cutoffs should be considered in the analysis as not totally impervious. Flexible steel sheet piles should cause negligible load to be transferred to the soil. Rigid cutoffs, such as a concrete cutoff, will transfer the unbalanced earth and water pressures to the structure and shall be accounted for in the analysis of the pile group.

h. Interaction effects. Deep foundations where spacings between individual piles are less than six times the pile width *B* cause interaction effects between adjacent piles from

overlapping of stress zones in the soil, Figure 5-2. In situ soil stresses from pile loads are applied over a much larger area and extend to a greater depth leading to greater settlement.

i. Pile spacing. Piles in a group should be spaced so that the bearing capacity of the group is optimum. The optimum spacing for driven piles is 3 to 3.5B (Vesic 1977) or 0.02L + 2.5B, where L is the embedded length of the piles (Canadian Geotechnical Society 1985). Pile spacings should be at least 2.5B.

3. Design for Vertical Loads

The methodology should provide calculations of the pile group capacity and displacements such that the forces are in equilibrium between the structure and the supporting piles and between the piles and soil supporting the piles. The allowable group capacity is the ultimate group capacity divided by the factor of safety. The factor of safety is usually 3 for pile groups, Table 3-2. Methods for analysis of axial load capacity and settlement are provided below.

a. Axial capacity of drilled shaft groups. The calculation depends on whether the group is in sands or clays. Installation in cohesionless sands causes stress relief and a reduced density of the sands during construction. The efficiency method is appropriate whether the pile cap is or is not in firm contact with the ground. Block failure, however, may occur when the base of the group overlies soil that is much weaker than the soil at the base of the piles. Group capacity in cohesive soil depends on whether or not the pile cap is in contact with the ground.

(1) Group capacity for cohesionless soil. Group ultimate capacity is calculated by the efficiency method for cohesionless soil

$$Q_{ug} = n \times E_g \times Q_u \tag{5-1}$$

where

Q_{ug} = group capacity, kips

n = number of shafts in the group

E_g = efficiency

Q_u = ultimate capacity of the single shaft

E_g should be > 0.7 for spacings = 3B and increases linearly to 1.0 for spacings = 6B where B is the shaft diameter or width (FHWA-HI-88-042). E_g should vary linearly for spacings between 3B and 6B. $E_g = 0.7$ for spacings $\leq$ 3B. The factor of safety of the group is the same as that of the individual shafts.

(2) Group capacity for cohesive soil. Groups with the cap in firm contact with the clay may fail as a block of soil containing the drilled shafts, even at large spacings between individual shafts. The ultimate group capacity is either the lesser of the sum of the individual capacities or the ultimate capacity of the block. The block capacity is determined by

$$Q_{ug} = 2L(H_L + H_W)C_{ua} + N_{cg} \times C_{ub} \times H_L \times H_W \tag{5-2}$$

where

L = depth of penetration meter (feet)

H_L = horizontal length of group meter (feet)

H_W = horizontal width of group meter (feet)

C_{ua} = average undrained shear strength of cohesive soil in which the group is placed kN/m^2 (ksf)

C_{ub} = undrained shear strength of cohesive soil at the base kN/m^2 (ksf)

N_{cg} = cohesion group bearing capacity factor

N_{cg} is determined by

$$N_{cg} = 5\left(1 + 0.2\frac{H_W}{H_L}\right)\left(1 + 0.2\frac{L}{H_W}\right) \quad \text{for } \frac{L}{H_W} \leq 2.5 \tag{5-3a}$$

$$N_{cg} = 7.5\left(1 + 0.2\frac{H_W}{H_L}\right) \quad \text{for } \frac{L}{H_W} > 2.5 \tag{5-3b}$$

The group capacity is calculated by the efficiency equation 5-1 if the pile cap is not in firm contact with the soil. Overconsolidated and insensitive clay shall be treated as if the cap is in firm contact with the ground.

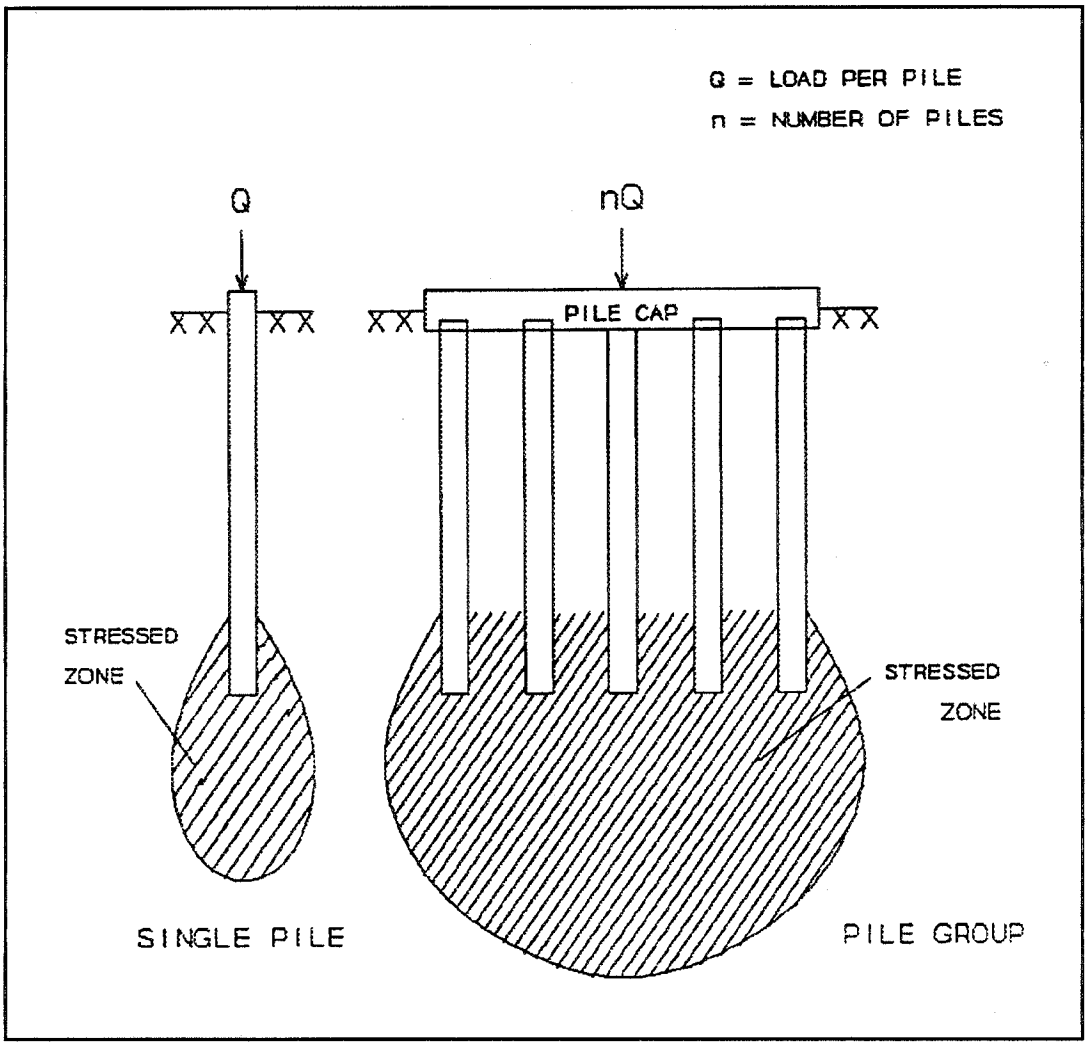

Figure 5-2. Stress zones in soil supporting piles

(a) Presence of locally soft soil should be checked because this soil may cause some driven piles or drilled shafts to fail. The equivalent mat method in Table 5-1 is recommended to calculate group capacity in soft clays, e.g. $C_u \leq 0.5$ ksf.

(b) The ultimate capacity of a group in a strong clay soil overlying weak clay may be estimated by assuming block punching through the weak underlying soil layer. Group capacity may be calculated by equation 5-2 using the undrained strength C_{ub} of the underlying weak clay. A less conservative solution is provided (FHWA-HI-88-042) by

$$Q_{ug} = Q_{ug,1} + \frac{Z_b}{10H_W}[Q_{ug,u} - Q_{ug,1}] \qquad (5\text{-}4)$$

$$\leq Q_{ug,u}$$

where

$Q_{ug,l}$ = group capacity if base at top of lower weak soil, kips

$Q_{ug,u}$ = group capacity in the upper soil if the weaker lower soil were not present, kips

Z_b = vertical distance from the base of the shafts in the group to the top of the weak layer, feet

H_W = least width of group, feet

Equation 5-4 can also be used to estimate the ultimate capacity of a group in a strong cohesionless soil overlying

a weak cohesive layer.

b. Axial capacity of driven pile groups. Driven piles are normally placed in groups with spacings less than 3*B* and joined at the ground surface by a concrete cap.

(1) Group capacity for cohesionless soil. Pile driving compacts the soil and increases end-bearing and skin friction resistance. Therefore, the ultimate group capacity of driven piles with spacings less than 3*B* can be greater than the sum of the capacities of the individual piles.

(2) Group capacity for cohesive soil. For this case, the ultimate capacity of a pile group is the lesser of the sum of the capacities of the individual piles or the capacity by block failure.

(a) The capacity of block failure is given by equation 5-2.

(b) The capacity of a pile group with the pile cap not in firm contact with the ground may be calculated by the efficiency method in equation 5-1.

(3) Uplift capacity. The ultimate uplift capacity of a pile group is taken as the lesser of the sum of the individual pile uplift capacities or the uplift capacity of the group considered as a block.

(a) Cohesionless soil. The side friction of pile groups in sands decreases with time if the piles are subject to vibration or lateral loads. The uplift capacity will be at least the weight of the soil and piles of the group considered as a block.

(b) Cohesive soil. The uplift capacity will include side friction and is estimated by

$$Q_{ug} = 2L\,(H_W + H_L)\,C_{ua} + W_g \qquad (5\text{-}5)$$

where

C_{ua} = average undrained shear strength along the perimeter of the piles, ksf

W_g = weight of the pile group considered as a block, kips

W_g also includes the weight of the soil within the group.

c. Settlement analysis. The settlement of a group of piles with load nQ (n - number of piles and Q = load per pile) can be much greater than the settlement of a single pile with load Q because the value of the stress zones of a pile group is much larger and extends deeper than that of a single pile, Figure 5-2. Hand calculation methods for estimating the settlement of pile groups are approximate. An estimate of settlement can also be obtained by considering the pile group as an equivalent mat as in Table 5-1, then calculating the settlement of this mat as given in chapter 5 of TM 5-818-1, "Soils and Geology; Procedures for Foundation Design of Buildings and Other Structures (Except Hydraulic Structures)."

(1) Immediate settlement. A simple method for estimating group settlement from the settlement of a single pile is to use a group settlement factor

$$\rho_g = g_f \rho \qquad (5\text{-}6a)$$

where

ρ_g = group settlement, feet

g_f = group settlement factor

ρ = settlement of single pile, feet

(a) The group settlement factor for sand (Pile Buck Inc. 1992) is

$$g_f = \left(\frac{H_W}{B}\right)^{0.5} \qquad (5\text{-}6b)$$

where H_W = width of the pile group and B is the pile diameter or width.

(b) The group settlement factor for clay (Pile Buck Inc. 1992) is

$$g_f = 1 + \sum_{i=1}^{n} \frac{B_i}{\pi s_i} \qquad (5\text{-}6c)$$

Table 5-1
Equivalent Mat Method of Group Pile Capacity Failure in Soft Clays

Step	Description
1	Replace group with a flexible mat of same dimensions as the group at some depth along the pile length; mat depth determined as follows:

Depth	Soil Condition
Ground Surface	Highly overconsolidated soil at the surface underlain by softer soil
2/3 of pile length from top	Group support obtained mostly from skin friction
Pile tip	End-bearing piles

2 Assume the mat carries the full group load

3 Distribute pressure on the mat to the underlying soft clay either by a line that makes a 60-degree angle with the horizontal or by Boussinesq theory; the 60-degree method reduces mat pressure by the ratio of mat area divided by area of soil enclosed by the 60-degree line at the selected depth

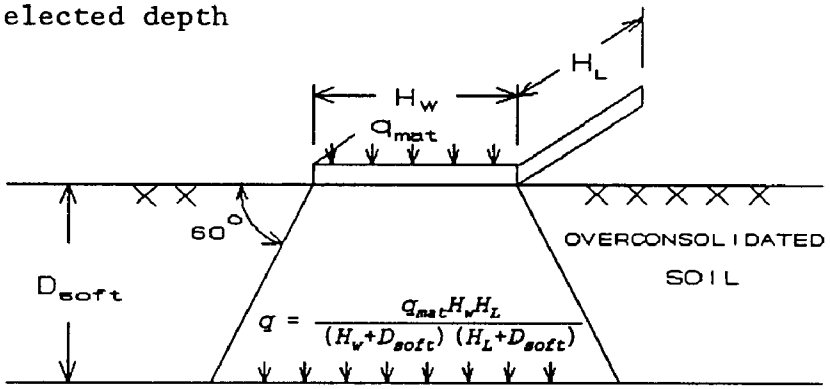

4 Compare the distributed pressure at the top of the soft clay with $9C_u$ where C_u is the average undrained shear strength of the soft clay

where n = number of piles in the group

where

n = number of piles in the group

s_i = distance from pile i to the location in the group where group settlement is to be calculated, feet

(2) Estimates using field soil test results. Standard penetration and cone penetration test data can provide useful estimates assuming the group can be represented by an equivalent single pile.

(a) Settlement of pile groups in a homogeneous sand deposit not underlain by a more compressible soil at greater depth (Meyerhof 1976) is

$$\rho_g = \frac{q\sqrt{H_w}}{N_{spt}} I \qquad (5\text{-}7a)$$

$$I = 1 - \frac{L}{8 H_w} \geq 0.5 \qquad (5\text{-}7b)$$

where

ρ_g = settlement of pile group, in.

q = net foundation pressure on the group, ksf

B_g = width of pile group, feet

I = influence factor

N_{spt} = average standard penetration resistance within the depth beneath the pile tip equal to the group width corrected to an effective overburden pressure of 2 kips per square foot, blows/feet

L = embedment depth of equivalent pile, feet

(b) The calculated settlement should be doubled for a silty sand.

(c) Maximum settlement estimated from static cone penetration tests (Meyerhof 1976) is

$$\rho_g = \frac{q H_w}{2 q_c} I \qquad (5\text{-}7c)$$

where q_c is the average cone tip resistance within depth H_W beneath the pile tip in the same units as q.

(3) Consolidation settlement. Long-term settlement may be estimated for pile groups in clay by the equivalent method in Table 5-2.

Table 5-2
Equivalent Mat Method for Estimating Consolidation Settlement of Pile Groups in Clay

Step	Description
1	Replace the group with a mat at some depth along the embedded pile length L; this depth is 2/3 of L for friction piles and L for end bearing piles.
2	Distribute the load from the mat to the underlying soil by Boussinesq theory or the 60-degree method.
3	Calculate settlement of soil layers below the mat by one-dimensional consolidation theory; any soil above the mat is assumed incompressible.
4	Multiply the calculated settlement by 0.8 to account for rigidity of the group.

d. Application. A square three by three group of nine steel circular closed-end pipe piles with diameter $B = 1.5$ feet is to be driven to an embedment depth $L = 30$ feet in the same soils as Figure 3-15. These soils are a 15-feet layer of clay over sand. Spacing is $4B$ and the horizontial width H_W is $15B = 15 \times 1.5 = 22.5$ feet. The group upper- and lower-bound estimates of ultimate and allowable capacity and expected settlement at the allowable capacity are to be calculated to provide guidance for the pile group design. Pile driver analysis with a load test will be conducted at the start of construction. The factor of safety to be used for this analysis is 3.

(1) Group ultimate capacity. The group ultimate capacity Q_{ug} is expected to be the sum of the ultimate capacities of the individual piles. These piles are to be driven into sand which will densify and increase the end-bearing capacity. From Table 3-7, the calculated lower-bound ultimate capacity is $Q_{u,l} = 317$ kips, and the upper-bound capacity is $Q_{u,u} = 520$ kips. Therefore, $Q_{ug,lo} = n \times Q_{u,l} = 9 \times 317 = 2{,}853$ kips and $Q_{ug,up} = 9 \times 520 = 4{,}680$ kips.

(2) Group allowable capacity. The allowable group upper- and lower-bound capacities are

$$Q_{ag,l} = \frac{Q_{ug,l}}{FS} = \frac{2,853}{3} = 951 \text{ kips}$$

$$Q_{ag,u} = \frac{Q_{ug,u}}{FS} = \frac{4,680}{3} = 1,560 \text{ kips}$$

The group allowable load is expected to be between 951 and 1,560 kips. Lower *FS* may be possible.

(3) Group settlement. Settlement at the allowable capacity will be greater than that of the individual piles. The settlement of each pile is to be initially determined from equation 3-38, then the group settlement is to be calculated from equation 5-6.

(a) The allowable lower- and upper-bound capacities of each individual pile is $Q_{a,l} = 317/3 = 106$ kips and $Q_{a,u} = 520/3 = 173$ kips. All the skin friction is assumed to be mobilized. Therefore, $Q_{s,l} = Q_{su,l} = 159$ kips $> Q_{a,l} = 106$ kips and $Q_{s,u} = Q_{su,u} = 231$ kips $> Q_u = 173$ kips. Base resistance will not be mobilized because the ultimate skin resistance Q_{su} exceeds the allowable capacity. From equation 3-38a, axial compression is

$$\rho_p = 12 \alpha_s Q_s \frac{L}{A E_p}$$

$$= 12 \times 0.5 \times Q_s \frac{30}{\pi \times 1 \times 5^2 \times 432,000}$$

$$= 0.00006 \times Q_s \text{ inch}$$

The elastic modulus of the pile is assumed similar to concrete $E_p = 432{,}000$ ksf because this pile will be filled with concrete. Lower- and upper-bound axial compression is therefore

$$\rho_{p,l} = 0.00006 \times 106 = 0.0063 \text{ inch}$$

$$\rho_{p,u} = 0.00006 \times 173 = 0.0104 \text{ inch}$$

(b) Tip settlement from load transmitted along the shaft length from equation 3-38c is

$$\rho_s = \frac{12 C_s Q_s}{L q_{bu}} = \frac{12 \times 0.05 \times Q_s}{30 \times q_{bu}} = \frac{0.02 Q_s}{q_{bu}} \text{ inch}$$

where

$C_s = [\, 0.93 + 0.16 (L/B_s)^{0.5} \,] C_b = [\, 0.93 + 0.16 (30/1.5)^{0.5} \,] (0.03) = 0.05$

lower-bound $q_{bu,l} = 89$ ksf

upper-bound $q_{bu,u} = 163$ ksf from Table 3-7

Lower- and upper-bound tip settlement from the load transmitted along the shaft length for $Q_{s,l} = 138$ kips and $Q_{s,u} = 231$ kips is

$$\rho_{s,l} = \frac{0.02 \times 159}{103} = 0.031 \text{ inch}$$

$$\rho_{s,u} = \frac{0.02 \times 231}{163} = 0.028 \text{ inch}$$

Total settlements for lower- and upper-bound capacities are

$$\rho = \rho_b + \rho_s$$

$$\rho_l = 0.006 + 0.036 = 0.042 \text{ inch}$$

$$\rho_u = 0.010 + 0.028 = 0.038 \text{ inch}$$

Total settlement ρ is about 0.04 inch.

(c) Group settlement factor g_f from equation 5-6b is

$$g_f = \left(\frac{H_w}{B} \right)^{0.5} = \left(\frac{22.5}{1.5} \right)^{0.5} = 3.87$$

Group settlement from equation 5-6a is

$$\rho_g = g_f \rho = 3.87 \times 0.04 = 0.15 \text{ inch}$$

4. Design for Lateral Loads[1]

a. Response to lateral loading of pile groups. There are two general problems in the analysis of pile groups: the computation of the loads coming to each pile in the group and the determination of the efficiency of a group of closely spaced piles. Each of these problems will be discussed in the following paragraphs.

(1) Symmetric pile group. The methods that are presented are applicable to a pile group that is symmetrical about the line of action of the lateral load. That is, there is no twisting of the pile group so that no pile is subjected to torsion. Therefore, each pile in the group can undergo two translations and a rotation. However, the method that is presented for obtaining the distribution of loading to each pile can be extended to the general case where each pile can undergo three translations and three rotations (Reese, O'Neill, and Smith 1970; O'Neill, Ghazzaly, and Ha 1977; Bryant 1977).

(2) Soil reaction. In all of the analyses presented in this section, the assumption is made that the soil does not act against the pile cap. In many instances, of course, the pile cap is cast against the soil. However, it is possible that soil can settle away from the cap and that the piles will sustain the full load. Thus, it is conservative and perhaps logical to assume that the pile cap is ineffective in carrying any load.

(3) Pile spacing. If the piles that support a structure are spaced far enough apart that the stress transfer between them is minimal and if only shear loading is applied, the methods presented earlier in this manual can be employed. Kuthy et al. (1977) present an excellent treatment of this latter problem.

b. Widely spaced piles. The derivation of the equations presented in this section is based on the assumption that the piles are spaced far enough apart that there is no loss of efficiency; thus, the distribution of stress and deformation from a given pile to other piles in the group need not be considered. However, the method that is derived can be used with a group of closely spaced piles, but another level of interation will be required.

(1) Model of the problem. The problem to be solved is shown in Figure 5-3. Three piles supporting a pile cap are shown. The piles may be of any size and placed on any batter and may have any penetration below the groundline. The bent may be supported by any number of piles but, as noted earlier, the piles are assumed to be placed far enough apart that each is 100 percent efficient. The soil and loading may have any characteristics for which the response of a single pile may be computed. The derivation of the necessary equations proceeds from consideration of a simplified structure such as that shown in Figure 5-4 (Reese and Matlock 1966; Reese 1966). The sign conventions for the loading and for the geometry are shown. A global coordinate system, a-b, is established with reference to the structure. A coordinate system, x-y, is established for each of the piles. For convenience in deriving the equilibrium equations for solution of the problem, the a-b axes are located so that all of the coordinates of the pile heads are positive. The soil is not shown, but as shown in Figure 5-4b, it is desirable to replace the piles with a set of "springs" (mechanisms) that represent the interaction between the piles and the supporting soil.

(2) Derivation of equations. If the global coordinate system translates horizontally Δh and vertically Δv and if the cordinate system, shown in Figure 5-4, rotates through the angle α_s, the movement of the head of each of the piles can be readily found. The angle α_s is assumed to be small in the derivation. The movement of a pile head x_t in the direction of the axis of the pile is

$$x_t = (\Delta h + b\alpha_s)\sin\theta + (\Delta v + a\alpha_s)\cos\theta \quad (5\text{-}8)$$

The movement of a pile head y_t transverse to the direction of the axis of the pile (the lateral deflection) is

$$y_t = (\Delta h + b\alpha_s)\cos\theta - (\Delta v + a\alpha_s)\sin\theta \quad (5\text{-}9)$$

The assumption is made in deriving equations 5-8 and 5-9 that the pile heads have the same relative positions in space before and after loading. However, if the pile heads move relative to each other, an adjustment can be made in equations 5-8 and 5-9 and a solution achieved by iteration. The movements computed by equations 5-8 and 5-9 will generate forces and moments at the pile head.

[1]Portions of this section were abstracted from the writings of Dr. L. C. Reese and his colleagues, with the permission of Dr. Reese.

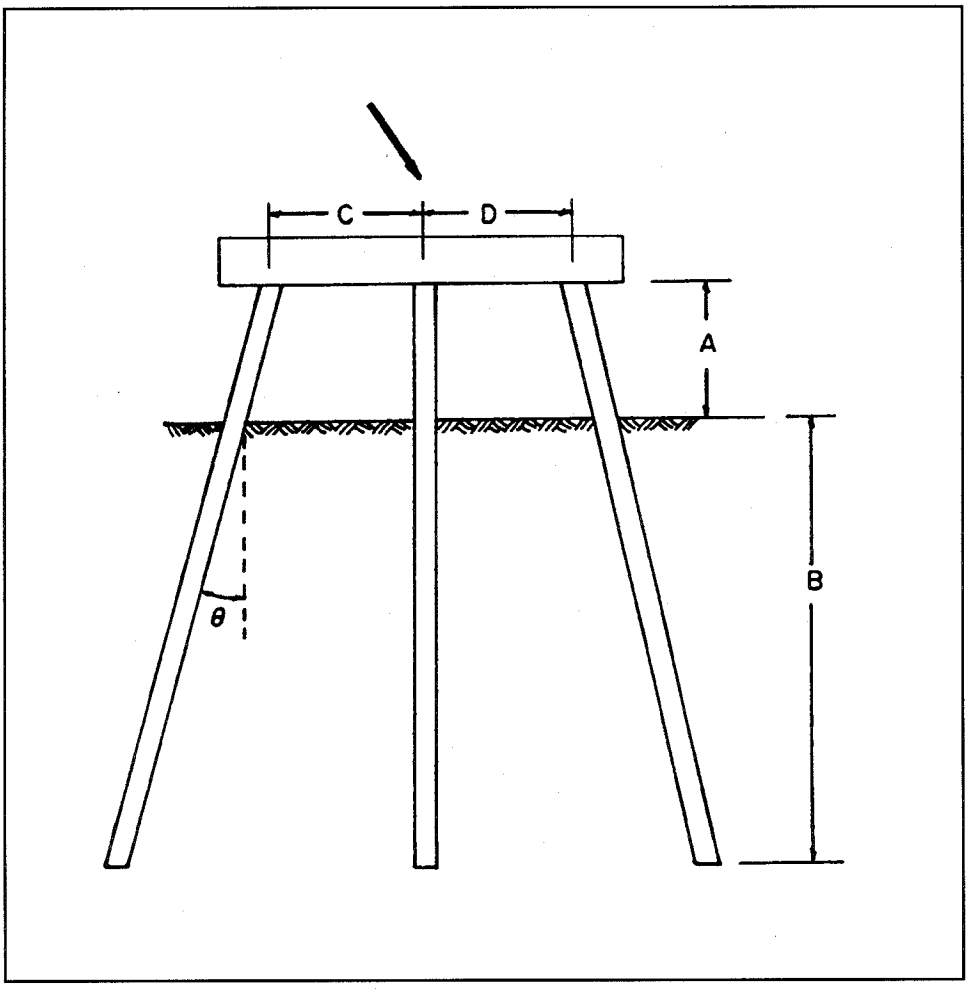

Figure 5-3. Typical pile-supported bent

The assumption is made that curves can be developed, usually nonlinear, that give the relationship between pile-head movement and pile-head forces. A secant to a curve is obtained at the point of deflection and called the modulus of pile-head resistance. The values of the moduli, so obtained, can then be used, as shown below, to compute the components of movement of the structure. If the values of the moduli that were selected were incorrect, iterations are made until convergence is obtained. Using sign conventions established for the single pile under lateral loading, the lateral force P_t at the pile head may be defined as follows:

$$P_t = J_y y_t \tag{5-10}$$

If there is some rotational restraint at the pile-head, the moment is

$$M_t = -J_m y_t \tag{5-11}$$

The moduli J_y and J_m are not single-valued functions of pile-head translation but are functions also of the rotation α_s of the structure. For batter piles, a procedure is given in Appendix D for adjusting values of soil resistance to account for the effect of the batter. If it is assumed that a compressive load causes a positive deflection along the pile axis, the axial force P_x may be defined as follows:

$$P_x = J_x x_t \tag{5-12}$$

It is usually assumed that P_x is a single-valued function of x_t A curve showing axial load versus deflection may be computed by one of the procedures recommended by several authors (Reese 1964; Coyle and Reese 1966; Coyle and

Sulaiman 1967; Kraft, Ray, and Kagawa 1981) or the results from a field load test may be used. A typical curve is shown in Figure 5-5a.

(3) Computer programs. Computer programs or nondimesional methods may be used to obtain curves showing lateral load as a function of lateral deflection and pile-head moment as a function of lateral deflection. The way the pile is attached to the superstructure must be taken into account in making the computations. Typical curves are shown in Figures 5-5b and 5-5c. The forces at the pile head defined in equations 5-10 through 5-12 may now be resolved into vertical and horizontal components of force on the structure, as follows:

$$F_v = -(P_x \cos\theta - P_t \sin\theta) \tag{5-13}$$

$$F_h = -(P_x \sin\theta + P_t \cos\theta) \tag{5-14}$$

The moment on the structure is

$$M_s = J_m y_t \tag{5-15}$$

The equilibrium equations can now be written, as follows:

$$P_v + \Sigma F_{v_i} = 0 \tag{5-16}$$

$$P_h + \Sigma F_{h_i} = 0 \tag{5-17}$$

$$M + \Sigma M_{s_i} + \Sigma a_i F_{v_i} + \Sigma b_i F_{h_i} = 0 \tag{5-18}$$

The subscript i refers to values from any "i-th" pile. Using equations 5-8 through 5-15, equations 5-16 through 5-18 may be written in terms of the structural movements. Equations 5-19 through 5-21 are in the final form.

$$P_v = \Delta v[\Sigma A_i] + \Delta h[\Sigma B_i] + \alpha_s[\Sigma a_i A_i + \Sigma b_i B_i] \tag{5-19}$$

$$P_h = \Delta v[\Sigma B_i] + \Delta h[\Sigma C_i] + \alpha_s[\Sigma a_i B_i + \Sigma b_i C_i] \tag{5-20}$$

$$M = \Delta v[\Sigma D_i + \Sigma a_i A_i + \Sigma b_i B_i] + \Delta h[\Sigma E_i + \Sigma a_i B_i + \Sigma b_i C_i] + \alpha_s[\Sigma a_i D_i + \Sigma a_i^2 A_i + \Sigma b_i E_i + \Sigma b_i^2 C_i + \Sigma 2 a_i b_i B_i] \tag{5-21}$$

where

$$A_i = J_{x_i} \cos^2\theta_i + J_{y_i} \sin^2\theta_i$$

$$B_i = (J_{x_i} - J_{y_i}) \sin\theta_i \cos\theta_i$$

$$C_i = J_{x_i} \sin^2\theta_i + J_{y_i} \cos^2\theta_i$$

$$D_i = J_{m_i} \sin\theta_i$$

$$E_i = -J_{m_i} \cos\theta_i$$

These equations are not as complex as they appear. For example, the origin of the coordinate system can usually be selected so that all of the b-values are zero. For vertical piles, the sine terms are zero and the cosine terms are unity. For small deflections, the J-values can all be taken as constants. Therefore, under a number of circumstances it is possible to solve these equations by hand. However, if the deflections of the group is such that the nonlinear portion of the curves in Figure 5-5 is reached, the use of a computer solution is advantageous. Such a program is available through the Geotechnical Engineering Center, The University of Texas at Austin (Awoshika and Reese 1971; Lam 1981).

(4) Detailed step-by-step solution procedure.

(a) Study the foundation to be analyzed and select a two-dimensional bent where the behavior is representative of the entire system.

(b) Prepare a sketch such that the lateral loading comes from the left. Show all pertinent dimensions.

(c) Select a coordinate center and find the horizontal component, the vertical component, and the moment through and about that point.

(d) Compute by some procedure a curve showing axial load versus axial deflection for each pile in the group; or, preferably, use the results from a field load test.

(e) Use appropriate procedures and compute curves showing lateral load as a function of lateral deflection and moment as a function of lateral deflection, taking into account the effect of structural rotation on the boundary conditions at each pile head.

(f) Estimate trial values of J_x, J_y, and J_m for each pile in the structure.

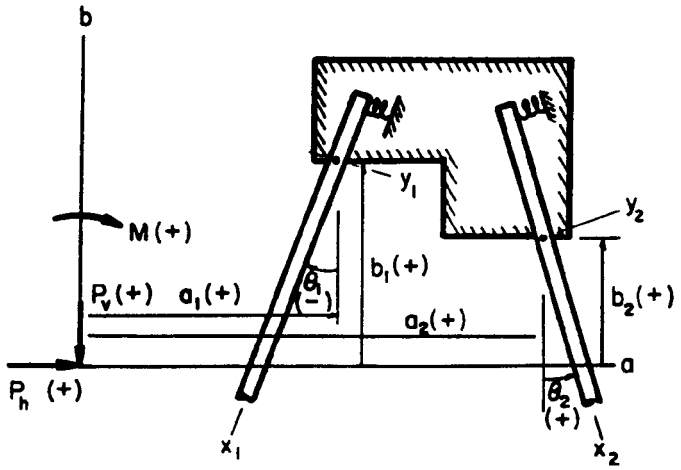

a. With piles shown

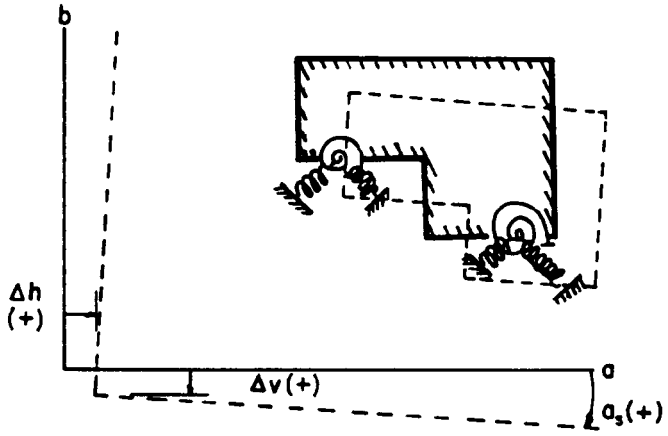

b. With piles represented as springs

Figure 5-4. Simplified structure showing coordinate systems and sign conventions

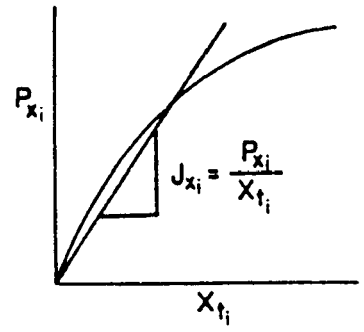

a. Axial pile resistance versus axial displacement.

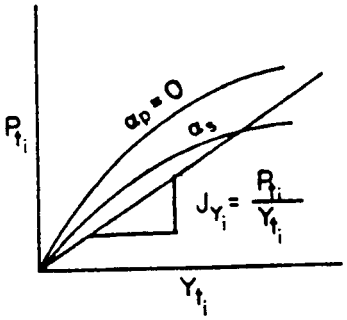

b. Lateral pile resistance versus lateral pile displacement.

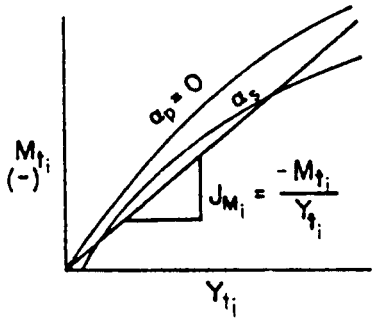

c. Moment at pile head versus lateral pile displacement for various rotations (α_p) of the pile head.

Figure 5-5. Set of pile resistance functions for a given pile

(g) Solve equations 5-19 through 5-21 for values of Δv, Δh, and α_s .

(h) Compute pile-head movements and obtain new values of J_x , J_y , and J_m for each pile.

(i) Solve equations 5-19 through 5-21 again for new values of Δv, Δh, and α_s .

(j) Continue iteration until the computed values of the structural movements agree, within a given tolerance, with the values from the previous computation.

(k) Compute the stresses along the length of each pile using the loads and moments at each pile head.

(5) Example problem. Figure 5-6 shows a pile-supported retaining wall with the piles spaced 8 feet apart. The piles are 14 inches in outside diameter with four No. 7 reinforcing steel bars spaced equally. The centers of the bars are on an 8-inch circle. The yield strength of the reinforcing steel is 60 kips per square inch and the compressive strength of the concrete is 2.67 kips per square inch. The length of the piles is 40 feet. The backfill is a free-draining, granular soil

with no fine particles. The surface of the backfill is treated to facilitate a runoff, and weep holes are provided so that water will not collect behind the wall. The forces P_1, P_2, P_s, and $_wP$ (shown in Figure 5-6) were computed as follows: 21.4, 4.6, 18.4, and 22.5 kips, respectively. The resolution of the loads at the origin of the global coordinate system resulted in the following service loads: P_v = 46 kips, P_h = 21 kips, and M = 40 foot-kips (some rounding was done). The moment of inertia of the gross section of the pile was used in the analysis. The flexural rigidity EI of the piles was computed to be 5.56×10^9 pounds per square inch. Computer Program PMEIX was run and an interaction diagram for the pile was obtained. That diagram is shown in Figure 5-7. A field load test was performed at the site and the ultimate axial capacity of a pile was found to be 176 kips. An analysis was made to develop a curve showing axial load versus settlement. The curve is shown in Figure 5-8. The subsurface soils at the site

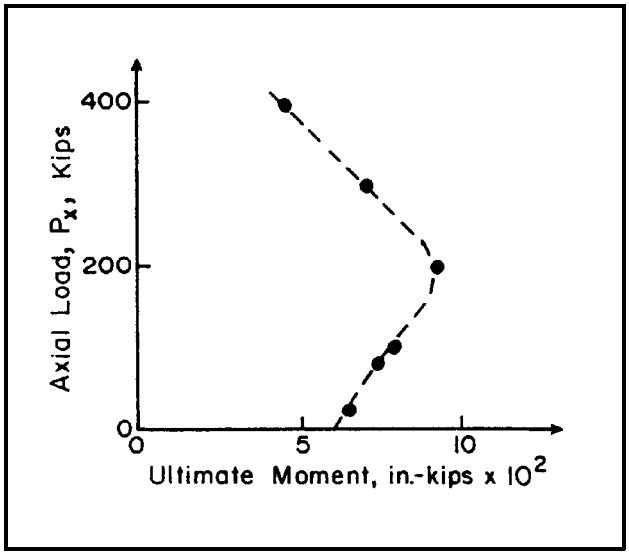

Figure 5-7. Interaction diagram of reinforced concrete pile

consist of silty clay. The water content averaged 20 percent in the top 10 feet and averaged 44 percent below 10 feet. The water table was reported to be at a depth of 10 feet from the soil surface. There was a considerable range in the undrained shear strength of the clay and an average value of 3 kips per square foot was used in the analysis. A value of the submerged unit weight of 46 pounds per cubic foot as employed and the value of g_{50} was estimated to be 0.005. In making the computations, the assumption was made that all of the load was carried by piles with none of the load taken by passive earth pressure or by the base of the footing. It was further assumed that the pile heads were free to rotate. As noted earlier, the factor of safety must be in the loading. Therefore, the loadings shown in Table 5-3 were used in the preliminary computations. Table 5-4 shows the movements of the origin of the global coordinate system when equation 5-19 through 5-21 were solved simultaneously. The loadings were such that the pile response was almost linear so that only a small number of iterations were

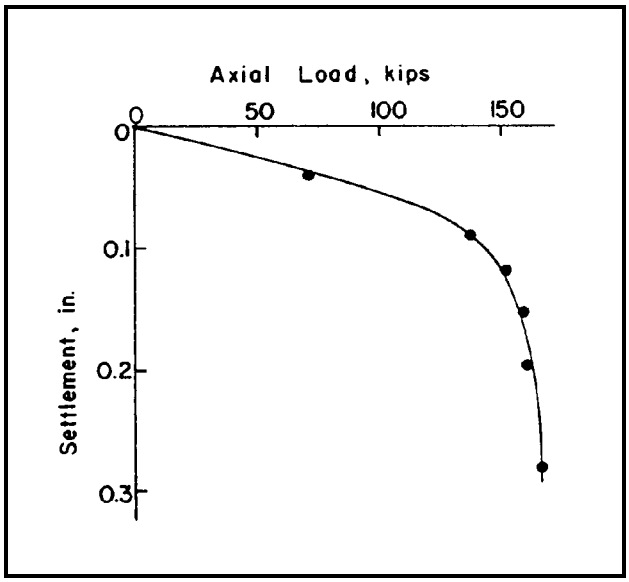

Figure 5-8. Axial load versus settlement for reinforced concrete pile

required to achieve converenge. The computed pile-head movements, loads, and moments are shown in Table 5-5.

(6) Verify results. The computed loading on the piles is shown in Figure 5-9 for Case 4. The following check is made to see that the equilibrium equations are satisfied.

$$\Sigma F_v = 24.2 + 97.2 \cos 14 - 14.3 \sin 14$$
$$= 24.2 + 94.3 - 3.5 = 115.0 \text{ kips OK}$$
$$\Sigma F_h = 15.2 + 14.3 \cos 14 + 97.2 \sin 14$$
$$= 15.2 + 13.9 + 23.6 = 52.7 \text{ kips OK}$$
$$\Sigma M = -(24.2)(1.5) + (97.2 \cos 14)(1.5) - (14.3 \sin 14)(1.5)$$
$$= -36.3 + 141.4 - 5.2$$
$$= 99.9 \text{ ft-kips OK}$$

Table 5-3
Values of Loading Employed in Analyses

Case	Loads, kips		moment, ft-kips	Comment
	P_v	P_h		
1	46	21	40	service load
2	69	31.5	60	1.5 times service load
3	92	42	80	2 times service load
4	115	52.5	100	2.5 times service load

Note: $P_v / P_h = 2.19$

Table 5-4
Computed Movements of Origin of Global Coordinate System

Case	Vertical movement Δv	Horizontal movement Δh	Rotation α
	in.	in.	rad
1	0.004	0.08	9×10^{-5}
2	0.005	0.12	1.4×10^{-4}
3	0.008	0.16	1.6×10^{-4}
4	0.012	0.203	8.4×10^{-5}

Thus, the retaining wall is in equilibrium. A further check can be made to see that the conditions of compatibility are Figure 5-8, an axial load of 97.2 kips results in an axial deflection of about 0.054 inch, a value in reasonable satisfied. One check can be made at once. Referring to agreement with the value in Table 5-5. Further checks on compatibility can be made by using the pile-head loadings and Computer Program COM622 to see if the computed deflections under lateral load are consistent with the values tabulated in Table 5-5. No firm conclusions can be made concerning the adequacy of the particular design without further study. If the assumptions made in performing the analyses are appropriate, the results of the analyses show the foundation to be capable of supporting the load. As a matter of fact, the piles could probably support a wall of greater height.

c. Closely spaced piles. The theory of elasticity has been employed to take into account the effect of a single pile on others in the group. Solutions have been developed (Poulos 1971; Banerjee and Davies 1979) that assume a linear response of the pile-soil system. While such methods are instructive, there is ample evidence to show that soils cannot generally be characterized as linear, homogeneous, elastic materials. Bogard and Matlock (1983) present a method in which the *p-y* curve for a single pile is modified to take into account the group effect. Excellent agreement was obtained between their computed results and results from field experiments (Matlock et al. 1980). Two approaches to the analysis of a group of closely spaced piles nder lateral load are given in the following paragraphs. One method is closely akin to the use of efficiency formulas, and the other method is based on the assumption that the soil within the pile group moves laterally the same amount as do the piles.

(1) Efficiency formulas. Pile groups under axial load are sometimes designed by use of efficiency formulas. Such a formula is shown as equation 5-22.

$$(Q_{ult})_G = E \times n \times (Q_{ult})_p \quad (5\text{-}22)$$

where

$(Q_{ult})_G$ = ultimate axial capacity of the group

E = efficiency factor (1 or < 1)

n = number of piles in the group

$(Q_{ult})_p$ = ultimate axial capacity of an individual pile

Various proposals have been made about obtaining the value of E; for example, McClelland (1972) suggested that the value of E should be 1.0 for pile groups in cohesive soil with center-to-center spacing of eight diameters or more and that E should decrease linearly to 0.7 at a spacing of three diameters. McClelland based his recommendations on results from experiments in the field and in the laboratory. It is of interest to note that no differentiation is made between piles that are spaced front to back, side by side, or spaced as some other angle between each other. Unfortunately, experimental data are limited on the behavior of pile groups under lateral load. Furthermore, the mechanics of the behavior of a group of laterally loaded piles are more complex than for a group of axially loaded piles. Thus, few recommendations have been made for efficiency formulas for laterally loaded groups. Two different recommendations have been made regarding the modification of the coefficient of subgrade reaction. The Canadian Foundation Engineering Manual (Canadian Geotechnical Society 1985) recommends that the coefficient of subgrade reaction for pile groups be equal to that of a single pile if the spacing of the piles in the group is eight diameters. For spacings smaller than eight diameters, the following ratios of the single-pile subgrade reaction were recommended: six diameters, 0.70; four diameters, 0.40; and three diameters, 0.25. The Japanese Road Association (1976) is less conservative. It is suggested that a slight reduction in the coefficient of horizontal subgrade reaction has no serious effect with regard to bending stress and that the use of a factor of safety should be sufficient in design except in the case where the piles get quite close together. When piles are closer together than two and one-half diameters, the following equation is suggested for computing a factor μ to multiply the coefficient of subgrade reaction for the single pile.

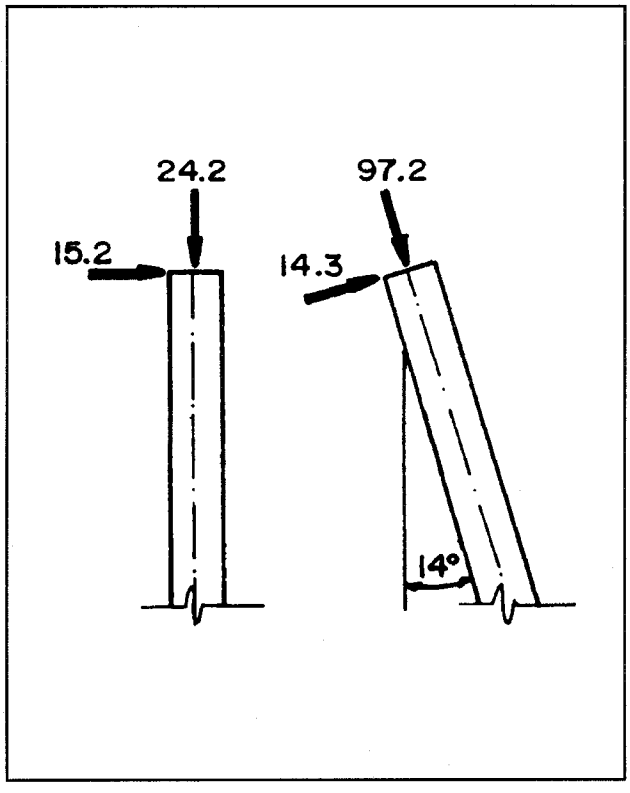

Figure 5-9. Pile loading - Case 4

$$\mu = 1 - 0.2(2.5 - L/D) \quad L < 2.5D \quad (5\text{-}23)$$

where

L = center-to-center distance between piles

D = pile diameter

Table 5-5
Computed Movements and Loads at Pile Heads

Case	Pile 1					Pile 2				
	x_t	y_t	P_x	P_t	M_{max}	x_t	y_t	P_x	P_t	M_{max}
	in.	in.	kips	kips	in.-kips	in.	in.	kips	kips	in.-kips
1	0.005	0.08	9.7	6.0	148	0.02	0.077	38.9	5.8	143
2	0.008	0.12	14.5	9.0	222	0.03	0.116	58.3	8.6	215
3	0.011	0.162	19.3	12.1	298	0.04	0.156	77.7	11.5	288
4	0.013	0.203	24.2	15.2	373	0.06	0.194	97.2	14.3	360

(2) Single-pile method. The single-pile method of analysis is based on the assumption that the soil contained between the piles moves with the group. Thus, the pile group that contained soil can be treated as a single pile of large diameter.

(3) A step-by-step procedure for single-pile method.

(a) The group to be analyzed is selected and a plan view of the piles at the groundline is prepared.

(b) The minimum length is found for a line that encloses the group. If a nine-pile (three by three) group consists of piles that are 1 foot square and three widths on center, the length of the line will be 28 feet.

(c) The length found in step b is considered to be the circumference of a pile of large diameter; thus, the length is divided by π to obtain the diameter of the imaginary pile having the same circumference of the group.

(d) The next step is to determine the stiffness of the group. For a lateral load passing through the tops of the piles, the stiffness of the group is taken as the sum of the stiffness of the individual piles. Thus, it is assumed that the deflection at the pile top is the same for each pile in the group and, further, that the deflected shape of each pile is identical. Some judgment must be used if the piles in the group have different lengths.

(e) Then, an analysis is made for the imaginary pile, taking into account the nature of the loading and the boundary conditions at the pile head. The shear and moment for the imaginary large-size pile is shared by the individual piles according to the ratio of the lateral stiffness of the individual pile to that of the group.

The shear, moment, pile-head deflection, and pile-head rotation yield a unique solution for each pile in the group. As a final step, it is necessary to compare the single-pile solution to that of the group. It could possibly occur that the piles in the group could have an efficiency greater than one, in which case the single-pile solutions would control.

(4) Example problem. A sketch of an example problem is shown in Figure 5-10. It is assumed that steel piles are embedded in a reinforced concrete mat in such a way that the pile heads do not rotate. The piles are 14HP89 by 40 feet long and placed so that bending is about the strong axis. The moment of inertia is 904 inches^4 and the modulus of elasticity of 30×10^6 pounds per square inch. The width of the section is 14.7 inches and the depth is 13.83 inches. The soil is assumed to be a sand with an angle of internal friction of 34 degrees, and the unit weight is 114 pounds per cubic foot. The computer program was run with a pile diameter of 109.4 inches and a moment of inertia of 8,136 inches^4 (nine times 904). The results were as follows:

$y_t = 0.885$ inch

$M_t = M_{max} = 3.60 \times 10^7$ in.-lb for group

$= 3.78 \times 10^6$ in.-lb for single pile

Bending stress = 25.3 kips / sq in.

The deflection and stress are for a single pile. If a single pile is analyzed with a load of 50 kips, the groudline deflection was 0.355 inch and the bending stress was 23.1 kips per square inch. Therefore, the solution with the imaginary large-diameter single pile was more critical.

5. Computer Assisted Analysis

A computer assisted analysis is a reasonable alternative for obtaining reliable estimates of the performance of pile groups. Several computer programs can assist the analysis and design of groups.

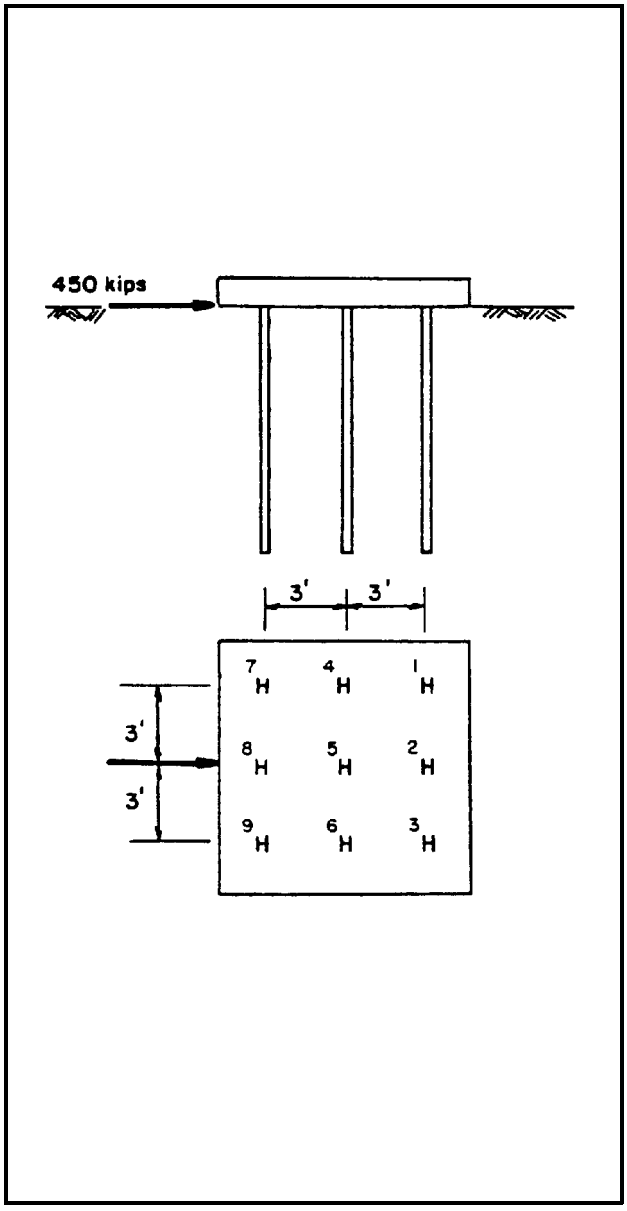

Figure 5-10. Plan and evaluation of foundation analyzed in example problem

a. CPGA. Program CPGA provides a three-dimensional stiffness analysis of a group of vertical and/or battered piles assuming linear elastic pile-soil interaction, a rigid pile cap, and a rigid base (WES Technical Report ITL-89-3). Maxtrix methods are used to incorporate position and batter of piles as well as piles of different sizes and materials. Computer program CPGG displays the geometry and results of program CPGA.

b. STRUDL. A finite element computer program such as STRUDL or SAP should be used to analyze the performance of a group of piles with a flexible base.

c. CPGC. Computer program CPGC develops the interaction diagrams and data required to investigate the structural capacity of prestressed concrete piles (WES Instruction Report ITL-90-2).

d. CPGD. Computer program (Smith and Mlakar 1987) extends the rigid cap analysis of program CPGA to provide a simplified and realistic approach for seismic analysis of pile foundations. Program CPGD (in development stage at WES) includes viscous damping and response-spectrum loading to determine pile forces and moments.

Chapter 6
Verification of Design

1. Foundation Quality

Construction can cause defects in driven piles or drilled shafts. Unfortunately, an installed deep foundation is mostly below the ground surface and cannot be seen. The quality of the foundation should be verified to ensure adequate structural integrity, to carry the required load without a bearing capacity failure, to limit displacements of the structure to within acceptable levels, and to avoid unnecessary overdesign of the foundation. This chapter describes methods commonly used to verify the capability of the foundation to support a structure. These methods are nondestructive and usually permit the tested piles or drilled shafts to be used as part of the foundation.

a. Indicators of problem with driven piles. Piles driven into soils with variable stratification that show driving records containing erratic data, which cannot be explained by the construction method, indicate possible pile damage. Failure to reach the prescribed tip elevation or penetration rate also indicates pile damage. Other indicators include drifting of the pile off location, erratic driving unexplained by the soil stratification, and a sudden decrease in driving resistance or interference with nearby piles as indicated by sound or vibration. A pile can also be damaged during extraction.

b. Indicators of problems with drilled shafts. Most problems with drilled shafts are related to construction deficiencies rather than design. Such problems result from inadequate information of the subsurface soil and groundwater conditions provided to the contractor, inadequate clean-out including the presence of water in the excavation prior to concrete placement, inadequate reinforcement, and other complications during concrete placement. Drilled shaft failures may result from neglecting vertical dimensional changes in shrinking and swelling soil as those described in TM 5-818-7.

2. Driven Piles

Piles can be bent or sheared during installation and can cause a reduction in pile capacity. Piles can also undergo excessive tensile stresses during driving, specifically when soil layers have variable density or strength or when there is no significant end bearing resistance. Field test procedures such as standard penetration tests, pile driving analysis (PDA) with the wave equation, restrikes, and pile load tests can determine the ability of the pile to carry design loads. Refer to paragraph 4, Chapter 6, for guidance on load tests. Typically 2 to 5 percent of the production piles should be driven as indicator piles, at the start of construction at locations specified by the design engineer or at suspicious locations to confirm the capability of the driven piles to support the structure. PDA should also be performed during the driving of indicator piles and some static load tests performed to calibrate wave equation analyses. Table 6-1 illustrates an example procedure for verifying pile design. Analyses by wave equation and pile driving are presented.

a. Wave equation analysis. The penetration resistance in blows/feet (or blows/inch) measured when the pile tip has been driven to the required depth can be used to calculate the ultimate bearing capacity and verify design. Wave equation analyses can relate penetration resistance to the static ultimate bearing capacity.

(1) Computer program GRLWEAP. A wave equation analysis is recommended, except for the simplest projects when adequate experience and data already exist, for estimating the behavior of pile driving and confirming pile performance. This analysis may be accomplished using program GRLWEAP (Goble et al. 1988), Wave Equation Analysis of Pile Driving, licensed to WES. Program GRLWEAP and user's manual with applications are available to offices of the Corps of Engineers. GRLWEAP models the pile driving and soil system by a series of elements supported by linear elastic springs and dashpots with assumed parameters, Figure 6-1. Each dashpot and spring represent a pile or soil element. Information required to use this program includes indentification of the hammer (or ram) and hammer cushion used, description of the pile, and soil input parameters. Hammer selection is simplified by using the hammer data file that contains all the required information for numerous types of hammers. A simple guide for selection of soil input parameters to model the soil resistance force is provided as follows:

(a) The soil resistance force consists of two components, one depends on pile displacement, and theother depends on pile velocity. Pile displacement dependent resistance models static soil behavior, and it is assumed to increase linearly up to a limiting deformation, which is the quake. Deformation beyond the quake requires no additional force. The pile velocity component models depend on soil damping charactertistics where the relationship between soil resistance and velocity is linear and the slope of such relationship is the damping constant. Quake and damping constants are required for both skin friction and end-bearing components. Table 6-2 gives recommended soil parameters, which should be altered depending on local experience. The distribution of soil resistance between skin friction and end bearing, which depend on the pile and soil bearing strata, is also required. End-bearing piles may have all of the soil resistance in end

Table 6-1
Procedure for Verifying Design and Structural Integrity of Driven Piles

Step	Procedure
1	Complete an initial wave equation analysis selecting soil damping constants J_c, quakes ρ_u, distribution of soil resistance between skin friction and end bearing and the ultimate bearing capacity Q_u. Use the proposed pile and driving system. Adjust driving criteria as needed to reduce pile stresses and to optimize pile driving.
2	Drive indicator piles, typically 2 to 5 percent of the production piles, at locations specified by the design engineer using driving criteria determined by the wave equation analysis. Complete additional wave equation analysis using actual hammer performance and adjust for changes in soil strength such as from freeze or relaxation. Drive to various depths and determine penetration resistances with the PDA using the Case method to determine the static ultimate bearing capacity Q_u.
3	Restrike the piles after a minimum waiting period, usually 1 day, using the PDA and Case methods to determine actual bearing capacity that includes soil freeze and relaxation.
4	Perform CAPWAPC analysis to calibrate the wave equation analysis and to verify field test results. Determine Q_u, hammer efficiency, pile driving stresses and structural integrity, and an estimate of the load-displacement behavior.
5	Perform static load tests to confirm the dynamic test results, particularly on large projects where savings can be made in foundation costs by use of lower factors of safety. Dynamic tests may also be inconclusive if the soil resistance cannot be fully mobilized by restriking or by large strain blows such as in high capacity soil, intact shale, or rock. Static load tests can be significantly reduced for sites where dynamic test results are reliable.
6	Additional piles should be dynamically tested during driving or restruck throughout pile installation as required by changes in soil conditions, load requirements, piles, or changes in pile driving.
7	Each site is unique and often has unforeseen problems. Changes may be required in the testing program, type and length of pile, and driving equipment. Waivers to driving indicator piles and load testing requirements or approval for deviations from these procedures must be obtained from HQUSACE/CEMP-ET.

bearing, while friction piles may have all of the soil resistance in skin friction.

(b) A bearing-capacity graph is commonly determined to relate the ultimate bearing capacity with the penetration resistance in blow/feet (or blows/inch). The penetration resistance measured at the pile tip is compared with the bearing-capacity graph to determine how close it is to the ultimate bearing capacity. The contractor can then determine when the pile has been driven sufficiently to develop the required capacity.

(c) Wave equation analysis also determines the stresses that develop in the pile. These stresses may be plotted versus the penetration resistance or the ultimate pile capacity to assist the contractor to optimize pile driving. The driving force can be adjusted by the contractor to maintain pile tensile and compressive stresses within allowable limits.

(d) GRLWEAP is a user friendly program and can provide results within a short time if the engineer is familiar with details of the pile driving operation. The analysis should be performed by Government personnel using clearly defined data provided by the contractor.

(2) Analysis prior to pile installation. A wave equation analysis should be performed prior to pile driving as a guide to select properly sized driving equipment and piles to ensure that the piles can be driven to final grade without exceeding the allowable pile driving stresses.

(3) Analysis during pile installation. Soil, pile, and driving equipment parameters used for design should be checked to closely correspond with actual values observed in the field during installation. Sound judgment and experience are required to estimate the proper input parameters for wave equation analysis.

(a) Hammer efficiencies provided by the manufacturer may overestimate energy actually absorbed by the pile in the field and

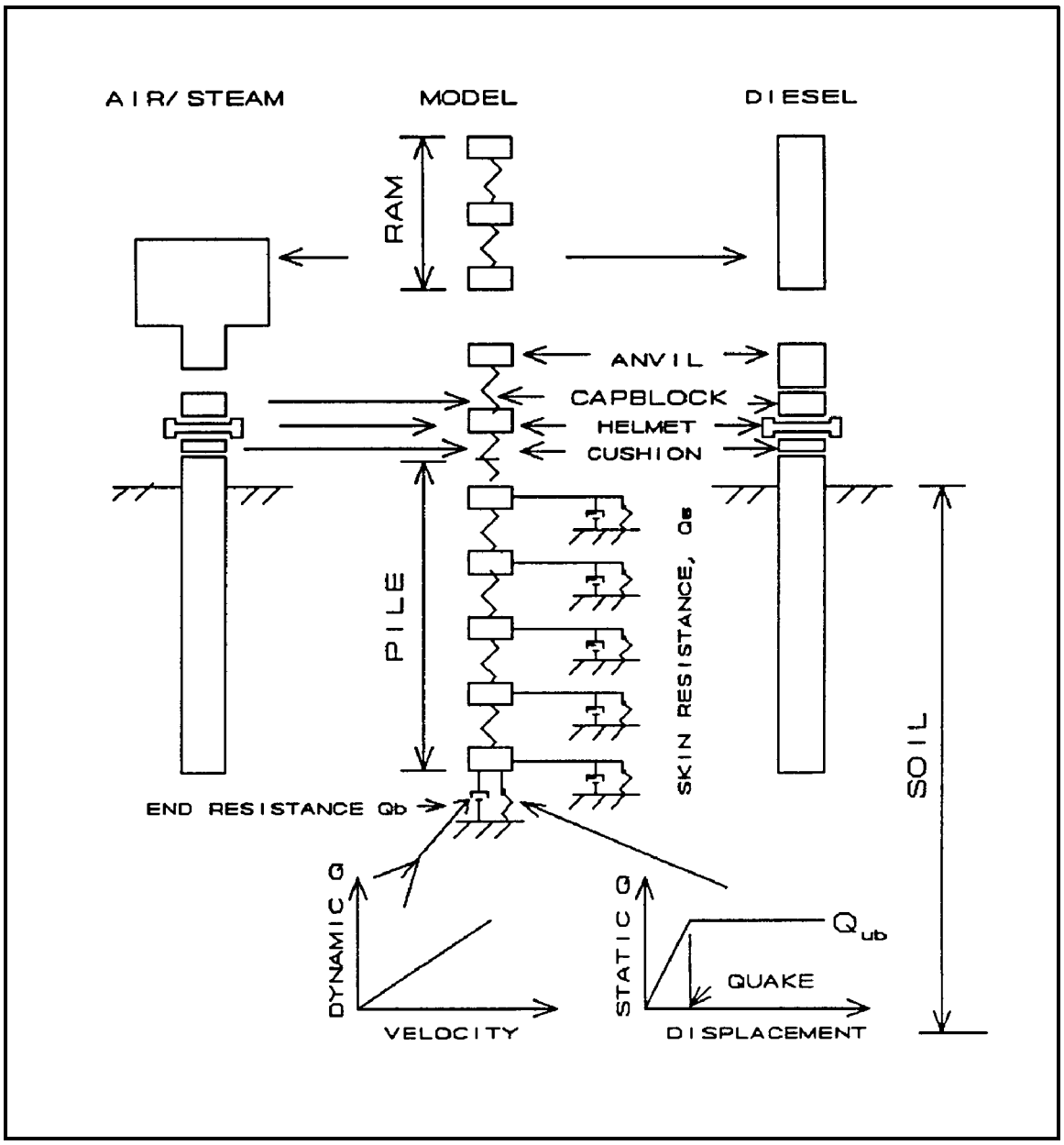

Figure 6-1. Schematic of wave equation model

may lead to an overestimate of the bearing capacity. Significant error in estimating ahmmer efficiency is also possible for driving batter piles. A bracket analysis is recommended for diesel hammers with variable strokes. Results of the PDA and ststic with variable strokes. Results of the PDA and static load tests described below and proper inspection can be used to make sure that design parameters are realistic and that the driven piles will have adequate capacity.

(b) Results of wave equation analysis may not be applicable if soil freeze (setup) occurs. Saturated sensitive clays and loose sands may lose strength during driving which can cause remolding and increasing pore water pressure. Densification of sands during driving contribute to a buildup of pore pressure. Strength regain is increased with time, after the soil freeze or setup. Coral sands may have exceptionally low penetration resistance during driving, but a reduction in pore pressure after driving and cementation that increases with time over a period of several weeks to months can contribute substantially to pile capacity. Significant cementation may not occur in several weeks.

(c) Penetration resistance is dense, final submerged sand, inorganic silts or stiff, fissured, friable shale, or clay stone can dramatically increase during driving, apparently from dilation and reduced pore water pressure. A "relaxation" (decrease) in penetration resistance occurs with time after driving. Driving equipment and piles shall be selected with sufficient capacity to overcome driving resistance or driving periodically delayed to allow pore water pressures to increse.

Table 6-2
Recommended Soil Parameters for Wave Equation (Copyright permission, Goble, Rausche, Likins and Associates, Inc. 1988)

	Damping Constants J_c, seconds/ft (seconds/m)		Quake ρ_u, inches (mm)	
Soil	**Skin**	**Tip**	**Skin**	**Tip[1]**
Cohesionless	0.05 (0.16)	0.15 (0.50)	0.10 (2.54)	B_b / 120
Cohesive	0.30 (0.90)	0.15 (0.50)	0.10 (2.54)	B_b / 120

[1] Selected tip quake should not be less than 0.05 inch. B_b is the effective tip (base) diameter; pipe piles should be plugged.

(d) The pile shall be driven to a driving resistance that exceeds the ultimate pile capacity determined from results of wave equation analysis or penetration resistance when relaxation is not considered. Driving stresses in the pile shall not exceed allowable stress limits. Piles driven into soils with freeze or relaxation effects should be restruck at a later time such as one or more days after driving to measure a more realistic penetration resistance for design verification.

(e) Analysis of the bearing capacity and performance of the pile by wave equation analysis can be contested by the contractor and resolved at the contractor's expense through resubmittals performed and sealed by a registered engineer. The resubmittal should include field verification using driving and load tests, and any other methods approved by the Government design engineer.

b. Pile driving analysis. Improvements in electronic instruments permit the measurement of data for evaluating hammer and driving system performance, pile driving stresses, structural integrity, and ultimate pile capacity. The required data may be measured and pile performance evaluated in fractions of a second after each hammer blow using pile driving analyzer equipments. PDA is also useful when restriking piles after some time following pile installation to determine the effects of freeze or relaxation on pile performance. The Case method (Pile Buck, Inc. 1988) developed at Case Institute of Technology (now Case Western Reserve University) is the most widely used technique. The CAPWAPC analytical method is also applied with results of the PDA to calibrate the wave equation analysis and to lead to reliable estimates of the ultimate static pile capacity provided soil freeze, relaxation, or long-term changes in soil characteristics are considered. The CAPWAPC method quakes and damping factors, and therefore, confirms input data required for the wave equation analysis.

(1) PDA equipment. PDA can be performed routinely in the field following a schematic arrangement shown in Figure 6-2. The system includes two strain transducers and two accelerometers bolted to the pile near its top, which feed data to the pile driving analyzer equipment. The oscilloscope monitors signals from the transducers and accelerometers to indicate data quality and to check for pile damage. The tape recorder stores the data, while an optional plotter can plot data. Digital computations of the data are controlled with a Motorola 68000 microprocessor with output fed to a printer built into the pile driving analyzer. The printer also documents input and output selections.

(a) The strain transducers consist of four resistance foil gauges attached in a full bridge.

(b) The piezoelectric accelerometers measure pile motion and consist of a quartz crystal that produces a voltage proportional to the pressure caused by the accelerating pile mass.

(c) Data can be sent from the pile driving analyzer to other equipment such as a plotter, oscilloscope, strip chart recorder, modem for transmitting data to a distant office or analysis center, and a computer. The computer can be used to analyze pile performance by the Case and CAPWAPC methods.

(2) Case Method. This method uses the force $F(t)$ and acceleration $\ddot{a}(t)$ measured at the pile top as a function of time during a hammer blow. The velocity $v(t)$ is obtained by integrating the acceleration. The PDA and its transducers were developed to obtain these data for the Case method.

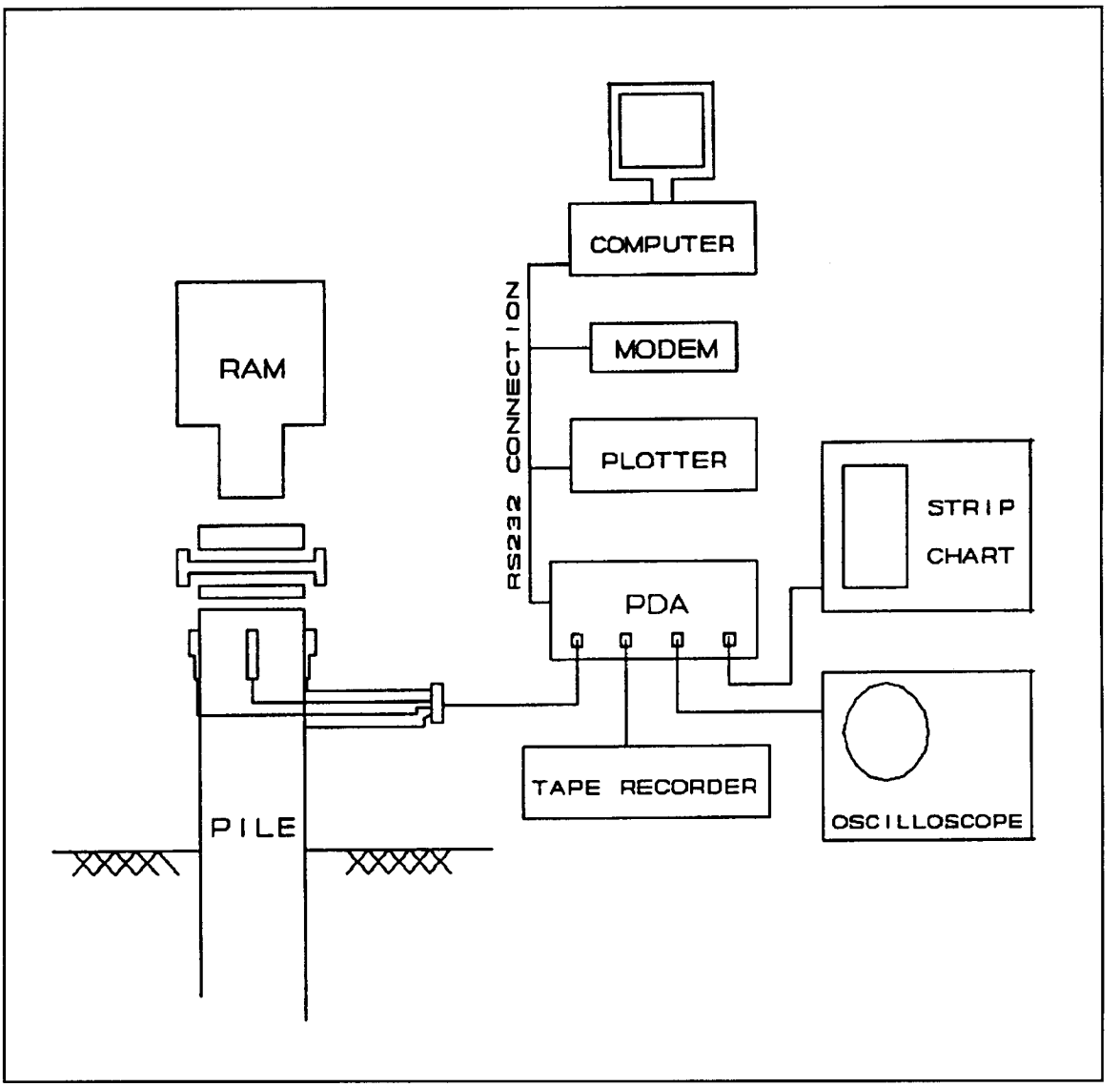

Figure 6-2. Schematic of field pile driving analyzer equipment

integrating the acceleration. The PDA and its transducers were developed to obtain these data for the Case method.

(a) The total soil resistance during pile driving R is initially calculated using wave propagation theory and assuming a uniform elastic pile and an ideal plastic soil as

$$R = \frac{F(t_1) + F(t_2) + Z_p[v(t_1) - v(t_2)]}{2} \quad (6\text{-}1)$$

where

$F(t)$ = force measured by a strain transducer at a selected time t

t_1 = first selected time

$t_2 = t_1 + 2L/c$

Z_p = pile impedance, $M_p c/L$

$v(t)$ = velocity determined by integration of the accelerometers measured as a function of time

M_p = pile mass

c = wave transmission speed in the pile

t_1 is often selected as the time at the first maximum velocity. R is the sum of the static soil (displacement dependent), Q_u and the dynamic (velocity dependent) D components are of the capacity.

(b) Static soil capacity Q_u can be calculated from R by

$$Q_u = R - J_c(2Z_p V_{top} - R) \quad (6\text{-}2)$$

where V_{top} is the velocity of the wave measured at the pile top at time t_1. Approximate damping constants J_c have already been determined for soils as given in Table 6-2 by comparing Case method calculations of static capacity with results of load tests. J_c can be fine tuned to actual soil conditions if load test results are available.

(c) Proper calculation of Q_u requires that the displacement obtained by integration of the velocity at time t_1, $v(t_1)$, exceeds the quake (soil compression) required for full mobilization of soil r esistance. Selection of time t_1 corresponding to the first maximum velocity is usually sufficient.

(d) A correction for ealy skin friction unloading causing a negative velocity may be required for long piles with high skin friction. The upper shaft friction may unload if the pile top is moving upward before the full resistance is mobilized. A proper correction can be made by adding the skin friction resistance that was unloaded to the mobilized soil resistance.

(e) Proper calculation to static resistance requires that freeze or relaxation effects are not present. Piles may be restruck after a waiting period such as 1 day or more to allow dissipation of pore water pressures.

(f) The driving force must be sufficient to cause the soil to fail; otherwise, ultimate capacity is only partially mobilized and the full soil resistance will not be measured.

(3) CAPWAPC method. This is an analytical method that combines field measured data with wave equation analysis to calculate the static ultimate bearing capacity and distribution of the soil resistance. Distribution of soil resistance, Q_u, and the pile load-displacement behavior calculated by the CAPWAPC method may be used to evaluate the damping constant J_c, quakes and soil resistances required in the Case method, and to confirm the determination of Q_u calculated using the Case method. The CAPWAPC method is often used as a supplement to load tests and may replace some load tests.

(a) The CAPWAPC method is begun using a complete set of assumed input parameters to perform a wave equation analysis. The hammer model, which is used to calculate the pile velocity at the top, is replaced by a velocity that is imposed at the top pile element. The imposed velocity is made equal to the

velocity determined by integration of the acceleration. The CAPWAPC method calculates the force required to give the imposed velocity. This calculated force is compared with the force measured at the pile top. The soil input parameters are subsequently adjusted until the calculated and measured forces and calculated and measured velocities agree as closely as practical such as illustrated in Figure 6-3. The CAPWAPC method may also be started by using a force imposed at the pile top rather than an imposed velocity. The velocity is calculated and then compared with the velocity measured at the pile top. The CAPWAPC method is applicable for simulating static and dynamic tests.

(b) A simulated static load test may be performed using the pile and soil models determined from results of a CAPWAPC analysis. The pile is incrementally loaded, and the force and displacements at the top of the pile are computed to determine the load-displacement behavior. Actual static load test results can be simulated within 10 to 15 percent of computed results if the available static resistance is fully mobilized and time dependent soil strength changes such as soil freeze or relaxation are negligible.

(c) Dynamic tests with PDA and the CAPWAPC method provide detailed information that can be used with load factor design and statistical procedures to reduce factors of safety and reduce foundation cost. The detailed information on hammer performance, driving system, and the pile material can be provided to the contractor to optimize selection of driving equipment and cushions, to optimize pile driving, to reduce pile stresses, to reduce construction cost, and to improve construction quality. The foundation will be of higher quality, and structural integrity is more thoroughly confirmed with the PDA method because more piles can be tested by restriking the pile than can be tested by applying actual static loads. PDA can also be used to simulate pile load test to failure, but the pile can still be used as part of the foundation, while actual piles loaded to failure may not be suitable foundation elements.

3. Drilled Shafts

Drilled shafts should be constructed adequately and certified by the inspector. Large shafts supporting major structures are sometimes tested to ensure compliance with plans and specifications. Sonic techniques may be used to ascertain homogeneity of the foundation. Sonic wave propagation with receiver embedded in the concrete is the most reliable method for detecting voids or other defects. Striking a drilled shaft as ina large strain test with PDA and wave equation analysis is recommended for analysis of the ultimate pile capacity and load-displacement behavior as decribed above for driven piles. A large strain test may be conducted by dropping a heavy load onto the head of the shaft using a crane. Static load tests are commonly performed on selected shafts or test shafts of large construction projects to verify shaft performance and efficiency of the design.

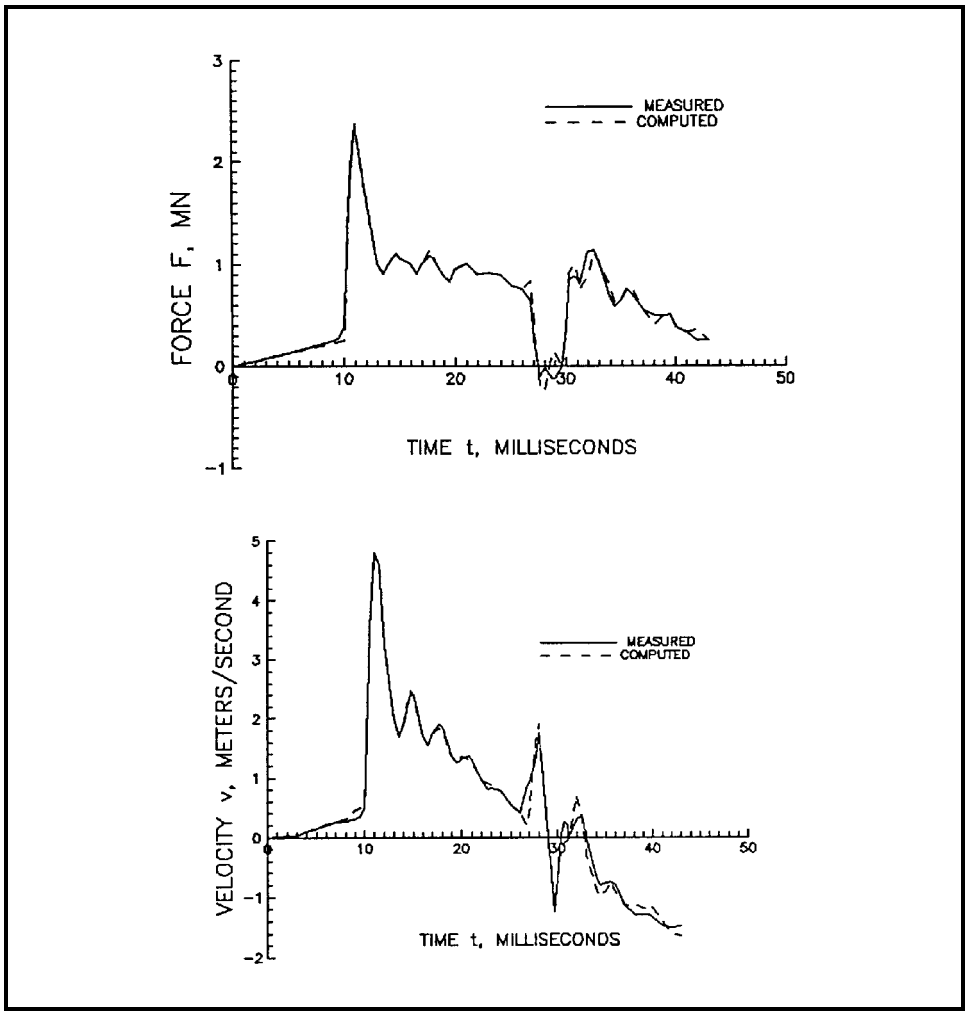

Figure 6-3. Example results of CAPWAPC analysis

a. Performance control. Continuous monitoring is essential to ensure that the boreholes are properly prepared to minimize loss of soil friction and end-bearing capacity and that the concrete mix is placed to achieve a continuous adequate shaft. Complete details of a drilled shaft construction control and an example of quality control forms may be found in FHWA-HI-88-042, "Drilled Shafts: Construction Procedures and Design Methods" and ADSC (1989) report, "Drilled Shaft Inspector's Manual." Construction and quality control include the following:

(1) Borehole excavation. Soil classification provided by all available boring logs in the construction area should be correlated with the visual description of soil or rock removed from the excavation. Any observed groundwater levels should also be recorded. Characteristics to be observed and determined include determined include location of the various strata, location and nature of the bearing stratum, and any seepage. The observer should also determine if the soil profile is substantially different from the one assumed for the design based on knowledge of the plans, specifications, and previous geotechnical analysis. The design engineer should be at the construction site during boring of the first holes to verify assumptions regarding the subsurface soil profile and periodically thereafter to check on requirements for any design modifications.

(a) Excavation details such as changes in the advance rate of the boring tool and changes in the soil cutting, groundwater observations, and bottom heave should be recorded. These details can be used to modify excavation procedure and improve efficiency in the event of problems as well as to provide a complete record for later reference.

Other important data include type of excavation (e.g., dry, cased, or slurry), time of initiation and completion of the boring, estimates of location of changes in the soil strata, and description of each soil stratum. Determine any evidence of pervious lenses and groundwater, problems encountered during excavating (e.g., caving, squeezing, seepage, cobbles, or boulders), and the location of the bearing stratum. A small diameter test boring from the excavation bottom can be made and an undisturbed sample recovered to test the bearing soil.

(b) The excavation should be checked for proper length, diameter, and underream dimensions. Any lateral deviations from the plan location and unintentional inclination or batter should be noted on the report and checked to be within the required tolerance. Provided that all safety precautions have been satisified, the underream diameter can be checked by placing the underream tool at the bottom of the excavation and comparing the travel of the kelly when the underreamer is extended to the travel when it is retracted in the barrel of the underream tool. Electronic calipers may be used if the excavation was made with slurry or the hole cannot be entered for visual inspection. Extreme safety precautions must be taken if an inspector enters an excavation to ensure no fall-in of material, and he should be provided with adequate air supply, communications and lifeline, and hoisting equipment. In the event of entry, a liner or casing should be in place to protect against fall-in. Fresh air may be pumped through hoses extending to the bottom. Minimum diameter of casing for personal inspection is 2 feet. An alternative to downhole inspection is to utilize ADSC drilled shaft inspectors manuals.

(c) Slurry used during excavation should be tested for compliance with mix specifications after the slurry is mixed and prior to placing in the excavation. These tests are described in Table 6-3 and should be performed by the Government and reported to construction management and the designer.

(d) The bottom of the excavation should be checked before placement of the reinforcement cage and concrete to ensure that all loose soil is removed, water has not collected on the bottom of open boreholes, and the soil is in the correct bearing stratum. Depth of water in an open borehole should be less than 2 inches. Casing should be clean, smooth, and undeformed.

(2) Placement of reinforcement. The reinforcement cage should be assembled prior to placement in the excavation with the specified grade, size, and number of bars. The cage should be supported with the specified horizontal stirrups or spirals either tied or welded in place as required to hold bars in place and prevent misalignment during concrete placement and removal of casing. The minimum spacing between bars should be checked to ensure compliance with specifications for adequate flow of concrete through the cage. The cage should be checked for placement in the specified position and adequately restrained from lateral movement during concrete placement.

(3) Concrete placement. The properties of the concrete mix and placement method must be closely monitored to avoid defects in the shaft. A record of the type of cement, mix proportions, admixtures, quantities, and time loaded on the truck should be provided on the delivery ticket issued by the concrete supplier. The lapse of time since excavation of the borehole and method of concrete placement, including details of the tremie used to place the concrete, should be recorded. Concrete slump should be greater than 6 inches and the amount of concrete placed in the excavation for each truck should be recorded. A plot of the expected quantity calculated from the excavation dimensions and the actual quantity should be prepared to indicate the amount and location of the concrete overrun or underrun. Excessive overruns or any underruns observed during concrete placement will require an investigation of the cause. Any unusual occurrence that affects shaft integrity should be described.

Table 6-3
Specifications for Bentonite Slurry

Property	Supplied During Excavation			Test Method
Density	Not less than necessary to bore shaft and less than 70 lb/cu ft	Mud density	–	Constant volume sample cup with lid connected to a balance gravity arm is filled with slurry so when placing the lid some slurry is forced out of a hole in the lid. Tap the edge of the cup to break up any entrained air or gas. Wipe excess slurry from the cup and lid. Place the balance arm into the fulcrum and move the rider on the balance arm to balance the assembly. Read the specific gravity from the scale on the balance.
Viscosity	30 to 50 sec	Marsh funnel	–	Place a finger over the bottom chute of the funnel and fill the funnel with slurry through a screen at the top of the funnel until the slurry level reaches the bottom of the screen (1 quart capacity). The slurry is allowed to flow from the funnel through the chute and number of seconds required to drain the funnel is recorded. Time measured is the viscosity.
Shear strength	0.03 psf to 0.2 psf (1.4 to 10 N/m^2)	Shearometer	–	The initial strength is determined by filling a container about 3 inches in diameter to the bottom line on a scale with freely agitated slurry. The scale is vertically mounted in the container. A thin metal tube is lowered over the scale and released. The tube is allowed to settle for 1 minute and the shear strength recorded on the scale reading at the top of tube . The 10-minute gel strength is determined in a similar manner except that 10 minutes is allowed to pass before the tube is lowered over the scale.
pH	9.5 to 12	Indicator paper	-	A pH electric meter of pH paper may be used.
Sand	2 % maximum by volume	API method	-	A specified amount of slurry is mixed in a marked tube. The content mixture is vigorously shaken, and all of it is then poured through a No. 200 mesh screen so that sand particles are retained on the screen. The sand particles are washed into a marked tube by fitting the large end of a funnel down over the top of the screen holder, then inverting the screen and funnel assembly. The tip of the funnel is fitted into the clear measuring tube and water sprayed from a wash bottle on the screen. The percent volume of sand is read from the marked measuring tube after the sand has settled.

b. Nondestructive tests. Routine inspection with nondestructive tests (NDT) using wave propagation shall be performed to check the quality of the installed drilled shafts. Additional special tests as indicated in the following paragraphs are performed if defects are suspected in some drilled shafts. Routine tests performed as part of the inspection procedure are typically inexpensive and require little time. Special tests to determine defects, however, are often time consuming, expensive, and performed only for unusual situations.

(1) Routine inspection tests. The most common routine NDT is to externally vibrate the drilled shaft by applying a sudden load as from a hammer or heavy weight dropped from a specified height. Signals from the wave are recorded by transducers and accelerometers installed near the top of the shaft or embedded in the concrete at some location in the length of the shaft. Access tubes may also be installed in the shaft for down-hole instrumentation to investigate the concrete between access tubes. Refer to FHWA-HI-88-042

for further information.

(a) The PDA procedure as discussed for driven piles may also be used for drilled shafts, even though it cannot be considered a routine test for NDT. The force-time and velocity-time traces ofo the vibration recorded on the oscilloscope caused by a dynamic load can be interpreted by an experienced technician to determine discontinuities and their location in the concrete.

(b) The wave pattern of large displacements caused by dropping sufficiently large weights from some specified height can be analyzed by the PDA procedure and CAPWAPC method to determine the ultimate bearing capacity and load-displacement behavior.

(c) Vibration from a hammer blow measured with embedded velocity transducers (geophones) can confirm any possible irregularities in the signal and shaft defects. The transducers are inexpensive and any number can be readily installed and sealed in epoxy-coated aluminum cases on the reinforcing cage with no delay in construction. The embedded receivers provide a much reduced noise level that can eliminate much of the requirement for signal processing.

(d) Forced vibrations induced by an electrodynamic vibrator over a load cell can be monitored by four accelerometers installed near the shaft head (Preiss, Weber, and Caiserman 1978). The curve of v_o / F_o , where v_o is the maximum velocity at the head of the drilled shaft and F_o is the applied force, is plotted. An experienced operator can determine the quality of the concrete such as discontinuities and major faults if the length of the shaft is known. Information below an enlarged section cannot be obtained.

(2) Access tubes and down-hole instruments. Metal or plastic tubes can be cast longitudinally into a drilled shaft that has been preselected for special tests. These tubes usually extend full length, are plugged at the lower end to keep out concrete, and are fastened to the rebar cage. Various instruments can be lowered down the access tubes to generate and receive signals to investigate the quality of the concrete.

(a) A probe that delivers a sonic signal can be inserted down a tube and signal receivers inserted in other tubes. One tube can check the quality of concrete around the tube or multiple tubes can check the concrete between the tubes.

(b) An acoustic transmitter can be inserted in a fluid-filled tube installed in a drilled shaft and a receiver inserted to the same depth in an adjacent tube. This test can also be performed on a drilled shaft with only a single tube using a probe that contains the receiver separated by an acoustic isolator. A single tube can be used to check the quality of concrete around the tube.

(c) A gamma-ray source can be lowered down one tube and a detector lowered down to the same depth in another tube to check the density of concrete between the source and detector. A change in the signal as the instruments are lowered indicates a void or imperfection in the concrete.

(3) Drilling and coring. Drilled shafts that are suspected of having a defect may be drilled or cored to check the quality of the concrete. Drilling is to make a hole into the shaft without obtaining a sample. Coring is boring and removal of concrete sample. Drilling and coring can indicate the nature of the concrete, but the volume of concrete that is checked is relatively small and drilling or coring is time consuming, costly, and sometimes misleading. The direction of drilling is difficult to control, and the hole may run out the side of the shaft or might run into the reinforcement steel. Experienced personnel and proper equipment are also required to ensure that drilling is done correctly and on time.

(a) Drilling is much faster than coring, but less information is gained. The drilling rate can infer the quality of concrete and determine if any soil is in the shaft. A caliper can measure the diameter of the hole and determine any anomalies.

(b) Coring can determine the amount of concrete recovery and the concrete samples examined for inclusions of soil or slurry. Compression tests can be performed to determine the strength of the concrete samples. The cores can also be checked to determine the concrete to soil contact at the bottom of the shaft.

(c) Holes bored in concrete can be checked with a television camera if such an instrument is available. A portion of a borehole can also be packed to perform a fluid pressure test to check for leaks that could be caused by defects.

(d) Defects of large size such as caused by the collapse of the excavation prior to concrete placement or if concrete is absent in some portion of the shaft can be detected by drilling or coring. Defects can be missed such as when the sides of a rock socket are smeared with remolded and weak material. Coring can also detect defects that appear to be severe but are actually minor. For example, coring can indicate weak concrete or poor material, or poor contact with the end bearing soil or rock in the region of the core,

but the remaining shaft could be sound and adequately supported by the soil.

c. Load tests. The only positive way to prove the integrity of a suspected drilled shaft is to perform a load test. Drilled shafts are often constructed in relatively large sizes and load tests are often not economically feasible. Replacing a suspected drilled shaft is often more economical than performing the load test.

(1) Application. Load tests as described in paragraph 4, Chapter 6, shall be performed for drilled shafts when economically feasible such as for large projects. Results of load tests can be used to reduce the *FS* from 3 to 2 and can increase the economy of the foundation when performed during design.

(2) Preload. An alternative to load tests is to construct the superstructure and to preload the structure to determine the integrity of the foundation. This test must be halted immediately if one or more drilled shafts show more settlement than is anticipated.

4. Load Tests

Field load tests determine the axial and lateral load capacity as a function of displacements for applied structural loads to prove that the tested pile or drilled shaft can support the design loads within tolerable settlements. Load tests are also used to verify capacity calculations and structural integrity using static equations and soil parameters. Soil parameters can be determined by laboratory and in situ tests, wave equation and pile driving analysis, and from previous experience. Load tests consist of applying static loads in increments and measuring the resulting pile movements. Some aspects of load tests that need to be considered are:

a. Categories of load tests. Types of load tests performed are proof tests, tests conducted to failure without internal instrumentation, and tests conducted to failure with instrumentation. Proof tests are not conducted to a bearing capacity failure of the pile or drilled shaft but usually to twice the design load. Tests conducted to failure without instrumentation determine the ultimate pile capacity Q_u, but do not indicate the separate components of capacity of end bearing Q_{bu} and skin resistance Q_{su}. Tests with internal instrumentation, such as strain gauges mounted on reinforcement bars of drilled shafts or mounted inside of pipe piles, will determine the distribution of load carried by skin friction as a function of depth and will also determine the end-bearing capacity when conducted to failure.

b. Limitations of proof tests. Many load tests performed today are "proof" tests, which are designed to prove that the pile can safely hold the design load or to determine the design load. Proof tests do not determine the ultimate capacity so that the pile is often designed to support a higher load than necessary and can cause foundation costs to be greater than necessary. Proof tests are not adequate when the soil strength may deteriorate with time such as from frequent cyclic loads in some soils. Coral sands, for example, can cause cementation that can degrade from cyclic loads.

c. Selecting and timing load tests. Load tests are always technically desirable, but not always economically feasible because they are expensive. These tests are most frequently performed to assist in the design of major structures with large numbers of piles where changes in length, size, and type of pile and installation method can provide significant cost savings. The costs of load tests should be compared with potential savings when using reduced safety factors permitted with the tests. Factors to be considered before considering load test are:

(1) Significance of structure. The type and significance of a structure could offset the added cost of load tests for a complex foundation when the consequences of failure would be catastrophic.

(2) Soil condition. Some subsurface investigations may indicate unusual or highly variable soils that are difficult to define.

(3) Availability of test site. Testing should not interfere with construction. Load tests should be conducted early after the site is prepared and made accessible. The contractor must wait for results before methods and equipment can be determined and materials can be ordered. Advantages of completing the testing program prior to construction include discovery of potential and resolution of problems, determination of the optimum installation procedure, determination of the appropriate type, length and size of the piles. Disadvantages include increased design time to allow for load tests and testing conditions and data extrated from a test site used in the design may not simulate actual construction conditions such as excavation, groundwater, and fill. Problems may also occur if different contractors and/or equipment are used during construction.

(4) Location. Test piles should be located near soil test borings and installed piezometers.

(5) Timing. Load tests of driven piles should be performed after 1 or more days have elapsed to allow

dissipation of pore water pressures and consideration of freeze or relaxation.

d. Axail load tests. Axial compressive load tests should be conducted and recorded according to ASTM D 1143. The quick load test described as an option in ASTM D 1143 is recommended for most applications, but this test may not provide enough time for some soils or clays to consolidate and may underestimate settlement for these soils. The standard load test takes much longer and up to several days to complete than the quick load test and will measure more of the consolidation settlement of compressible soils than the quick load test procedure. However, neither the standard test nor the quick test will measure all of the consolidation settlement. The cyclic load test will indicate the potential for deterioration in strength with time from repeated loads. Procedures for load tests are presented:

(1) Quick load test. The load is applied in increments of 10 to 15 percent of the proposed design load with a constant time interval between load increments of 2 minutes or as specified. Load is added until continuous jacking is required to maintain the test load (plunging failure) or the capacity of the loading apparatus is reached, whichever comes first.

(2) Standard load test. Load is applied in increments of 25 percent of the design load and held until the rate of settlement is not more than 0.01 inch/hour but not longer than 2 hours. Additional load increments are applied until twice the design load is reached. The load is then removed in decrements of 50, 100 and 200 percent of the design load for rebound measurements. This is a proof test if no further testing is performed. A preferred option of the standard load test is to reload the pile in increments of 50 percent of the design load until the maximum load is reached. Loads may then be added at 10 percent of the design load until plunging failure or the capacity of the equipment is reached. This option is recommended to evaluate the ultimate pile capacity.

(3) Repeated load test. The standard load test is initially performed up to 150 percent of the design load, allowing 20 minutes between load increments. Loads are removed in decrements equal to the load increments after 1 hour at the maximum applied load. Load is reapplied in increments of 50 percent of the design load allowing 20 minutes between increments until the previous maximum load is reached. Additional load is then applied and removed as described in ASTM D 1143. This test is useful to determine deterioration in pile capacity and displacements from cyclic loads.

(4) Tension test. Axial tension tests may be conducted according to ASTM D 3689 to provide information on piles that must function in tension or tension and compression. Residual stresses may significantly influence results. A minimum waiting period of 7 days is therefore required following installation before conducting this test, except for tests in cohesive soil where the waiting period should not be less than 14 days.

(5) Drilled shaft load test using Osterberg Cell. Load tests are necessary so that the design engineer knows how a given drilled shaft would respond to design loads. Two methods are used to load test drilled shaft: the Quick Load Test Method described in ASTM D 1143 standard, and the Osterberg Cell Method.

(a) Unlike the Quick Load ASTM test method which applies the load at the top of the drilled shaft, the Osterberg cell test method applies the load to the bottom of the shaft. The cell consists of inflatable cylindrical bellow with top and bottom plates slightly less than the diameter of the shaft. The cell is connected to double pipes, with the inner pipe attached to the bottom and the outer pipe connected to the top of the cell (Figure 6-4). These two pipes are separated by a hydraulic seal at the top with both pipes extended to the top of the shaft. The outer pipe is used as a conduit for applying fluid pressure to the previously calibrated cell. The inner pipe is used as a tell-tale to measure the downward movement of the bottom of the cell. It is also used to grout the space between the cell and the ground surface and create a uniform bearing surface. Fluid used to pressurize the cell is mixed with a small amount of water - miscible oil. The upward movement of the shaft is measured by dial gauge 1 placed at the top of the shaft (Figure 6-4). Downward movement is measured by dial gauge 2 attached to the top of the inner pipe above the point where it emerges from the outer pipe through the hydraulic seal.

(b) After drilling the shaft, the Osterberg cell is welded to the bottom of the reinforcing cage, lifted by crane, and inserted carefully into the hole. After proper installation and testing, the cell is grouted by pumping a carefully monitored volume of grout through the inner pipe to fill the space between the cell and the bottom of the hole. When the grout is set, concrete is pumped to fill the hole to the desired level and the casing is pulled. After concrete has reached the desired strength, the cell is pressurized internally to create an upward force on the shaft and an equal and opposite downward force in end bearing. As pressure increases, the inner pipe moves downward while the outer pipe moves upward. The upward movement is a function of the weight of the drilled shaft and the friction

and/or adhesion mobilized between the surface concrete and the surrounding soil.

(c) The dial gauges are usually attached to a reference beam supported by two posts driven into the ground a sufficient distance apart (i.e., 10 feet or two shaft diameters, whichever is larger) (Figure 6-4) to eliminate the influence of shaft movement during the test. The difference in reading between dial gauge 1 and dial gauge 2 at any pressure level represents the elastic compression of the concrete. The load downward-deflection curve in end bearing and the load upward- movement curve in skin friction can be plotted from the test data to determine the ultimate load of the drilled shaft. Failure may occur in end bearing or skin friction. At that point the test is considered complete. Osterberg cells can be constructed as large as 4 feet in diameter to carry a load equivalent to 6,000 tons of surface load.

(6) Analysis of capacity. Table 6-4 illustrates four methods of estimating ultimate capacity of a pile tested to failure. Three methods should be used when possible, depending on local experience and preference, to determine a suitable range of probable ultimate capacity. The methods given in Table 6-4 give a range of Q_u from 320 to 467 kips for the same test data.

(7) Effects of layered soils. Layered soils may cause the test piles to have a different capacity than the service piles if the test piles have tips in a different stratum. Consolidation of a cohesive layer supporting the tip load may also cause the load to be supported by another layer. The support of a pile could change from friction to end bearing or the reverse depending on the strata.

e. Lateral load test. This test is used to verify the stiffness used in design. The cyclic reduction factor used in design can be verified if the test pile is loaded for approximately 100 cycles. Some aspects of the lateral load test are:

(1) Monotonic and cyclic lateral load tests should be conducted and recorded according to ASTM D 3966. Tests should be conducted as close to the proposed structure as possible and in similar soil.

(2) Lateral load tests may be conducted by jacking one pile against another, thus testing two adjacent piles. Loads should be carried to failure.

(3) Groundwater will influence the lateral load response of the pile and should be the same as that which will exist during the life of the structure.

(4) The sequence of applying loads is important if cyclic tests are conducted in combination with a monotonic lateral load test. This may be done by first selecting the load level of the cyclic test using either load or deflection guidelines. The load level for the cyclic test may be the design load. A deflection criterion may consist of loading the piles to a predetermined deflection and then using that load level for the cyclic load test. Using the cyclic load level, the test piles would be cyclically loaded from zero loading to the load level of the cyclic load test. This procedure should be repeated for the required number of cycles. Dial gauge readings of lateral deflection of the pile head should be made at a minimum at each zero load level and at each maximum cyclic load level. The test pile should be loaded laterally to failure after the last loading cycle. The last loading cycle to failure can be superimposed on the initial loading cycle to determine the lateral load-deflection curve of the pile to failure.

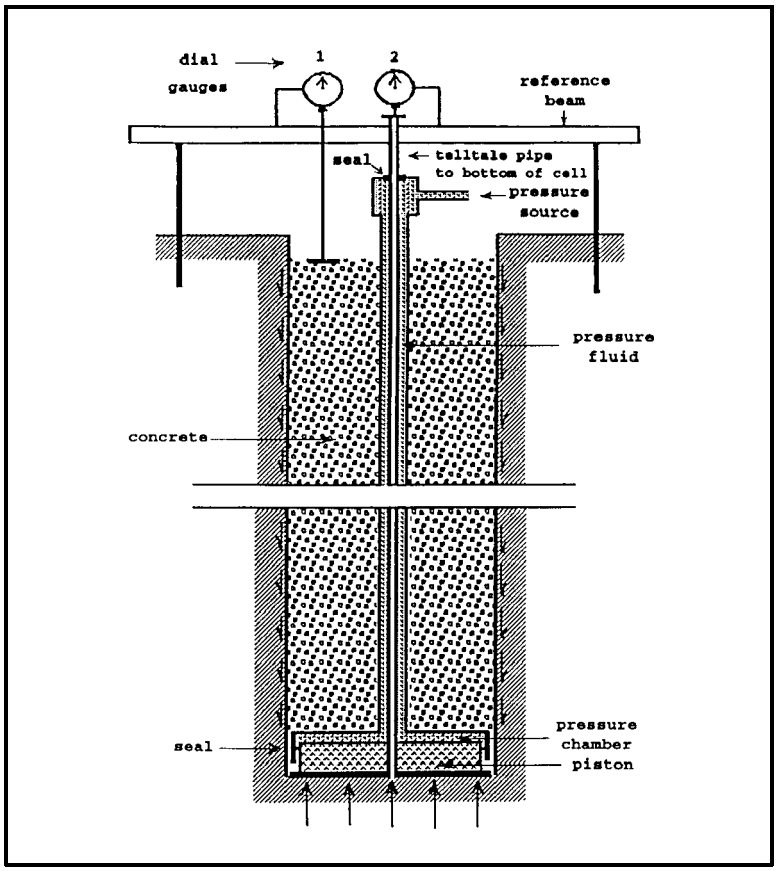

Figure 6-4. Typical Osterberg cell load test (from Osterberg 1995)

Table 6-4
Methods of Estimating Ultimate Pile Capacity from Load Test Data

Method	Procedure	Diagram
Tangent (FHWA-RD-IR-77-8)	1. Draw a line tangent to the curve at the origin 2. Draw another line tangent to the curve at the point on the curve with slope equivalent to 1 inch for 40 kips of load 3. Ultimate bearing capacity is the load at the intersection of the two tangent lines	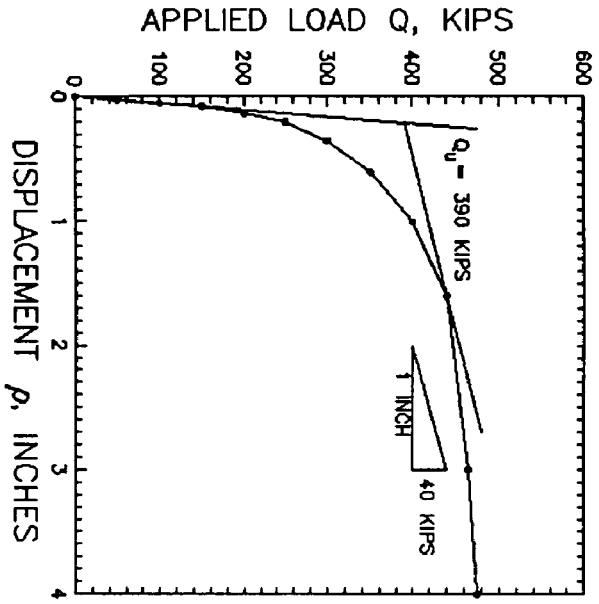
Limit Value (Davisson 1972)	1. Draw a line with slope $\frac{\pi B^2}{4L} \cdot E_p$ where B = pile diameter, inches; E_p = Young's pile modulus, kips/inch²; L = pile length, inches 2. Draw a line parallel with the first line starting at a displacement of 0.15 + B/120 inch at zero load 3. Ultimate bearing capacity is the load at the intersection of the load –displacement curve with the line of step 2	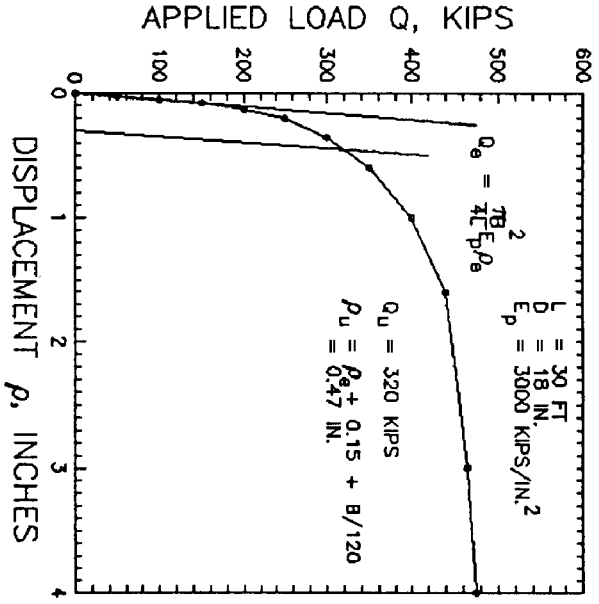

Table 6-4 (Concluded)

Method	Procedure	Diagram
80 Percent (Hansen 1963)	1. Plot load test results as $\sqrt{\rho}/Q$ vs. ρ 2. Draw straight line through data points 3. Determine the slope a and intercept b of this line 4. Ultimate bearing capacity is $Q_u = \frac{1}{2\sqrt{ab}}$ 5. Ultimate deflection is $\rho_u = b/a$	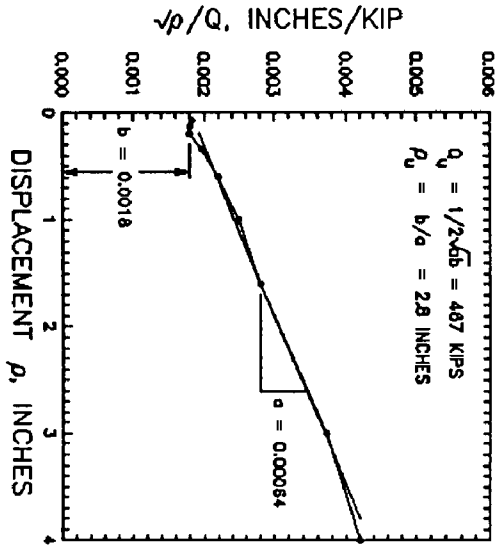
90 Percent (Hansen 1963)	1. Calculate 0.9Q for each load Q 2. Find $\rho_{0.9Q}$, displacement for load of 0.9Q, for each Q from Q vs. ρ plot 3. Determine $2\rho_{0.9Q}$ for each Q and plot vs. Q on the chart with the load test data of Q vs. ρ 4. Ultimate bearing capacity is the load at the intersection of the two plots of data	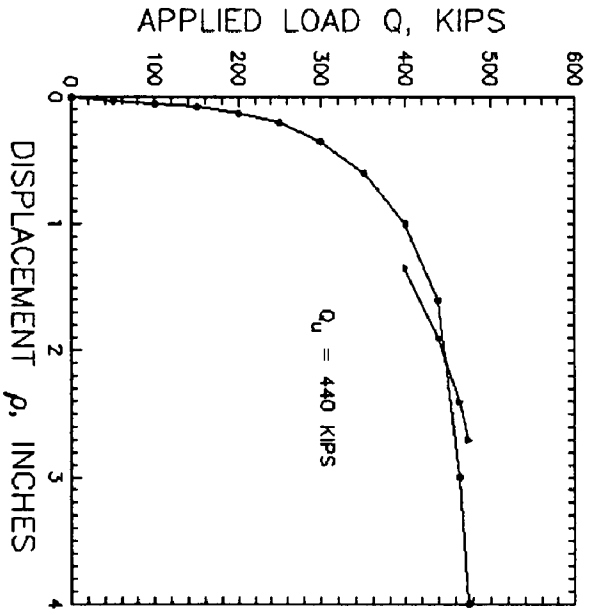

Appendix A
References and Bibliography

A-1. Required Publications

Departments of the Army and the Navy

NAVFAC DM-7.1
Soil Mechanics

TM 5-818-1
Soils and Geology; Procedures for Foundation Design of Buildings and Other Structures (Except Hydraulic Structures)

TM 5-818-7
Foundations in Expansive Soils

TM 5-849-1
Pile Driving Equipment

[1]Federal Specifications

TT-W00571J
Wood Preservation: Treating Practices

[2]U.S. Department of Transportation

FHWA-DP-66-1 (Revision 1)
Manual on Design and Constuction of Driven Pile Foundations, April 1986

FHWA-RD-IR-77-8
User's Manual for the Texas Quick-Load Method for Foundation Load Testing, 1977

FHWA-TS-78-209
Guidelines for Cone Penetration Test Performance and Design, 1978

FHWA-RD-83-059
Allowable Stresses in Piles, 1983

[1]Naval Publications and Form Center, 5801 Tabor Avenue, Philadelphia, PA 19120.

[2]Federal Highway Administration , Office of Implementation, 6300 Georgetown Pike, McLean, Virginia 22101

FHWA-RD-85-106
Behavior of Piles and Pile Groups Under Lateral Load, 1985

FHWA-HI-88-042
Drilled Shafts: Construction Procedures and Design Methods, 1988

FHWA-DP-66-1
Manual on Design and Construction of Driven Pile Foundation, 1986

U.S. Army Engineer Waterways Experiment Station 1975. U.S. Army Engineer Waterways Experiment Station. 1975. "Background Theory and Documentation of Five University of Texas Soil-Structure Interaction Computer Programs," Miscellaneous Paper K-75-2, Vicksburg, MS.

U.S. Army Engineer Waterways Experiment Station 1984. U.S. Army Engineer Waterways Experiment Station, 1984 (Feb). "User's Guide: Computer Program for Soil-Structure Interaction Analysis of Axially Loaded Piles (CAXPILE)," Instruction Report K-84-4, Vicksburg, MS.

U.S. Army Engineer Waterways Experiment Station 1992. U.S. Army Engineer Waterways Experiment Station. 1992. "User's Guide for Concrete Strength Investigation and Design (CASTR) in Accordance with ACI 318-89," Instruction Report ITL-87-2 (Revised), Vicksburg, MS.

U.S. Army Engineer Waterways Experiment Station 1989. U.S. Army Engineer Waterways Experiment Station. 1989. "User's Guide: Pile Group Analysis (CPGA) Computer Program," Technical Report ITL-89-3, Vicksburg, MS.

U.S. Army Engineer Waterways Experiment Station 1990. U.S. Army Engineer Waterways Experiment Station. 1990. "User's Guide: Pile Group/Concrete Pile Analysis Program (CPGC) Preprocessor to CPGA Program," Instruction Report ITL-90-2, Vicksburg, MS.

American Association of State Highway and Transportation Officials (AASHTO) 1989. American Association of State Highway and Transportation Officials (AASHTO), 14th edition, 444 North Capitol Street NW, Suite 225, Washington, DC 20001.

Standard Specification for Highway Bridges
Standard Specification for Highway Bridges

[3]**American Concrete Institute 1986**
American Concrete Institute. 1986. "Use of concrete in Buildings: Design, Specifications, and Related Topics," *Manual of Concrete Practice*. Parts 3 and 4.

[3]**American Concrete Institute 1989**
American Concrete Institute. 1989. "Building Code Requirements for Reinforced Concrete," ACI Report No. 318-89.

[3]**American Concrete Institute 1974**
American Concrete Institute. 1974. "Recommen-dations for Design, Manufacture and Installation of Concrete Piles," ACI Report No. 543R-74.

[3]**American Concrete Institute 1985**
American Concrete Institute. 1985. "Ultimate Strength Design Handbook, Volume I: Slabs, 1984; Columns," ACI Report No. SP 17.

Association of Drilled Shaft Contractors 1989
Association of Drilled Shaft Contractors (ADSC). 1989. "Drilled Shaft Inspector's Manual," First Edition, P.O. Box 280379, Dallas, TX.

American Institute of Steel Construction 1986
American Institute of Steel Construction (AISC). 1986. "Load and Resistance Factor Design," First Edition, *Manual of Steel Construction*, 1 E. Wacker Drive, Chicago, IL.

American Institute of Steel Construction 1989
American Instiute of Steel Construction (ASIC). 1989. "Allowable Stress Design," 9th Edition, *Manual of Steel Construction*, 1 E. Wacker Drive, Chicago, IL.

[4]**American Society for Testing and Materials**

ASTM A 252
(1993) Specification for Welded and Seamless Steel Pipes

ASTM D 25
(1991) Specification for Round Timber Piles

ASTM D 1143
(1987) Piles Under Static Axail Compressive Load

ASTM D 1586
(1992) Penetration Test and Split-Barrel Sampling of Soils

ASTM D 2435
(1990) One-Dimensional Consolidation Properties of Soils

ASTM D 2487
(1993) Classification of Soils for Engineering Purposes

ASTM D 2899
(1986) Method for Establishing Design Stresses for Round Timber Piles

ASTM D 3200
(1986) Establishing Recommended Design Stresses for Round Timber Construction Poles

ASTM D 3441
(1986) Deep, Quasi-Static, Cone and Friction-Cone Penetration Tests of Soil

ASTM D 3689
(1990) Individual Piles Under Static Axial Tensile Load

ASTM D 3966
(1990) Piles Under Lateral Loads

ASTM D 4546
(1990) One-Dimensional Swell or Settlement Potential of Cohesive Soils Wood

American Society for Testing and Materials
American Society for Testing and Materials (ASTM). Steel-Piping, Tubing, Fitting, Vol 01.01.

American Society for Testing and Materials
American Society for Testing and Materials. "Steel-Structural, Reinforcing, Pressure Vessel, Railway," ASTM Vol 01.04.

American Society for Testing and Materials
American Society for Testing and Materials. "Soil and Rock; Dimension Stone; Geosynthetics,"ASTM Vol 04.08.

American Society for Testing and Materials
American Society for Testing and Materials. "Soil and Rock (II): D4943-latest; Geosynthetics," ASTM Vol 04.09.

American Wood Preservers Institute 1977-1979
American Wood Preservers Institute. 1977-1979. "Standards for Creosoted-Wood Foundation Piles," 1945

[3]American Concrete Institute (ACI), P.O. Box 19150, Redford Station, Detroit, MI 48219

[4]American Society for Testing and Materials (ASTM), 1916 Race Street, Philadelphia, PA 19103

Old Gallows Road, Suite 405, Vienna, VA, C1-C12.

International Conference of Building Officials 1991
International Conference of Building Officials. 1991. "Uniform Building Code," 5360 South Workman Mill Road, Whittier, CA.

Pile Buck, Inc. 1988
Pile Buck, Inc. 1988. "Testing Methods of Driven Piles," *Pile Buck Annual*, P.O. Box 1056, Jupiter, FL, Chapter 13, pp 297-318.

Pile Buck, Inc. 1992
Pile Buck, Inc. 1992. "Design of Pile Foundations," *Foundations*, P.O. Box 1056, Jupiter, FL, pp 1-69.

Precast and Prestressed Concrete Institute 1988
Precast and Prestressed Concrete Institute. 1988. "Recommended Practice for the Design of Prestressed Concrete Columns and Walls," *PCI Committee on Prestressed Concrete Columns, PCI Journal*, Vol 33, No. 4, pp 56-95.

A-2. Related Publications

American Petroleum Institute 1987
American Petroleum Institute. 1987 (Apr). "Recommended Practice for Planning, Designing, and Constructing Fixed Offshore Platforms, API Recommended Practice 2A (RP 2A)," Seventeenth Edition.

Awoshika and Reese 1971
Awoshika, K., and Reese, L. C. 1971 (Feb). "Analysis of Foundation with Widely Spaced Batter Piles," Research Report 117-3F, Project 3-5-68-117, Center for Highway Research, University of Texas at Austin.

Baguelin, Jézéquel, and Shields 1978
Baguelin, F., Jézéquel, J. F., and Shields, D. H. 1978. *The Pressuremeter and Foundation Engineering*, Trans Tech Publications.

Banerjee and Davies 1979
Banerjee, P. K., and Davies, T. G. 1979 (May). "Analysis of Some Reported Histories of Laterally Loaded Pile Groups." *Proceedings*, Numerical Methods in Offshore Piling, The Institute of Civil Engineers, London, pp 101-108.

Barker et al. 1991
Barker, R. M., et al. 1991. "Manual for the Design of Bridge Foundations," National Cooperative Highway Research Program Report 343, Transportation Research Board, 2101 Constitution Avenue, Washington, DC.

Bieniawski 1984
Bieniawski, Z. T. 1984. *Rock Mechanics Design in Mining and Tunneling*, A. A. Balkema, Rotterdam/Boston.

Bogard and Matlock 1983
Bogard, D., and Matlock, H. 1983 (Apr). "Procedures for Analysis of Laterally Loaded Pile Groups in Soft Clay," *Proceedings*, Geothechnical Practice in Offshore Engineering, American Society of Civil Engineers, New York, NY.

Bowles 1968
Bowles, J. E. *Foundation Analysis and Design*, Appendix A, McGraw-Hill, NY.

Broms 1964a
Broms, B. B. 1964a. "Lateral Resistance of Piles in Cohesive Soils," *Journal of the Soil Mechanics and Foundations Division*, American Society of Civil Engineers, New York, NY,Vol 90, pp 27-63.

Broms 1964b
Broms, B. B. 1964b. "Lateral Resistance of Piles in Cohesionless Soil," *Journal of the Soil Mechanics and Foundations Division*, American Society of Civil Engineers, New York, NY, Vol 90, pp 123-156.

Broms 1965
Broms, B. B. 1965. "Design of Laterally Loaded Piles," *Journal of Soil Mechanics and Foundations Division*, American Society of Civil Engineers, New York, NY, Vol 91, pp 79-99.

Bryant 1977
Bryant, L. M. 1977. "Three-Dimensional Analysis of Framed Structures with Nonlinear Pile Foundations," Unpublished Dissertation, University of Texas at Austin, Austin, TX.

Canadian Geotechnical Society 1985
Canadian Geotechnical Society. 1985. "Canadian Foundation Engineering Manual," 2nd Edition, BiTech Publishers Ltd., 801-1030 W. Georgia Street, Vancouver, B.C.

Cox, Reese, and Grubbs 1974
Cox, W. R., Reese, L. C., and Grubbs, B. R. 1974. "Field Testing of Laterally Loaded Piles in Sand," *Proceedings*, 6th Annual Offshore Technology Conference Paper No. OTC 2079, Houston, TX pp 459-472.

Coyle and Reese 1966
Coyle, H. M., and Reese, L. C. 1966. "Load Transfer for Axially Loaded Piles in Clay," *Proceedings*, American Society of Civil Engineers, New York, NY, Vol 92, No.SM2, pp 1-26.

Coyle and Sulaiman 1967
Coyle, H. M., and Sulaiman, I. H. 1967. "Skin Friction for Steel Piles in Sand, " *Proceedings*, American Society of Civil Engineers, New York, NY, Vol 93, No. SM6, pp 261-278.

Davisson 1970
Davisson, M. T. 1970. "Lateral Load Capacity of Piles," *Highway Research Record*, Transportation Research Board, 2101 Constitution Avenue, Washington, DC.

Davisson 1972
Davisson, M. T. 1972. "High Capacity Piles," *Proceedings Lecture Series, Innovations in Foundation Construction*, Illinois Section, American Society of Civil Engineers, New York, NY.

Davisson and Robinson 1965
Davisson, M. T., and Robinson, K. E. 1965. "Bending and Buckling of Partially Embedded Piles," *Proceedings 6th International Conference on Soil Mechanics and Foundation Engineering*, Montreal, Canada, University of Toronto Press, 63a George Street, Toronto ONM5S1A6, pp 243-246.

Deere 1968
Deere, D. V. 1968. "Geological Considerations," *Rock Mechanics in Engineering Practice*, K. G. Stagg and O. C. Zienkiewica, New York, NY, Chapter 1.

Det norske 1977
Det norske, V. 1977. "Rules for the Design, Construction, and Inspection of Offshore Structure," Veritasveien 1, 1322 HØ vik, Norway.

Donald, Sloan, and Chiu 1980
Donald, I. B., Sloan, S. W., and Chiu, H. K. 1980. "Theoretical Analyses of Rock-socketed Piles," *Proceedings International Conference on Sturctural Foundations on Rock*, Sydney, Australia, A. A. Balkema, Rotterdam/Boston.

Fleming et al. 1985
Fleming, W. G. F., et al. 1985. *Pile Engineering*, Blackie and Son, Ltd., Glasgo, Scotland.

George and Wood 1977
George, P., and Wood, D. 1977. *Offshore Soil Mechanics*, Cambridge University Engineering Department, Cambridge, MA.

Goble, Rausche, Likins and Associates, Inc. 1988
Goble, Rausche, Likins and Associates, Inc. 1988. (GRL), *GRLWEAP Wave Equation Analysis of Pile Driving*. Available from GRL, 4535 Emery Industrial Parkway, Cleveland, OH.

Hansen 1963
Hansen, J. B. 1963. "Hyperbolic Stress-strain Response: Cohesive Soils," *Discussion Journal of the Soil Mechanics and Foundations Division*, American Society of Civil Engineers, New York, NY, Vol 89, No. SM4.

Hetenyi 1946
Hetenyi, M. I. 1946. *Beams on Elastic Foundation*, University of Michigan Press, Ann Arbor, MI.

Horvath and Kenney 1979
Horvath, R. G., and Kenney, T. C. 1979. "Shaft Resistance of Rock Socketed Drilled Piers," *Proceedings Symposium on Deep Foundations*, American Society of Civil Engineers, Atlantic, GA.

International Conference of Building Officials 1991
International Conference of Building Officials. 1991. "Uniform Building Code," Whitter, CA.

Jamiolkowski 1977
Jamiolkowski, M. 1977. "Design of Laterally Loaded Piles,"General Lecture, International Conference on Soil Mechanics and Foundation Engineering, Tokyo, Japan.

Japanese Road Association 1976
Japanese Road Association. 1976 (May). "Road Bridge Substructure Design Guide and Explanatory Notes, Designing of Pile Foundations," p 67.

Kraft, Focht, and Amarasinghe 1981
Kraft, L. M., Jr., Focht, J. A., and Amarasinghe, S. R. 1981. "Friction Capacity of Piles Driven into Clay, " *Journal of Geotechnical Engineering Division*, Vol 107, pp 1521-1541.

Kraft, Ray, and Kagawa 1981
Kraft, L. M., Ray, R. P., and Kagawa, T. 1981. "Theortical t-z Curves," *Journal of the Geotechnical Engineering Division*, American Society of Civil Engineers, New York, NY, Vol 107, pp 1543-1561.

Kuthy et al. 1977
Kuthy, R. A. et al. 1977 (Apr). "Lateral Load Capacity of

Vertical Pile Groups," Research Report 47, Engineering Research and Development Bureau, New York State Department of Transportation, Albank, NY.

Kubo 1965
Kubo, K. 1965. "Experimental Study of the Behavior of Laterally Loaded Piles," *Proceedings*, Sixth International Conference on Soil Mechanics and Foundation Engineering, Montreal, Vol 2, pp 275-279.

Lam 1981
Lam, P. 1981. "Computer Program of Analysis of Widely Spaced Batter Piles," Unpublished thesis, University of Texas at Austin, Austin, TX.

Matlock 1970
Matlock, H. 1970. "Correlations for Design of Laterally Loaded Piles in Soft Clay," *Proceedings*, 2nd Annual Offshore Technology Conference, Paper No. OTC 1204, Houston, TX, pp 577-594.

Matlock and Reese 1961
Matlock, H., and Reese, L. C. 1961. "Foundation Analysis of Offshore Pile-Supported Structures," *Proceedings*, Fifth International Conference, International Society of Soil Mechanics and Foundation Engineering, Paris, France, Vol 2, pp 91-97.

Matlock et al. 1980
Matlock, H., et al. 1980 (May). "Field Tests of the Lateral Load Behavior of Pile Groups in Soft Clay," *Proceedings*, 12th Annual Offshore Technology Conference, Paper No. OTC 3871, Houston, TX.

McCelland 1972
McCelland, B. 1972 (Jun). "Design and Performance of Deep Foundations," *Proceedings*, Specialty Conference on Performance of Earth and Earth Supported Structures, Purdue University, Soil Mechanics and Foundations Division, American Society of Civil Engineers .

McCelland and Focht 1958
McCelland, B., and Focht, J. A. 1958. "Soil Modulus for Laterally Loaded Piles," *Transactions*, American Society of Civil Engineers, Vol 123, pp 1049-1086.

Meyerhof 1976
Meyerhof, G. G. 1976. "Bearing Capacity and Settlement of Pile Foundations," *Journal of Geotechnical Engineering*, American Society of Civil Engineers, New York, NY, Vol 102, GT3, pp 197-228.

Meyerhof 1983
Meyerhof, G. G. 1976. "Scale Effects of Ultimate Pile Capacity," *Journal of Geotechnical Engineering*, American Society of Civil Engineering, New York, NY, Vol 109, No. 6, pp 797-806.

Nordlund 1963
Nordlund, R. L. 1963. "Bearing Capacity of Piles in Cohesionless Soils," *Journal of the Soil Mechanics and Foundations Division*, American Society of Civil Engineers, Vol 89, pp 1-36.

Nottingham and Schmertmann 1975
Nottingham, L., and Schmertmann, J. 1975. "An Investigation of Pile Capacity Design Procedures," Final Report D629 to Florida Department of Transportation from Department of Civil Engineering, University of Florida.

O'Neill 1983
O'Neill, M. W. 1983 (Apr). "Group Action in Offshore Piles," *Proceedings*, Geotechnical Practice in Offshore Engineering, American Society of Civil Engineers.

O'Neill, Ghazzaly, and Ha 1977
O'Neill, M. W., Ghazzaly, O. I., and Ha, H. B. 1977. "Analysis of Three-Dimensional Pile Groups with Nonlinear Soil Response and Pile-Soil-Pile Interaction," *Proceedings* 9th Annual Offshore Technology Conference, Houston, TX, Vol II, Paper No. 2838, pp 245-256.

Osterberg 1995
Osterberg, J. O. 1995. "The Osterberg CELL for Load Testing Drilled Shafts and Driven Piles," report for U.S. Department of Transportation, Federal Highway Administration, by J. O. Osterberg, Ltd., Aurora, CO.

Peck 1976
Peck, R. B. 1976. "Rock Foundations for Structures," *Proceedings ASCE Specialty Conference on Rock Engineering for Foundations and Slopes*, Boulder, CO.

Poulos 1971
Poulos, H. G. 1971. "Behavior of Lateally Loaded Piles: II - Pile Groups," *Proceedings*, American Society of Civil Engineers, Vol 97, No. SM5, pp 733-751.

Poulos and Davis 1980
Poulos, H. G., and Davis, E. H. 1980. *Pile Foundation Analysis and Design*, Wiley, New York.

Prakash and Sharma 1989
Prakash, S., and Sharma, H. D. 1989. *Pile Foundations in Engineering Practice*, Wiley, New York.

Preiss, Weber, and Caiserman 1978
Preiss, K., Weber, H., and Caiserman, A. 1978. "Integrity Testing of Bored Piles and Diaphragm Walls," *Transactions*, South African Institution of Civil Engineers, Vol 20, No. 8, pp 191-196.

Randolph and Wroth 1978
Randolph, M. F., and Wroth, C. P. 1978. "Analysis of Deformation of Vertically Loaded Piles," *Journal of the Geotechnical Engineering Division*, American Society of Civil Engineers, New York, NY, Vol 104, No. GT12, pp 1465-1488.

Reese 1964
Reese, L. C. 1964 (Feb). "Load versus Settlement for an Axially Loaded Pile," *Proceedings*, Part II, Symposium on Bearing Capacity of Piles, Central Building Research Institute, Roorkee, pp 18-38.

Reese 1966
Reese, L. C. 1966 (Apr). "Analysis of a Bridge Foundation Supported by Batter Piles," *Proceedings*, 4th Annual Symposium on Engineering Geology and Soil Engineering, Moscow, ID, pp 61-73.

Reese 1984
Reese, L. C. 1984 (Jul). *Handbook on Design of Piles and Drilled Shafts Under Lateral Load*, U. S. Department of Transportation, Federal Highway Administration, FHWA-IP-84-11, p 360.

Reese, Cox, and Koop 1974
Reese, L. C., Cox, W. R., and Koop, F. D. 1974. "Analysis od Laterally Loaded Piles in Sand," *Proceedings*, 5th Annual Offshore Technology Conference, Paper No. OTC 2080, Houston, TX, pp 473-485.

Reese, Cox, and Koop 1975
Reese, L. C., Cox, W. R., and Koop, F. D. 1975. "Field Testing and Analysis of Laterally Loaded Piles in Stiff Clay," *Proceedings*, 7th Annual Offshore Technology Conference, Paper No. OTC 2312, Houston, TX, pp 672-690.

Reese and Matlock 1956
Reese, L. C., and Matlock, H. 1956. "Non-Dimensional Solutions for Laterally Loaded Piles with Soil Modulus Assumed Proportional to Depth," *Proceedings Eighth Texas Conference on Soil Mechanics and Foundation Engineering*, Special Publication No. 29, Bureau of Engineering Research, University of Texas, Austin, TX.

Reese and Matlock 1966
Reese, L. C., and Matlock, H. 1966. "Behavior of a Two-Dimensional Pile Group Under Inclined and Eccentric Loading," *Proceedings*, Offshore Exploration Conference, Long Beach, CA, pp 123-140.

Reese, O'Neill, and Smith 1970
Reese, L. C., O'Neill, M. W., and Smith, R. E. 1970 (Jan). "Generalized Analysis of Pile Foundations," *Proceedings*, American Society of Civil Engineers, Vol 96, No. SM1, pp 235-250.

Reese and Welch 1975
Reese, L. C., and Welch, R. C. 1975 (Feb). "Lateral Loading of Deep Foundations in Stiff Clay," *Journal of the Geotechnical Engineering Division*, American Society of Civil Engineers, Vol 101, No. GT7, pp 633-649.

Reese and Wright 1977
Reese, L. C., and Wright, S. J. 1977. "Drilled Shaft Manual - Construction Procedures and Design for Axial Loading," Vol 1, U.S. Department of Transportation, Implementation Division, Implementation Package 77-21.

Saul 1968
Saul, W. E. 1968. "Static and Dynamic Analysis of Pile Foundations," *Journal of the Structural Division*, American Society of Civil Engineers, Vol 94, pp 1077-1100.

Scott 1969
Scott, C. R. 1969. *An Introduction to Soil Mechanics and Foundations*, Applied Science Publishers Ltd., Ripple Road, Barking, Essex, England, p 310.

Seed and Reese 1957
Seed, H. B., and Reese, L. C. 1957. "The Action of Soft Clay Along Friction Piles," *Transactions*, American Society of Civil Engineers, New York, NY, Vol 122, pp 731-753.

Smith and Mlakar 1987
Smith, W. G., and Mlakar, P. F. 1987. "Lumped Parameter Seismic Analysis of Pile Foundations," Report No. J650-87-008/2495, Vicksburg, MS.

Stewart and Kulhawy 1980
Stewart, J. P., and Kulhawy, F. H. 1980. "Behavior of Drilled Shafts in Axial Uplift Loading," Geotechnical Engineering Report 80-2, School of Civil and Environmental Engineering, Cornell University, Ithica, NY.

Stewart and Kulhawy 1981
Stewart, J. P., and Kulhawy, F. H. 1981. "Experimental Investigation of the Uplift Capacity of Drilled Shaft Foundations in Cohesionless Soil," Contract Report B-49 (6), Niagara Mohawk Power Corporation, Syracuse, NY.

Tomlinson 1980
Tomlinson, M. J. 1980. *Foundation Design and Construction*, Fourth Edition, Pitman Publishing Limited, 128 Long Acre, London WC2E 9AN, UK.

Tomlinson 1987
Tomlinson, M. J. 1987. *Pile Design and Construction Practice*, Viewpoint Publications.

Vesic 1971
Vesic, A. S. 1971. "Breakout Resistance of Object Embedded in Ocean Bottom," *Journal of the Soil Mechanics and Foundation Division*, American Society of Civil Engineers, New York, NY, Vol 97, SM9, pp 1183-1205.

Vesic 1977
Vesic, A. S. 1977. "Design of Pile Foundations," *National Cooperative Highway Research Program Synthesis of Highway Practice*, No. 42, Transportation Research Board, 2101 Constitution Avenue, Washington, DC.

Vijayvergiya and Focht 1972
Vijayvergiya, V. N., and Focht, J. A., Jr. 1972. "A New Way to Predict Capacity of Piles in Clay," *Proceedings*, 4th Annual Offshore Technology Conference, Paper No. OTC Paper 1718, Houston, TX.

Vijayvergiya 1977
Vijayvergiya, V. N. 1977. "Load-Movement Characteristics of Piles," *Port 77 Conference*, American Society of Civil Engineers, New York, NY.

Welch and Reese 1972
Welch, R. C., and Reese, L. C. 1972 (May). "Laterally Loaded Behavior of Drilled Shafts," Research Report No. 3-5-65-89, Center for Highway Research, University of Texas at Austin, Austin, TX.

Wolff 1990
Wolff, T. F. 1990. "User's Guide: Pile Group Interference Probabilistic Assessment (CPGP) Computer Program," U.S. Army Engineer Waterways Experiment Station, Vicksburg, MS.

Appendix B
Pipe Piles

B-1. Dimensions and Properties.

Table B-1 lists the dimensions and properties for design of some of the more commonly used sizes of pipe piles. The source of this information is Pile Buck, Inc. (1988) or FHWA-DP-66-1 (Revision 1), "Manual on Design and Construction of Driven Piles Foundations."[1] Data from this table are used for analysis of design stresses in stell piles, Chapter 2, in applications of tabuluar members. For reference to a particular member, use designation $PPB_o \times t_w$ where B_o is the outside diameter in inches and t_w is the wall thickness in inches. I is the moment of inertia, inches^4, and determined by $I = Ar^2$. $A = \pi t_w(B_o - t_w)$, the cross-sectional area of the tube, inches^2. S is the elastic section modulus, inches^3, and r is the radius of gyration, inches. The External Collapse Index in the last column is a nondimensional function of the diameter to the wall thickness ratio and is for general guidance only. The higher the number, the greater is the resistance to collapse. Refer to ASTM A 252 for material specifications.

[1]References are listed in Appendix A.

Table B-1
Dimensions and Properties for Design of Pipe Piles

Designation and Outside Diameter	Wall Thickness	Area A	Weight per Foot	Section Properties			Area of Exterior Surface	Inside Cross-Sectional Area	Inside Volume	External Collapse Index
				I	S	r				
in.	in.	$in.^2$	lb	$in.^4$	$in.^3$	in.	ft^2/ft	$in.^2$	yd^3/ft	!
PP10	.109	3.39	11.51	41.4	8.28	3.50	2.62	75.2	.0193	62
	.120	3.72	12.66	45.5	9.09	3.49	2.62	74.8	.0192	83
	.134	4.15	14.12	50.5	10.1	3.49	2.62	74.4	.0191	116
	.141	4.37	14.85	53.1	10.6	3.49	2.62	74.2	.0191	135
	.150	4.64	15.78	56.3	11.3	3.48	2.62	73.9	.0190	163
	.164	5.07	17.23	61.3	12.3	3.48	2.62	73.5	.0189	214
	.172	5.31	18.05	64.1	12.8	3.48	2.62	73.2	.0188	247
	.179	5.52	18.78	66.6	13.3	3.47	2.62	73.0	.0188	279
	.188	5.80	19.70	69.8	14.0	3.47	2.62	72.7	.0187	324
	.203	6.25	21.24	75.0	15.0	3.46	2.62	72.3	.0186	409
	.219	6.73	22.88	80.5	16.1	3.46	2.62	71.8	.0185	515
	.230	7.06	24.00	84.3	16.9	3.46	2.62	71.5	.0184	588
	.250	7.66	26.03	91.1	18.2	3.45	2.62	70.9	.0182	719
PP10-3/4	.109	3.64	12.39	51.6	9.60	3.76	2.81	87.1	.0224	50
	.120	4.01	13.62	56.6	10.5	3.76	2.81	86.8	.0223	67
	.125	4.17	14.18	58.9	11.0	3.76	2.81	86.6	.0223	76
	.141	4.70	15.98	66.1	12.3	3.75	2.81	86.1	.0221	109
	.150	5.00	16.98	70.2	13.1	3.75	2.81	85.8	.0221	131
	.156	5.19	17.65	72.9	13.6	3.75	2.81	85.6	.0220	148
	.164	5.45	18.54	76.4	14.2	3.74	2.81	85.3	.0219	172
	.172	5.72	19.43	80.0	14.9	3.74	2.81	85.0	.0219	199
	.179	5.94	20.21	83.1	15.5	3.74	2.81	84.8	.0218	224
	.188	6.24	21.21	87.0	16.2	3.73	2.81	84.5	.0217	260
	.219	7.25	24.63	100	18.7	3.72	2.81	83.5	.0215	414
	.230	7.60	25.84	105	19.6	3.72	2.81	83.2	.0214	480
	.250	8.25	28.04	114	21.2	3.71	2.81	82.5	.0212	605
	.279	9.18	31.20	126	23.4	3.70	2.81	81.6	.0210	781
	.307	10.1	34.24	137	25.6	3.69	2.81	80.7	.0208	951
	.344	11.2	38.23	152	28.4	3.68	2.81	79.5	.0205	1,180
	.365	11.9	40.48	161	29.9	3.67	2.81	78.9	.0203	1,320
	.438	14.2	48.24	189	35.2	3.65	2.81	76.6	.0197	1,890
	.500	16.1	54.74	212	39.4	3.63	2.81	74.7	.0192	2,380

Note: Metric properties of pipe piles are available from the American Institute of Steel Construction, 1 E. Wacker Drive, Chicago, IL 60601.

Table B-1 (Continued)

Designation and Outside Diameter	Wall Thickness	Area A	Weight per Foot	Section Properties			Area of Exterior Surface	Inside Cross-Sectional Area	Inside Volume	External Collapse Index
				I	S	r				
in.	in.	$in.^2$	lb	$in.^4$	$in.^3$	in.	ft^2/ft	$in.^2$	yd^3/ft	!
PP12	.134	5.00	16.98	87.9	14.7	4.20	3.14	108	.0278	67
	.141	5.25	17.86	92.4	15.4	4.19	3.14	108	.0277	78
	.150	5.58	18.98	98.0	16.3	4.19	3.14	108	.0277	94
	.172	6.39	21.73	112	18.6	4.18	3.14	107	.0274	142
	.179	6.65	22.60	116	19.4	4.18	3.14	106	.0274	161
	.188	6.98	23.72	122	20.3	4.18	3.14	106	.0273	186
	.203	7.52	25.58	131	21.8	4.17	3.14	106	.0272	235
	.219	8.11	27.55	141	23.4	4.17	3.14	105	.0270	296
	.230	8.50	28.91	147	24.6	4.16	3.14	105	.0269	344
	.250	9.23	31.37	159	26.6	4.16	3.14	104	.0267	443
	.281	10.3	35.17	178	29.6	4.14	3.14	103	.0264	616
	.312	11.5	38.95	196	32.6	4.13	3.14	102	.0261	784
PP12-3/4	.109	4.33	14.72	86.5	13.6	4.47	3.34	123	.0317	30
	.125	4.96	16.85	98.8	15.5	4.46	3.34	123	.0316	45
	.134	5.31	18.06	106	16.6	4.46	3.34	122	.0315	56
	.150	5.94	20.19	118	18.5	4.46	3.34	122	.0313	78
	.156	6.17	20.98	122	19.2	4.45	3.34	122	.0313	88
	.164	6.48	22.04	128	20.1	4.45	3.34	121	.0312	103
	.172	6.80	23.11	134	21.1	4.45	3.34	121	.0311	118
	.179	7.07	24.03	140	21.9	4.45	3.34	121	.0310	134
	.188	7.42	25.22	146	23.0	4.44	3.34	120	.0309	155
	.203	8.00	27.20	158	24.7	4.44	3.34	120	.0308	196
	.230	9.05	30.75	177	27.8	4.43	3.34	119	.0305	286
	.250	9.82	33.38	192	30.1	4.42	3.34	118	.0303	368
	.281	11.0	37.42	214	33.6	4.41	3.34	117	.0300	526
	.312	12.2	41.45	236	37.0	4.40	3.34	115	.0297	684
	.330	12.9	43.77	248	39.0	4.39	3.34	115	.0295	776
	.344	13.4	45.58	258	40.5	4.39	3.34	114	.0294	848
	.375	14.6	49.56	279	43.8	4.38	3.34	113	.0291	1,010
	.406	15.7	53.52	300	47.1	4.37	3.34	112	.0288	1,170
	.438	16.9	57.59	321	50.4	4.36	3.34	111	.0285	1,350
	.500	19.2	65.42	362	56.7	4.33	3.34	108	.0279	1,760

Table B-1 (Continued)

Designation and Outside Diameter	Wall Thickness	Area A	Weight per Foot	Section Properties			Area of Exterior Surface	Inside Cross-Sectional Area	Inside Volume	External Collapse Index
				I	S	r				
in.	in.	$in.^2$	lb	$in.^4$	$in.^3$	in.	ft^2/ft	$in.^2$	yd^3/ft	!
PP14	.134	5.84	19.84	140	20.0	4.90	3.67	148	.0381	42
	.141	6.14	20.87	147	21.1	4.90	3.67	148	.0380	49
	.150	6.53	22.19	157	22.4	4.90	3.67	147	.0379	59
	.156	6.78	23.07	163	23.2	4.89	3.67	147	.0378	66
	.172	7.47	25.40	179	25.5	4.89	3.67	146	.0377	89
	.179	7.77	26.42	186	26.5	4.89	3.67	146	.0376	101
	.188	8.16	27.73	195	27.8	4.88	3.67	146	.0375	117
	.203	8.80	29.91	209	29.9	4.88	3.67	145	.0373	147
	.210	9.10	30.93	216	30.9	4.88	3.67	145	.0373	163
	.219	9.48	32.23	225	32.2	4.87	3.67	144	.0372	185
	.230	9.95	33.82	236	33.7	4.87	3.67	144	.0370	215
	.250	10.8	36.71	255	36.5	4.86	3.67	143	.0368	277
	.281	12.1	41.17	285	40.7	4.85	3.67	142	.0365	395
	.344	14.8	50.17	344	49.2	4.83	3.67	139	.0358	691
	.375	16.1	54.57	373	53.3	4.82	3.67	138	.0355	835
	.438	18.7	63.44	429	61.4	4.80	3.67	135	.0348	1,130
	.469	19.9	67.78	457	65.3	4.79	3.67	134	.0345	1,280
	.500	21.2	72.09	484	69.1	4.78	3.67	133	.0341	1,460
PP16	.134	6.68	22.71	210	26.3	5.61	4.19	194	.0500	28
	.141	7.02	23.88	221	27.6	5.61	4.19	194	.0499	33
	.150	7.47	25.39	235	29.3	5.60	4.19	194	.0498	39
	.164	8.16	27.74	256	32.0	5.60	4.19	193	.0496	52
	.172	8.55	29.08	268	33.5	5.60	4.19	193	.0495	60
	.179	8.90	30.25	278	34.8	5.59	4.19	192	.0494	67
	.188	9.34	31.75	292	36.5	5.59	4.19	192	.0493	78
	.203	10.1	34.25	314	39.3	5.59	4.19	191	.0491	98
	.219	10.9	36.91	338	42.3	5.58	4.19	190	.0489	124
	.230	11.4	38.74	354	44.3	5.58	4.19	190	.0488	144
	.250	12.4	42.05	384	48.0	5.57	4.19	189	.0485	185
	.281	13.9	47.17	429	53.6	5.56	4.19	187	.0481	264
	.312	15.4	52.27	473	59.2	5.55	4.19	186	.0478	362

Table B-1 (Concluded)

Designation and Outside Diameter	Wall Thickness	Area A	Weight per Foot	Section Properties			Area of Exterior Surface	Inside Cross-Sectional Area	Inside Volume	External Collapse Index
				I	S	r				
in.	in.	$in.^2$	lb	$in.^4$	$in.^3$	in.	ft^2/ft	$in.^2$	yd^3/ft	!
PP16	.344	16.9	57.52	519	64.8	5.54	4.19	184	.0474	487
(cont'd)	.375	18.4	62.58	562	70.3	5.53	4.19	183	.0470	617
	.438	21.4	72.80	649	81.1	5.50	4.19	180	.0462	874
	.469	22.9	77.79	691	86.3	5.49	4.19	178	.0458	1,000
	.500	24.3	82.77	732	91.5	5.48	4.19	177	.0455.	1,130

(Sheet 4 of 4)

Appendix C
Computer Program Axiltr

C-1. Organization

Program AXILTR, AXIal Load-Transfer, consists of a main routine and two subroutines. The main routine feeds in the input data, calculates the effective overburden stress, and determines whether the load is axial down-directed, pullout, or if uplift/downdrag forces develop from selling or consolidating soil. The main routine also prints out the computations. Subroutine BASEL calculates the displacement at the base for given applied down-directed loads at the base. Subroutine SHAFL evaluates the load transferred to and from the shaft for relative displacements between the shaft and soil. An iteration scheme is used to cause the calculated applied loads at the top (butt) to converge within 10 percent of the input load applied at the top of the shaft.

a. Input data. Input data are illustrated in Table C-1 with descriptions given in Table C-2.

Table C-1
Input Data

Line	Input Parameters	Format Statement
1	TITLE	20A4
2	NMAT NEL DX GWL LO IQ IJ	2I5,2F6.2,3I5
3	I J K SOILP DS DB	3I5,3F10.3
4	E50 (Omitted unless K = 2, 5, 9)	E13.3
5	LLL	I5
6	MAT GS EO WO PS CS CC C PHI AK PM (Lines 5 repeated for each material M = 1,NMAT)	I3,3F6.2,F7.0,2F7.2,
7	ALPHA (Omitted unless I = 6) (α input for each material MAT = 1,NMAT)	7F10.5
8	M IE(M) (Line 8 repeated for each element M and number of soil IE(M). Start with 1. The last line is NEL NMAT)	2I5
9	RFF GG (Omitted unless K = 7, 8, 9)	F6.3,E13.3
10	(Omitted unless K = 3, 4, 5, 6)	
10a	NCA (<12)	I5
10b	T(M,1)... T(M,11) (Input for each curve M = 1,NCA	11F6.2
10c	S(M) (Input on new line for each M = 2,11; S(1) input in program as 0.00)	F6.3
11	(Omitted unless I = 5)	
11a	NCC (<12)	I5
11b	FS(N) ZEPP(N) NCUR (Input on new line for each N = 1,NCC)	2F10.3,I5
12	(Omitted unless J = 0)	
12a	NC (>1)	I5
12b	EP(M) ZEP(M) (Input on new line for each M = 1,NC; at least a top and bottom term required)	E13.3,F6.2

Table C-1 (Concluded)

Line	Input Parameters	Format Statement
13	R(M) S(M) (Omitted unless K = 6; repeat on new line for each M = 1,IJ)	F10.5,F15.3
14	STRUL SOILP XA	3F15.2
15	NON (Omitted unless XA < 0.0)	I5

Table C-2
Description of Input Parameters (Continued)

Line	Parameter	Description
1	TITLE	Name of problem
2	NMAT	Total number of materials
	NEL	Total number of elements
	DX	Thickness of each element, ft (usually 0.5 or 1.0 ft)
	GWL	Depth to groundwater level, ft
	LO	Amount of output data = 0 Extensive data output used to check the program = 1 Shaft load-displacement behavior and detailed load distribution-displacement response along shaft length for input top load prior to and following soil distribution-displacement response along shaft length for input top load prior to and following soil movement (load transfer, load, shaft compression increment, and shaft movement at given depth = 2 Shaft load-displacement behavior and load distribution-displacement response along shaft length for input top load prior to and following soil movement = 3 Shaft load-displacement behavior and load distribution-displacement response along shaft length for input top load on shaft following soil movement
	IQ	Total number of shaft increments (shaft length/element thickness); top of shaft at ground surface
	IJ	Number of points for shaft load-displacement behavior (usually 12, but maximum 19 for PARAMETER statement = 40
3	I	Magnitude of reduction factor α applied to total (undrained) or effective (drained) shear strength for skin friction resistance = 0 α = 1 (usually used for drained strength) = 1 α = sin ($\pi x/L$), x = depth, ft; L = shaft length, ft = 2 α = 0.6 = 3 α = 0.45 = 4 α = 0.3 = 5 α = Permits maximum skin friction input as a function of depth, psf (see line 11) = 6 α = is input for each material (see line 7)
	J	Option for elastic shaft modulus = 0 shaft modulus input = 1 shaft modulus set to near infinity

(Sheet 1 of 3)

Table C-2 (Continued)

Line	Parameter	Description
	K	Option for load-transfer functions (see Figure 3-22)

Base	Shaft
= 0 Consolidation	Seed and Reese
= 1 Vijayvergiya	Seed and Reese
= 2 Reese and Wright	Seed and Reese
= 3 Consolidation	Input (see line 10)
= 4 Vijayvergiya	Input (see line 10)
= 5 Reese and Wright	Input (see line 10)
= 6 Input (see line 13)	Input (see line 10)
= 7 Consolidation	Kraft, Ray, and Kagawa
= 8 Vijayvergiya	Kraft, Ray, and Kagawa
= 9 Reese and Wright	Kraft, Ray, and Kagawa

	SOILP	Pressure on top layer of soil exerted by surrounding structure, fill, etc., psf
	DS	Diameter shaft, ft
	DB	Diameter base, ft
4	E50	Strain at 1/2 maximum deviator stress, Equation 3-34
5	LLL	Option for type of shear failure at base = 0 Local shear failure, Equation 3-24 or $N_c = 7$ = 1 General shear failure, Equation 3-10 or $N_c = 9$
6	MAT	Number of material
	GS	Specific gravity
	EO	Initial void ratio
	WO	Initial water content, percent
	PS	Swell pressure, psf
	CS	Swell index
	CC	Compression index
	C	Cohesion, psf; = undrained strength for total stress analysis; effective cohesion c' or zero for effective stress analysis
	PHI	Angle of shearing resistance ϕ; = 0 for total stress analysis
	AK	Coefficient of lateral earth pressure
	PM	Maximum past pressure, psf (program sets PM = PS if PM input < PS)
7	ALPHA	Reduction factor α_a for each material MAT, Equations 3-26, Table 3-5, Table 3-9,; used when option I = 6, Line 3
8	M	Number of element
	IE(M)	Material number of soil, MAT
9	RFF	Hyperbolic reduction factor R for Kraft, Ray, and Kagawa model, Equation 3-35; use 1.0 if not known
	GG	Shear modulus G, psf, Equation 3-35
10		Input data for shaft load-transfer curves (k = 3, 4, 5, 6)
10a	NCA	Total number of shaft load-transfer curves to input, < 12
10b	T(M,1)... ..T(M,11)	Skin friction ratio of developed shear strength/maximum mobilized shear strength of each shaft load-transfer curve; 11 values required for each load-transfer curve, the first value T(1,1) = 0.0
10c	S(M)	Movement in inches for all of the T(M,1)...T(M,11) curves; only 10 values required from S(2)...S(11); S(1) = 0.0 in code; if S(M) in the code is okay (0.0, 0.05, 0.1, 0.15, 0.2, 0.23, 0.3, 0.45, 0.75, 1.05, 1.5 inches)

Table C-2 (Concluded)

Line	Parameter	Description
11		Input data for maximum skin friction as a function of depth
	NCC	Total number of maximum skin friction terms to input, <12; program interpolates maximum skin friction between depths
11a	FS(N)	Maximum skin friction f-, for point N, psf
11b	ZEPP(N)	Depth for the maximum skin friction for point N, ft
11c	NCUR	Number of the shaft load-transfer curve input M in line 10; applicable to the maximum skin friction for point N (Repeat 11a, 11b, 11c for each N = 1,NCC)
12		Input data for shaft elastic modulus as function of depth; program interpolates the elastic modulus between depths
	NC	Total number of terms of elastic modulus and depth, > 1
12a	EP(M)	Elastic modulus of shaft at point M, psf
12b	ZEP(M)	Depth for the elastic modulus of shaft at point M, ft (An elastic modulus and depth term are required at least at the top and bottom of the shaft)
13		Input data for base displacements if K = 6 (The number of input terms or R(M) and S(M) equals IJ -1, line 2
13a	R(M)	Base displacement, in. (The first displacement is 0.0 inches and already input in the program)
13b	S(M)	Base load for displacement R(M), pounds; the base load for 0.0 displacement is approximated as the overlying soil weight and already input in the program
14		Structural load, pressure on adjacent soil at the ground surface, and depth of the active zone for heave input for each problem for evaluation of specific load distribution-placement computations
14a	STRUC	Structural vertical load on top of shaft, pounds
14b	SOILP	Pressure on top layer on soil exerted by surrounding structure, fill, etc., psf
14c	XA	Depth of the active zone for heave, ft; = 0.01 yields load-displacement behavior for zero soil movement; a saturated soil profile is assumed when comp uting soils movement; < 0.0 program goes to line 15 below
15	NON	Execution stops if 0; program goes to line 1 if > 0

(Sheet 3 of 3)

(1) The program is set to consider up to a total of 40 soil types and 100 soil elements. Figure C-1 provides and example layout of soil types and elements used in AXILTR.

(2) The program can accommodate up to 18 points of the load-displacement curve. This capacity may be altered by adjusting the PARAMETER statement in the program.

(3) The input data are placed in a file, "DALTR.TXT." These data are printed in output file, "LTROUT.TXT," illustrated in Table C-3a.

b. Output data. Results of the computations by AXILTR are printed in LTROUT.TXT illustrated in Table C-3b. Table C-3c provides a description of calculations illustrated in Table C-3b.

(1) Load-displacement data are placed in file LDCOM.DAT for plotting by graphic software.

(2) Load-depth data for a given applied load on the pile top are placed in file LDSP.DAT for plotting by graphic software.

(3) Displacement-depth data for a given applied load on the pile top are placed in file MDEP.DAT for plotting by graphic software.

C-2. Application

The pullout, uplift, and downdrag capabilities of AXILTR are illustrated by two example problems. The accuracy of these solutions can be increased by using more soil layers, which increases control over soil input parameters such as swell pressure, maximum past pressure, and shear strength.

a. Pullout and uplift. Table C-4 illustrated input data required to determine performance of a 2-feet-diameter drilled shaft 50 feet long constructed in an expansive clay soil of two layers, NMAT = 2. The shaft is underdreamed of two layers, NMAT = 2. The shaft is underdreamed

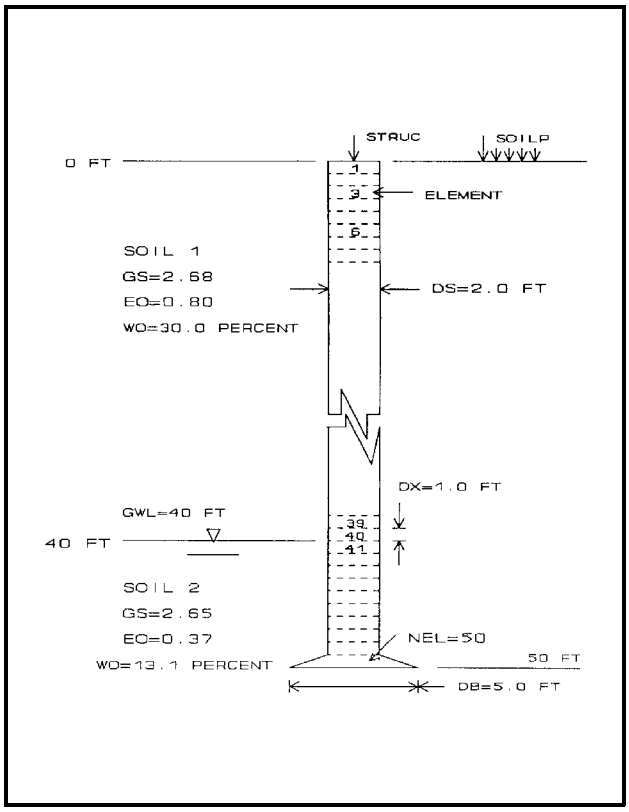

Figure C-1. Schematic diagram of soil and pile elements

with a 5-foot-diameter bell. Soil beneath the shaft is nonexpansive. The shaft is subject to a pullout force of 300 kips. Refer to Figure C-1 for a schematic representation of this problem.

(1) Bearing capacity. The alpha skin friction and local shear base capacity models are selected. Option to input the reduction factor " (I = 6) was used. The selected "'s for the two soils is 0.9. A high " was selected because expansive soil increases pressure against the shaft, which may raise the skin friction.

(2) Load-transfer models. The Kraft, Ray, and Kagawa skin friction and the Vijayvergiya base load-transfer models (K = 8) were selected. Two points for the elastic modulus of the shaft concrete were input into the program.

(3) Results. The results are plotted in Figure C-2 for a pullout force of 300,000 pounds. Results of the computation placed in files “LTROUT.TXT” are shown in Table C-5.

(a) Total and base ultimate bearing capacity is about 1,200 and 550 kips, respectively (Figure C-2a). Base and total capacity is 250 and 600 kips, respectively, if settlement is limited to 0.5 inch, which is representative of an *FS* of approximately 2.

(b) The distribution of load with depth, Figure C-2b, is a combination of the shapes indicated in Figures 3-15 and 3-16, because both pullout and uplift forces must be resisted.

(c) The shaft will heave approximately 0.7 inch, while the soil heaves more than 11 inches at the ground surface (Figure C-2c).

b. Downdrag. Table C-6 illustrates input data required to solve for the performance of the same drilled shaft and soil described in the previous example problem, but the soil is wetter with a much lower swell pressure. Soil shear strength is assumed not to change significantly from the previous example. This shoft is subject to a 150-kip load in addition to the downdrag forces from the settling soil.

(1) Bearing capacity. The alpha skin friction and local shear bearing-capacity models are selected similar to the previous example. Option to input the reduction factor α’s are 0.55 and 0.3 for the surface and deeper soils, respectively.

Table C-3. Output Data

a. Repeat of Input Data (See Table C-1)

Line	Input Parameters	Format Statement
1	TITLE	20A4
2	NMAT= NEL= DX= FT GWL= FT LO= IQ (SHAFT INC)= IJ (NO.LOADS=	I5,I5,F6.2,F6.2 I5,I5,I5
3	I= J= K= SOILP= PSF DS= FT DB= FT	I5,I5,I5,F10.2 F10.2 F10.2
4	(If K = 2, 5, 9) E50	 E13.3
5	LOCAL SHEAR FAILURE AT BASE - LLL = 0 Or GENERAL SHEAR FAILURE AT BASE - LLL = 1	I5 I5
6	MAT GS EO WO (%) PS(PSF) CS CC CO(PSF) PHI K PM(PSF)	I3,3F6.2,F7.0,27.2, F7.0,2F6.2,F7.0
7	(If I = 6) ALPHA =	2(7F10.5)
8	ELEMENT NO OF SOIL	I5,10X,I5
9	(If K = 7, 8, 9) REDUCTION FACTOR= SHEAR MODULUS=	 F6.3,3X,E13.3
10	(If K = 3, 4, 5, 6) NO. OF LOAD-TRANSFER CURVES(<12)?=	 I5
	For each curve 1 to NCA: CURVE	 I5
	RATIO SHR DEV, M=1, 11 ARE MOVEMENT (IN.) FOR LOAD TRANSFER M= IS INCHES	11F6.3 I5,F6.3
11	(If I = 5 NO OF SKIN FRICTION-DEPTH TERMS (<12)? ARE SKIN FRICTION (PSF) DEPTH(FT) CURVE NO	 I5 F10.3,F10.3,I5
12	If J = 0) E SHAFT (PSF) AND DEPTH(FT):	 4(E13.3,2X,F6.2)
13	(If K = 6) BASE DISPLACEMENT(IN.), BASE LOAD(LB) > FOR POINTS	 F10.2,I5

b. Output Calculations

Line	Input Parameters	Format Statement
1	BEARING CAPACITY= POUNDS	F13.2
2	DOWNWARD DISPLACEMENT	
3	(Omitted unless LO = 0,1) POINT BEARING(LB)=	 F13.2

(Sheet 1 of 3)

Table C-3 (Continued)

Line	Input Parameters	Format Statement
4	(Omitted unless LO = 0,1) DEPTH LOAD TRANS TOTAL LOAD COM OF INCR TOTAL MOVMT FT LB LB INCHES INCHE S 5E13.5,I5	
5	TOP LOAD TOP MOVEMENT BASE LOAD BASE MOVEMENT LB INCHES LB INCHES	4E13.5
6	NEGATIVE UPWARD DISPLACEMENT	
7	TOP LOAD TOP MOVEMENT BASE LOAD BASE MOVEMENT LB INCHES LB INCHES	E13.5
8	STRUC LOAD (LB) SOILP (PSF) ACTIVE DEPTH (FT) (Line 14 of Table C-2)	F10.0,2F10.2
9	BELL RESTRAINT(LB)=	F13.2
10	(If STRUL < 0.0 See Line 14, Table C-2) FIRST ESTIMATE OF PULLOUT RESTRAINT(LB)=	F13.2
11	LOAD-DISPLACEMENT BEHAVIOR	
12	(If LO <2) EFFECTS OF ADJACENT SOIL	
13	INITIAL BASE FORCE(LB)= (If LO = 0) BASE FORCE(LB)=	F13.2
14	DISPLACEMENT (INCHES)= FORCE= POUNDS	F8.4,F12.2
15	ITERATIONS=	I5
16	DEPTH(FT) LOAD(LB) SHAFT MVMT(IN) SOIL MVMT(IN)	F7.2,2X,E13.5, 2F15.5

c. Description of Calculations

Line	Program Prints	Description
1	BEARING CAP...	End-bearing capacity, pounds
2	DOWNWARD DISPL	Load-displacement behavior for zero soil movement in downward direction for IJ points
3	POINT BEARING	Load at bottom of shaft prior to shaft load-transfer calculation, pounds
4	DEPTH	Depth, ft
	LOAD TRANS	Load transferred at given depth along shaft, pounds
	TOTAL LOAD	Total load on shaft at given depth, pounds
	COM OF INCR	Incremental shaft compression at given depth, inches
	TOTAL MOVMT	Shaft-soil relative movement at given depth, inches
	INTER	Number of iterations to complete calculations
5	TOP LOAD	Load at top of shaft, pounds
	TOP MOVEMENT	Displacement at top of shaft, inches
	BASE LOAD	Load at bottom of shaft, pounds
	BASE MOVEMENT	Displacement at bottom of shaft, inches

Table C-3 (Concluded)

Line	Input Parameters	Format Statement
6	NEGATIVE UPWARD	Load-displacement behavior for zero soil movement in upward direction for IJ points
7	Same as item 5	
8	STRUC LOAD(LB)	Load applied on top of shaft, pounds
	SOILP(PSF)	Pressure applied on top of adjacent soil, psf
	ACTIVE DEPTH	Depth of soil beneath ground surface subject to soil heave, ft
9	BELL RESTRAINT	Restraining resistance of bell, pounds
10	FIRST ESTIMATE	Initial calculations of pullout resistance prior to iterations for structural loads less than zero, pounds
11	LOAD-DISPLACE	Load-shaft movement distribution for given structural load
12	EFFECTS OF ADJ	Effects of soil movement considered in load-displacement behavior
13	INITIAL BASE	Initial calculation of force at bottom of shaft prior to iterations
14	DISPLACEMENT	Displacement at bottom of shaft after 100 iterations, inches
	FORCE=	Force at bottom of shaft, pounds after 100 iterations, pounds
15	ITERATIONS	Total number of iterations to converge to solution
16	DEPTH(FT)	Depth, feet
	LOAD(LB)	Load at given depth, pounds
	SHAFT MVMT(IN.)	Shaft displacement, inches
	SOIL MVMT(IN.)	Soil movement, inches

(Sheet 3 of 3)

(2) Load-transfer models. The Seed and Reese skin friction and Reese and Wright base load-transfer models were selected (K = 2). Two points for the elastic modulus of the shaft concrete were input into the program.

(3) Results. The results are plotted in Figure C-3 for a downward applied load of 150 kips. Results of the computation placed in file LTROUT.TXT are illustrated in Table C-7.

(a) Total and base ultimate bearing capacity (Figure C-3a) is about 550 and 880 kips, respectively. Base and total capacity is about 200 and 500 kips, respectively, if settlement is limited to 0.5 inch. The *FS* is approximately 1.8 relative to total pile capacity. The program does not add the vertical plunging failure liens to the curves in Figure C-3a, which leaves the calculated displacement load relationships nearly linear.

(b) The distribution of load with depth (Figure C-3b) is representative of downdrag indicated in Figure 3-21. The load on the shaft base is nearly 300 kips or double the applied load at the ground surface.

(c) The shaft will settle approximately 1 inch, while the soil settles about 2 inches at the ground surface (Figure C-3c). The soil is heaving near the ground surface, which counters the settlement from downdrag. Maximum settlement is about 3.5 inches at 10 feet of depth.

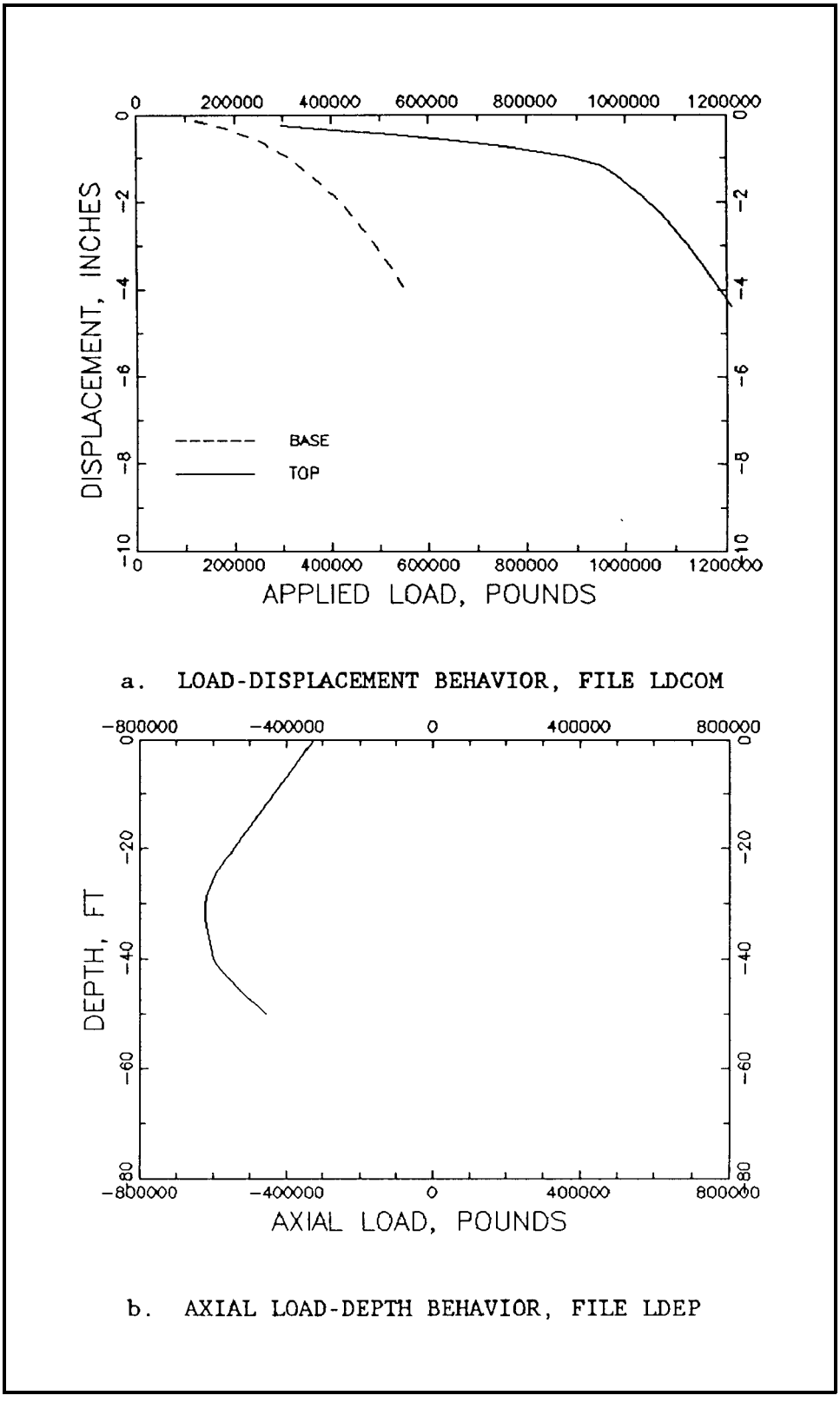

a. LOAD-DISPLACEMENT BEHAVIOR, FILE LDCOM

b. AXIAL LOAD-DEPTH BEHAVIOR, FILE LDEP

Figure C-2. Plotted output for pullout and uplift problems (Continued)

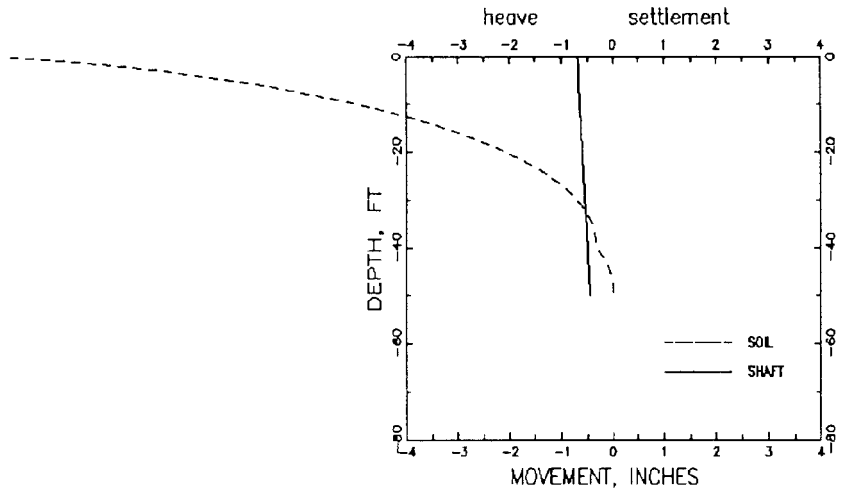

c. DISPLACEMENT-DEPTH BEHAVIOR, FILE MDEP

Figure C-2. (Concluded)

Table C-4
Listing of Data Input for Expansive Soil, File DATLR.TXT

```
          EXPANSIVE SOIL
      2  50       1.0     40.          2     50      16
      6   0         8          0.0          2.0              5.00
      0
1     2.68        .8          30.         4800.       .1        .2        2000.      .0         .7          7000.
2     2.65        .37         13.1        6000.       .1        .2        4000.      .0         2.          10000.
   0.9                        0.9
    1     1
   41     2
   50     2
  .900        1.600E+05
    2
    4.333E 08       .0
    4.333E 08   50.0
-300000.                      .0                      50.
      0.                      .0                      -1.0
    0
```

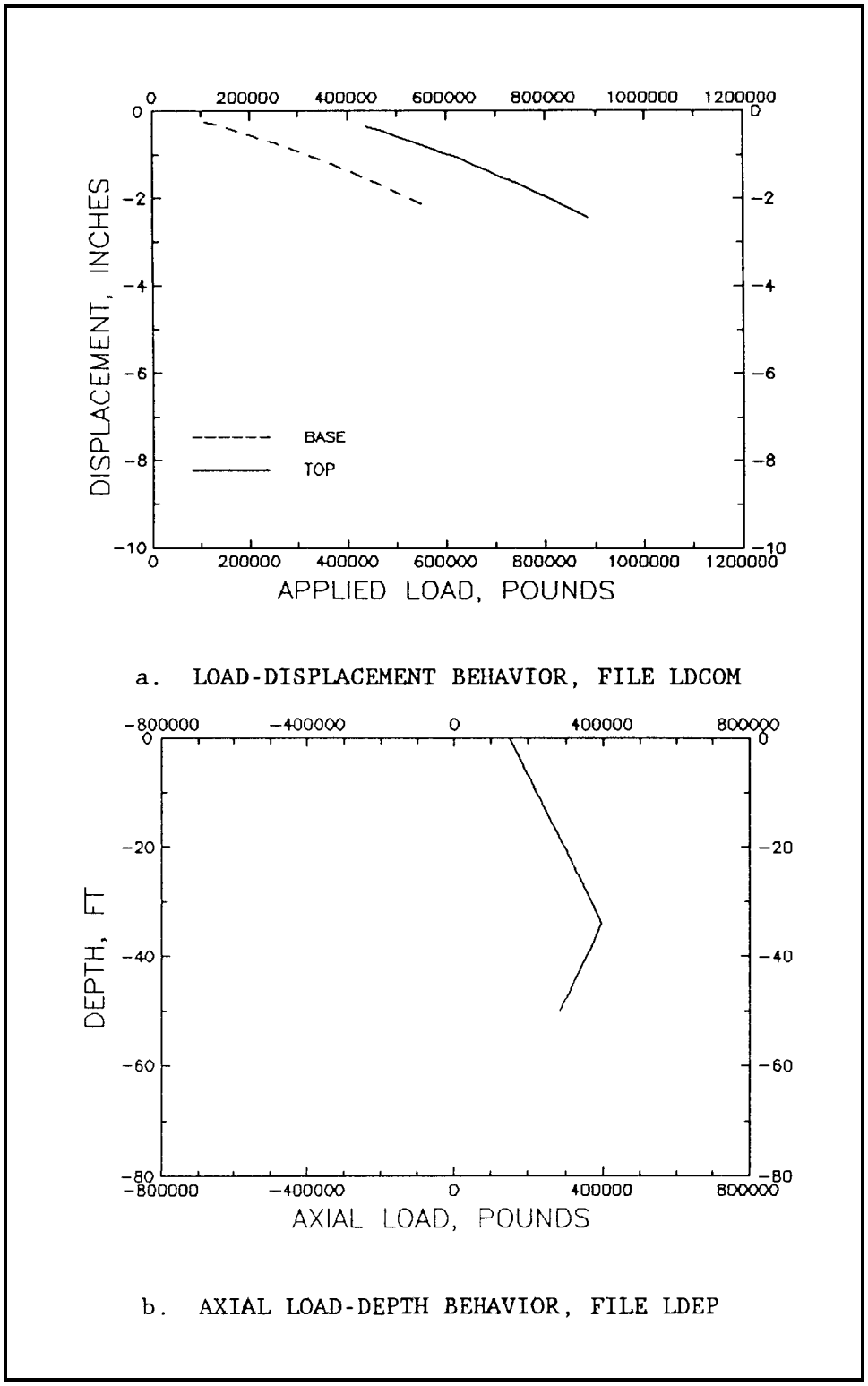

Figure C-3. Plotted output for drowndrag problem

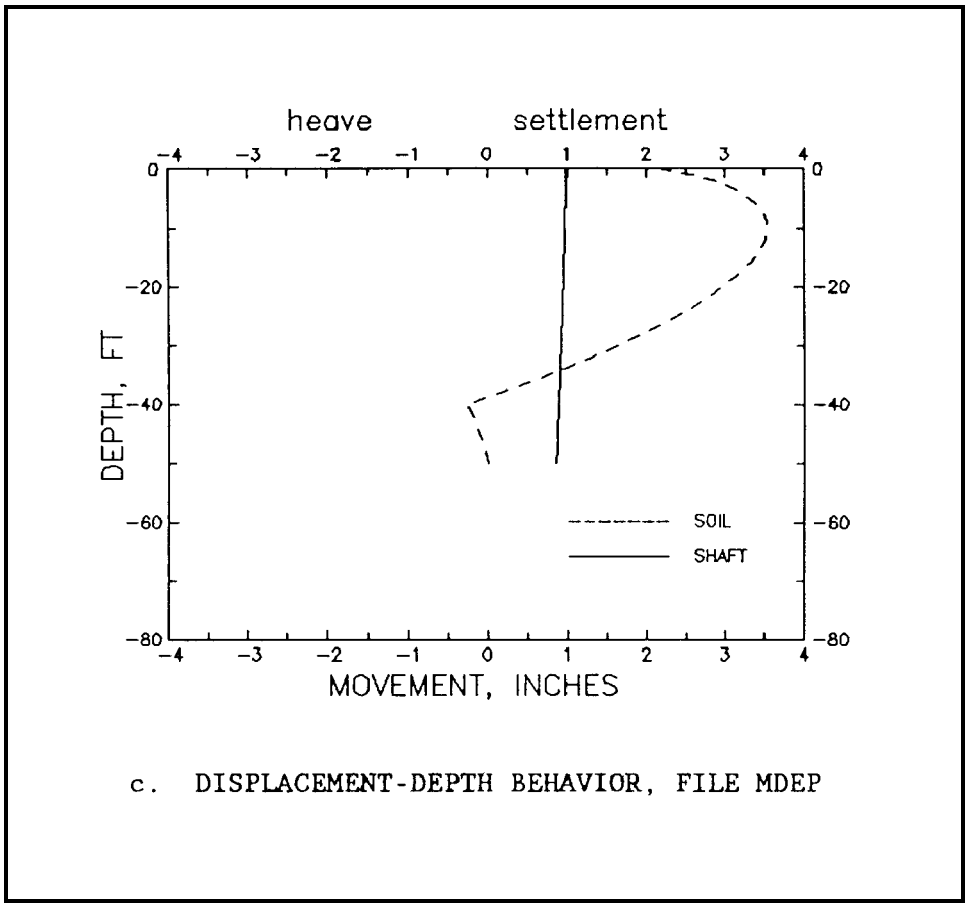

Figure C-3. (Concluded)

Table C-5
Listing of Output for Pullent and Uplift Problem

EXPANSIVE SOILS

NMAT= 2 NEL= 50 DX= 1.00 FT GWL= 40.00 FT
LO= 2 IQ (SHAFT INC)= 50 IJ (NO. LOADS)= 16

I= 6 J= 0 K= 8 SOILP= 0.00 PSF
DS= 2.00 FT
DB= 5.00 FT

LOCAL SHEAR FAILURE AT BASE - LLL= 0

MAT	GS	EO	WO(%)	PS(PSF)	CS	CC	CO(PSF)	PHI	K	PM(PSF)
1	2.68	0.80	30.00	4800.	0.10	0.20	2000.	0.00	0.70	7000.
2	2.65	0.37	13.10	6000.	0.10	0.20	4000.	0.00	2.00	100000.

ALPHA= 0.90000 0.9000

ELEMENT	NO OF SOIL
1	1
2	1
.	1
.	1
40	1
41	2
42	2
.	2
.	2
50	2

REDUCTION FACTOR = 0.900 SHEAR MODULUS= 0.160E+06

E SHAFT(PSF) AND DEPTH(FT):
0.433E+09 0.00 0.433E+09 50.00

BEARING CAPACITY= 549778.69 POUNDS

DOWNWARD DISPLACEMENT

TOP LOAD POUNDS	TOP MOVEMENT INCHES	BASE LOAD POUNDS	BASE MOVEMENT INCHES
0.24017E+06	0.17714E+00	0.10946E+06	0.99065E-01
0.34507E+06	0.26781E+00	0.13882E+06	0.15855E+00
0.45773E+06	0.37719E+00	0.16817E+06	0.23526E+00
0.58421E+06	0.50996E+00	0.19753E+06	0.33139E+00
0.71040E+06	0.66509E+00	0.22688E+06	0.44915E+00
0.82982E+06	0.84256E+00	0.25624E+06	0.59070E+00
0.92817E+06	0.10432E+01	0.28559E+06	0.75826E+00
0.97601E+06	0.12587E+01	0.31494E+06	0.95401E+00
0.10054E+07	0.14978E+01	0.34430E+06	0.11801E+01
0.10347E+07	0.17694E+01	0.37365E+06	0.14388E+01
0.10641E+07	0.20758E+01	0.40301E+06	0.17323E+01
0.10934E+07	0.24192E+01	0.43236E+06	0.20627E+01
0.11228E+07	0.28017E+01	0.46172E+06	0.24323E+01
0.11521E+07	0.32256E+01	0.49107E+06	0.28432E+01
0.11815E+07	0.36930E+01	0.52042E+06	0.32977E+01
0.12108E+07	0.42061E+01	0.54978E+06	0.37979E+01

(Sheet 1 of 3)

Table C-5 (Continued)

NEGATIVE UPWARD DISPLACEMENT

TOP LOAD POUNDS	TOP MOVEMENT INCHES	BASE LOAD POUNDS	BASE MOVEMENT INCHES
-0.18590E+05	-0.37138E-02	0.00000E+00	0.00000E+00
-0.31134E+05	-0.16708E-01	0.00000E+00	-0.10000E-01
-0.43689E+05	-0.29706E-01	0.00000E+00	-0.20000E-01
-0.68793E+05	-0.55704E-01	0.00000E+00	-0.40000E-01
-0.11899E+06	-0.10770E+00	0.00000E+00	-0.80000E-01
-0.21806E+06	-0.21160E+00	0.00000E+00	-0.16000E+00
-0.38024E+06	-0.41089E+00	0.00000E+00	-0.32000E+00
-0.61240E+06	-0.78911E+00	0.00000E+00	-0.64000E+00
-0.69610E+06	-0.14531E+01	0.00000E+00	-0.12800E+01
-0.69610E+06	-0.27331E+01	0.00000E+00	-0.25600E+01
-0.69610E+06	-0.52931E+01	0.00000E+00	-0.51200E+01
-0.69610E+06	-0.10413E+02	0.00000E+00	-0.10240E+02
-0.69610E+06	-0.20653E+02	0.00000E+00	-0.20480E+02
-0.69610E+06	-0.41133E+02	0.00000E+00	-0.40960E+02
-0.69610E+06	-0.82093E+02	0.00000E+00	-0.81920E+02
-0.69610E+06	-0.16401E+03	0.00000E+00	-0.16384E+03

STRUC LOAD(LB)	SOILP(PSF)	ACTIVE DEPTH(FT)
-300000.	0.00	50.00

BELL RESTRAINT(LB)= 44915.44

FIRST ESTIMATE OF PULLOUT RESTRAINT(LB)= 541894.31

LOAD-DISPLACEMENT BEHAVIOR

INITIAL BASE FORCE(LBS)= -788275.25

DISPLACEMENT(INCHES)= -0.2475 FORCE= -66776819 POUNDS

DISPLACEMENT(INCHES)= -0.4975 FORCE= -532357.44 POUNDS

DISPLACEMENT(INCHES)= -0.6525 FORCE= -449443.94 POUNDS

INTERATIONS= 262

DEPTH(FT)	LOADS(LB)	SHAFT MVMT(IN.)	SOIL MVMT(IN.)
0.00	-0.32427E+06	-0.88276	-11.94514
1.00	-0.33520E+06	-0.87985	-10.67843
2.00	-0.34613E+06	-0.87685	-9.72980
3.00	-0.35706E+06	-0.87385	-8.92906
4.00	-0.36799E+06	-0.87055	-8.22575
5.00	-0.37892E+06	-0.86726	-7.59519
6.00	-0.38985E+06	-0.86387	-7.02274
7.00	-0.40078E+06	-0.86039	-6.49865
8.00	-0.41171E+06	-0.85681	-6.01600
9.00	-0.42264E+06	-0.85313	-5.56958
10.00	-0.43357E+06	-0.84936	-5.15537
11.00	-0.44450E+06	-0.84549	-4.77014
12.00	-0.45543E+06	-0.84152	-4.41124
13.00	-0.46636E+06	-0.83746	-4.07648
14.00	-0.47729E+06	-0.83330	-3.76401
15.00	-0.48822E+06	-0.82904	-3.47223
16.00	-0.49915E+06	-0.82469	-3.19976

Table C-5 (Concluded)

DEPTH(FT)	LOADS(LB)	SHAFT MVMT(IN.)	SOIL MVMT(IN.)
17.00	-0.51008E+06	-0.82024	-2.94538
18.00	-0.52101E+06	-0.81570	-2.70805
19.00	-0.53194E+06	-0.81105	-2.48680
20.00	-0.54287E+06	-0.80632	-2.28080
21.00	-0.55380E+06	-0.80148	-2.08927
22.00	-0.56473E+06	-0.79655	-1.91153
23.00	-0.57566E+06	-0.79153	-1.74696
24.00	-0.58613E+06	-0.78641	-1.59498
25.00	-0.59556E+06	-0.78120	-1.45506
26.00	-0.60381E+06	-0.77591	-1.32673
27.00	-0.61073E+06	-0.77056	-1.20953
28.00	-0.61621E+06	-0.76515	-1.10306
29.00	-0.62027E+06	-0.75970	-1.00692
30.00	-0.62304E+06	-0.75422	-0.92078
31.00	-0.62444E+06	-0.74872	-0.84428
32.00	-0.62465E+06	-0.74321	-0.77713
33.00	-0.62386E+06	-0.73771	-0.71902
34.00	-0.62223E+06	-0.73222	-0.66969
35.00	-0.61992E+06	-0.72674	-0.62887
36.00	-0.61710E+06	-0.72129	-0.59633
37.00	-0.61390E+06	-0.71587	-0.57183
38.00	-0.61049E+06	-0.71047	-0.55516
39.00	-0.60701E+06	-0.70510	-0.54610
40.00	-0.60360E+06	-0.69977	-0.54447
41.00	-0.59487E+06	-0.69448	-0.46514
42.00	-0.58401E+06	-0.68929	-0.39155
43.00	-0.57119E+06	-0.68420	-0.32363
44.00	-0.55675E+06	-0.67922	-0.26128
45.00	-0.54103E+06	-0.67439	-0.20443
46.00	-0.52416E+06	-0.66969	-0.15300
47.00	-0.50642E+06	-0.66515	-0.10692
48.00	-0.48799E+06	-0.66077	-0.06611
49.00	-0.46897E+06	-0.65655	-0.03049
50.00	-0.44994E+06	-0.65250	0.00000

STRUC LOAD(LB)	SOILP(PSF)	ACTIVE DEPTH(FT)
0.	0.00	-1.00

Table C-6
Listing of Data Input for Settling Soil

```
          SETTLING SOIL
       2  50        1.0      40.          2      50      16
       6   0          2          0.0          2.0                5.00
           0.010
       0

1      2.68        .8          30.          1200.        .05       .1          2000.      .0          .7          4000.
2      2.65        .37         13.1         6000.        .05       .1          4000.      .0          2.          10000.
   0.55                        0.3
    1      1
   41      2
   50      2
    2
    4.333E 08      .0
    4.333E 08   50.0
150000.                        .0                       50.
   0.              .0                      -1.0
    0
```

Table C-7
Listing of Output for Downdrag Problem

SETTLING SOILS

NMAT= 2 NEL= 50 DX= 1.00 FT GWL= 40.00 FT
LO= 2 IQ (SHAFT INC)= 50 IJ (NO. LOADS)= 16

I= 6 J= 0 K= 8 SOILP= 0.00 PSF
DS= 2.00 FT
DB= 5.00 FT

E50= 0.100E-01

LOCAL SHEAR FAILURE AT BASE - LLL= 0

MAT	GS	EO	WO(%)	PS(PSF)	CS	CC	CO(PSF)	PHI	K	PM(PSF)
1	2.68	0.80	30.00	1200.	0.05	0.10	2000.	0.00	0.70	4000.
2	2.65	0.37	13.10	6000.	0.05	0.10	4000.	0.00	2.00	10000.

ALPHA= 0.55000 0.3000

Table C-7 (Continued)

ELEMENT	NO OF SOIL
1	1
2	1
.	1
.	1
40	1
41	2
42	2
.	2
.	2
50	2

E SHAFT(PSF) AND DEPTH(FT):
0.433E+09 0.00 0.433E+09 50.00
BEARING CAPACITY= 549778.69 POUNDS

DOWNWARD DISPLACEMENT

TOP LOAD POUNDS	TOP MOVEMENT INCHES	BASE LOAD POUNDS	BASE MOVEMENT INCHES
0.43825E+06	0.36209E+00	0.10946E+06	0.24071E+00
0.47316E+06	0.46787E+00	0.13882E+06	0.33163E+00
0.50252E+06	0.57771E+00	0.16817E+06	0.42854E+00
0.53187E+06	0.69319E+00	0.19753E+06	0.53108E+00
0.56122E+06	0.81401E+00	0.22688E+06	0.63896E+00
0.59058E+06	0.93992E+00	0.25624E+06	0.75193E+00
0.61993E+06	0.10707E+01	0.28559E+06	0.86977E+00
0.64929E+06	0.12061E+01	0.31494E+06	0.99228E+00
0.67864E+06	0.13461E+01	0.34430E+06	0.11193E+01
0.70800E+06	0.14904E+01	0.37365E+06	0.12507E+01
0.73735E+06	0.16389E+01	0.40301E+06	0.13862E+01
0.76671E+06	0.17945E+01	0.43236E+06	0.15259E+01
0.79606E+06	0.19481E+01	0.46172E+06	0.16695E+01
0.82541E+06	0.21085E+01	0.49107E+06	0.18170E+01
0.85477E+06	0.22727E+01	0.52042E+06	0.19682E+01
0.88412E+06	0.24405E+01	0.54978E+06	0.21231E+01

Table C-7 (Continued)

NEGATIVE UPWARD DISPLACEMENT

TOP LOAD POUNDS	TOP MOVEMENT INCHES	BASE LOAD POUNDS	BASE MOVEMENT INCHES
-0.19877E+05	-0.38437E-02	0.00000E+00	0.00000E+00
-0.44463E+05	-0.18937E-01	0.00000E+00	-0.10000E-01
-0.69052E+05	-0.34038E-01	0.00000E+00	-0.20000E-01
-0.11821E+06	-0.64239E-01	0.00000E+00	-0.40000E-01
-0.21272E+06	-0.12447E+00	0.00000E+00	-0.80000E-01
-0.31375E+06	-0.22746E+00	0.00000E+00	-0.16000E+00
-0.36937E+06	-0.40225E+00	0.00000E+00	-0.32000E+00
-0.36937E+06	-0.72225E+00	0.00000E+00	-0.64000E+00
-0.36937E+06	-0.13623E+01	0.00000E+00	-0.12800E+01
-0.36937E+06	-0.26423E+01	0.00000E+00	-0.25600E+01
-0.36937E+06	-0.52023E+01	0.00000E+00	-0.51200E+01
-0.36937E+06	-0.10322E+02	0.00000E+00	-0.10240E+02
-0.36937E+06	-0.20562E+02	0.00000E+00	-0.20480E+02
-0.36937E+06	-0.41042E+02	0.00000E+00	-0.40960E+02
-0.36937E+06	-0.82002E+02	0.00000E+00	-0.81920E+02
-0.36937E+06	-0.16392E+02	0.00000E+00	-0.16384E+03

STRUC LOAD(LB)	SOILP(PSF)	ACTIVE DEPTH(FT)
150000.	0.00	50.00

BELL RESTRAINT(LB)= 44915.44

LOAD-DISPLACEMENT BEHAVIOR

POINT BEARING(LB)= 37465.96

DEPTH FEET	LOAD TRANS POUNDS	TOTAL LOAD POUNDS	COM OF INCR INCHES	TOTAL MVMT INCHES	ITER
0.49500E+02	0.35018E+04	0.40968E+05	0.34571E-03	0.82732E-01	2
0.48500E+02	0.35181E+04	0.44486E+05	0.37665E-03	0.83108E-01	2
0.47500E+02	0.35358E+04	0.48022E+05	0.40775E-03	0.83516E-01	2
0.46500E+02	0.35550E+04	0.51577E+05	0.43900E-03	0.83955E-01	2
0.45500E+02	0.35756E+04	0.55152E+05	0.47043E-03	0.84425E-01	2
0.44500E+02	0.35976E+04	0.58750E+05	0.50205E-03	0.84928E-01	2
0.43500E+02	0.36210E+04	0.62371E+05	0.53386E-03	0.85461E-01	2
0.42500E+02	0.36459E+04	0.66017E+05	0.56589E-03	0.86027E-01	2
0.41500E+02	0.36722E+04	0.69689E+05	0.59815E-03	0.86625E-01	2
0.40500E+02	0.37000E+04	0.73389E+05	0.63064E-03	0.87256E-01	2
0.39500E+02	0.32524E+04	0.76641E+05	0.66129E-03	0.87917E-01	2
0.38500E+02	0.32804E+04	0.79921E+05	0.69008E-03	0.88607E-01	2
0.37500E+02	0.33096E+04	0.83231E+05	0.71913E-03	0.89327E-01	2
0.36500E+02	0.33400E+04	0.86571E+05	0.74844E-03	0.90075E-01	2
0.35500E+02	0.33717E+04	0.89943E+05	0.77802E-03	0.90853E-01	2
0.34500E+02	0.34046E+04	0.93347E+05	0.80789E-03	0.91661E-01	2
0.33500E+02	0.34378E+04	0.96786E+05	0.83805E-03	0.92499E-01	2
0.32500E+02	0.34741E+04	0.10026E+06	0.86852E-03	0.93368E-01	2
0.31500E+02	0.35107E+04	0.10377E+06	0.89931E-03	0.94267E-01	2

Table C-7 (Continued)

0.30500E+02	0.35487E+04	0.10732E+06	0.93042E-03	0.95197E-01	2
0.29500E+02	0.35879E+04	0.11091E+06	0.96188E-03	0.96159E-01	2
0.28500E+02	0.36284E+04	0.11454E+06	0.99369E-03	0.97153E-01	2
0.27500E+02	0.36703E+04	0.11821E+06	0.10259E-02	0.98179E-01	2
0.26500E+02	0.37135E+04	0.12192E+06	0.10584E-02	0.99237E-01	2
0.25500E+02	0.37581E+04	0.12568E+06	0.10913E-02	0.10033E+00	2
0.24500E+02	0.37857E+04	0.12946E+06	0.11246E-02	0.10145E+00	2
0.23500E+02	0.38093E+04	0.13327E+06	0.11581E-02	0.10261E+00	2
0.22500E+02	0.38337E+04	0.13711E+06	0.11918E-02	0.10380E+00	2
0.21500E+02	0.38588E+04	0.14097E+06	0.12257E-02	0.10503E+00	2
0.20500E+02	0.38845E+04	0.14485E+06	0.12598E-02	0.10629E+00	2
0.19500E+02	0.39110E+04	0.14876E+06	0.12941E-02	0.10758E+00	2
0.18500E+02	0.39382E+04	0.15270E+06	0.13287E-02	0.10891E+00	2
0.17500E+02	0.39661E+04	0.15667E+06	0.13636E-02	0.11027E+00	2
0.16500E+02	0.39947E+04	0.16066E+06	0.13987E-02	0.11167E+00	2
0.15500E+02	0.40241E+04	0.16468E+06	0.14340E-02	0.13111E+00	2
0.14500E+02	0.40542E+04	0.16874E+06	0.14696E-02	0.11458E+00	2
0.13500E+02	0.40850E+04	0.17282E+06	0.15055E-02	0.11608E+00	2
0.12500E+02	0.41166E+04	0.17694E+06	0.15417E-02	0.11762E+00	2
0.11500E+02	0.41490E+04	0.18109E+06	0.15781E-02	0.11920E+00	2
0.10500E+02	0.41821E+04	0.18527E+06	0.16148E-02	0.12082E+00	2
0.95000E+01	0.42159E+04	0.18949E+06	0.16518E-02	0.12247E+00	2
0.85000E+01	0.42506E+04	0.19374E+06	0.16891E-02	0.12416E+00	2
0.75000E+01	0.42860E+04	0.19802E+06	0.17268E-02	0.12588E+00	2
0.65000E+01	0.43222E+04	0.20235E+06	0.17647E-02	0.12765E+00	2
0.55000E+01	0.43592E+04	0.20670E+06	0.18030E-02	0.12945E+00	2
0.45000E+01	0.43970E+04	0.21110E+06	0.18416E-02	0.13129E+00	2
0.35000E+01	0.44355E+04	0.21554E+06	0.18805E-02	0.13317E+00	2
0.25000E+01	0.44749E+04	0.22001E+06	0.19198E-02	0.13509E+00	2
0.15000E+01	0.45152E+04	0.22453E+06	0.19594E-02	0.13705E+00	2
0.50000E+00	0.45562E+04	0.22908E+06	0.19994E-02	0.13905E+00	2

Table C-7 (Concluded)

INITIAL BASE FORCE(LB)= 355177.69
ITERATIONS= 81

DEPTH(FT)	LOADS(LB)	SHAFT MVMT(IN.)	SOIL MVMT(IN.)
0.00	0.14992E+06	0.98875	2.15238
1.00	0.15721E+06	0.98740	2.58505
2.00	0.16451E+06	0.98598	2.85868
3.00	0.17108E+06	0.98450	3.05836
4.00	0.17909E+06	0.98295	3.20933
5.00	0.18638E+06	0.98134	3.32392
6.00	0.19367E+06	0.97967	3.40946
7.00	0.20096E+06	0.97793	3.47082
8.00	0.20852E+06	0.97612	3.51146
9.00	0.21554E+06	0.97425	3.53398
10.00	0.22283E+06	0.97232	3.54040
11.00	0.23013E+06	0.97033	3.53233
12.00	0.23742E+06	0.96827	3.51109
13.00	0.24471E+06	0.96614	3.47778
14.00	0.25200E+06	0.96395	3.43333
15.00	0.25929E+06	0.96170	3.97853
16.00	0.26658E+06	0.95938	3.31409
17.00	0.27387E+06	0.95700	3.24058
18.00	0.28116E+06	0.95455	3.15857
19.00	0.28845E+06	0.95204	3.06850
20.00	0.29575E+06	0.94946	2.97082
21.00	0.30304E+06	0.94683	2.86589
22.00	0.31033E+06	0.94412	2.75408
23.00	0.31762E+06	0.94135	2.63568
24.00	0.32491E+06	0.93852	2.51098
25.00	0.33220E+06	0.93563	2.38025
26.00	0.33949E+06	0.93267	2.24373
27.00	0.34678E+06	0.92964	2.10165
28.00	0.35407E+06	0.92655	1.95420
29.00	0.36137E+06	0.92340	1.80157
30.00	0.36866E+06	0.92018	1.64396
31.00	0.37595E+06	0.91690	1.48152
32.00	0.38324E+06	0.91355	1.31441
33.00	0.39019E+06	0.91014	1.14278
34.00	0.39292E+06	0.90669	0.96503
35.00	0.38861E+06	0.90325	0.77876
36.00	0.38207E+06	0.89985	0.58423
37.00	0.37554E+06	0.89651	0.38165
38.00	0.36901E+06	0.89323	0.17124
39.00	0.36248E+06	0.89000	-0.04679
40.00	0.35595E+06	0.88684	-0.27224
41.00	0.34864E+06	0.88373	-0.23257
42.00	0.34133E+06	0.88069	-0.19578
43.00	0.33403E+06	0.87771	-0.16181
44.00	0.32672E+06	0.87480	-0.13064
45.00	0.31941E+06	0.87195	-0.10222
46.00	0.31211E+06	0.86917	-0.07650
47.00	0.30480E+06	0.86645	-0.05346
48.00	0.29749E+06	0.86380	-0.03305
49.00	0.29018E+06	0.86121	-0.01524
50.00	0.28288E+06	0.85868	0.00000

STRUC LOAD(LB)	SOILP(PSF)	ACTIVE DEPTH(FT)
0.	0.00	-1.00

Appendix D
Modification of *p-y* Curves for Battered Piles

a. Kubo (1965) and Awoshika and Reese (1971)[1] inves-tigated the effect of batter on the behavior of laterally loaded piles. Kubo used model tests in sands and full-scale field experiments to obtain his results. Awoshika and Reese tested 2-inch diameter piles in sand. The value of the constant showing the increase or decrease in soil resistance as a function of the angle of batter may be obtained from the line in Figure D1. The "ratio of soil resistance" was obtained by comparing the groundline deflection for a battered pile with that of a vertical pile and is, of course, based purely on experiment.

b. The correction for batter is made as follows: (1) enter Figure D1 with the angle of batter, positive or negative, and obtain a value of the ratio; (2) compute groundline deflection as if the pile were vertical; (3) multiply the deflection found in (2) by the ratio found in (1); (4) vary the strength of the soil until the deflection found in (3) is obtained; and (5) use the modified strength found in (4) for the further computations of the behavior of the pile that is placed on a batter. The method outlined is obviously approximate and should be used with caution. If the project is large, it could be desirable to perform a field test on a pile installed with a batter.

[1]References are listed in Appendix A.

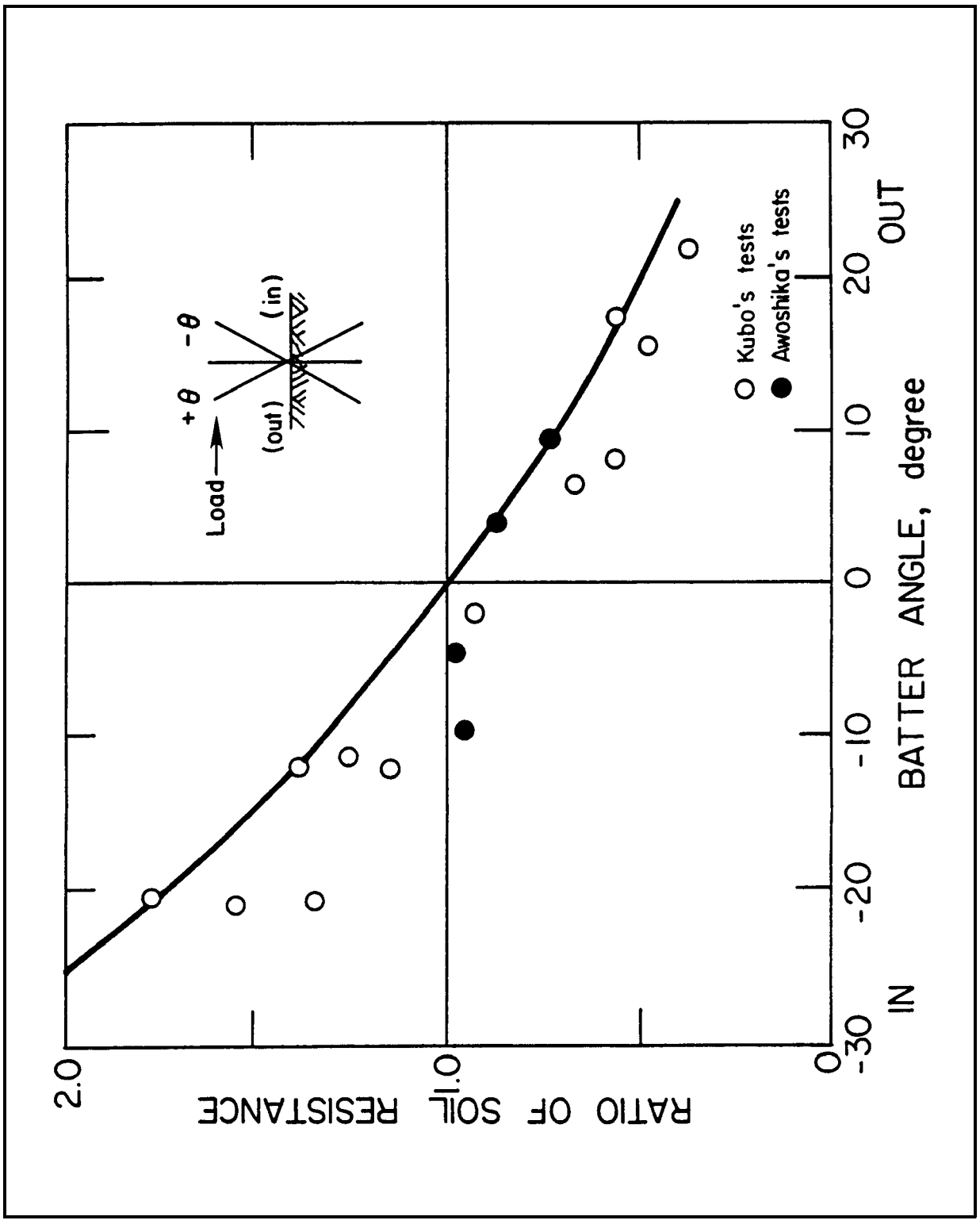

Figure D1. Modification of *p-y* curves for battered piles (after Kubo (1965), and Awoshika and Reese (1971))